Design and Synthesis of Nickel *N*-Heterocyclic Carbene Catalyst Systems and Their Application in the Cross-Coupling of Silyloxyarenes

by

Wesley Layne Pein

A dissertation submitted in partial fulfillment
of the requirements for the degree of
Doctor of Philosophy
(Chemistry)
in the University of Michigan
2021

Doctoral Committee:

Professor John Montgomery, Chair
Assistant Professor Timothy Cernak
Associate Professor Corinna Schindler
Professor John Wolfe

Wesley Layne Pein

pein@umich.edu

ORCID iD: 0000-0002-4626-9043

Dedication

The completion of my doctoral studies would not have been possible in the absence of so many factors. Most fundamentally, however, it would not have been at all possible to attempt without the tenacity and collective sacrifices of my forebearers who endured 400 years of slavery and many more thereafter of oppression. Their bravery, relentlessness, and determination to constantly strive for a better future paved the way for me to have the right and the opportunity to pursue this education; which, I have seen to the finish at the highest level. The burden of combating institutional racism in the United States of America and abroad is seemingly never ending. However, I partly take solace from a monologue in "The Lord of the Rings" where the character, Samwise Gamgee, describes how in the face of adversity, the heroes "…had lots of chances of turning back only they didn't. Because they were holding onto something." Frodo went on to ask, "What are we holding on to, Sam?" to which Sam replied "That there's some good in this world, Mr. Frodo. And it's worth fighting for." Certainly, that is worth holding on to. With that, this thesis is dedicated to those who had lots of chances of turning back only they did not and those of the future that will not turn back either.

This is dedicated to the slaves that endured and clung to the hope that one day they may be delivered. This is dedicated to Harriet Tubman, and others who aided and abetted in the escape of slaves from the wicked south. This is dedicated to the 54th Massachusetts Regiment who played a critical role in securing our freedom from bondage during the American Civil War. This is dedicated to visionaries like Frederick Douglas, Dr. Martin Luther King Jr., and Malcom X who sought to not only attain freedom on paper, but to see it infect every part of our lifestyle. This is

dedicated to intellectuals like Booker T. Washington and William Edward Burghardt Du Bois who advocated strongly for Blacks to advance socioeconomically and to reap the benefits of education, respectively. This is dedicated to the first Black chemists like Dr. Percy Lavon Julian, who forged a path for us in the field. This is dedicated to artists like Sam Cooke who made hopeful music chronicling how one day, change would come only to never see it come fully to fruition. This is dedicated to the Trayvon Martins and George Floyds whose time was cut far too short by the institutional racism in this nation. Most importantly, this thesis is dedicated to the bright, young future of Black America. Whoever you are, wherever you are from, may you find comfort and inspiration in that there ain't no mountain high, ain't no mountain low, ain't no river wide enough to keep you from reaching your dreams.

Acknowledgements

I would like to thank the support that I have received from my advisor, John Montgomery. I came into graduate school at 21 and rough around the edges. Over the course of my doctoral studies, I most appreciate John's patience with me as I stumbled and grew into an independent scientist. Additionally, I would be remiss not to thank the National Science Foundation (NSF) for their support via two NSF-AGEP awards, and Rackham Graduate School for providing me with a Rackham Merit Fellowship. I would also like to thank the members of my dissertation committee being Professor Tim Cernak, Professor Corinna Schindler, and Professor John Wolfe for showing up over the years and for their helpful suggestions and kind support. I would also like to thank all members of the Montgomery lab both past and present. I have felt incredibly lucky to have such a great group of people around me. I would like to thank Dr. Eric Wiensch, for being such a great collaborator and friend. Also, I would like to thank Dr. Alex Nett for his leadership and guidance over the years. I would like to thank Dr. Alex Rand and Dr. Annabel Ansel for contributing to the editing of my thesis.

I am so grateful for all my incredible friends from home to college, to graduate school, I have been blessed to meet so many wonderful people. High on that list is my undergraduate advisor, Professor Michael Leonard, to whom I am eternally grateful. Lastly, I would especially like to thank my family with special attention to my grandmother, Margy Pein, grandfather, Lieutenant. Colonel Heiko Pein, and my mother, Jamie Pein.

Table of Contents

List of Tables

List of Figures

List of Abbreviations

α: alpha

Acac: acetylacetone

Ar: aryl

β: beta

Bpin: pinacolboron

Bu: butyl

Bz: benzoyl

c: cyclo

C: Celsius

cat: catalyst

COD: cylcooctadiene

Cp: cyclopentadienyl

CPME: *cyclo*-pentyl methyl ether

Cu: copper

CV: cyclic voltametry

DCE: 1,2-dichloroethane

DCM: dichloromethane

DDQ: 2,3-dichloro-5,6,-dicyano-1,4-benzoquinone

DG: directing group

DFT: density functional theory

DME: dimethoxyethane

DMF: dimethylformamide

DMSO: dimethyl sulfoxide

Dppf: 1,1'-Bis(diphenylphosphino)ferrocene

DPV: differential pulse voltammetry

dr: diastereomeric ratio

EI: electron impact

er: enantiomeric ratio

Et: ethyl

EtOAc: ethyl acetate

Equiv.: equivalent

EPR: electron paramagnetic resonance

GC-FID: gas chromatography-flame ionization detector

GCMS: gas chromatography-mass spectrometry

Fe: iron

h: hour

HOMO: highest-occupied molecular orbital

HRMS: high resolution mass spectroscopy

hv: ultraviolet light

i: iso

i-Bu: isobutyl

i-Pr: isopropyl

IMes: 1,3-bis(2,4,6-trimethylphenyl)-1,3-dihydro-2H-imidazol-2-ylidene

IPr: 1,3-bis(2,6-diisopropylphenyl)-1,3-dihydro-2H-imidazol-2-ylidene

IPr^{Me}: 4,5-dimethyl-1,3-bis(2,4,6-triisopropylphenyl)-4,5-dihydro-imidazolium

IPr*OMe: N,N'-Bis(2,6-bis(diphenylmethyl)-4-methoxyphenyl)imidazole-2-ylidene

L: ligand

Ln: a number of ligands

LG: leaving group

LUMO: lowest-occupied molecular orbital

μ: micro

M: molarity, transition metal

Me: methyl

mg: milligram

n-Bu: butyl

n-Hex: hexyl

n-Pent: pentyl

n-Pr: propyl

NHC: n-heterocyclic carbene

Ni: nickel

NMR: nuclear magnetic resonance

Pd: palladium

PG: protecting group

Ph: phenyl

Piv: pivalate

Pr: propyl

R: generic group

r.t.: room temperature

SET: single electron transfer

SAR: structure activity relationship

SIMes•HCl: 1,3-dimesityl-4,5-dihydro-1H-imidazol-3-ium chloride

SIPr•HCl: 1,3-bis(2,6-diisopropylphenyl)-4,5-dihydro-1H-imidazol-3-ium chloride

t: tertiary

t-Bu: tert-butyl

TBS: tert-butyldimethyl silyl

TBDPS: tert-butyldiphenylsilyl

TES: triethylsilyl

Tf: triflate

THF: tetrahydrofuran

TIPS: triisopropylsilyl

TMS: trimethylsilyl

X: halogen, leaving group, generic group

Abstract

The invention of transition-metal catalyzed cross-coupling reactions has fundamentally changed how chemists approach the synthesis of small molecules. Moreover, the ability to perform reactions catalytically while employing Earth abundant first row transition-metals has had positive impacts regarding sustainability. In addition to environmental considerations, first row transition-metals, like nickel, have been found to possess reactivity that is complementary to metals like palladium, which has implications for how the metal performs in the various elementary steps of catalytic processes. These insights have arisen from the study, design, and development of nickel catalyst systems, which have propelled the invention of catalytic strategies for the formation of a wide array of C–C and C–heteroatom bond forming reactions. The nature of reaction development and catalyst design are intimately related as achieving the development of novel bond forming reactions relies upon innovative advances that reduce the limitations associated with existing catalyst systems to provide enhanced performance, or to make the catalysts, themselves, more accessible. An account of these efforts in the context of C–O bond functionalization and air-stable, discrete nickel(0) (Ni(0)) *n*-heterocyclic carbene (NHC) catalysts are described, herein.

Chapter 1 is largely oriented towards the utility of phenol derivatives as electrophilic coupling partners with low-reactivity C–O bonds being of main interest. The challenges regarding the activation of these low-reactivity C–O bonds is discussed, as well as current strategies to overcome their inherently low-reactivity. Although low-reactivity C–O bonds are challenging to activate, their functionalization is of import as possessing electrophilic coupling partners that range in reactivity enables highly selective sequential couplings, resulting from leveraging the

orthogonal reactivity of each electrophile. Chapter 2 chronicles the utility of aryl boronic acids in organic synthesis, with particular attention paid to their role in cross-coupling reactions. The synthesis of these compounds spanning from traditional approaches to modern techniques, which includes the state of the art in the borylation of low-reactivity C–O bonds. The limitations of these strategies are covered and the development of a borylation of silyloxyarenes is described along with synthetic demonstrations that highlight the ability of silyloxyarenes to be used orthogonally to other electrophiles.

Chapter 3 entails the advantages of catalysis, and the transition metal catalysts we rely upon to mediate these processes, with special attention to nickel, have evolved. For the purposes of this dissertation, nickel catalysts have been categorized as 1) Ni(II) salts, 2) discrete Ni(II) pre-catalysts, 3) Ni(0) pre-catalysts, 4) air-stable Ni(0) pre-catalysts, and 5) discrete air-stable Ni(0) pre-catalysts. The advantages and disadvantages, activation strategies, and synthesis of each category are described in detail. Preliminary work regarding progress towards the synthesis of an air-stable, discrete Ni(0) NHC complex from nickel (II) (Ni(II)) precursors and NHC salts is described.

Chapter 1

Nickel-Catalyzed Couplings of Phenol Derivatives to and Their Implications on Sequential Couplings

1.1 The Importance of Base-Metal Catalysis

As scientists, we have a responsibility to develop catalytic processes that enable novel reactivity, improve upon existing protocols, are cost-effective, and are more sustainable than their predecessors. To capture the spirit of this mandate, attention has been turned to base-metal catalysis due to the natural abundance of these metals, which encompasses this broad mandate.[1] Aside from the aforementioned well-defined, tangible outcomes, another direction is dedicated towards basic research, which aims to expand our knowledge regarding the fundamental reactivity of the catalysts that mediate these processes. Nickel is one such base-metal that has received a great deal of attention more recently. From these efforts, the scientific community has learned that nickel possesses complementary properties to other *d*10 metals, such as 1) its propensity for conducting challenging oxidative additions, 2) its ease of coordination and migratory insertion to olefins, and 3) that it is nimble in conducting odd electron chemistry via single electron transfer (SET) processes.[2]

1.2 Motivation for Utilizing Phenol Derivatives as Electrophiles in Cross-Coupling Reactions

Phenol derivatives are an attractive class of cross-coupling partner due to the abundance and diversity of their derivatives. Additionally, they display a broad range of reactivity depending on the nature of the protecting group employed. Furthermore, the phenol moiety is highly

conserved in natural products and so methodologies to functionalize these handles for diversification is advantageous for structure activity relationship (SAR) studies in the context of medicinal chemistry.[3] Another significant application of C–O bonds comes in the degradation of lignan polymers containing several subunits, which are bound by low-reactivity C–O bonds.[4] This is of import as the degradation of lignan is a promising strategy in making progress towards reducing humanity's reliance upon the petroleum stream for commodity chemicals. Lastly, in addressing limitations surrounding the functionalization of low-reactivity C–O bonds, advances in other related areas like catalyst development may occur as advances in this area are essential to the activation of these challenging bonds.

1.2.1 Low-Reactivity Phenol Derivatives

Pseudohalides like aryl triflates, tosylates, etc have been fairly-well studied in nickel-catalyzed cross-coupling reactions.[5] While less studied, less reactive electrophiles such as esters, carbamates, and ethers have begun to receive more attention over the last 15 years. The reactivity of each is described by following trend (Figure 1-1).[2,6–8]

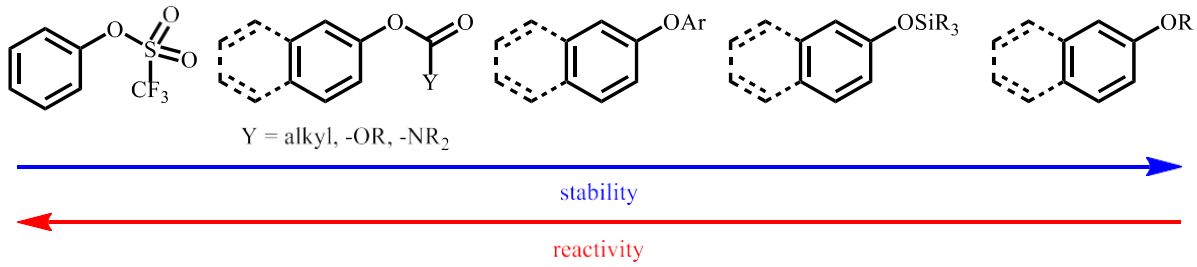

Figure 1-1. Reactivity scale of phenol derivatives towards transition-metal catalyzed couplings.

The differences in relative reactivity between aryl triflates and electrophiles like aryl carbonates, carbamates, and pivalates are easily discernable.[2] However, distinguishing the difference in reactivity between the latter grouping and other electrophiles on the scale is less

obvious and must be determined by rigorous empirical testing combined with the support of theoretical experiments. One such study was conducted by Nelson and co-workers in 2017 which utilized a discrete Ni(0) complex which utilized 1,1'-Bis(diphenylphosphino)ferrocene (dppf) and cyclooctadiene (COD) as ligands (Figure 1-2).[9]

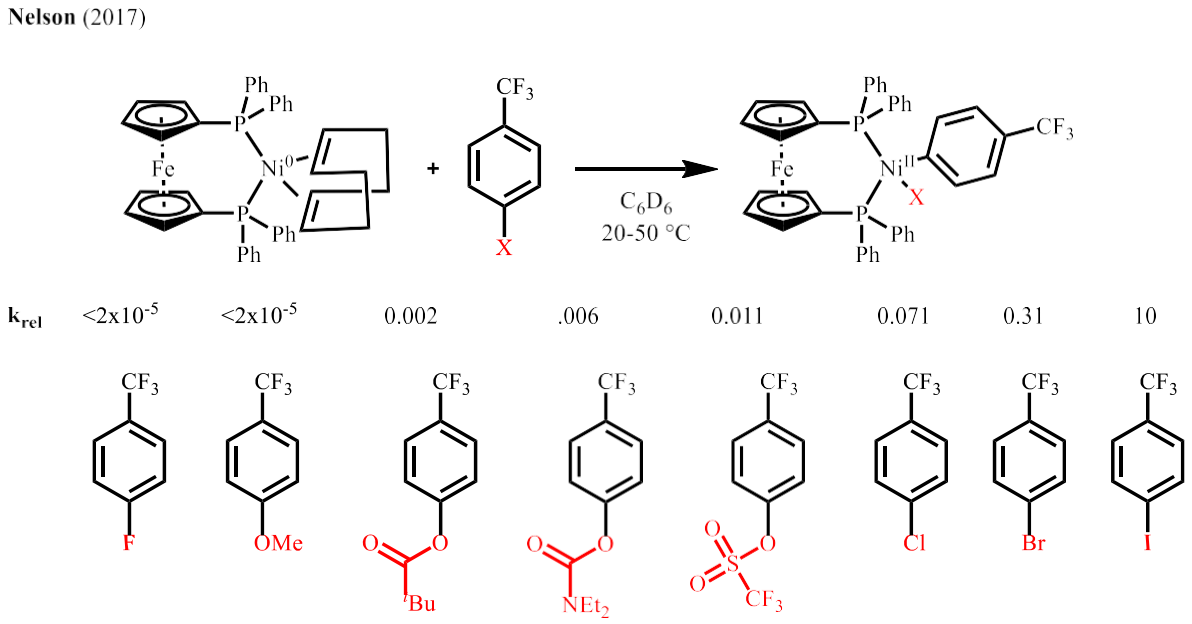

Figure 1-2. Relative rates of oxidative addition between various aryl electrophiles.

However, to our knowledge, no such studies have been conducted concerning the relative rate of oxidative addition to silyloxyarenes by nickel. While not as precise, an anticipated trend in reactivity can be rationalized via a pka argument (Figure 1-3).

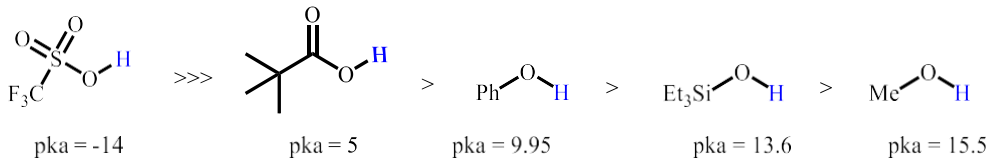

Figure 1-3. pka of parent acid of leaving groups mentioned in (Figure 1-1).

While these data may not correlate perfectly with reactivity observed in cross-coupling reactions, they do at least provide a loose template for what to expect; which, led the Montgomery group to believe that the functionalization of silyloxyarenes should be possible.

1.2.2 Challenges of Activating Low-Reactivity Phenol Derivatives

In general, two properties of easily activatable electrophilic coupling partners are that they possess a weak C–X bond and that within the structure of the leaving group, there may exist directing group functionality, such as in the case of triflates, or pyridyl ethers (Figure 1-4).

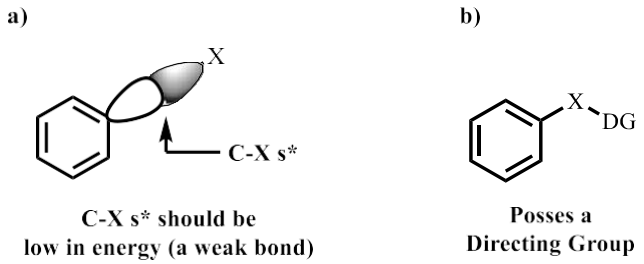

Figure 1-4. Favorable properties of aryl electrophiles. a) possessing a weaker C–X bond, and b) containing a directing group within the structure of the leaving group.

Although low-reactivity C–O bonds represent an appealing class of aryl electrophile as their enhanced stability allows them to be carried through several synthetic operations only to be activated at the opportune time, thus providing the potential for late state functionalization, they tend to be limited to polyaromatic frameworks. This is colloquially known as the naphthyl problem. This is largely attributed to the fact that they do not possess properties of ideal electrophiles. For example, low-reactivity C–O bonds are not well polarized, whereas pseudohalides are. This leads to a higher lying lowest occupied molecular orbital (LUMO), in comparison, which confers increased bond strength to low reactivity C–O bonds thus making them more challenging to activate (Figure 1-5).

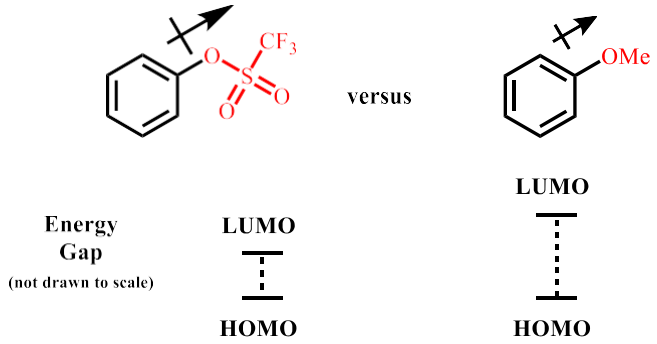

Figure 1-5. Inductive consideration regarding C–O bond strength and relation to LUMO energy.

Aryl methyl ethers, represent a prime example of an unpolarized C–O bond. However, reactivity can still be broadly seen so long as they are polyaromatic systems like the naphthalene core, because the extended π system, supplies a lower lying LUMO; which, leads to a more facile oxidative addition (Figure 1-6). Due to the higher LUMO energies of low-reactivity C–O bonds, electron rich metals are ideal agents for the functionalization of these bonds due to the higher energy of their highest occupied molecular orbital (HOMO).

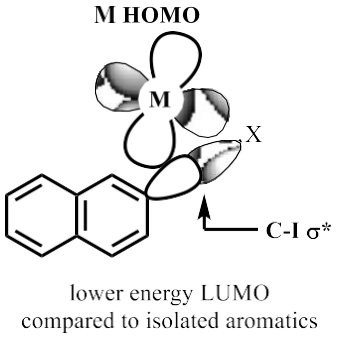

Figure 1-6. Molecular orbital representation of a metal HOMO bonding with the LUMO of the C–X bond.

However, as conjugation decreases as in the case of biphenyls, and systems that are completely isolated, electronically, the issue of a higher lying LUMO is exacerbated and typically results in the low reactivity C–O bond being intractable except in cases where the nucleophile is highly reactive as in the case of Kumada couplings.

1.2.3 Silyloxyarenes as a Competent Class of Phenolic Electrophile

Initially discovered by Wenkert and co-workers,[6] in a one-off experiment, silyloxyarenes had been found to participate in couplings with organometallic nucleophilic coupling partners. Aside from this, however, silyloxyarenes have seen limited action in cross-coupling and remain largely unexplored otherwise. Therefore, the Montgomery group became interested in investigating this underexplored class of low-reactivity C–O electrophile to determine if it displayed favorable reactivity on aromatic scaffolds that go beyond naphthalene-based systems. These efforts resulted in the disclosure of four coupling reactions, all of which, demonstrate the inclusion of large numbers of isolated aromatic substrates (Figure 1-7).[10–13]

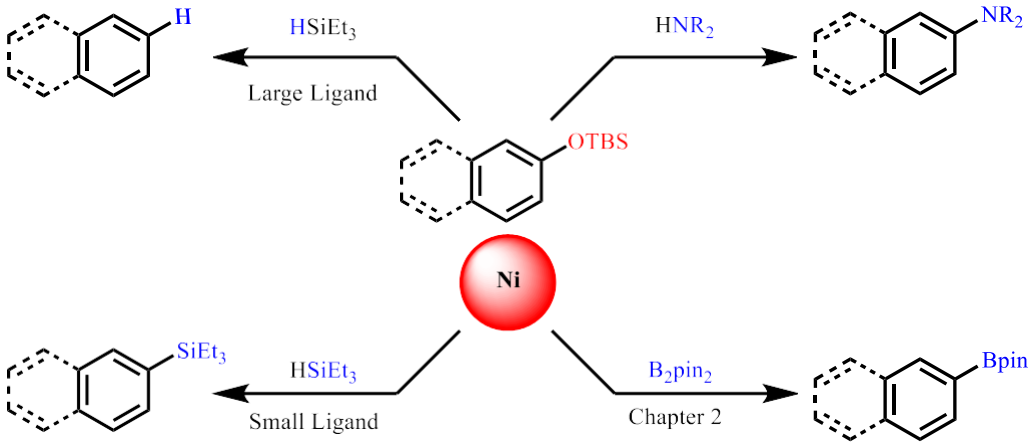

Figure 1-7. Coupling reactions of silyloxyarenes.

1.3 Orthogonal Reactivity and Sequential Couplings

The expansion of viable electrophiles in cross-coupling reactions provides more flexibility in how molecules are assembled. Having an array of electrophiles that possess orthogonal reactivity to each other allows for sequential couplings to be conducted wherein, no additional deprotection/activation steps are required. This leads to the design of streamlined synthetic routes, which save time, money, and materials.

Organohalides represent a robust class of aryl electrophile due to their ease of activation. However, the low abundance of some organohalides, particularly aryl iodides, necessitates the preparation of these species, which can be a multistep process. These considerations led to the development of alternative electrophiles for use in cross coupling reactions from abundant feedstocks, one class being phenol derivatives as discussed, previously.[8]

In principle, there are two main methods in which orthogonal reactivity can be accomplished 1) through substrate control wherein the inherent reactivity of the electrophile is variable, or 2) via catalyst control where chemoselectivity is determined strictly by choice of catalyst system (Figure 1-8).

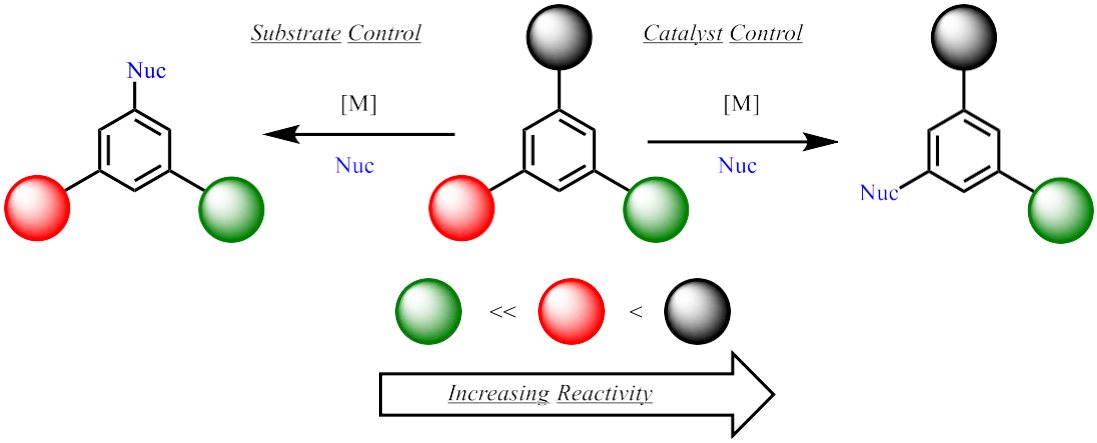

Figure 1-8. Conceptual scheme regarding orthogonal reactivity in cross-coupling reactions.

In the case of substrate control, the most reactive electrophilic position would react first followed by the second most reactive site, so on and so forth. Whereas, in the case of catalyst control, the inherent reactivity of the electrophile can be overcome via the nature of the catalyst system regardless of the inherent reactivity (Figure 1-9).[14, 15]

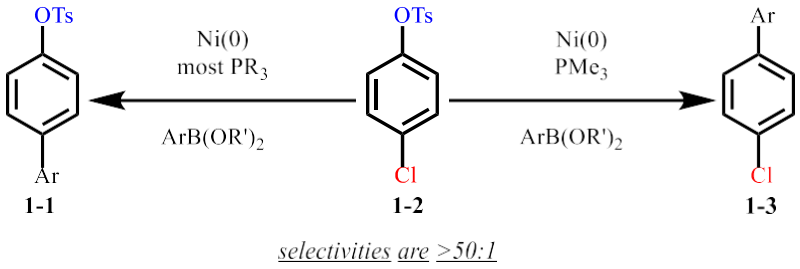

Figure 1-9. Catalyst control in the functionalization of **1-2**.

In either case, these strategies permit the sequential coupling of substrates with multiple electrophilic sites without the need for deprotection/activation steps, which enables the expedient build-up of molecular complexity from simple starting materials (Figure 1-10).

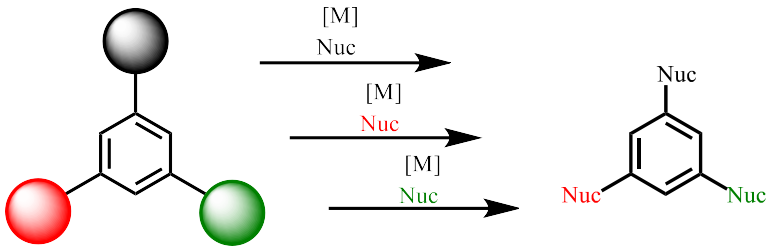

Figure 1-10. Hypothetical sequence of couplings with high chemoselectivity.

Studies by the Montgomery group have demonstrated that silyloxyarenes are not activable by a wide range of phosphine ligands ranging in steric and electronic profiles in the optimization of several coupling reactions. In contrast, aryl methyl ethers are readily functionalized by nickel catalyst systems that employ phosphine ligands. With this information, it was hypothesized that **1-4** could be selectively functionalized via catalyst control instead of relying upon the innate reactivity of the aryl electrophiles present. In a previous report, it was demonstrated that an electron rich Ni-NHC catalyst system, amination could be done with exquisite selectivity for the silyloxyarene site of **1-4**, to furnish **1-5**, which could then be further functionalized to provide **1-6**. Conversely, the less reactive methyl ether of **1-4** could be engaged first by a nickel-phosphine

catalyst system to deliver alkylation ipso to the methyl ether, leaving the silyloxyarene untouched, affording **1-7**. This could then subsequently be converted to the aniline derivative. These reactions highlight the power of orthogonally activatable electrophiles (Figure 1-11).[12]

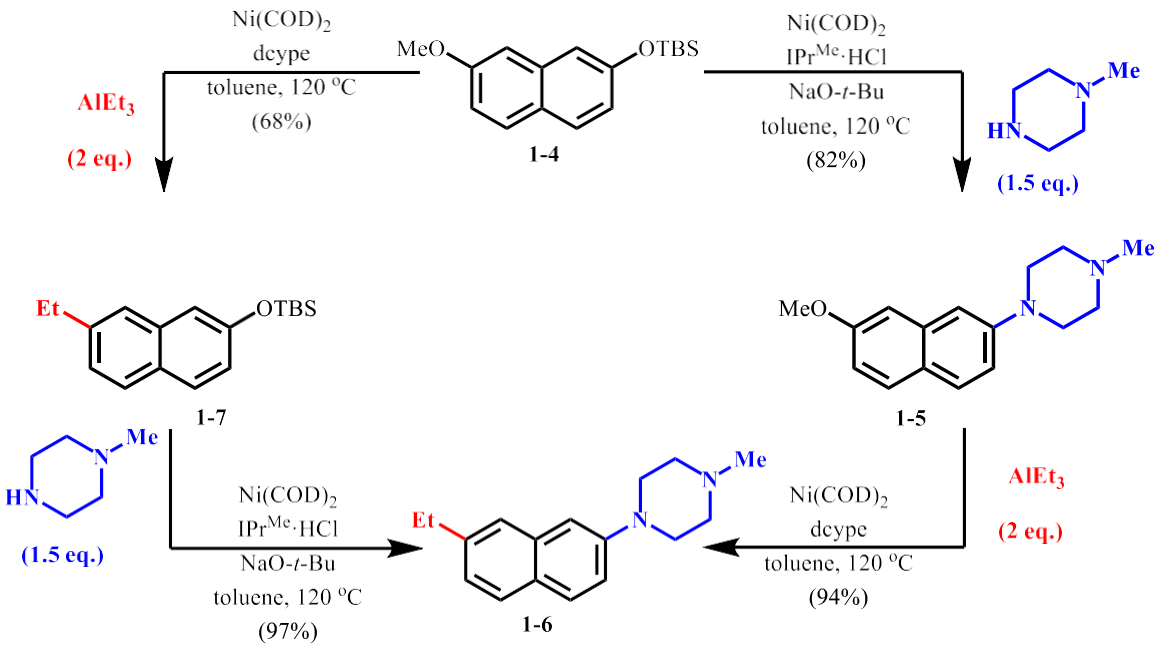

Figure 1-11. Orthogonal reactivity of aryl methyl ethers to silyloxyarenes via catalyst control.

The orthogonal reactivity of a series of aryl electrophiles was then leveraged to perform the following sequential coupling also previously reported by the Montgomery group (Figure 1-12).[12] The naphthyl system, **1-7**, was methylated to give a naphthalene system possessing two electrophilic positions in the methyl ether and the halide, **1-8**. Generally, palladium has difficulty functionalizing aryl electrophiles that are less reactive than pseudohalides without directing groups.[2] Ergo, it was hypothesized that applying standard Suzuki conditions to **1-8** in the presence of **1-9**, would lead to exclusive functionalization of the aryl bromide. Notably, the boronic acid installed two other electrophilic sites in the formation of **1-10** being the silyloxy group and the aryl chloride, which were unaffected under these reaction conditions.

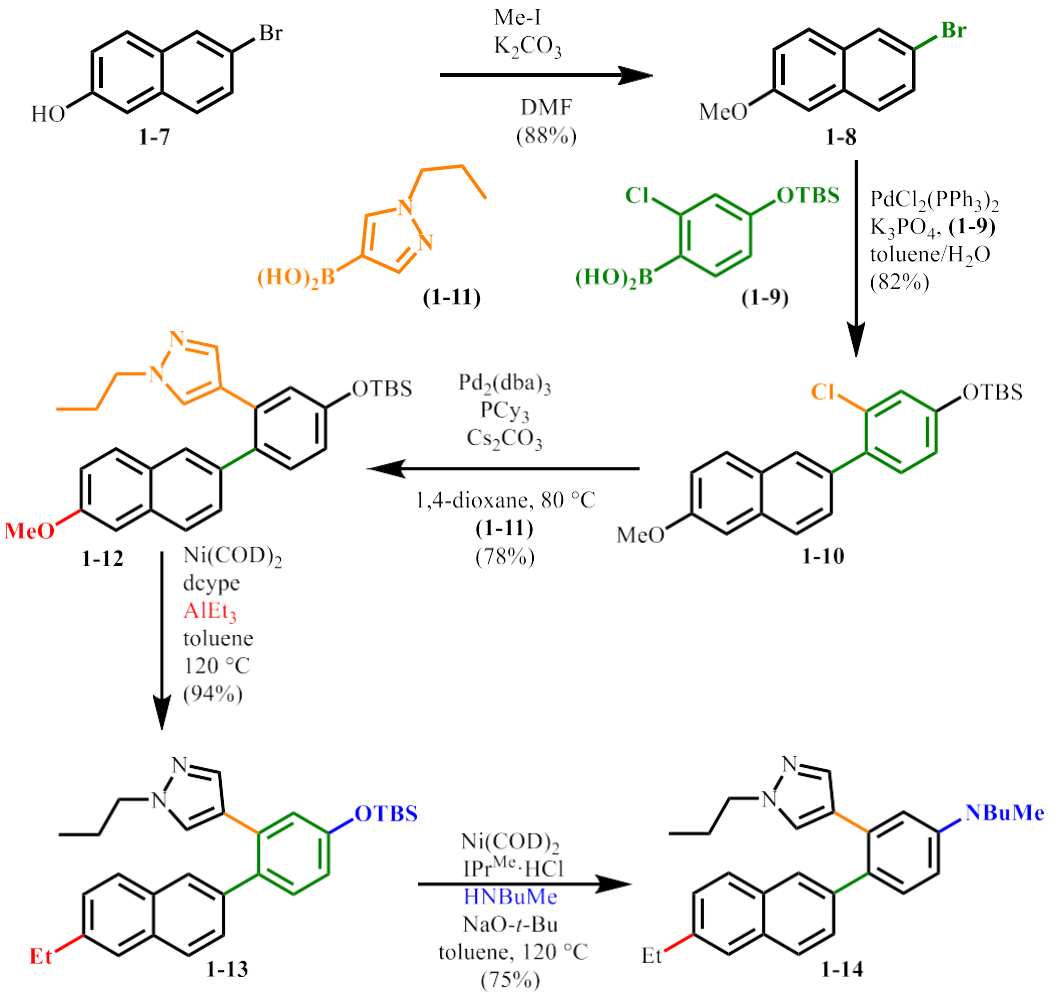

Figure 1-12. Sequential coupling demonstration.

As a result, a scaffold possessing three electrophilic positions was generated. A second Suzuki reaction, this time on **1-10**, was conducted, resulting in conversion of the aryl chloride to the value added, pyrazole substrate, **1-12**. Subsequently, alkylation of the methyl ether was conducted providing **1-13**. Finally, the silyloxyarene was aminated, furnishing **1-14**. Aside from the methylation of **1-7**, four cross-coupling reactions were conducted in high yields and excellent selectivity without the need for deprotection/activation steps demonstrating the power of orthogonal reactivity to facilitate sequential couplings.

1.4 Summary of Phenol Derivatives and Their Role in Orthogonal Reactivity

Phenol derivatives represent a desirable chemical feedstock for synthetic transformations as they are abundant, diverse in structure, and highly modular regarding their reactivity. Recently, many studies have been produced, which sought to expand the utility of low-reactivity C–O bonds by developing protocols that are more inclusive of isolated aromatic systems. This range in reactivity in addition to various other classes of electrophiles sets the stage for sequential couplings that provide the expedient formation of highly decorated molecules without the need for activation and deprotection steps from simple starting materials. Moreover, the study and design of catalyst systems to better address the needs of these programs is vital.

Chapter 2

Nickel-Catalyzed *Ipso*-Borylation of Silyloxyarenes

(This chapter was partially published in: Pein, W.; Wiensch, E.; Montgomery, J. *Org. Lett*. **2021**, *23*, 4588–4592 - https://doi.org/10.1021/acs.orglett.1c01280)

2.1 Introduction

The employment of earth-abundant base-metals for catalysis is of great interest due to their sustainability, affordability, and unique reactivity, as compared to precious metals.[1,2] Due to this, nickel catalysis has been rigorously investigated to ascertain the distinct chemical properties which differentiate it from its congener palladium, such as nickel's propensity to conduct challenging oxidative additions as in the case of low-reactivity C─O bonds, for example.[2,6,8,16] Employing C─O electrophiles over traditional halides is desirable due to phenols being cheap, commodity chemicals possessing a rich diversity of structures, substitution patterns, and representation in natural products. Furthermore, C─O bond activation offers opportunities for orthogonal reactivity to halide electrophiles as their reactivity can be modulated through prudent choice of protecting group (Chapter 1).[9,14,17] This enables aryl scaffolds that possess multiple electrophilic sites to be engaged in sequential couplings via judicious selection of catalyst system. The same reactivity paradigm that allows for chemoselective activation between aryl halides and pseudohalides, as compared to other phenol derivatives, necessitates more forcing conditions for the less reactive electrophiles. For example, employing low-reactivity C─O electrophiles, such as, pivalates, carbamates, or simple ethers often require either harsh, organometallic nucleophilic coupling partners such as Grignard reagents, highly activated naphthol-derived electrophiles, and/or

directing groups that promote reactivity.[18] To bridge this gap, we utilized silyloxyarenes as coupling partners. Although silyloxyarenes have most commonly used in reactions with activated nucleophilic coupling partners,[18–21] recent reports from our lab show that electron-rich Ni-NHC catalyst systems facilitate the reduction, silylation, and amination of silyloxyarenes in a manner that is inclusive of isolated aromatic systems without the need for *ortho*-directing groups.[12,13] Building upon these seminal reports, systematic investigations were undertaken to expand this class of reactions to include borylation, as aryl boronic acid pinacol esters serve as excellent synthetic handles for downstream functionalization[22–24] and can also be utilized as precursors for medicinally relevant boronic acids[25] (Figure 2-1).

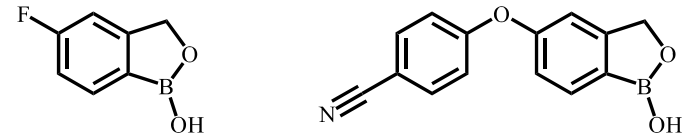

2-1
Kerydinâ (Tavaborole)

2-2
EucrisaÔ (Crisaborole)

Figure 2-1. Pharmaceutically relevant examples of aryl boronic acids.

Traditional protocols to access aryl boronic acids involve the treatment of organolithium reagents with borates.[26–28] Alternative methods have also been described for light-mediated and transition-metal catalyzed reactions enabling the borylation of aryl halides and aryl C–H bonds.[29] More recently, C–O electrophiles have been utilized as precursors to aryl boronic acids, although opportunities for improvement include avoiding easily hydrolyzed activating groups and providing improved reactivity with isolated aromatic ring substrates.[30–34]

To address the above limitations regarding borylation of C–O bonds, silyloxyarenes offer several promising attributes. They offer ease of synthesis and possess well-understood reactivity

profiles, owing to detailed investigations of silyl ethers as protecting groups. This latter understanding gives rise to predictable strategies to tune their reactivity and stability across a range of reaction conditions,[35–37] enabling them to be carried through several synthetic steps, functionalized without additional deprotection and activation steps, thus leaving them available for further functionalization. Given the balance between the stability and reactivity of silyloxyarenes in comparison to other inert C–O electrophiles (Chapter 1), this study sought to enable the inclusion of substrates that go beyond naphthyl systems while using attractive diboron coupling partners to form highly coveted aryl boronic acid derivatives.

2.2 Utility of Aryl Boronic Acids in Organic Synthesis

Many of the desirable properties of boron stem from its unfilled p-orbital, which results in a sp^2 geometry and Lewis acidic nature of organoboron species (Figure 2-2). The Lewis acidity of boron is highly modular and can be finely tuned via the manipulation of the steric and electronic properties of its substituents. This empty p orbital allows for coordination of Lewis base (LB) to form boronates, which are then suitably activated to undergo transmetallation in cross-coupling reactions.

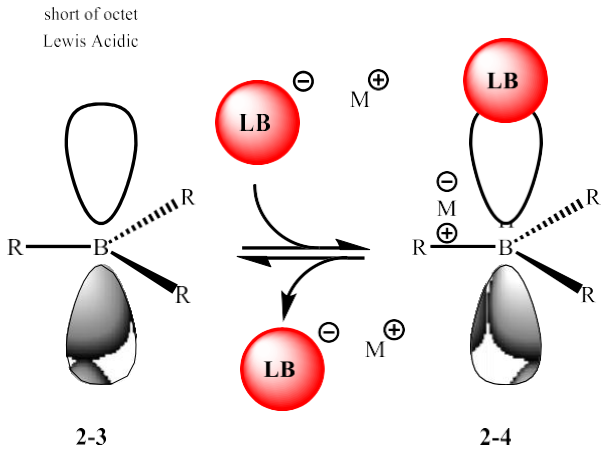

Figure 2-2. Molecular orbital representation regarding the origins of boron's Lewis acidic properties.

Due to the development of a number of methods that use boron nucleophile, the relatively high abundance in the Earth's crust, and the largely non-toxic nature of boron-containing compounds, the synthesis of organoboron compounds have been an area of great investigation in the synthetic community (Figure 2-3).[38]

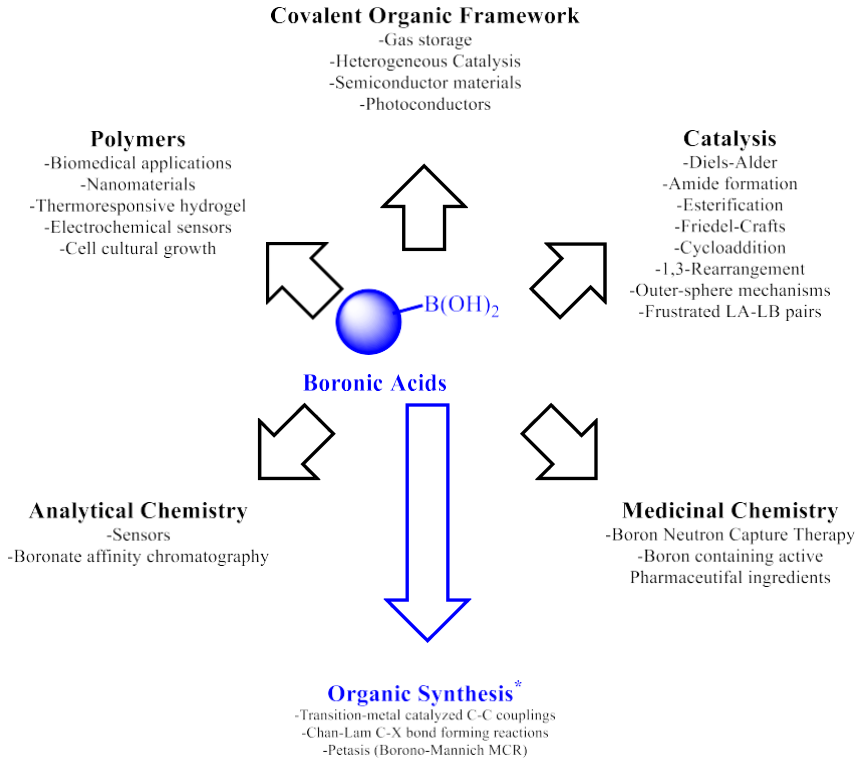

Figure 2-3. Applications of boronic acids in synthesis.

While the use of boron-containing compounds has been adopted by numerous sectors inside and out of the chemistry community, this chapter will cover the application of aryl boronic acids in organic synthesis (Figure 2-4).

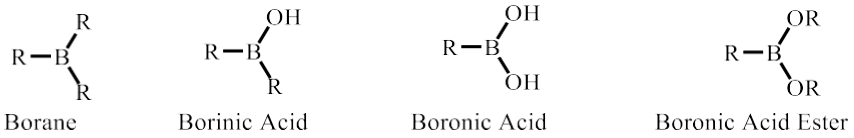

Figure 2-4. Nomenclature of common boron species.

Several key transformations regarding aryl boronic acids will be discussed followed by select examples of their employment in the context of pharmaceuticals.[38] For the purposes of this discussion, it should be assumed unless otherwise noted that aryl boronic acid esters possess similar reactivity to aryl boronic acids and so similar conclusions can be drawn regarding their reactivity.

2.2.1 Applications of Aryl Boronic Acids in Cross-Coupling Reactions

Transition-metal catalyzed cross-coupling reactions revolutionized synthesis. Previously inaccessible motifs are now assembled in an expedient fashion from simple, commercially available chemical feedstocks. One such feedstock comes in the form of aryl boronic acids, which are featured in a myriad of cross-coupling reactions (Figure 2-5).

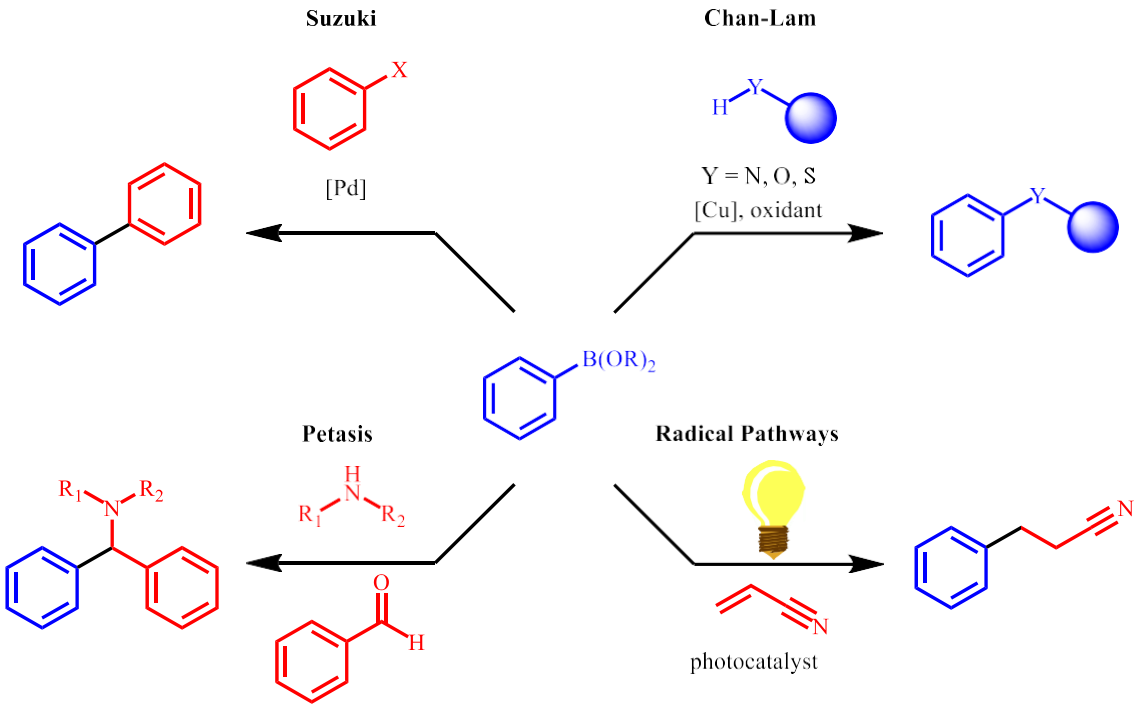

Figure 2-5. Applications of aryl boronic acids.

Over the course of this section, each class of synthetic transformation shown in (Figure 2-5) shall be summarized.

2.2.1.1 The Chan-Lam Coupling

In 1998, Chan, Evan, and Lam near simultaneously reported the coupling of aryl boronic acids and nucleophilic heteroatoms using a copper catalyst, which is now known as the Chan-Lam reaction.[24,39,40] While the reaction is traditionally facilitated by copper, other $M(II)X_2$ salts, such as nickel, can be employed, as well. Since this is a cross-nucleophile coupling, $Cu(II)X_2$ salts are utilized in combination with stoichiometric quantities of oxidant to re-oxidize the catalyst following the reductive elimination that furnishes the coupled products. The nature of the oxidant can vary widely; some common examples of oxidants include silver salts, peroxides, and air. Finally, non-nucleophilic bases are required to activate the boronic acid, thus priming it for coupling. A generic representation regarding the simplified mechanism for this reaction can be seen, below (Figure 2-6). Assisted by base, the amine nucleophile undergoes ligand exchange with the Cu(II) salt. The boron nucleophile then transmetallates to copper. Another equivalent of $Cu(II)X_2$ enters the catalytic cycle and undergoes a disproportionation reaction yielding a Cu(I)X species and Cu(III), which then reductively eliminates to produce the desired product and put forth another equivalent of Cu(I)X, which are then subsequently be oxidized back to $Cu(II)X_2$ to complete the catalytic cycle.

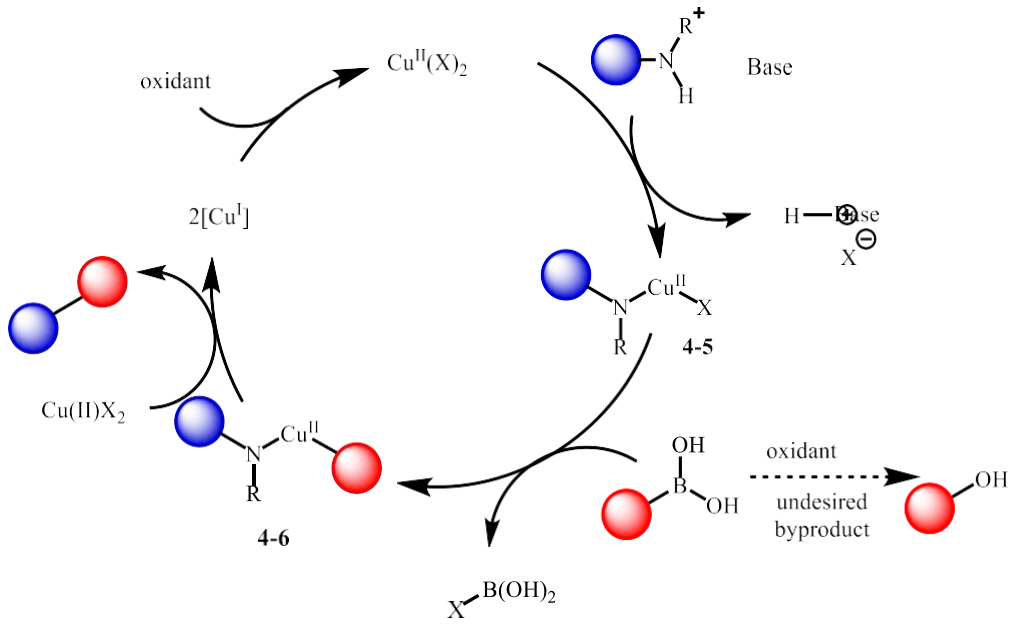

Figure 2-6. General mechanism for a Chan-Lam reaction.

A common disadvantage of this method, however, is the decomposition of the boronic acids via protodeboronation, or oxidation. The latter of which results in conversion to the corresponding oxygen nucleophile. As a result, this reaction has been studied extensively and many strategies exist to mitigate byproduct formation by judicious optimization of conditions, specifically, with respect to the oxidant.[41] Oxidative processes have their advantages, one large one being that they can be run open to air, and in some cases, air alone is enough to facilitate the reaction. The operational advantages and the tremendous diversity of chemical transformations that can be conducted via the Chan-Lam reaction have made its presence in the synthesis of pharmaceuticals ubiquitous (Figure 2-7).

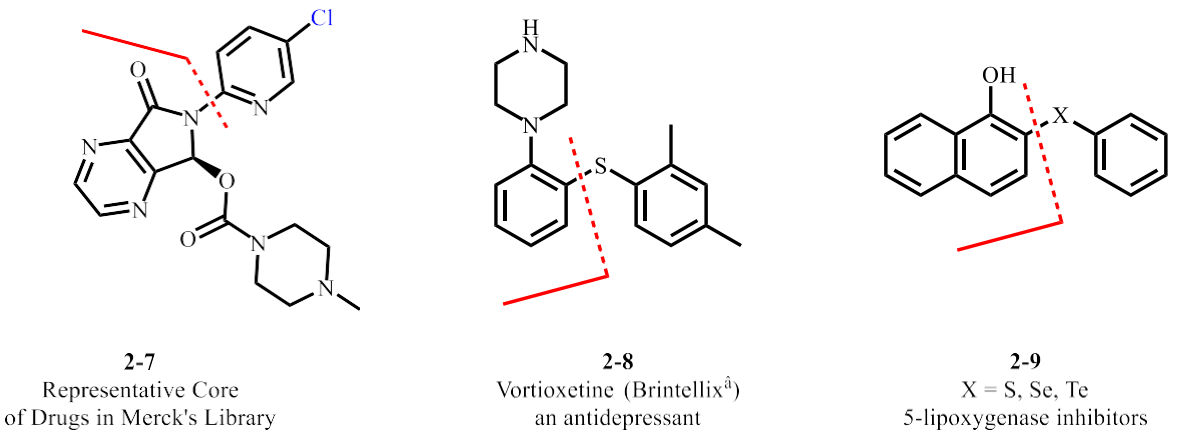

2-7
Representative Core
of Drugs in Merck's Library

2-8
Vortioxetine (Brintellix®)
an antidepressant

2-9
X = S, Se, Te
5-lipoxygenase inhibitors

Figure 2-7. Drug targets made from Chan-Lam reactions.

2.2.1.2 The Petasis Reaction

The Petasis reaction was developed in 1993 by Nicos Petasis and company.[42] These reactions typically involve the formation of a C–N and C–C using an amine, aldehyde, and boronic acid. Generally, this reaction is not catalyzed by a transition metal, however, there are cases in which palladium has been employed to promote the reaction, such as in the case of aryl sulfonamides, formaldehyde, and boronic acids. This process involves *in-situ* condensation of an amine with the aldehyde, forming an iminium ion followed by subsequent trapping by an aryl, alkyl or vinyl boronic acid (Figure 2-8).[43]

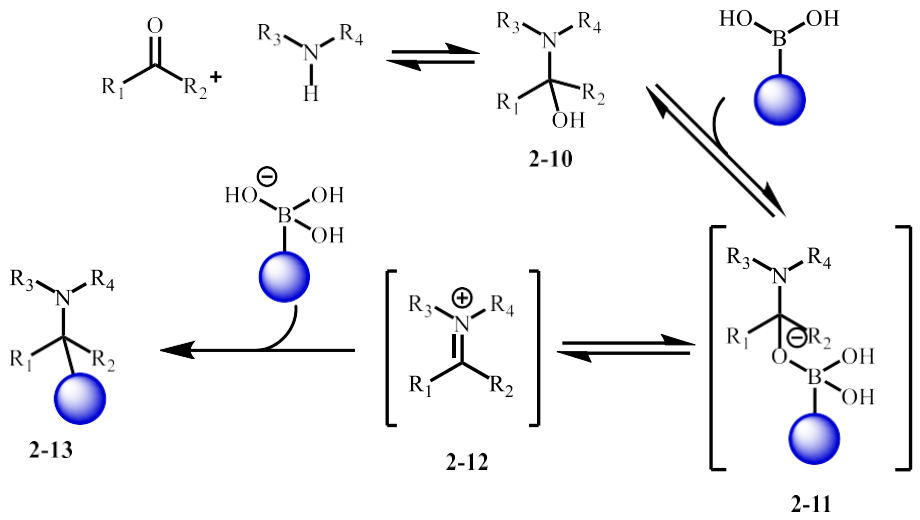

Figure 2-8. Mechanism for the Petasis reaction.

This reaction is attractive because it is generally executed without a transition metal, affords C–C bonds, is not particularly air-sensitive, and represents a base/acid free protocol that provides value added materials expediently from simply, highly diversifiable starting materials. Lastly, like in the case of the Chan-Lam reaction, the coupling partners that can be employed in these reactions are diverse in each category. A representative example comes from the Kilinski group in 2008, where they synthesized Clopidogrel in just two steps in 44% overall yield, thereby highlighting the ability of this three-component reaction for an expedited synthesis (Figure 2-9).

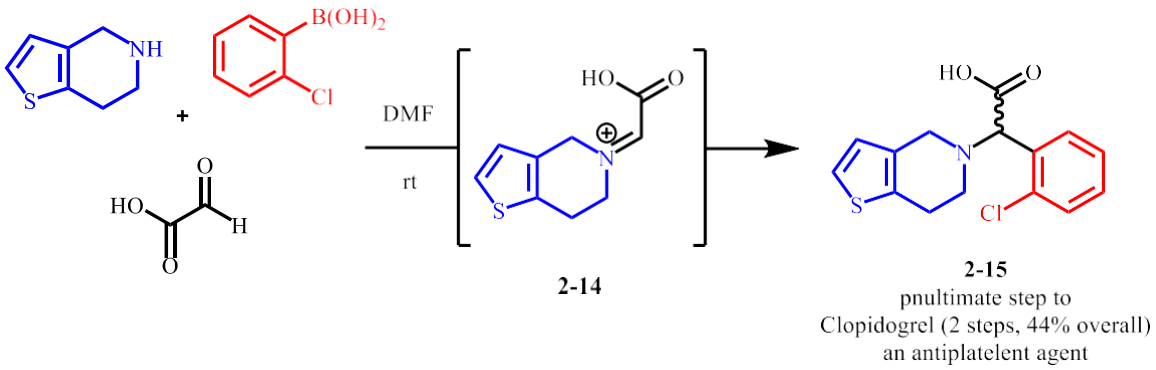

Figure 2-9. Expedient synthesis of an active pharmaceutical ingredient.

2.2.1.3 The Suzuki-Miyuara Reaction

The Suzuki reaction represents the one of the most common uses of boronic acids in both academia and in industry. Developed in 1979, and then later awarded the Nobel Prize in 2010, notable advantages of this reaction are the low catalyst loadings and the wide array of palladium catalyst systems that can be employed. For example, palladium on carbon is one such catalyst system, which does not require an exogenous ligand, greatly reducing the cost on scale. Relative to other coupling reactions, the solvent systems are environmentally friendly as combinations of water and an organic solvent such as ethanol, or ethereal solvents are common. Furthermore, these reactions are highly functional group tolerant and can typically yield synthetically useful quantities of product in short reaction times and at relatively low temperatures. Additionally, like the Chan-Lam reaction, a myriad of boronic acid derivatives can be engaged successfully in the coupling. The key difference being that in this reaction, the other coupling partner comes in the form of an electrophilic coupling partner, which have historically been aryl halides.

The Suzuki reaction easily accommodates a large array of functionalities and can be catalyzed by a large set of catalyst systems, making the reaction highly amenable to the generation of libraries of compounds and complex molecule synthesis. Some examples of complex targets that resulted in drug molecules can be found, below (Figure 2-10).[44]

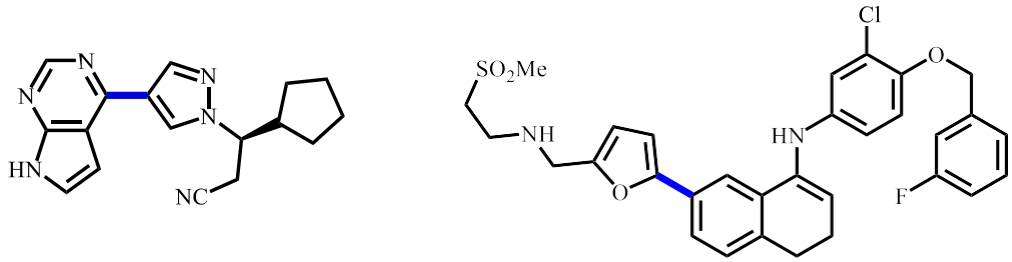

2-16
Ruxolitinib

2-17
Lapatinib

Figure 2-10. Therapeutics featuring a Suzuki-Miyuara as the critical step.

2.2.2 Utilization as Radical Precursors

In addition to being formidable nucleophilic coupling partners, aryl boronic acids can also serve as arene radical precursors. There are many more examples, however, these representative examples shall suffice for the purposes of this discussion. Aryl boronic acids can be converted to aryl radicals *in situ* by a variety of methods. These methods range from being metal-mediated to excitation with light using an organo-catalyst (Figure 2-11).[45–47]

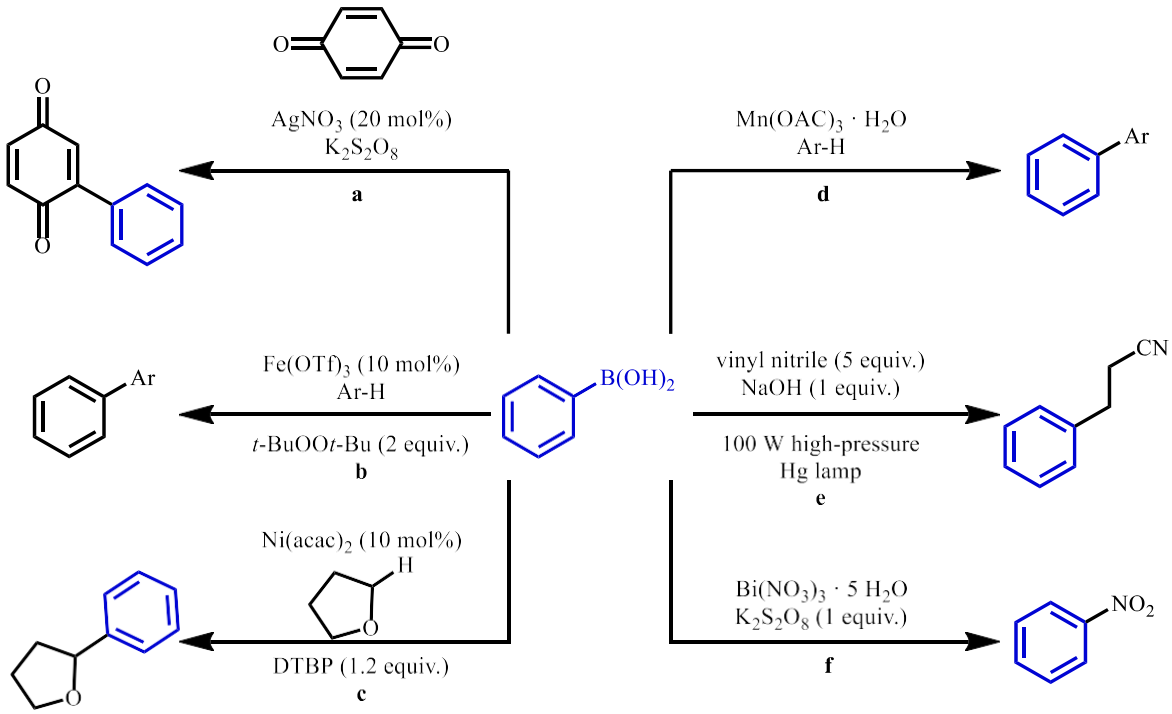

Complete Conditions: (a) $PhCF_3/H_2O$(1:1), 60 °C, 3-24 h, **(b)** 4,7-bis(4-(trifluoromethyl)phenyl) 1,10- phenanthroline (10 mol%), 80 °C, 24 h, **(c)** PPh_3 (10 mol%), K_3PO_4 (1 equiv.), 100 °C, 16 h, **(d)** reflux, 0.5 h, **(e)** 1, 10-phenanthroline (0.5 equiv.), dichlorobenzene (0.5 equiv.), CH_3CN/H_2O 9/1, **(f)** toluene, 80 °C, 12 h.

Figure 2-11. Aryl boronic acids as radical precursors in SET processes.

Boronic acids are well suited for the generation of organic radicals through the use of strongly oxidizing reagents. Lewis base first coordinates to the boronic acid to form a boronate.

Then, oxidation of this electron rich species yields a radical cation. This then decomposes to the aryl radical and a neutral boron species.

Aryl boronic acids and their derivatives represent a highly valuable class of compound due to their versatility in organic synthesis. They can be utilized in many transformations ranging from acting as a competent nucleophile in transition-metal catalyzed cross-coupling reactions, to serving as radical precursors in single electron transfer (SET) processes.

2.3 Synthesis of Aryl Boronic Acids

2.3.1 Traditional Synthesis of Aryl Boronic Acids

The first synthesis of an aryl boronic acid was achieved in 1880 by Michaelis and Becker.[38] While this synthesis did indeed afford the desired material, it had several limitations which largely concerned the sourcing of the starting materials. The production of boron trichloride at the time was conducted by the burning of amorphous boron in the presence of chlorine gas (Figure 2-12). Meanwhile, the utilization of diphenyl mercury is not attractive either given the perils of mercury poisoning, and finally the added steps required to reach the desired product.

2-18

Figure 2-12. First reported synthesis of an aryl boronic acid.

Following this initial report, in 1909, Grignard reagents emerged as an alternative method to form aryl boronic acids without the use of mercury. Additionally, the utilization of trialkoxyboranes typically used in these reactions has the advantage of being sourced from borax, which is a cheap, commercially available reagent that is easy to handle (Figure 2-13).[48] Some

drawbacks of this method, however, are that a Grignard must be pre-formed, and that over arylation is possible, in addition to the fact that Grignards display very low functional group compatibility.

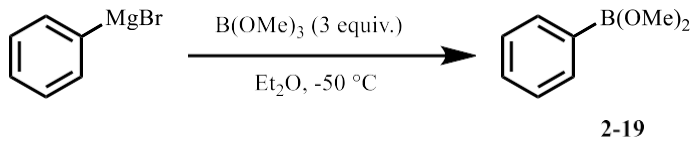

2-19

Figure 2-13. Synthesis of aryl boronic acid derivatives via Grignard reagents.

In 1986, the Haubold group provided and alternative protocol which utilized aryl silanes, which circumnavigated the use of Grignard reagents (Figure 2-14).[49] Additionally, the employment of tribromoborane as the boron source eliminated the previous need to utilize stannanes for the analogous coupling. However, these conditions are still rather harsh, necessitating further exploration in the synthesis of aryl boronic acids.

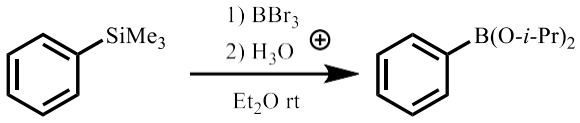

2-20

Figure 2-14. Aryl boronic acid derivatizes from aryl silanes.

Although these previous methods had certain advantages, there was still room for improvement. To address some of these limitations, Brown developed a lithiation protocol in 1983 (Figure 2-15).[49] While *n*-BuLi is a strong base, it is a highly efficient reagent and is regarded as a reliable standard for such transformations. This is in part, because the *n*-BuLi byproducts are volatile gases, which give clean reaction profiles. Also examined in this work was the effect of the sterics surrounding the alkoxyborane and how that related to over-arylation.

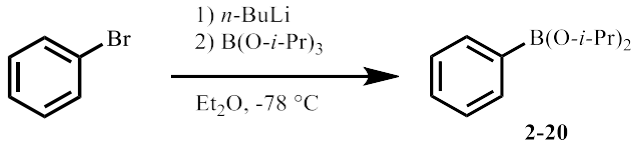

Figure 2-15. Lithiation of aryl bromides to provide aryl boronic acid derivatives.

Ultimately, they empirically found that tri-isopropyl borate provided excellent yields (>90%) of the desired product. Once the aryl borate is in hand, it can be hydrolyzed to the boronic acids, converted to trifluoro potassium salts, or undergo substitution with various diols to afford aryl boronic acid esters. To this day, this protocol serves as the foundation for how aryl boronic acids are synthesized.

2.3.2 Modern Approaches for the Synthesis of Aryl Boronic Acids

While lithiation chemistry is an effective strategy for the synthesis of aryl boronic acid derivatives, limitations regarding functional group tolerance, the use of stoichiometric base, and safety concerns are still problematic. Therefore, in the past 30 years, a tremendous effort has been dedicated to developing alternative strategies to achieve the synthesis of this quintessential class of nucleophilic coupling partner. Largely, these efforts have been encompassed by transition-metal catalyzed coupling reactions of aryl electrophiles and nucleophilic boron species. In addition, several radical pathways mediated by photochemical and electrochemical methodologies have been developed, as well.

2.3.2.1 The Miyuara-Suzuki Borylation

Discovered in 1995 by the Miyuara group, the borylation of aryl halides and pseudohalides using palladium catalysis and diboron reagents and related protocols have encompassed one of the most widely utilized pathways to synthesize aryl boronic acid derivatives in a catalytic matter (Figure 2-16).[50]

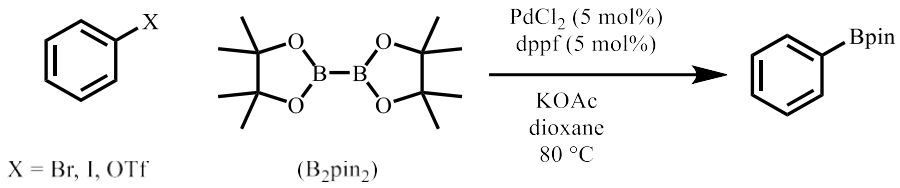

Figure 2-16. Miyuara borylation of aryl halides via palladium catalysis.

Miyuara borylation reactions are typically mediated by a palladium catalyst, which performs oxidative addition on an aryl electrophile such as a halide, or pseudohalide (Figure 2-17). Stoichiometric quantities of Lewis base then serve to activate the diboron source towards transmetallation. Reductive elimination then affords the desired aryl boronic acid ester species.

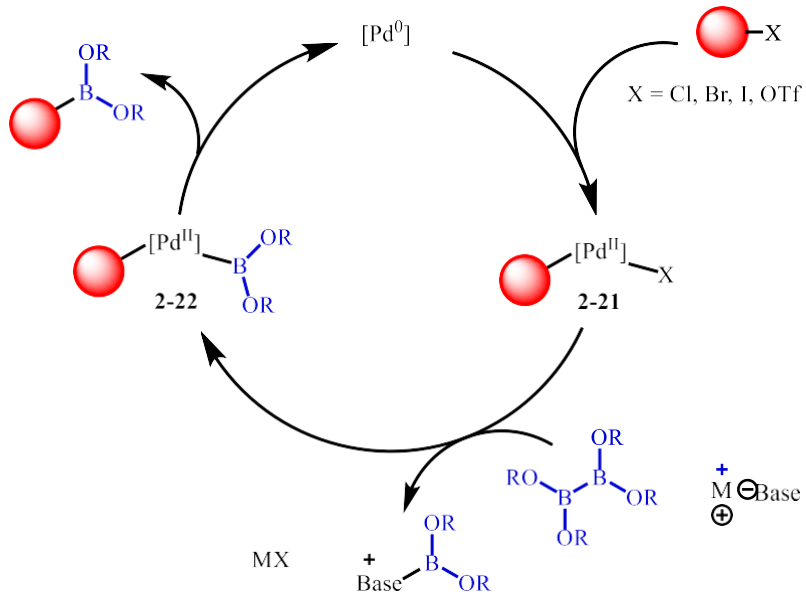

Figure 2-17. Mechanism for a generic Miyuara-Suzuki borylation.

Later on, Murata discovered that the more affordable pinacol borane (HBpin)[14] boron source could be used as opposed to the diboron, bis(pinacolato)diboron (B_2pin_2). This greatly enhanced both the atom economy and affordability of the reaction. Importantly, this reaction tolerates a broad array of functionalities, making it amenable to the expedient synthesis of complex

molecules. Some potential drawbacks of this method, however, are that these conditions are similar to Suzuki-Miyuara couplings, and so the resulting biphenyl byproducts can sometimes be observed. However, this is typically not an issue so long as the borylation reagent is more nucleophilic, and/or present in higher concentrations than the resulting aryl boronic ester. The other major byproduct that is typically observed results from protodeboronation of the desired product, or the borylation reagent, itself. However, these issues are typically well resolved during the optimization process.

In addition to diboron species and HBpin that are commonly used, aminoboranes can be utilized in these couplings too, as discovered by the Vaultier group in 2003 (Figure 2-18).[51]

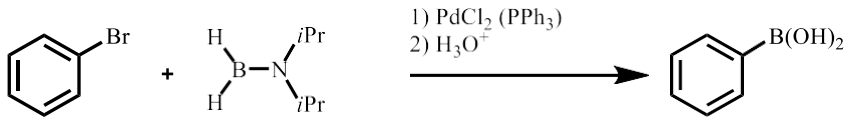

Figure 2-18. Borylation of aryl halides via aminoboranes.

Otherwise, identical from the Miyuara borylation, the utilization of the aminoboranes provides a convenient alternative to the employment of diboron reagents. The resulting aryl(dialkylamino)boranes can then by hydrolyzed under mildly acidic conditions to provide the corresponding aryl boronic acids in excellent yields.

Since their discovery in 1995, several other protocols inspired by the Miyuara group have been reported. The variations on the theme tend to involve the invention of base-free borylations, protocols that are catalyzed by base-metals, and/or detailing the employment of other classes of aryl electrophile.[52]

2.3.2.2 Borylation via C─H Activation

An equally important strategy to borylate compounds involves C─H activation as pioneered and popularized largely by Hartwig and co-workers.[53,54,55] A major advantage of C─H activation is that pre-functionalization of the parent arene is not required as the C─H bond, itself, serves as the electrophilic position. This work initially involved the borylation of alkanes but was soon extended to the stoichiometric borylation of arenes by pre-formed iron complexes. These iron complexes could then be irradiated in the presence of arenes to afford good yields of aryl boronic esters (Figure 2-19).[56]

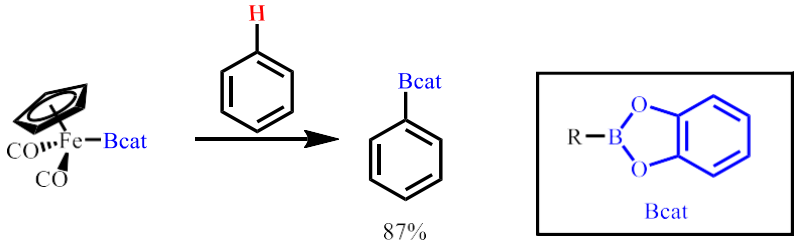

Figure 2-19. Seminal borylation of arenes via C–H functionalization.

However, selectivity issues become problematic on substituted arenes, such as toluene, where regiocontrol is often poor and directing groups are required. Furthermore, catalytic methods to perform these transformations would be greatly preferred. Hartwig and co-workers, were able to achieve both of these aims through the employment of an iridium catalyst featuring highly predictable regioselectivity outcomes with exquisite site-selectivity could be achieved especially in the case of heteroarenes (Figure 2-20).[57]

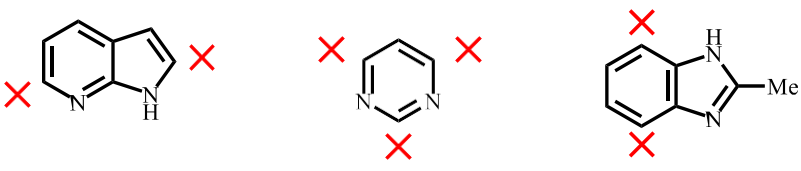

2-23 **2-24** **2-25**

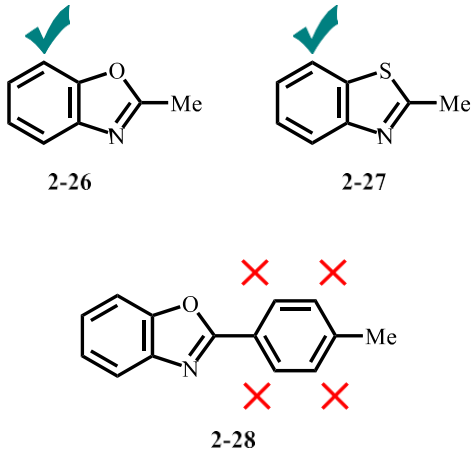

Figure 2-20. Trends regarding regioselectivity outcomes in the C─H borylation of heteroarenes. The red X indicates no borylation and the green checkmark represents preferred sites of borylation based upon empirical findings.

A culmination of many studies revealed that C─H borylation *ortho* and alpha to free N─H or basic nitrogen atoms were never observed. In contrast, borylation occurs preferentially at positions *ortho* to oxygen, or sulfur over less-activated positions. Lastly, though electronics play an integral role in determining regioselectivity, sterics are still of import and borylation preferentially occurs away from sites featuring *ortho* substitution. In recent years, several groups have contributed to developing C─H borylation strategies that do not rely upon precious metals like iridium.[58]

These guidelines are excellent for making informed synthetic decisions. Even so, C─H borylation is not adequate to address every possible synthetic challenge and as such, those such gaps wherein selectivity is an issue can be addressed in a complementary fashion by protocols that utilize pre-functionalized scaffolds.

2.3.2.3 Borylation via Radical Processes

The other main strategy by which aryl boronic acids are synthesized comes in the form of radical processes that are mediated either electrochemically, or by light. In this section, a

representative example of each borylation protocol will be featured accompanied by the advantages and disadvantages of each strategy.

2.3.2.3.1 Electrochemical Borylation

Electrochemical reactions, in general, are an attractive means to synthesize molecules, because they can be done at large scales and embody many of the principles of green chemistry, which has been defined as "…the utilization of a series of principles that reduce or eliminate the use or generation of dangerous substances during the design, fabrication, or application of chemical products."[59] Electrochemistry meets the following criterion of this definition being that 1) electrons are intrinsically clean reagents, 2) room temperature is generally suitable, which cuts on energy demands and reduces the chances of dangerous, run away reactions, 3) low volatility solvents can be used such as ionic liquids, which reduce the risk of atmospheric contamination, and 4) the heterogeneity of the catalysts ensures easy separation from products, which permits catalysts to be easily reusable and product to be free of undesired metal contamination. From an operational standpoint, the reaction setups are typically simple and can be far less expensive to implement than other techniques, such as in the case of non-electrochemically mediated reactions conducted in batch reactors.[59] For these reasons, combined with the utility of aryl boronic acids, Fangyang and co-workers were interested in developing an electrochemical procedure to convert aryl iodides into aryl boronic acid pinacol esters (Figure 2-21).[60]

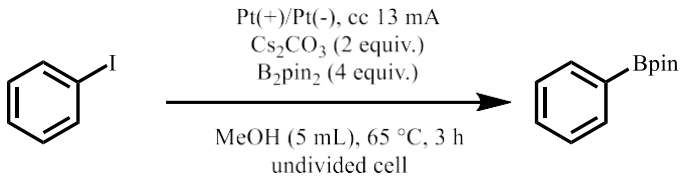

Figure 2-21. Electrochemical mediated conversion of aryl iodides to aryl boronic acid pinacol esters.

The method possessed a good substratrate scope, wherein substrates bearing both electron withdrawing and donating substituents converted to desired product in moderate to good yields. Based upon electron paramagnetic resonance (EPR), cyclic voltametry (CV), and differential pulse voltammetry (DPV) experiments in conjunction with the support of relevant literature, the authors propose that the reaction begins with the reduction of the aryl iodide to the radical anion (Figure 2-22) This fragments to provide aryl radical and the iodide anion. The aryl radical can then coordinate to the p-orbital of a boron of the diboron species. Lewis base then forms the boronate species. This species fragments to yield desired product and a radical anion, which is then oxidized through a SET process.

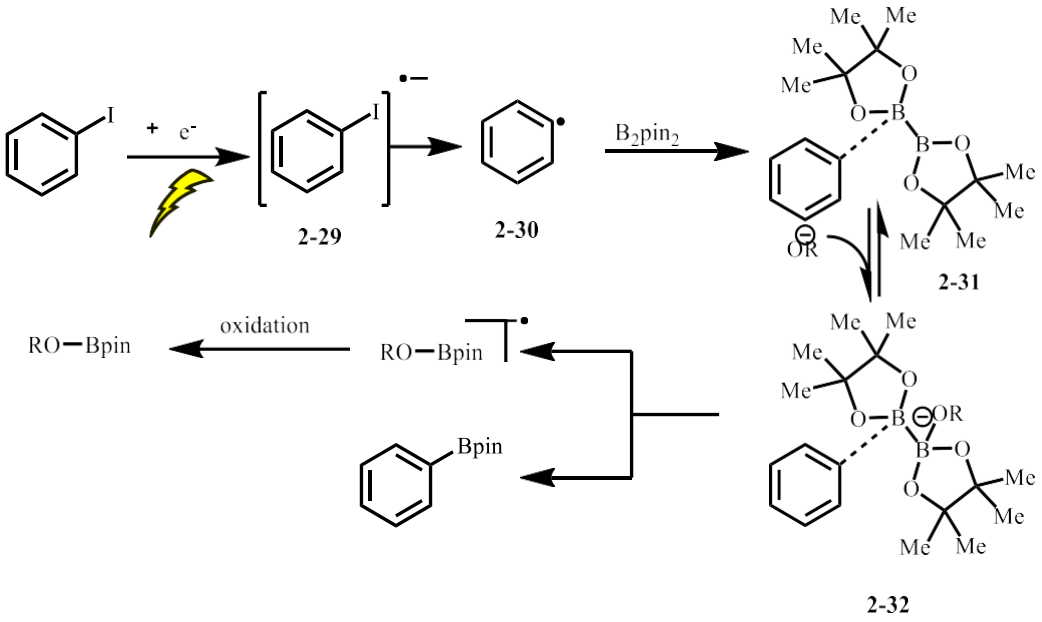

Figure 2-22. Mechanism for the electrochemical conversion of aryl iodides to aryl boronic acid pinacol esters.

2.3.2.3.2 Photoredox Mediated Borylation

Although not as scalable as electrochemically mediated reactions, at least not in batch, photochemical strategies for the synthesis of organic molecules also meet many of the pre-

requisites for representing a green protocol. One such example of this is in the conversion of aryl phosphates, halides, and tetramethyl ammonium salts into aryl boronic acid esters by Oleg Larionov and co-workers (Figure 2-23).[29] An additional benefit of the chemistry is that it is transition metal free and conducted either at room temperature, thus requiring no additional input of energy. The scope of the reaction is impressively broad encompassing a large array of functionality and heterocycles across over 50 examples. Notably, the same conditions, save for minor adjustments, accommodate each aryl electrophile merely by adjusting to the appropriate wavelength.

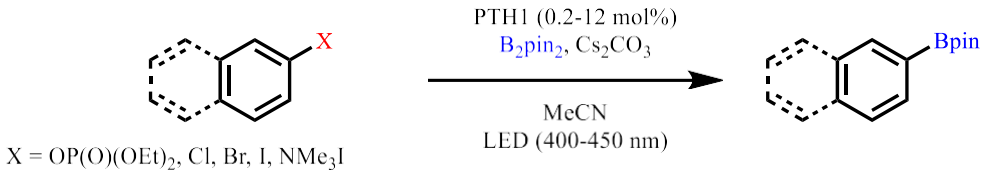

Figure 2-23. Photoredox method to convert aryl electrophiles to aryl boronic acid pinacol esters.

A variety of mechanistic studies were conducted, which encompass data from radical clock, nuclear magnetic resonance (NMR), fluorescence quenching, and density functional theory (DFT) experiments, which in conjunction with the literature, led the authors to propose the following mechanism (Figure 2-24). When the photocatalyst bonded to carbonate via hydrogen bonding is subjected to ultraviolet light (*hv*), it reaches an excited singlet state. Once in the singlet excited state, the aryl phosphonate is reduced by the photocatalyst, forming a radical anion and the oxidized photocatalyst via proton coupled electron transfer. The radical anion then decomposes into the phosphonate anion and the aryl radical, which abstracts a Bpin from B_2pin_2 resulting in the desired product and a radical Bpin species. The addition of base creates a radical anion, which can then be oxidized by the photocatalyst, thus completing the catalytic cycle.

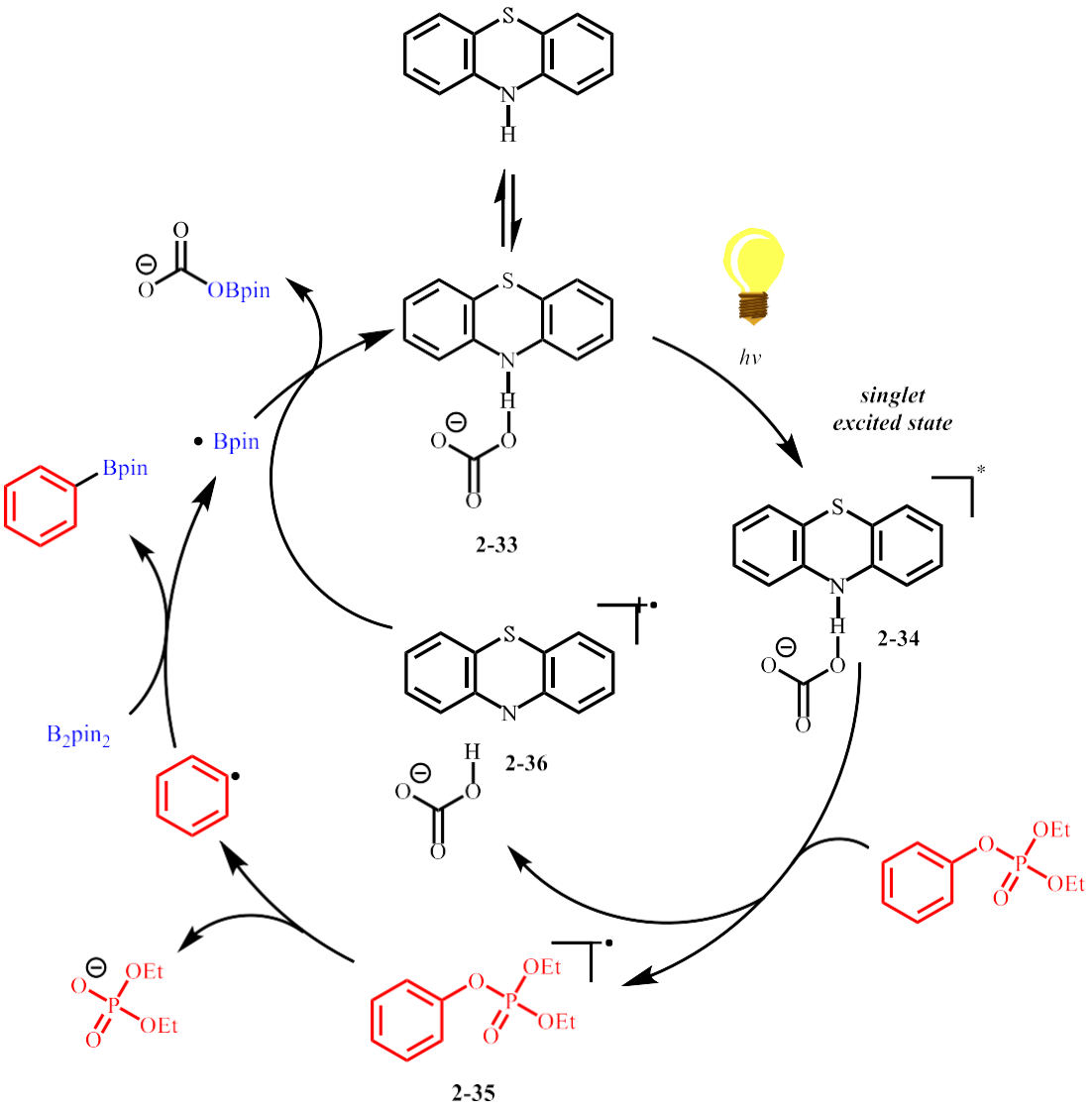

Figure 2-24. Mechanism for the photoredox mediated conversion of aryl electrophiles to aryl boronic acid pinacol esters.

2.3.3 Summary of synthesis of aryl boronic acid derivatives

Miyuara-Suzuki reactions, C–H functionalization, and radical mediated pathways create a triumvirate of paradigms by which to synthesis aryl boronic acid derivatives. Though powerful,

room still exists for further development as each overarching strategy has its limitations. C–H functionalization has many advantages, one of the most impressive being that lack of need for pre-functionalization, however, in cases where regioselectivity outcomes become burdensome to overcome, pre-functionalization returns to being an attractive alternative, once again. Along this vein, the Miyuara-Suzuki reaction would then be the heir apparent as methods under this manifold are excellent in affording aryl boronic acid esters from aryl halides and pseudohalides. However, less reactive C–O bonds are traditionally excluded and are just more recently being explored. Visible light provides an entry way to incorporate challenging to functionalize phenol derivatives like phosphonates in radical processes. While many aryl electrophiles can be tolerated, they must be amenable to reduction via SET processes. As such, silyloxyarenes represent an ideal agent to fill this gap as they 1) provide an entry way for the introduction of low-reactivity C–O electrophiles, which possess orthogonal reactivity to aryl halides and pseudohalides traditionally used in Miyuara-Suzuki couplings and 2) they also provide orthogonal to methods that employ visible light as they are not vulnerable to reduction via SET processes (Figure 2-25).

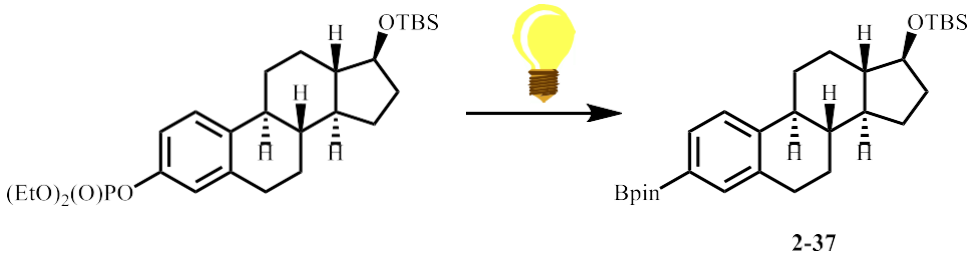

2-37

Figure 2-25. Example of orthogonality between a phosphonate C–O bond and a silyl ether C–O bond.

2.4 Borylation of Low-Reactivity C–O Electrophiles

2.4.1 Borylation of Low-Reactivity C(sp^2)─O Bonds

As previously discussed, phenols represent an attractive entry into aryl electrophiles. Due to their accumulation abundant feedstocks, and because of their wide range of reactivity, which can be fine-tuned by the introduction of various protecting groups (Figure 2-26).[6,32,34]

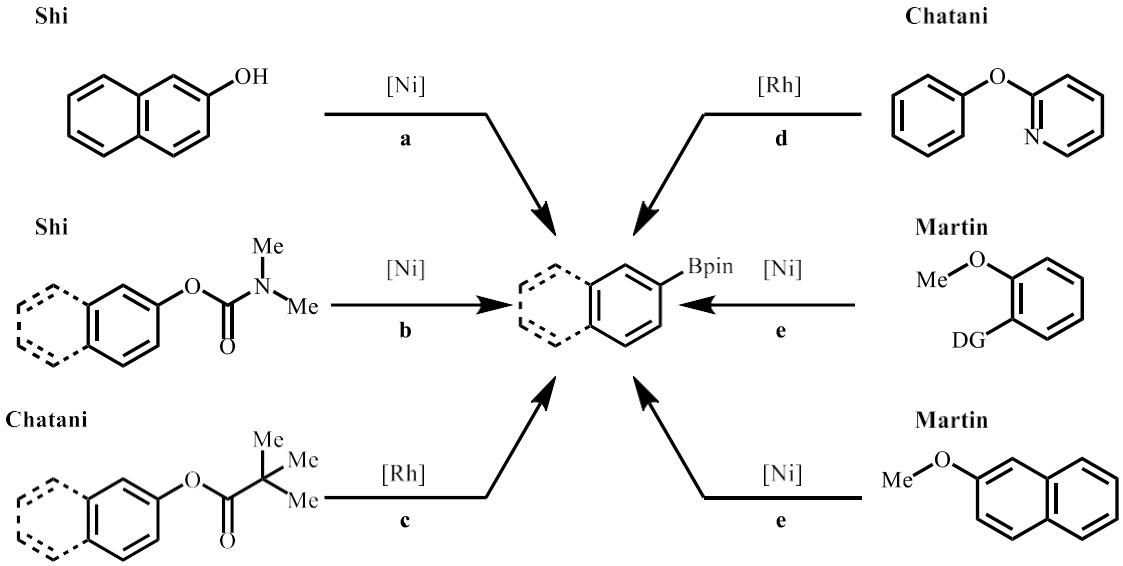

Complete Conditions: a) $Ni(COD)_2$ (10 mol%), IAd (40 mol%), B_2pin_2 (2.0 equiv.), toluene, 90 °C, 12 h, **b)** $Ni(PCy_3)_2Cl_2$ (5 mol%), K_3PO_4 or NaO-*t*-Bu (1.0 equiv.), B_2nep_2, toluene/DME (1/1), 100 °C, **c)** $[RhCl(COD)]_2$ (10 mol%), $P(4\text{-}MeOC_6H_4)_3$ (0.6 equiv.), B_2nep_2, toluene, 130 °C, **d)** $[RhCl(COD)]_2$ (5 mol%), ligand (10 mol%), PCy_3, $IMes^{Me}$, or $IMXy^{Me}$ (10 mol%), B_2pin_2, toluene, 100-160 °C, **e)** $Ni(COD)_2$ (10 mol%), PCy_3 (20 mol%), B_2nep_2 (2 equiv.), CsF (3.0 equiv.), toluene, 95 - 120 °C.

Figure 2-26. Synthetic approaches to access aryl boronic acid derivatives from inert C–O electrophiles.

Shi and co-workers demonstrated that the direct conversion of naphthalen-2-ol to the desired boronic acid pinacol ester in moderate yield. Unfortunately, further attempts to optimize the reaction were unsuccessful and this stands as a single example. However, by protection with an adequate functional group, various phenol derivatives have undergone successful borylation. The Shi group also demonstrated that aryl carbamates could be borylated using a nickel catalyst in

the presence of either tribasic potassium phosphate, or *tert*-butoxide bases, which serve to activate the diboron species. Notably, the C─N bond can also be leveraged for cross coupling reactions, however, in this case amongst others, exclusive reactivity with the C(sp^2)─O bond is observed. Although the reaction possesses an impressive substrate scope and can tolerate various functionalities, isolated aromatic systems require over 48 h to observe appreciable yields.

Although borylations of allylic pivalates is known to be catalyzed by nickel, the only known report of borylation of aryl pivalates utilizes a rhodium catalyst. Despite high reaction temperatures, the reaction was competent at producing desired product in high yields in the cases wherein naphthyl systems were employed. However, isolated aromatic systems were not well tolerated, which can be explained by the naphthyl problem as outlined in chapter 1. Chatani and co-workers were able to observe moderate yield of an alkenyl pivalate. Gratifyingly, they were able to demonstrate that a naphthalene-based scaffold hosting a bromide and pivalate could be sequentially couple with high reactivity in the presence of each other and a methyl ether.

Pyridyl ethers have found use as another low-reactivity C─O electrophile that can be used to install boronic esters from phenols. These are attractive substrates, because pyridyl ethers are commonly utilized as directing groups in C─H functionalization reactions, setting the stage for functionalization preceding the interconversion of the ethereal bond. In that same manor, they can aid in the activation of the adjacent aryl C─O bond resulting in borylation and effectively, serve as a traceless directing group for C─H functionalization of aryl boronic esters.

Lastly, despite their resilience to transition metal activation, methyl ethers have also been employed are aryl electrophiles in nickel-catalyzed borylations by the Martin group. This work demonstrated the viability of inert C─O bonds as being competent electrophiles in cross-coupling reactions, particularly in the transformation of aryl methyl ethers to aryl boronic esters. By

switching the identity of the coupling partner, they were able to successfully to install either boronic acid pinacol, or neopentyl esters. One limitation that is typically true in inert C─O bond functionalization is that this reaction is largely limited to naphthyl systems. However, they were able to overcome the innate lack of reactivity by employing *ortho*-directing groups in some cases.

2.4.2 Borylation of Inert C(sp^3)─O Bonds

In addition to the borylation of inert aryl C─O electrophiles, benzyl functionalities can be borylated, as well. Unlike the borylation of phenols, which must be pre-activated with a protecting group, borylation of benzyl alcohols can sometimes be conducted directly from the alcohol (Figure 2-27).[61]

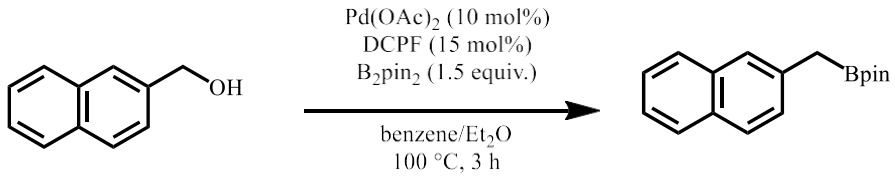

Figure 2-27. Palladium catalyzed borylation of napththyl methanols.

These reactions are highly efficient and more attractively, do not require exogenous base. It is hypothesized that the alcohol, itself, plays an integral role in not only activating the diboron species, but in docking the metal. Interestingly, they observe excellent selectivity for this process, despite the possible side products that could be formed, such as those resulting from the aldehyde, being formed from coordination of benzyl alcohol to the metal and subsequent β-hydride elimination.

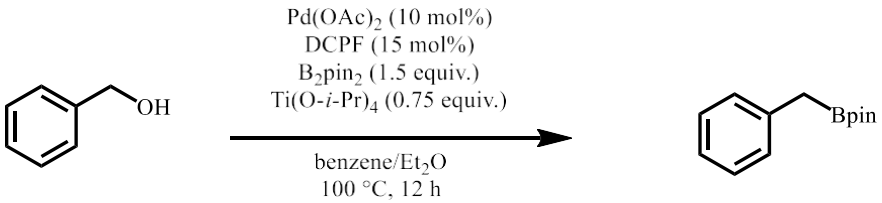

Figure 2-28. Palladium catalyzed borylation of benzyl alcohols with the assistance of a Lewis acid.

Although the stated reaction conditions (Figure 2-27) were only able to functionalize naphthyl benzyl alcohols, Ti(O-*i*-Pr)$_4$ could be employed as a Lewis acid in sub-stoichiometric quantities to overcome the difficulties of C–O activation leading to the inclusion of isolated aromatics (Figure 2-28).[61]

Refreshingly, an alternative protocol to functionalize benzyl alcohols can be accomplished by a more abundant, environmentally friendly catalyst in copper (Figure 2-29).[62] They too employ Ti(O-*i*-Pr)$_4$ as a Lewis acid activator and are able to isolate high yields of the desired product, including those that do not contain extended π-systems.

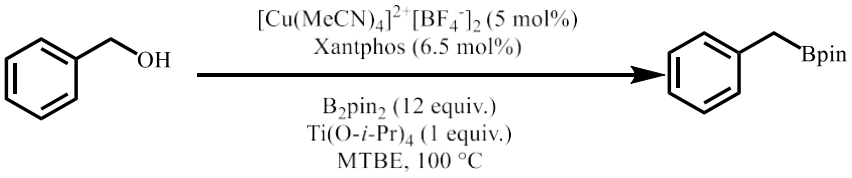

Figure 2-29. Copper catalyzed borylation of benzyl alcohols with the assistance of a Lewis acid.

Borylations featuring a simple acetyl protecting group are exceedingly rare, presumably due to the lessened stability to Lewis bases, which are typically required to promote activation of the diboron species (Figure 2-30).[63]

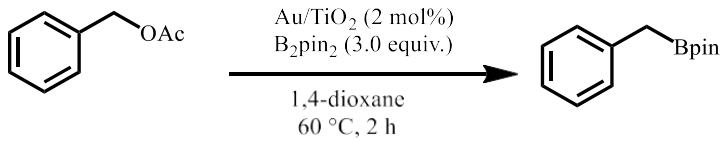

Figure 2-30. Gold-Titanium salt catalyzed borylation of benzyl alcohols.

In this case, no exogenous base is required, however, as the acetate, itself, is sufficient to activate the diboron species following C─O bond cleavage (Figure 2-31).

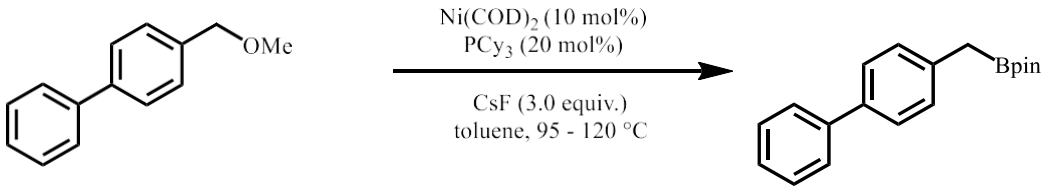

Figure 2-31. Nickel catalyzed borylation of benzyl methyl ethers.

In the same report as the borylation of aryl methyl ethers, the Martin group discovered that their reaction conditions were also amenable to the conversion of benzyl methyl ethers to boronic acid pinacol esters (Figure 2-32).[34] Excitingly, they are able to afford several naphthalene systems, including one with α-substitution, which opens the door for enantiospecific couplings of enantiopure benzyl methyl ethers.

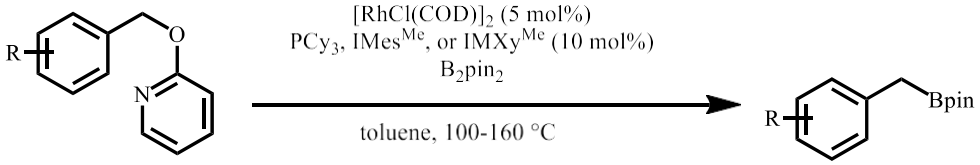

Figure 2-32. Rhodium catalyzed borylation of benzyl pyridyl ethers.

Finally, benzyl pyridyl ethers can also be deoxygenated to form the corresponding benzylic boronic acid pinacol esters in a similar fashion to their aryl counterparts under rhodium catalysis and elevated temperatures (Figure 2-32).[64]

2.4.3 Summary of Ipso-Borylation of Low-Reactivity C–O Bonds via Transition Metal Catalysis

Valuable work has been conducted regarding functional group interconversion strategies of inert C–O electrophiles spanning from ethers, to esters, to carbamates. Although these advances have represented significant progress in the field, the common denominator of many of these reactions is the limitation of being restricted largely to naphthyl systems. While some electrophiles, such as carbamates, permit the use of isolated aromatic systems, they often require elevated temperatures and prolonged reaction times. One potential alterative to using carbamates to activate C–O bonds is to utilize an alternative functional group that provides higher stability than a pivalate, but greater reactivity than an amide. While silyloxyarenes are inert to a number of transformations, they still possess a reactivity profile that permits the functionalization of isolated aromatic scaffolds without the presence of directing groups, or electronic biases.[12,13]

2.5 Results and Discussion

2.5.1 Optimization of the Nickel-Catalyzed *Ipso*-Borylation of Silyloxyarenes

Optimization efforts utilizing a *tert*-butyldimethyl silane (TBS)-protected substrate were first conducted based on our previous studies of silyloxyarene aminations and reductions, wherein electron rich Ni-NHC catalyst systems were shown to be effective in conjunction with *tert*-butoxide bases in toluene. $Cu(OAc)_2$ was essential to obtain appreciable yields of desired product, which we hypothesize aids in the transmetallation step (Figure 2-33).[12,13,65]

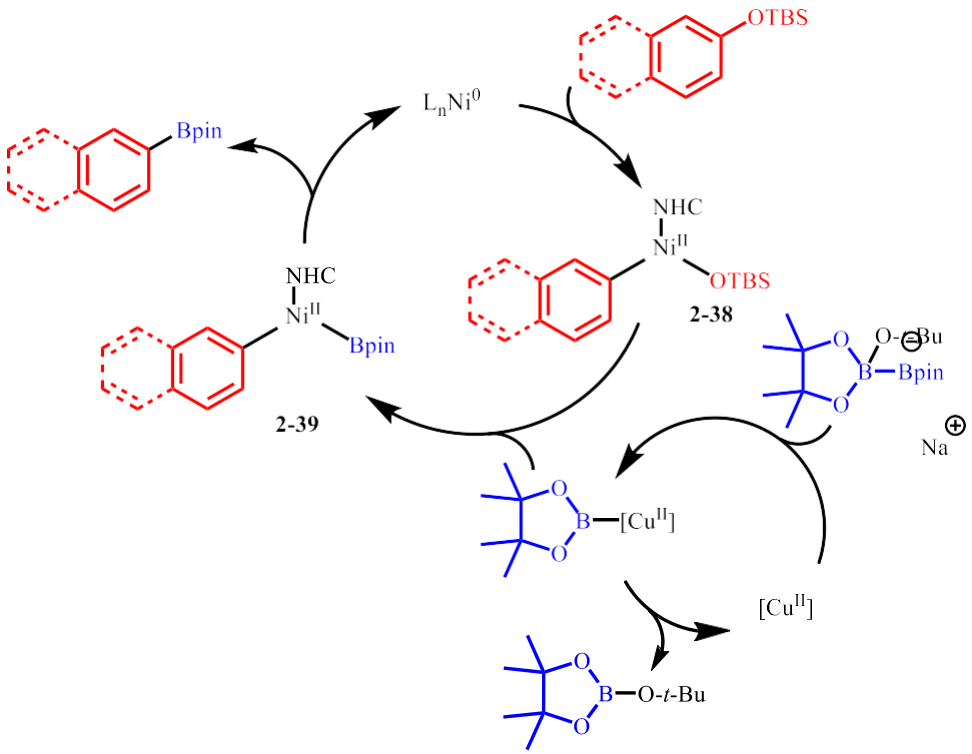

Figure 2-33. Initial proposed mechanism for the nickel catalyzed borylation of silyloxyarenes.

Under these conditions, however, modest yields and over-borylation of the desired product provided a mixture of regioisomers (Figure 2-34) along with borylation of the toluene solvent were observed.[66,67]

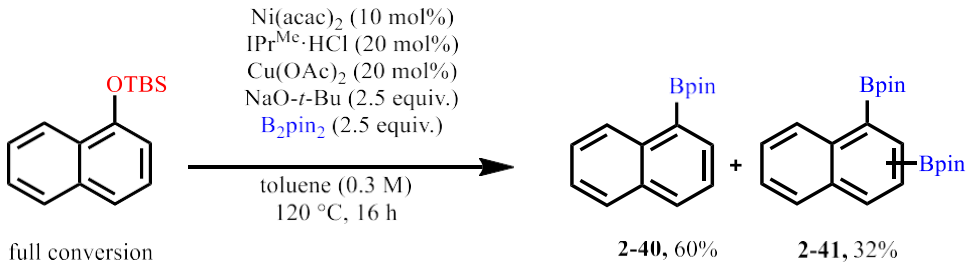

Figure 2-34. Preliminary hit for the nickel catalyzed borylation of silyloxyarenes.

Further optimization was conducted with a silylated 3-phenylphenol derivative as the model substrate, as we anticipated that optimization around this substrate would address the challenges of C–O activations in biphenyls and isolated aromatic systems. To eliminate side product formation resulting from the borylation of solvent, non-arene solvents were investigated, beginning with ethereal solvents that matched the boiling point profile for the requisite reaction temperature (entries 1-2, Table 2-1). The utilization of cyclopentyl methyl ether (CPME) as the solvent greatly enhanced the yield of the desired product and eliminated solvent-derived side products. Furthermore, it was found that in this solvent, $Cu(OAc)_2$ was no longer required to promote the reaction, though it did not hinder yields (entry 3, Table 2-1).

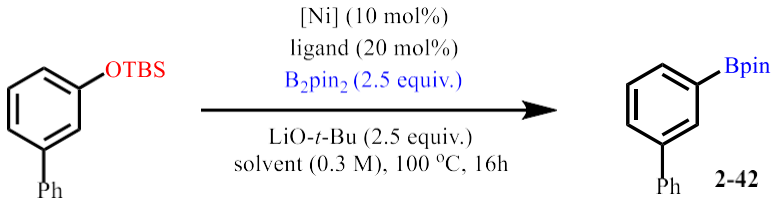

entry	metal	ligand	yield[a]
1	$Ni(acac)_2$	IPr^{Me}•HCl	32%[b]

2	$Ni(acac)_2$	IPr^{Me}•HCl	82%[c]
3	$Ni(acac)_2$	IPr^{Me}•HCl	80%
4	$NiBr_2$	IPr^{Me}•HCl	49%
5	$Ni(COD)_2$	IPr^{Me}•HCl	48%
6	$Ni(acac)_2$	PCy_3	NP
7	$Ni(PPh_3)_2Cl_2$	NA	NP
8	$Ni(acac)_2$	ICy•HCl	Trace
9	$Ni(acac)_2$	IAd•HCl	NP
10	$Ni(acac)_2$	IMes•HCl	8%
11	$Ni(acac)_2$	$IMes^{Me}$•HCl	14%
12	$Ni(acac)_2$	IPr^{*OMe}•HCl	5%
13	$Ni(acac)_2$	IPr•HCl	57%

Table 2-1. Re-optimization for the Ipso-borylation of silyloxyarenes with isolated aromatics. [a] Yields were determined by ^1H NMR analysis using CH_2Br_2 as an internal standard. [b] Dioxane used instead of CPME. [c] $Cu(OAc)_2$ (20 mol%) used as an additive. [d] NaO-*t*-Bu used instead of LiO-*t*-Bu. [e] B_2pin_2 (2.0equiv.) and LiO-*t*-Bu (2.0 equiv.) used instead of B_2pin_2 (2.5 equiv.) and LiO-*t*-Bu (2.5 equiv.). [f] B_2pin_2 (3.0 equiv.) and LiO-*t*-Bu (3.0 equiv.) used instead of B_2pin_2 (2.5 equiv.) and LiO-*t*-Bu (2.5 equiv.).

Representative Ni(0) and Ni(II) salts were screened, but were not found to be as effective as $Ni(acac)_2$ (entries 4-5, . Phosphine ligands were ineffective (entry 6-7, Table 2-1) whether $Ni(acac)_2$ was used, with the employment of a nickel pre-catalysts in $Ni(PPh_3)_2Cl_2$. This is consistent with other couplings of silyloxyarenes, wherein phosphine ligands are completely

ineffective.[12,13] When investigationg NHC ligands, it was found that NHCs with *n*-alkyl substituents did not effectively promote the reaction (entries 8-9, Table 2-1). However, *n*-arylated NHC ligands like IMes did provide some of the desired product and this yield could be enhanced by methylating the backbone of the NHC (entries 10-11, Table 2-1). Although IPr*^{OMe}•HCl had been effective in reductions of silyloxyarenes, it was not effective in the borylation reaction. (entry 12, Table 2-1). This is likely attributed to the enhanced steric bulk, which potentially inhibits the transmetallation step. A balance was struck between electron richness of the NHC and its steric profile in IPr•HCl (entry 13, Table 2-1). However, dimethylation of the NHC backbone was required in order to make the NHC electron rich enough to effectively promote the reaction as in the case of entry 3 (Table 2-1).

Having determined the ideal catalyst system and garnering an idea of an effective solvent system, other solvents, bases, and equivalents of diboron reagent and base were screened. Other ethereal solvents such as 1,4-dioxane and THF were examined and proved to be relatively ineffective as low yields were observed (entries 2-3, Table 2-2). A more polar solvent, such as acetonitrile, was tested with the hypothesis that the base would be more soluble and therefore more efficiently activate the diboron species, however, it was found that this completely inhibited the reaction (entry 4, Table 2-2). Alternatively, alkane solvents were tested, but to no avail (entry 5, Table 2-2). Consistent with previous couplings of silyloxyarenes, the choice of counterion of the base had a dramatic effect on the performance of the reaction.[65,68] The results indicated that LiO-*t*-Bu was optimal as NaO-*t*-Bu delivered product, albeit in slightly lower yields, and KO-*t*-Bu proved ineffective (entries 7-8, Table 2-2). *Tert*-butoxide bases have been used to access a highly electron-rich nickalate species *in-situ*, which can then conduct oxidative addition of the silyloxyarene, which might explain the unique reactivity observed with this class of reagent. It is

also possible that alkoxide bases play multiple roles in this reaction, such as the activation of the diboron species, and therefore other base additives were next examined (entries 9-12, Table 2-2). Ultimately, these multiple-base systems hindered the reaction in most cases, or resulted in compelet loss of reactivity, therefor LiO-*t*-Bu was utilized. Lastly, equivalents of B_2pin_2 were reduced to mitigate overborylation byproduct; however yields were greatly reduced, while increasing B_2pin_2 offered a neglible change in yield (entries 13-14, Table 2-2).

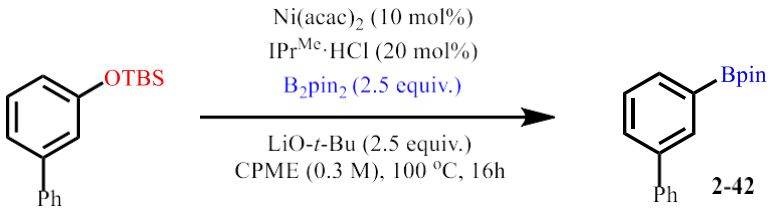

entry	variation	yield[a]
1	none	82%
2	1,4-dioxane for CPME	34%
3	THF for CPME	24%
4	acetonitrile for CPME	NP
5	*n*-heptane for CPME	NP
6	DCE for CPME	72%
7	NaO-*t*-Bu for LiO-*t*-Bu	72%
8	KO-*t*-Bu for LiO-*t*-Bu	32%
9	Add 0.5 equiv CsF	49%
10	Add 2.5 equiv NaOAc	41%
11	LHMDS for LiO-*t*-Bu	NP
12	Add 2.5 equiv Li_2CO_3	29%
13	2.0 equiv. of B_2pin_2 and base	41%

14	3.0 equiv. of B_2pin_2 and base	80%

Table 2-2. Solvent and base screening for the nickel catalyzed borylation of silyloxyarenes.

Finally, a short screening of aryl electrophiles was conducted to 1) determine if OSi(*t*-Bu)Me_2 was still the best silyl group for this transformation and 2) to see what other aryl electrophiles could be tolerated under the reaction conditions. Indeed, the -Si(*t*-Bu)Me_2 silyl group still provided the highest yields of desired products, with more sterically demanding silyl groups providing greatly diminishing yields and significant quantities of starting material (entries 1-3, Table 2-3).

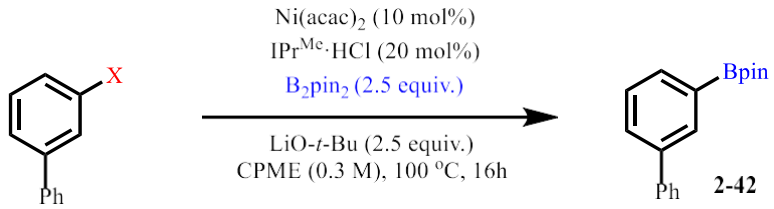

entry	variation	yield[a]
1	OSi(*t*-Bu)Me_2	82%
2	OSi(*i*-Pr)$_3$	61%[c]
3	OSi(*t*-Bu)Ph_2	64%
4	OMe	5%
5	OCON(Et)$_2$	76%
6	OPiv	trace
7	OTf	74%
8	F	72%

Table 2-3. Electrophile screening in the nickel catalyzed borylation of silyloxyarenes.

In the case of methyl ethers, mostly starting material was observed, which was not surprising as methyl ethers tend to require naphthyl systems in order to be activated and work best with phosphine ligands (entry 4,Table 2-3). Good reactivity was observed in the case of the carbamate, which proved to be robust under the reaction conditions (entry 5,

Table **2-3**). However, using pivalates did not result in the desired product, and in fact, much of the mass balance was deprotected starting material (entry 6,

Table **2-3**). Lastly, aryl triflates and fluorides were amenable to activation under these conditions (entries 7-8,

Table **2-3**). From these data, we can conclude that arenes containing a silyloxyarene and a methyl ether could be coupled with exquisite selectivity on this scaffold, favoring functionalization of the silyloxyarene. However, other aryl electrophiles would provide competing side reactivity under these conditions. Therefore, a different catalyst system would need to be employed to see high selectivity in a sequential coupling. This could be achieved merely by not using NHC ligands in the IMes, or IPr series.

2.5.2 Substrate Scope for the Nickel Catalyzed *Ipso*-Borylation of Silyloxyarenes

With optimized conditions in hand, the scope for the ipso-borylation of silyloxyarenes was explored (Table 2-4). The substrate scope of this transformation was quite broad, providing good to excellent yields for a variety of silyloxyarenes without deviating from the standard conditions, and in no cases was Suzuki byproduct derived from further reaction of the aryl Bpin observed. For naphthyl and biphenyl systems, full conversion was generally observed, wherein the remaining mass-balance could be accounted for by over-borylation of the desired product, resulting in a

mixture of regioisomers. Unfortunately, optimization efforts did not improve conversion of starting material to desired product, however, it is worth noting that borylation can be achieved at both the 1- and 2-position of the naphthyl (compounds **2-40** and **2-43**, Table 2-4). A more favorable product distribution was observed in the case of the less activated biphenyl (compound **2-42**, Table 2-4) systems, although reduced yields due to over-borylation were still observed to some extent. A biphenyl system possessing substitution at the 4-position proved to be less susceptible to this issue, providing excellent yield of the desired product, likely due to the substrate inhibiting over-borylation due to its increased steric profile (compound **2-44**, Table 2-4).

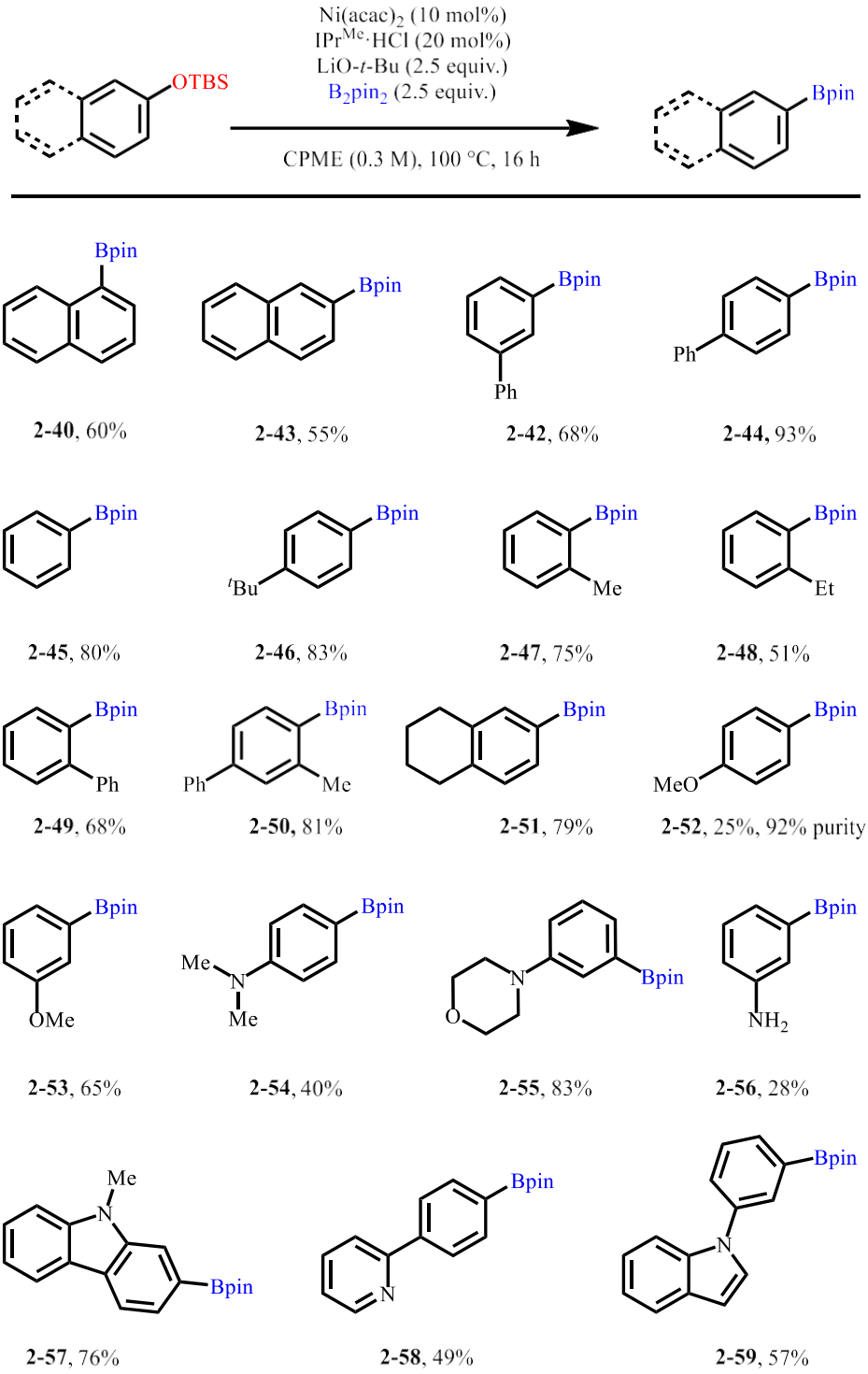

Table 2-4. Substrate scope for the nickel catalyzed borylation of silyloxyarenes.

Notably, these conditions can be used to convert silyloxyarenes on isolated aromatic systems in excellent yields, and in most cases, the remainder of the mass balance was typically

starting material and small quantities proto-deboronation product (compounds **2-45** and **2-46**, Table 2-4)**.** The reaction proved to be tolerant of sterics both at the *ortho*-position in addition to *ortho*- and *meta*-sites around the ring even in isolated aromatics (compounds **2-47**-**2-48, 2-51**, Table 2-4). Tolerance to sterics was demonstrated when biphenyl scaffolds were subjected to reaction conditions (compounds **2-49** and **2-50**, Table 2-4). Next, electron-donating substrates were examined, and it was found that oxygen and nitrogen groups could be tolerated (compounds **2-53, 2-55**, Table 2-4); however, when an electron-donating group was at the *para*-position, decreases in yield were observed (compounds **2-52, 2-54**, Table 2-4). Notably, it was also shown that methyl ethers, which can serve as electrophiles in subsequent coupling reactions, were well tolerated. Though in modest yield, the reaction proceeded on an unprotected aniline (compound **2-56**, Table 2-4) and a variety of heterocycles including indoles, carbazoles, and pyridines in good yields (compounds **2-57–2-59**, Table 2-4).

Benzylic silyl ethers were also effective substrates in the synthesis of benzylic boranes, providing good yields of benzyl boronic pinacol esters, even in the case of non-polyaromatic substrates (compounds **2-62** and **2-63**, Table 2-5). Notably, an electron-rich methoxy group was still tolerated, showcasing the orthogonal reactivity of these two electrophiles (compound **2-63**, Table 2-5). Though the yields for benzylic substrates are moderate, the borylation of methyl ethers cannot tolerate benzylic methyl ethers that contain isolated aromatic systems, representing an advancement in the area.[15]

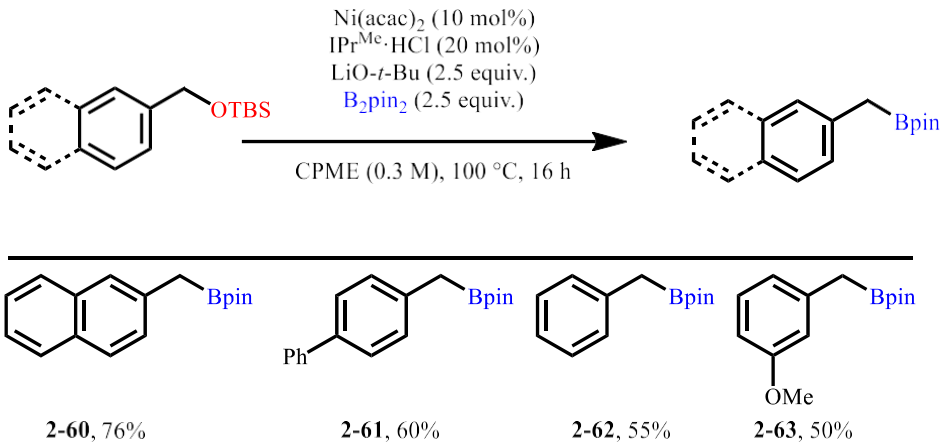

Table 2-5. Substrate scope for the nickel catalyzed borylation of benzyl silyl ethers.

2.5.3 Reluctant Substrates in the Nickel Catalyzed *Ipso*-Borylation of Silyloxyarenes

Although the reaction displayed a broad scope, there were some limitations to the chemistry (Table 2-6). Isolated aromatic substrates possessing ketone, ester, or amide functionality were not tolerated under the reaction conditions yielding no desired product (**2-64-2-67**, Table 2-6). Instead, complex mixtures resulted in conjunction with returned starting material. The pyridine substrate (**2-68**, Table 2-6) also did not perform well, although a pyridine ring can be incorporated in the case of a biphenyl substrate (**2-58**, Table 2-6). This negative result discouraged us from pursuing other heteroaryl substrates wherein the silyloxy group was directly appended. Unprotected indoles and even those protected with a methyl, a Boc, or a Ts were not tolerated returning starting material in all cases. However, moderate yields were attainable in the case of n-arylated indoles (**4-59**, Table 2-4). Lastly, no conversion of the nitrile containing group was observed, offering only returned starting material, which is likely attributed to catalyst poisoning.

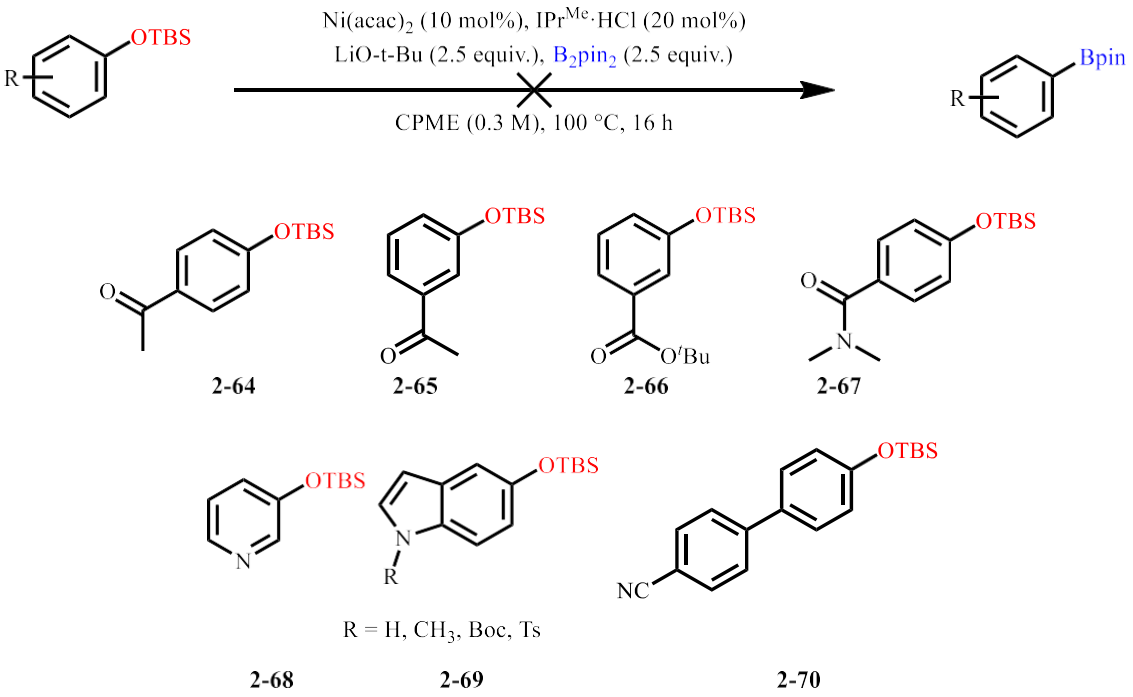

Table 2-6. Scope of challenging substrates to engage in the nickel catalyzed borylation of silyloxyarenes.

2.5.4 Synthetic Utility of the Nickel Catalyzed *Ipso*-Borylation of Silyloxyarenes

To highlight the synthetic utility of this method, we were interested in demonstrating how the orthogonal reactivity of silyloxyarenes to other classes of electrophiles to leverage iterative, chemoselective cross-couplings. Achieving selectively between various C(sp^2)–O and C(sp^3)–O bonds were next examined (Figure 2-35). Firstly, the stability of silyloxyarenes under palladium catalysis was shown, as **4-71** (Figure 2-35a) underwent Buchwald-Hartwig amination to afford **4-72** (Figure 2-35a) in good yield.[69] The unfunctionalized silyloxyarene was then engaged in the borylation reaction under standard conditions to afford **2-73** (Figure 2-35a) in moderate yield. Secondly, experiments were carried out determine if the borylation of silyloxyarenes was selective for either the sp^2 C–O or the sp^3 C–O (Figure 2-35b). To probe this, **2-74** (Figure 2-35b) was subjected to the standard borylation conditions, which resulted in the formation of **2-75** (Figure 2-35b) in good yield. However, diborylation of both silyloxy groups was also observed, resulting

in a mixture of **4-75** (Figure 2-35b) and the analogous diborylated product. Scaffold **2-74** (Figure 2-35b) was also subjected to amination conditions, which were previously reported, resulting in a high yield of **2-76** (Figure 2-35b) with no evidence of over-amination.

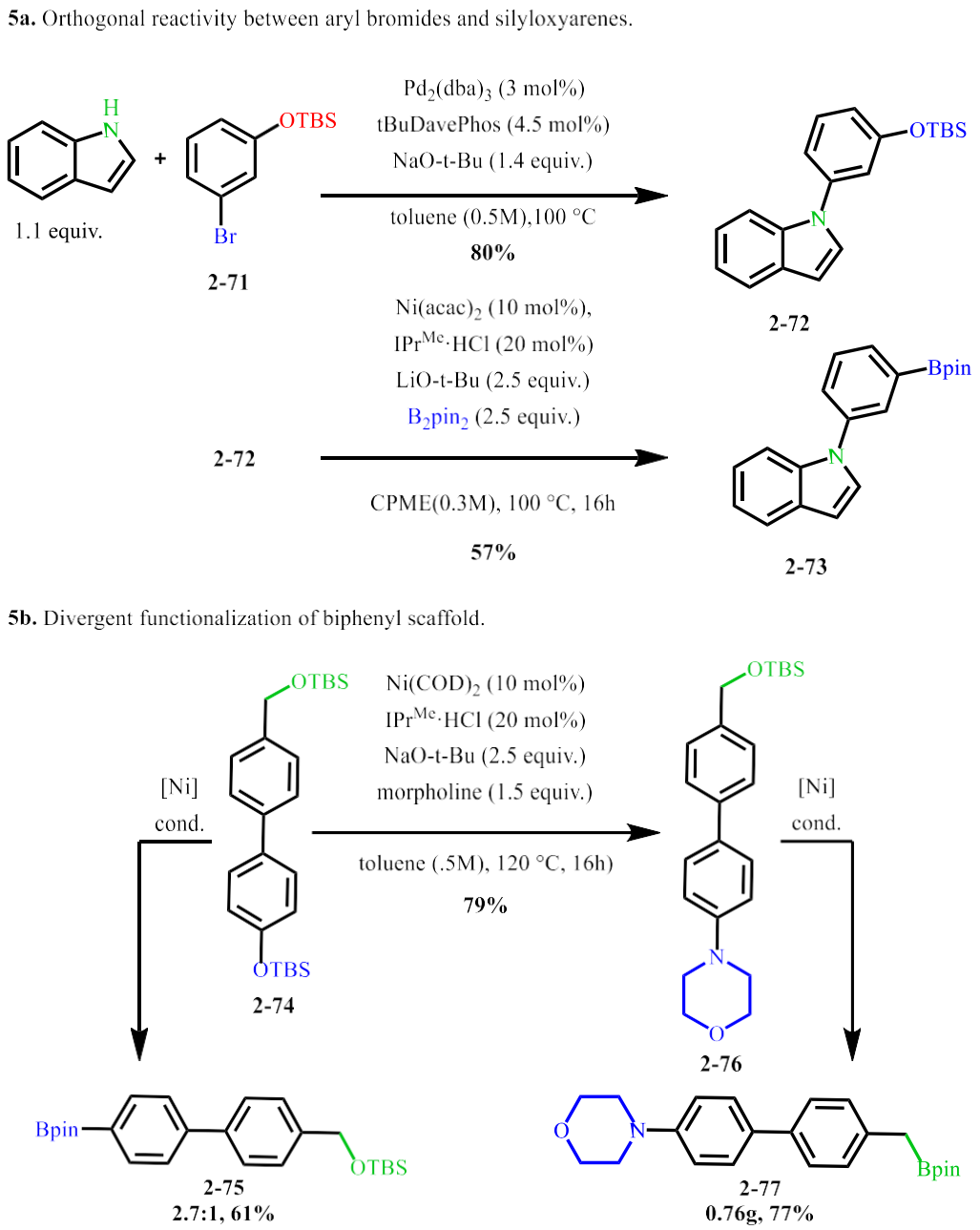

Figure 2-35. Synthetic demonstrations for the nickel catalyzed borylation of silyloxyarenes.

The C(sp^3)–O could then be functionalized subsequently to afford the borylated compound in good yield **2-77** (Figure 2-35b). Overall, this represents a modular process and allows access to a generous level of diversity with regards biphenyl core-scaffolds, which are ubiquitous in pharmaceuticals. For example, the structure **2-77** represents a fragment related to the core structure of fexaramine, which is a drug currently under investigation as an agonist of the farnesoid X receptor.[70]

2.5.5 Mechanistic Considerations for the Nickel Catalyzed *Ipso*-Borylation of Silyloxyarenes

A plausible mechanism for this reaction involves a traditional Ni(0)/Ni(II) cycle, wherein oxidative addition to the silyloxyarene would occur, followed by transmetallation of the diboron species and reductive elimination from the borylated arene (Figure 2-36).

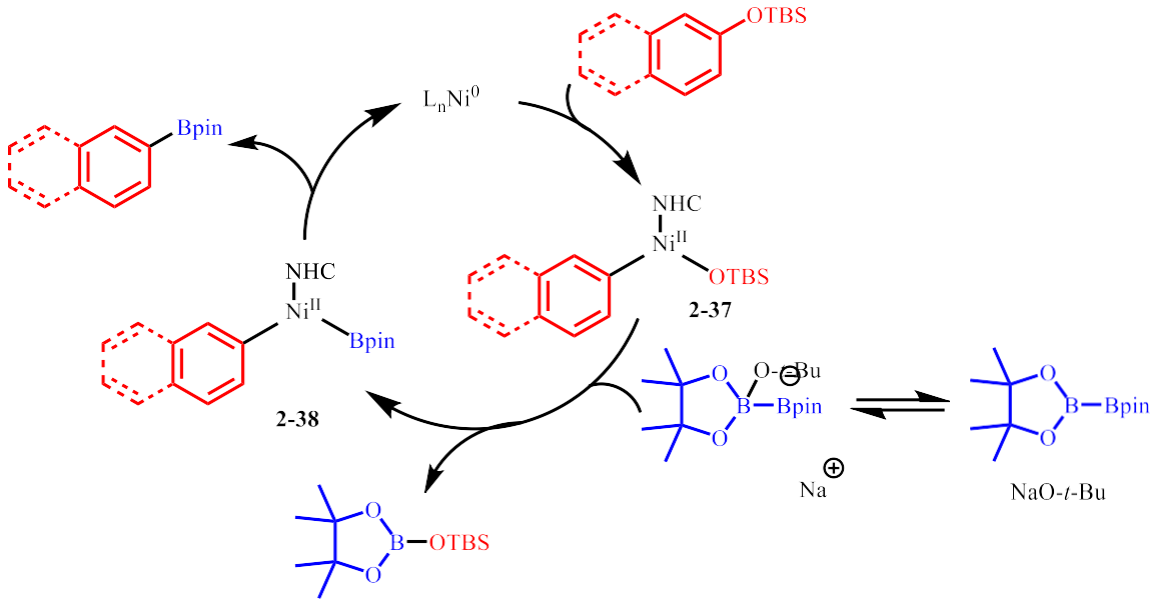

Figure 2-36. Copper free mechanism for the nickel catalyzed borylation of silyloxyarenes.

However, in recent years, an increasing number of mechanistic studies regarding the functionalization of low-reactivity of C−O bonds suggest that alternative mechanisms involving Ni(I) species or Ni(0) ate complexes may be operative.[71–73]

2.6 Conclusions Regarding the Nickel Catalyzed *Ipso*-Borylations of Silyloxyarenes

In summary, an effective nickel-catalyzed ipso-borylation of silyl ethers has been developed.[10,11] This method provides rare demonstrations of the direct functionalization of the C−O bond of silyloxyarenes and is distinguished by the inclusion of several isolated aromatic substrates including those with heterocyclic functionality. These features address several limitations regarding alternative approaches for the catalytic functional group interconversion of low-reactivity C(sp2)−O bonds to C(sp2)−Bpin products. The orthogonality of this method to other classes of arene and heteroarene cross couplings was demonstrated by chemoselective Buchwald−Hartwig amination of an aryl bromide followed by borylation of a silyloxyarene functionality. Additionally, in another bifunctional substrate, initial chemoselective amination of a silyloxyarene group was followed by borylation of a benzyloxysilane functionality. This method represents a promising technology for the functionalization of silyl protected phenols including those with isolated aromatic ring systems while possessing orthogonal reactivity to other classes of aryl electrophiles

Chapter 3

Synthesis of Air-Tolerant Discrete Nickel (0) Pre-Catalysts from Nickel (II) Salts and N-Heterocyclic Carbene Salts

3.1 Introduction

Scientists are charged with developing innovative, novel technologies and providing multi-faceted solutions for complex problems. Chemists contribute to this aim at a foundational level. In the Montgomery laboratory, an emphasis is placed on developing methodologies to facilitate the rapid formation of complex scaffolds, starting from simple precursors, in the hopes that they might facilitate the synthesis of high-performance therapeutics, agrochemicals, and/or materials. As discussed in Chapter 1, nickel is an excellent metal to facilitate these goals as it is sustainable and possesses complementary properties to those exhibited by other *d*10 metals. In more specific terms, the ideal catalyst is described, below (Figure 3-1).[74]

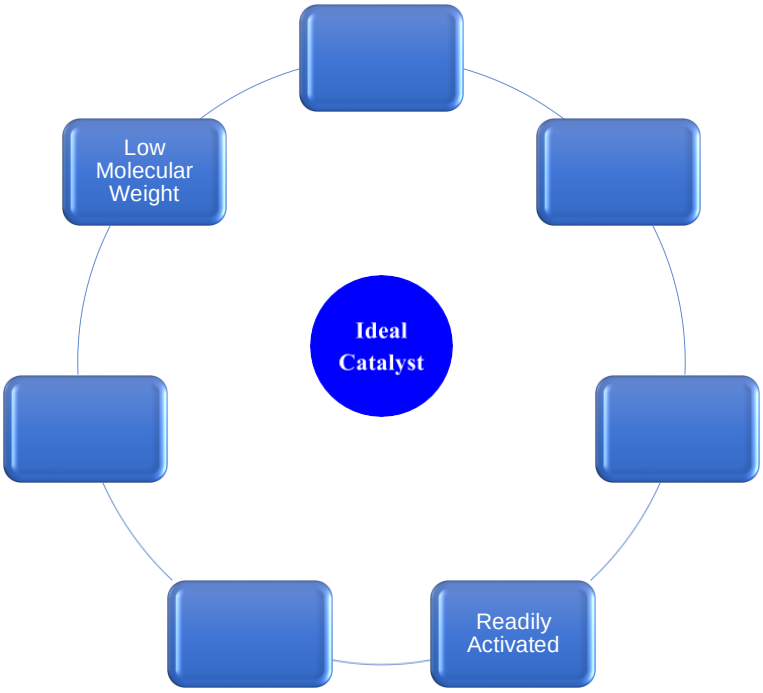

Figure 3-1. Attributes of an ideal catalyst system.

The most common oxidation state of available nickel pre-catalysts is Ni(II). However, a larger quantity of transformations exist wherein Ni(0) is required to achieve successful catalysis. Ni(II) salts can still be used to this end; however, the metal must then be reduced *in situ*, which is typically achieved either by the reagents in the parent reaction, or via the addition of an exogenous reductant. Key issues regarding this approach exist primarily in cases where 1) the reduction is inefficient, which typically leads to higher catalyst loadings, 2) reactions that are sensitive to the stoichiometry of metal to ligand, which is challenging to consistently create under this manifold, 3) the reactants are incapable of reducing the metal, and 4) the exogenous reductant is not compatible with the starting materials and/or facilitates undesirable side reactions. In addition, an exogenous reductant diminishes atom economy, and thus negatively affects sustainability.

An eloquent solution to some of these issues have been addressed by the Jameson group and others, which has contributed an impressive collection of air-stable Ni(II) pre-catalysts over

the years. This approach eliminates concerns regarding metal to ligand stoichiometry, and the need for an exogenous reductant as the nucleophilic partner in a variety of coupling reactions serves as the source of reduction. These advancements in nickel pre-catalysts have represented excellent contributions in nickel catalysis in the context of organic synthesis. That being said, some limitations do exist. One major limitation is that reduction to Ni(0) from the Ni(II) salt is still required, which can potentially lead to induction periods. Inefficiencies in catalyst reduction can lead to the enablement of undesirable side pathways in some cases.

Ni(0) pre-catalysts can circumnavigate some of these issues being that they begin with the desired oxidation state. However, very few Ni(0) pre-catalysts exist, with the most common Ni(0) pre-catalyst being nickel bis(cyclooctadiene) ($Ni(COD)_2$), which is highly air sensitive. This requires the use of oxygen-free environments such as gloveboxes for storage and handling, making transformations which rely on this pre-catalyst less accessible. Additionally, COD ligands can prove detrimental in several transformations, as they can inhibit catalysis and lead to side product formation. An approach that provides the most inclusion of solutions for the aforementioned challenges comes with the advent of air-stable/tolerant discrete nickel (0) pre-catalyst systems. Several catalyst systems of this nature have been reported including discrete Ni-NHC catalyst systems that employ acrylates and fumarates, which are less air sensitive. The largest challenge facing these catalysts is derived from the undesirable starting materials that are currently utilized to synthesize these complexes, including free NHC and $Ni(COD)_2$. A more efficient synthetic route to these species would make them more broadly accessible to the synthetic community. In this chapter, progress regarding the in-situ reduction of Ni(II) salts and the development of Ni(II) and Ni(0) pre-catalysts will be reviewed, as well as the evolution of the synthesis of our discrete Ni(0)-

NHC pre-catalysts from Ni(II) and NHC salts, in an effort to make them more broadly accessible to the synthetic community will be discussed (Figure 3-2).

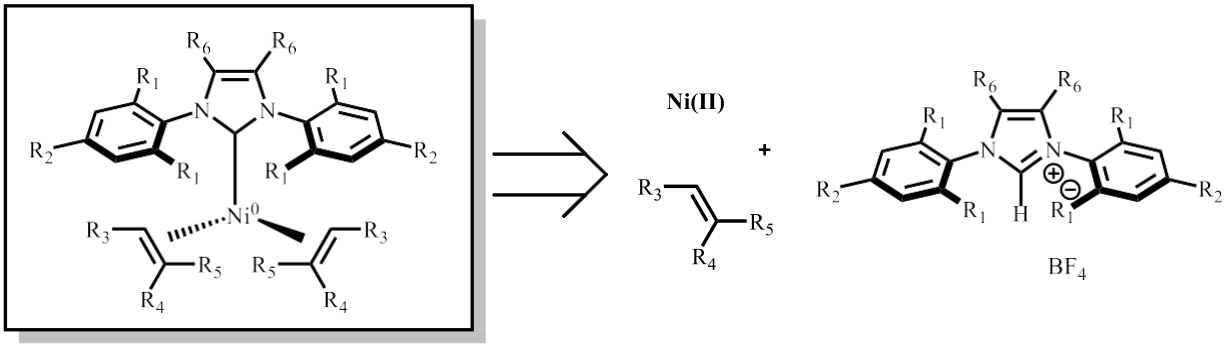

Figure 3-2. Refined synthesis of discrete Ni(0)-NHC complexes from Ni(II) and NHC salts.

3.2 Ni(II) Salts

Ni(II) salts are a convenient starting point for in nickel catalysis as they are air and water stable. This stability eliminates the need for a glovebox for storage, or chemical manipulations, which makes them much more accessible to the community. In cases where coupling reactions are water sensitive, these salts can be dried by heating the salt under high vacuum using Schlenk techniques. Analogously, many ligands commonly employed in cross-coupling reactions can also be stored on the benchtop and dried, if need be, leading up to the time when one desires to run the reaction. For air sensitive ligands such as phosphines, detrimental oxidation can be avoided by utilizing the protonated phosphine salt, which can simply be deprotonated *in situ*. For oxidative processes, or Ni(II) redox neutral reactions, the native oxidation state of the catalyst is sufficient (Figure 3-3).[75–79]

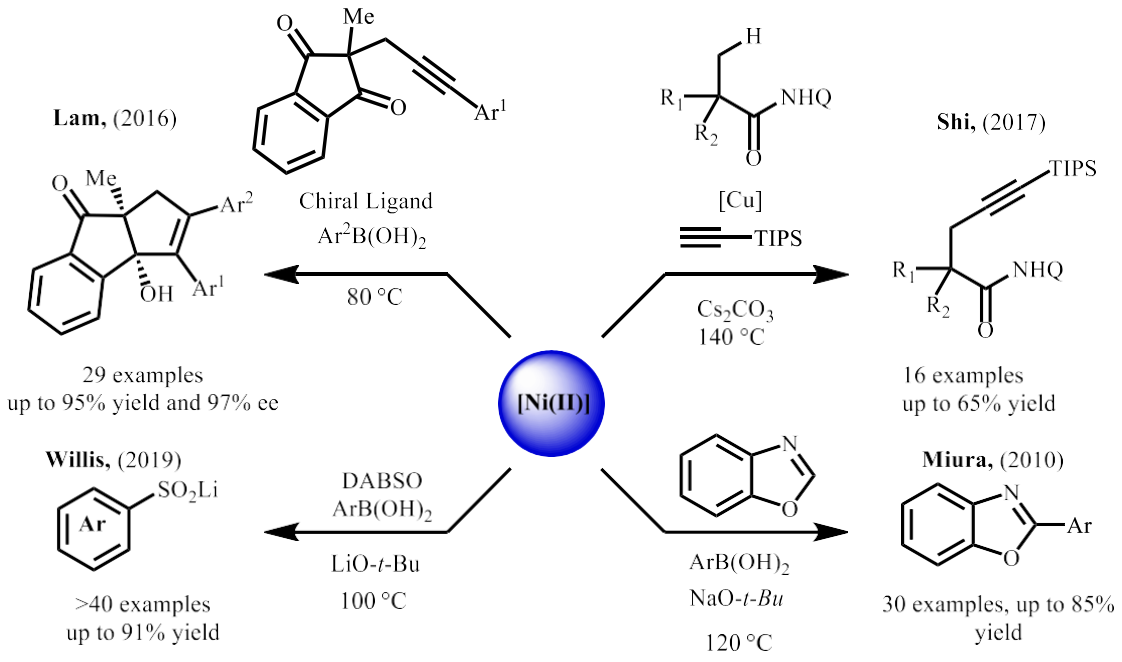

Figure 3-3. Reactions catalyzed by Ni(II) redox neutral, or oxidative pathways.

On the other hand, in reactions wherein Ni(0) is required, *in situ* reduction of the Ni(II) source is necessary. This means that reduction of the catalyst is solely dependent on the nature of the reaction conditions. In these cases, reduction of the Ni(II) source is often dependent on the class of reaction. The main mechanisms of activation can be divided into the follow three groups 1) metal reductants, 2) reactants that lead to reductive elimination, or 3) reacts leading to β-hydride elimination.

3.2.1 Reduction Mechanisms of Ni(II) Salts

3.2.1.1 Reductive Couplings (Mn, Zn, and other exogenous reductants)

One of the most common way to access Ni (0) for reactions, involves the use of an exogenous reductant, especially in the case of cross-electrophile couplings. Ni(II) salts can be readily reduced by both organic and metallic reductants and each have seen use, depending on the situation (Figure 3-5).[80]

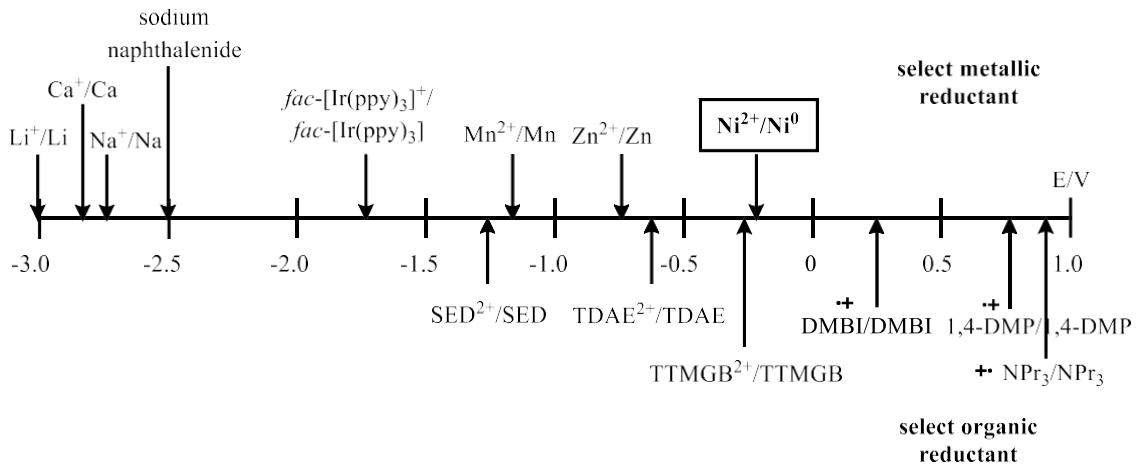

Figure 3-4. Reduction potentials of select metallic and organic reductants.

This method of reduction is most often utilized in the case of reductive couplings, which are most generally defined as reactions wherein the product(s) have been reduced. For the purposes of this discussion, however, reductive couplings will hence forth be referred to as reactions where an exogenous metal, or organic reductant is employed to reduce the metal to conduct reduction(s) on the metal to keep it in the catalytically relevant oxidation state throughout the course of the catalytic cycle. Advantages of reductive couplings are 1) they reduce the metal salt *in-situ*, 2) tend to be less sensitive to air as stoichiometric reductant is employed, and 3) this manifold permits the execution of cross-electrophile couplings, which would be otherwise impossible without a reductant. Representative examples of reactions mediated by exogenous reductants can be found, below (Figure 3-5).

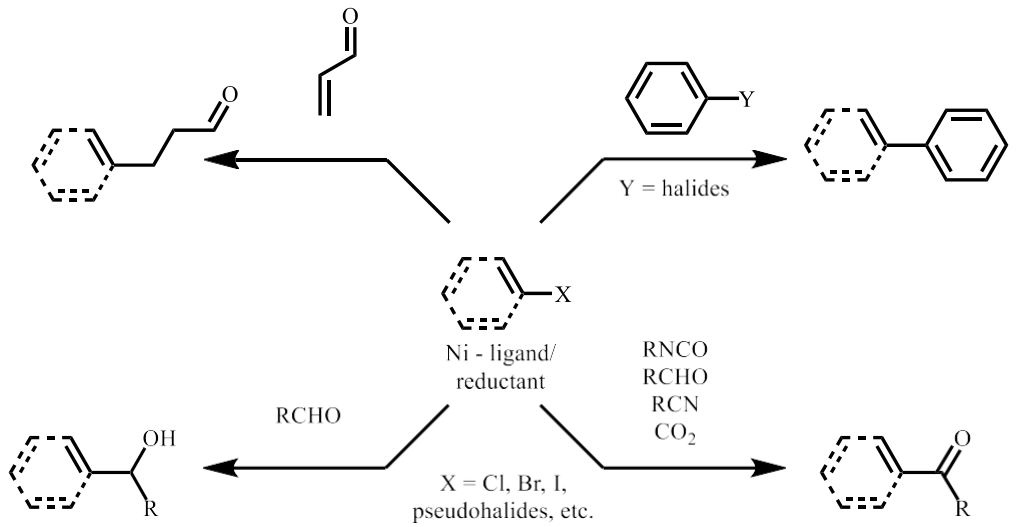

Figure 3-5. Reductive couplings wherein the Ni(II) salt is reduced *in situ* via mild metal reductants like Mn(0) and Zn(0).

In reductive cross-couplings, the reductant also serves to activate coupling partners and attenuate the oxidation state of the metal throughout the catalytic cycle. For example, recently published work from the Montgomery group has demonstrated that intercepting Ni(II) oxidative cyclization adducts with alkyl halides to provide tetrasubstituted olefins (Figure 3-6). Here, the Ni(II) salt is reduced by Mn(0) to form Ni(0) *in situ*. Another equivalent of Mn(0) enters at the end of the catalytic cycle to turn-over the nickel catalyst.

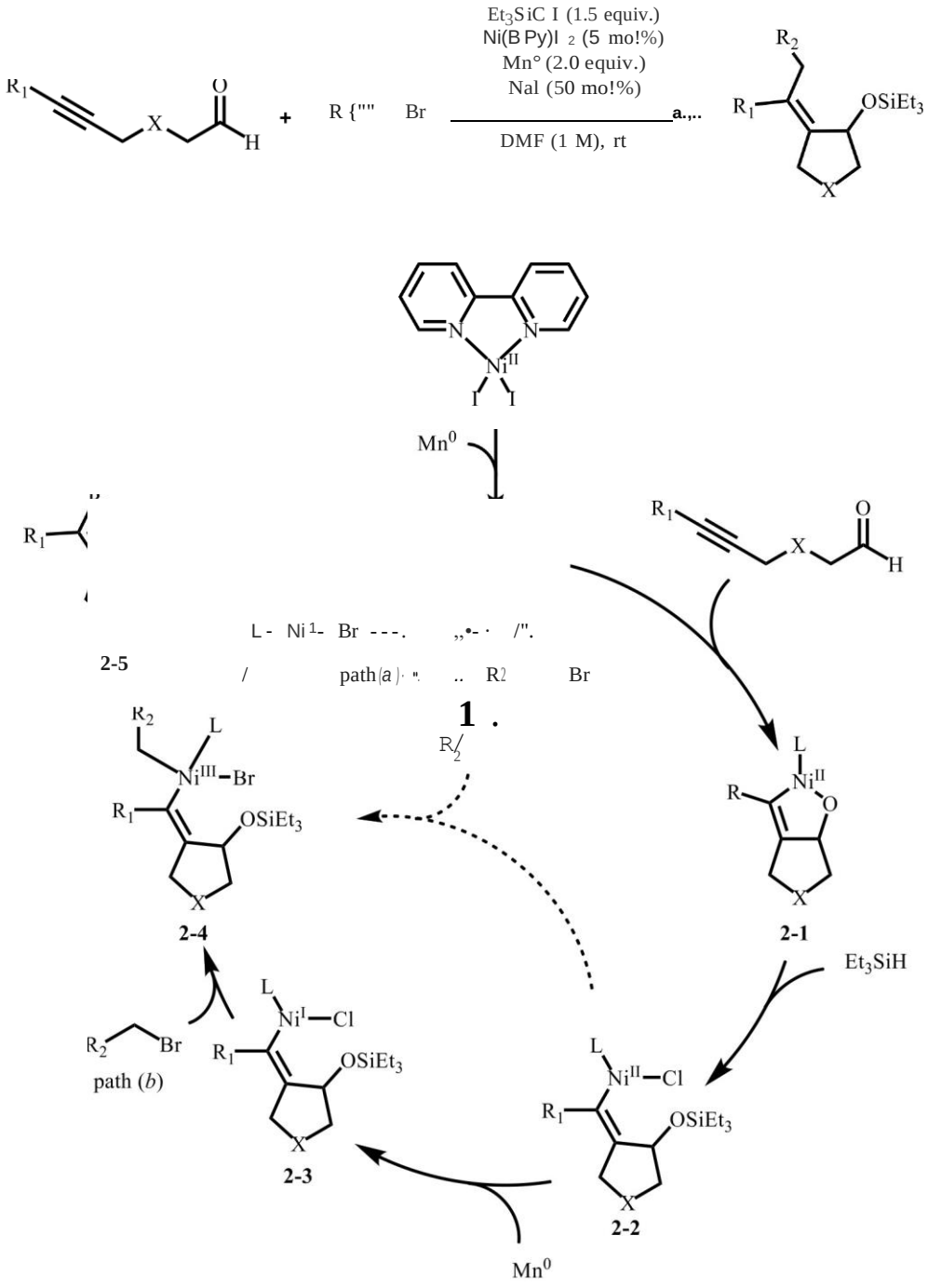

Figure 3-6. Proposed mechanism for the reductive coupling of aldehydes, alkynes, and alkyl halides.

3.2.1.2 Reduction of Metal via Reductive Elimination

Reduction via reductive elimination involves the Ni(II) salts being reduced *in situ* via nucleophilic coupling partners (Figure 3-7). Kumada, Negishi, Stille, Suzuki, and Hiyama-Denmark couplings are most well-known for this mechanism of action. Once two equivalents of nucleophile are ligated to the metal, subsequent reductive elimination furnishes the catalytically relevant Ni(0) species, which can then engage with the electrophile of the reaction.

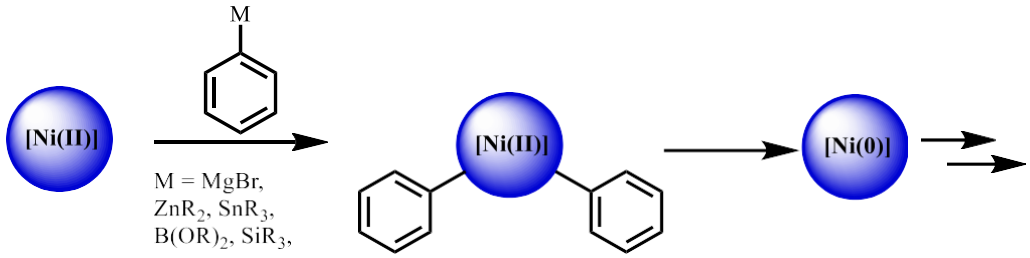

Figure 3-7. Reduction of Ni(II) salts via transmetallation followed by subsequent reduction.

3.2.1.3 Reduction of Metal via β–Hydride Elimination

The last major process by which Ni(II) salts are reduced *in situ* is through β-elimination. Most commonly these occur through the coordination of amine nucleophiles bearing β-hydrogens. In the presence of base, nitrogen nucleophiles undergo ligand exchange with a X ligand of the Ni(II) salt. Next, β-hydrogen elimination occurs, followed by deprotonation to afford the catalytically relevant Ni(0) species, along with the imine byproduct (Figure 3-8).

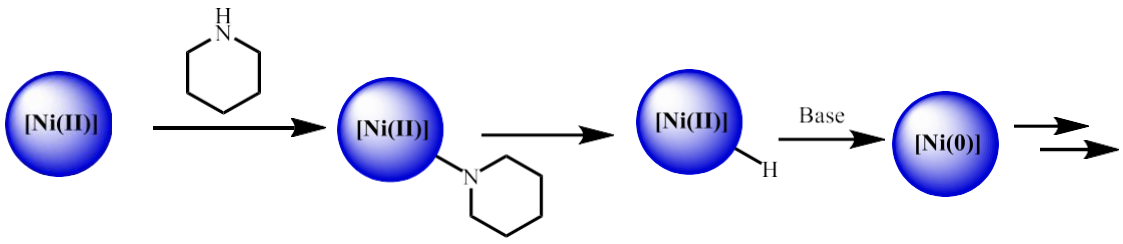

Figure 3-8. Reduction of Ni(II) salts via β-Hydrogen elimination.

Another strategy to reduce Ni(II) salts under this manifold is by utilizing solvents that contain or can degrade to provide trace quantities of amines with β-hydrogens. One example is seen in the Heck reaction of aryl iodides, wherein $Ni(acac)_2$ is utilized as a pre-catalyst (Figure 3-9).

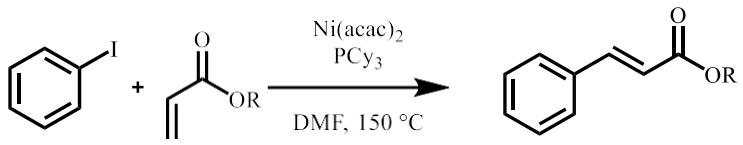

Figure 3-9. Reduction of Ni(II) salt via advantageous amine present in solution.

In this case, there is no obvious reductant for the presented transformation. The aryl iodide could be classified as an oxidant. Further, the olefin itself cannot reduce the metal on its own. There is no acetate, nor air, present to facilitate the reduction of nickel via oxidation of the phosphine ligand. Potentially unsuspectingly, the dimethyl formamide (DMF) is what serves as the source of reductant, as at elevated temperatures decomposition of DMF begins, resulting in increasing quantities of dimethyl amine, which can thus reduce the metal salt (Figure 3-8).

3.2.2 Summary of the Reduction of Ni(II) Salts

Ni(II) salts are advantageous with respect to the convenience and expediency in which cross-coupling reactions can be setup. Moreover, their stability to air and moisture makes the chemistry highly accessible to labs that are limited to Schlenk techniques for air-sensitive chemistry. However, drawbacks to Ni(II) salts as pre-catalysts exist in cases where the catalytically relevant species is Ni(0), and so reduction of the Ni(II) salt must be done *in situ.* Although this is manageable in a wide variety of coupling reactions, instances where reduction of the Ni(II) salt is inefficient can leading to pro-longed reaction times and may also lead to off-cycle reactivity. These

challenges have been sought to be addressed through discrete Ni(II) pre-catalysts (*vida infra*), which enable more efficient reduction processes.

3.3 Ni(II) Pre-Catalysts

Discrete Ni(II) Pre-Catalysts possess the advantages of Ni(II) salts, and offer unique properties, as well. The additional benefits are that the ratio of ligand to nickel is known more precisely. Further, these systems often come with mechanisms of reduction that occur in sub-stoichiometric quantities, which are easily separated from desired products. Finally, exogenous additives are typically not necessary, although exceptions exist (Figure 3-10).

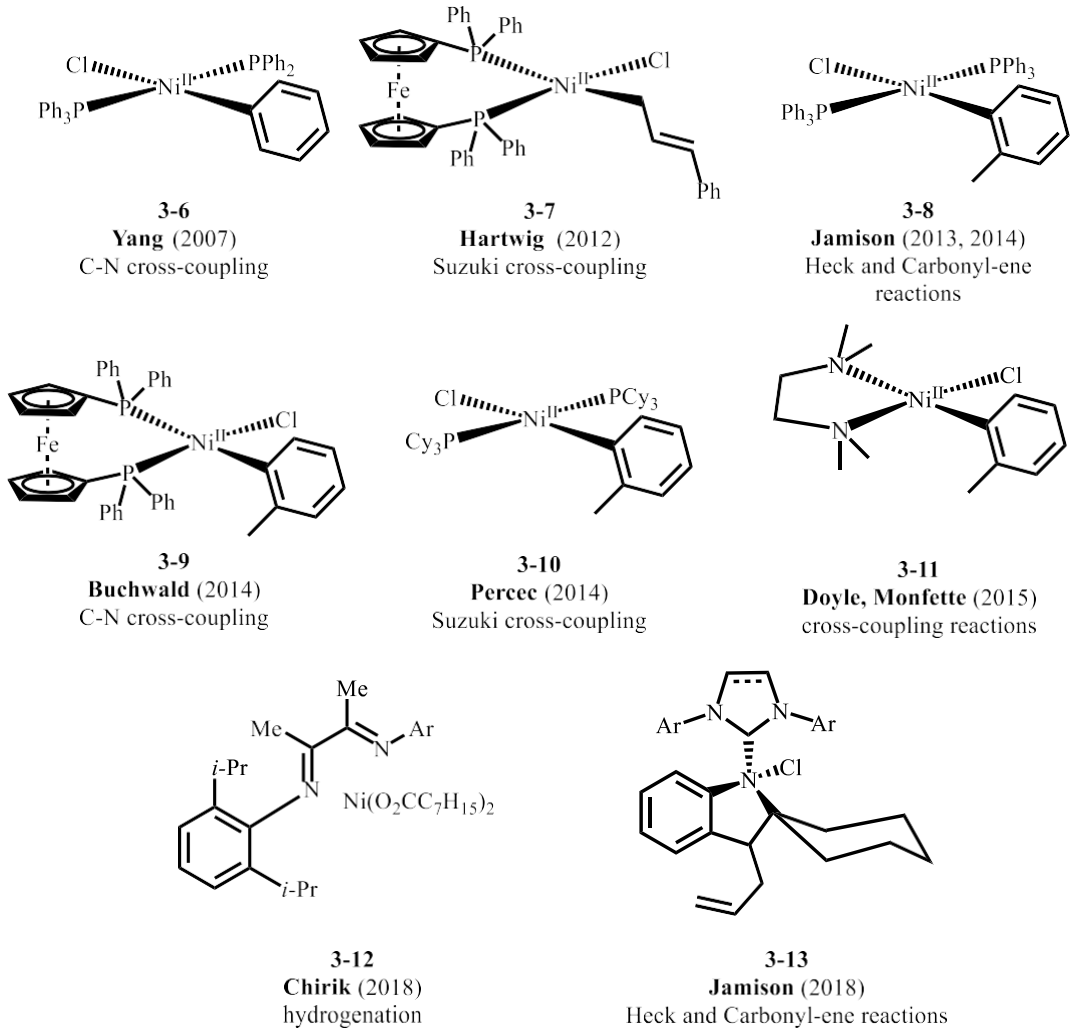

Figure 3-10. Select examples of discrete Ni(II) pre-catalysts designed to enable efficient reduction of Ni(II).

Many groups have benefited the synthetic community through their contributions to expanding known nickel pre-catalysts to choose from. In this work, facile reduction of catalyst occurs *in situ* under the specified manifold, allowing for highly efficient couplings. Additionally, these pre-catalysts are straightforward to make. Most often, Ni(II) salts are treated with the desired ratio of L-type ligand, followed by the addition of a Grignard reagent to provide the desire X-type aryl ligand (Figure 3-11).

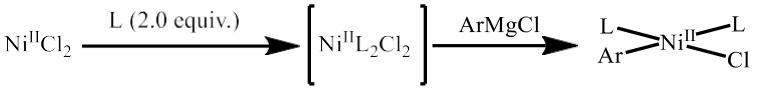

Figure 3-11. Representative, generic synthesis of Ni(II) pre-catalysts.

Synthetic methodologies to access these Ni(II) pre-catalysts are easy and practical. Often, they can be conducted as one-pot protocols. This enables these strategies to be highly modular, permitting for the expedient synthesis of catalyst libraries. A pertinent example regarding the efficiency of these discrete complexes was conducted by Jameson and co-workers in 2018, in the context of an ene-reaction of olefins and aldehydes. The discrete Ni(II) pre-catalyst, **2-13**, performed noticeable better in a direct comparison to an *in-situ* prep with $Ni(COD)_2$ (Figure 3-12).

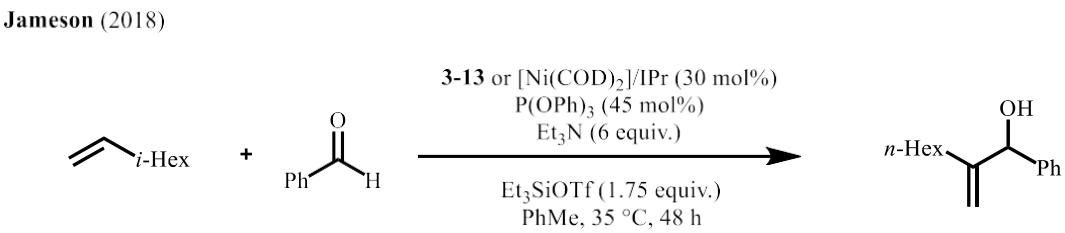

Figure 3-12. Time study of product formation with respect to catalyst employed.

In summary, these contributions have greatly advanced the scientific community's ability to conduct catalysis across a variety of transformations. The advantages of known stoichiometric ratios of ligand to metal, and enhanced efficiency of catalyst formation outweigh the concerns regarding the need to pre-synthesize them. Even then, the synthesis of these complexes is highly modular. However, some disadvantages are that catalysts loadings can be high. The largest consequence of this is that the byproduct of nickel reduction is equal to the catalyst loading, and so if loadings are too high, large quantities of waste are generated. To address these concerns various groups explored the synthesis of Ni(0) pre-catalysts.

3.4 Ni(0) Pre-Catalysts

To avoid protocols that rely upon the *in-situ* reduction of the nickel catalyst, the employment of Ni(0) pre-catalysts that begin the reaction in the catalytically relevant oxidation state are highly attractive. The first discrete source of Ni(0) sources developed by Ludwig Mond in 1889. He and his colleagues serendipitously discovered that $Ni(CO)_4$ could be formed from the heating of nickel oxide in the presence of carbon monoxide, which could subsequently be plated out, to give nickel ore in the coveted zero-oxidation state. In 1960, Gunther Wilke reported the first synthesis of binary metal-olefin complexes in his studies concerning reactions between olefins and nickel salts (Figure 3-13).

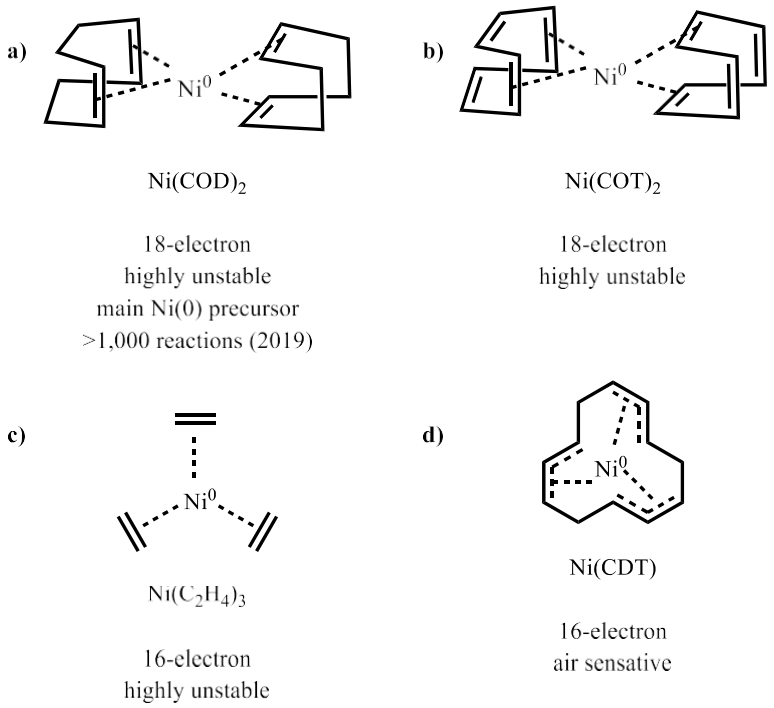

Figure 3-13. Olefin bound Ni(0) pre-catalysts.

This resulted in the development of several Ni(0) pre-catalysts; however, it was $Ni(COD)_2$ that ultimately became the standard Ni(0) pre-catalyst even in present times. This robust complex

has been used to facilitate over 1,000 chemical transformations, as of 2019. However, $Ni(COD)_2$ does have some disadvantages. Unfortunately, the greatest advantage of $Ni(COD)_2$ being that it is already in the catalytically relevant oxidation state is also its greatest weaknesses, in that it is highly air-sensitive, and must be stored in a glovebox. Traditional synthesis of $Ni(COD)_2$ has entailed the reduction of Ni(II) salts via reductants, such as sodium metal (Figure 3-4) in the presence of COD. Due to the hazards of sodium metals, more user-friendly reductions were then developed which employed DIBAL. More recently, however, the synthetic community has sought to develop even safer, less complicated protocols for the synthesis of this commodity pre-catalyst accompanied by easy, clean isolations of the desired complex. The most recent results of these efforts are as follows (Figure 3-14).

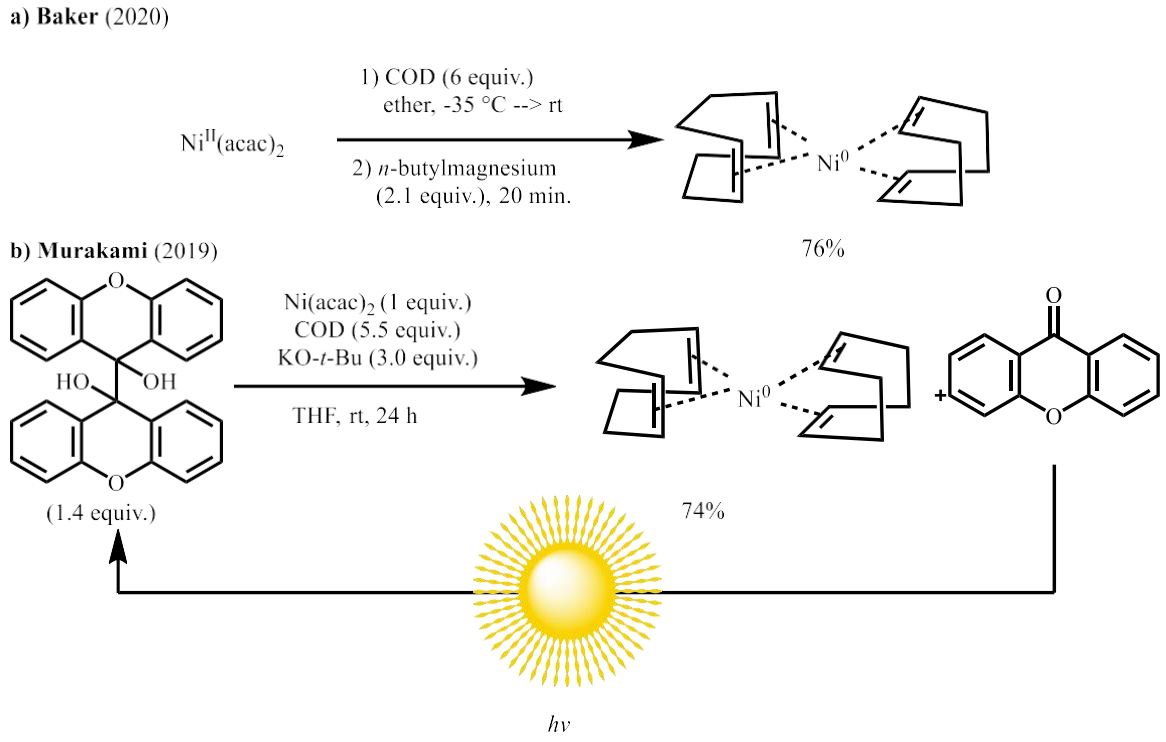

Figure 3-14. Modern synthetic protocols to access $Ni(COD)_2$.

First, Baker and co-workers developed an expedient protocol for the large-scale synthesis of $Ni(COD)_2$ via a relatively safe organometallic reagent in *n*-dibutylmagnesium in the presence of super stoichiometric quantities of COD. Another strategy, developed by Murakami, utilizes the power of the sun to create a dimer of xanthone. This diol can then be deprotonated by base *in-situ* to provide ketyl radicals, which then reduce the $Ni(acac)_2$ to provide $Ni(COD)_2$.

In addition to air-sensitivity, another disadvantage of the $Ni(COD)_2$ pre-catalyst is that the COD ligand can inhibit desired reactions by competitively occupying coordination sites, or by reacting, itself, under the reaction conditions. The latter commonly occurs in the case of C─H functionalization. Work by the Montgomery group has demonstrated how COD's off-cycle activity can be detrimental, thus requiring unnecessarily forceful conditions to produce an appreciable yield of product. $Ni(COD)_2$ pre-catalyst systems required temperatures of 80 °C, and only achieved yields in the 50s after an hour, having achieved no conversion at all at room temperature (Figure 3-15).[81]

Montromgery (2015)

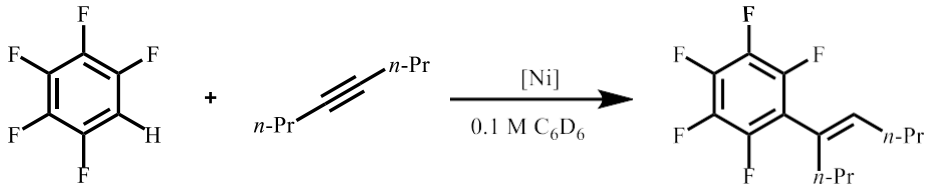

Figure 3-15. LLHT coupling of alkynes and arenes.

After careful study of the reaction, it was found that once oxidative addition to the C–H bond is complete, the resulting nickel-hydride can then insert into the COD ligand and participate in chain-walking events that prevent the catalyst from facilitating the desired reaction (Figure 3-16).[81]

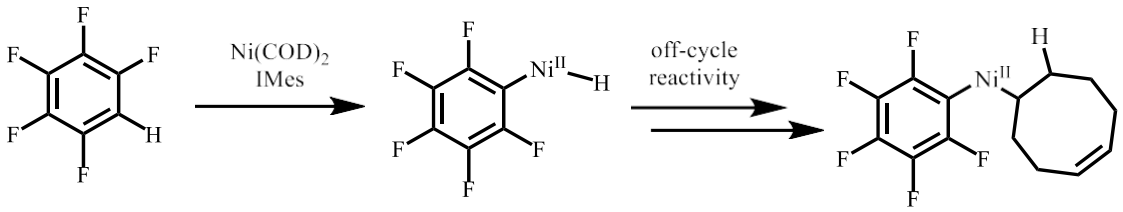

Figure 3-16. Ni-H chain-walking as an unproductive, inhibitive side pathway.

Overall, these findings illustrate the importance of Ni(0) catalyst systems that do not rely on the employment of COD ancillary ligands. This work, combined with others over the years justified the further development of Ni(0) pre-catalysts that did not contain the COD ligand (Figure 3-17).

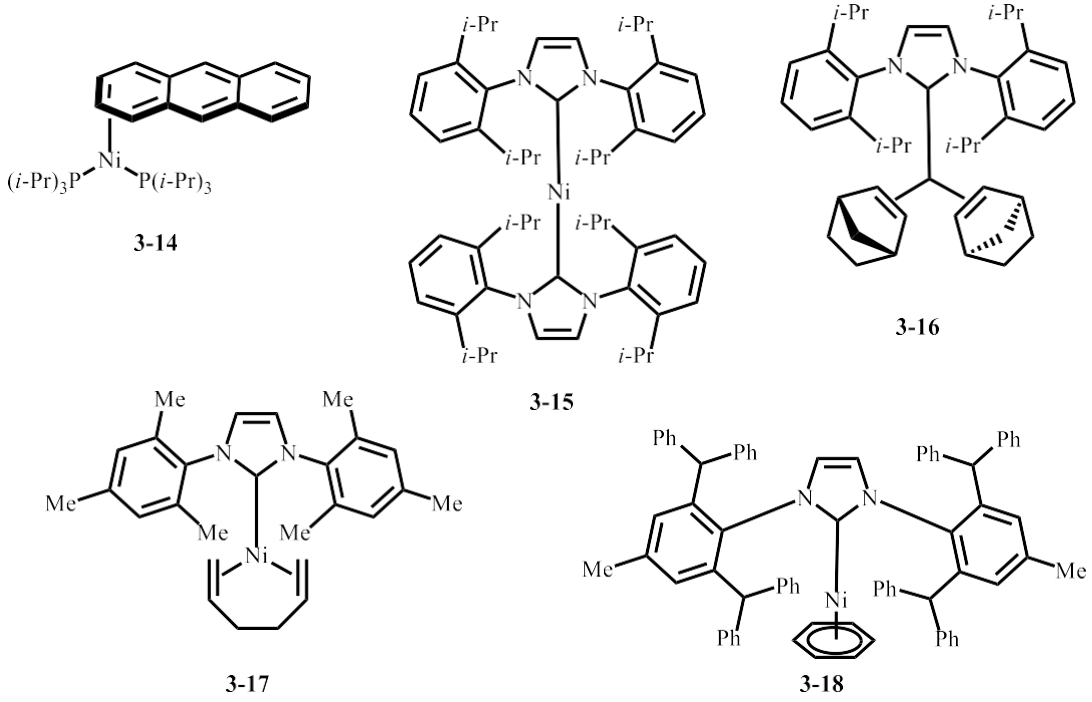

Figure 3-17. Ni(0) pre-catalysts that do not possess COD as a ligand.

In the same study wherein the detrimental effects of $Ni(COD)_2$ in the context of LLHT chemistry, it was found that catalyst **3-17** (Figure 3-17) facilitated the reaction (Figure 3-15) at

room temperature, providing full conversion to desired product after just one hour.[81] This result cemented the advantages of excluding COD in situations where nickel hydrides are present.

Furthermore, even in cases where the COD ligand is not an issue, the *in-situ* generation of catalyst systems can instead prove problematic as inefficient formation of catalyst system can lead to undesired side pathways. For example, previous work from the Montgomery lab has shown that in the reductive cross-coupling between enones and alkynes, *in-situ* protocols were irreproducible, and provide poor yields of the skipped diene resulted (Figure 3-18).[82]

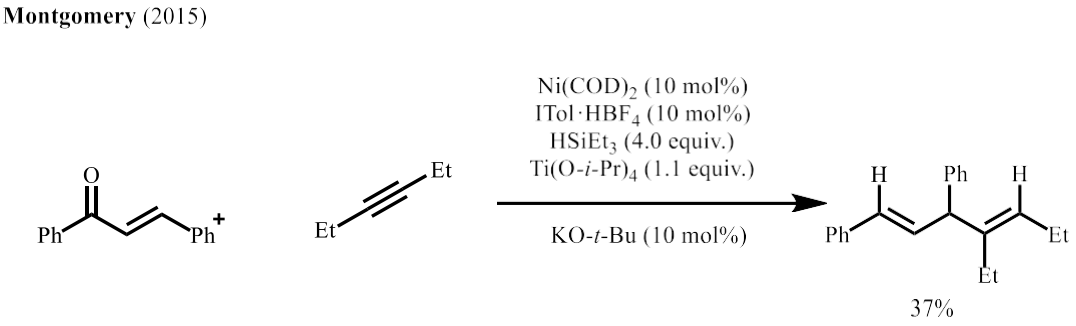

Figure 3-18. Inefficient catalyst formation leads to low yields and irreproducible results.

The inconsistency in the chemistry was thought to arise from inefficiencies in catalyst formation, resulting in the indulgence of undesired side reactions caused by an ill-defined ratio of ligand to metal. Montgomery and co-workers hypothesized that this could be overcome by the synthesis of a discrete Ni(0)-NHC pre-catalyst with a known ratio of ligand to metal, thus poised for participation in the catalytic cycle. This would also remove need for further activation, and ultimately result in consistent, and higher yields of desired product (Figure 3-19).

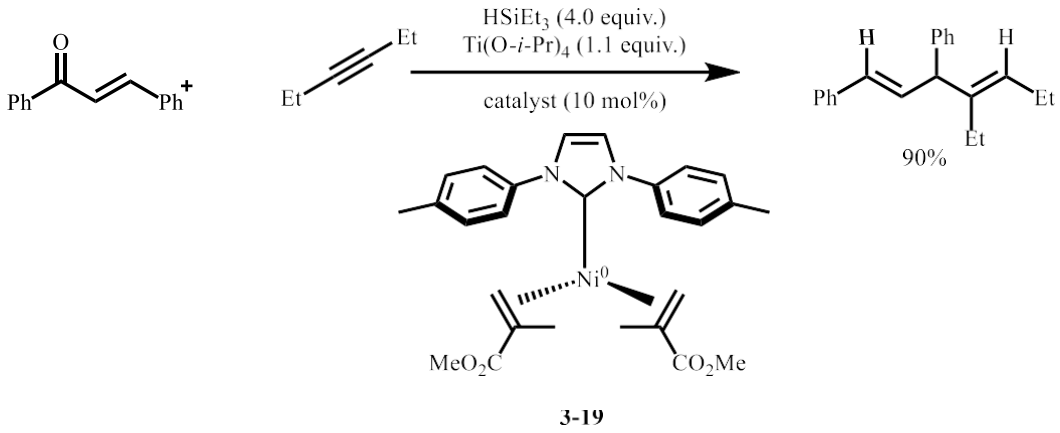

3-19

Figure 3-19. The utilization of a discrete Ni(0) pre-catalyst to enhance performance in contrast to an existing *in-situ* catalyst protocol.

While this represented a significant advancement in the field of Ni(0) pre-catalysts, there was a desire to keep working as to make the catalysts as broadly useful and accessible as possible. A chief aim to bring this goal to fruition would be innovation regarding enhancing the air stability. This led to work that studied the effect of the ancillary ligands, to determine if stronger π-acidic ligands could be utilized to confer air-stability onto the nickel pre-catalyst. To address the issues concerning air-stability of Ni(0) complexes, variability in the reliability of *in-situ* generated Ni(0) catalyst systems, and the detrimental side reactivity of COD ligands, the Montgomery group invested effort in developing air-tolerant/stable discrete Ni(0) pre-catalysts. This work resulted in three commercially available catalysts. When these discrete Ni(0) catalysts were employed, excellent yields of the desired product were consistently observed across aminations and couplings of aldehydes and alkynes. In contrast to *in-situ* protocols, this strategy ensures that the user knows the metal to ligand stoichiometry, the quantity of active catalyst, and that the catalyst is in the desired oxidation state. This work led to a number of novel compounds, which are now reported compounds in addition to those which were made commercially available being **3-24**, **3-26**, and **3-27** (Figure 3-20).[83]

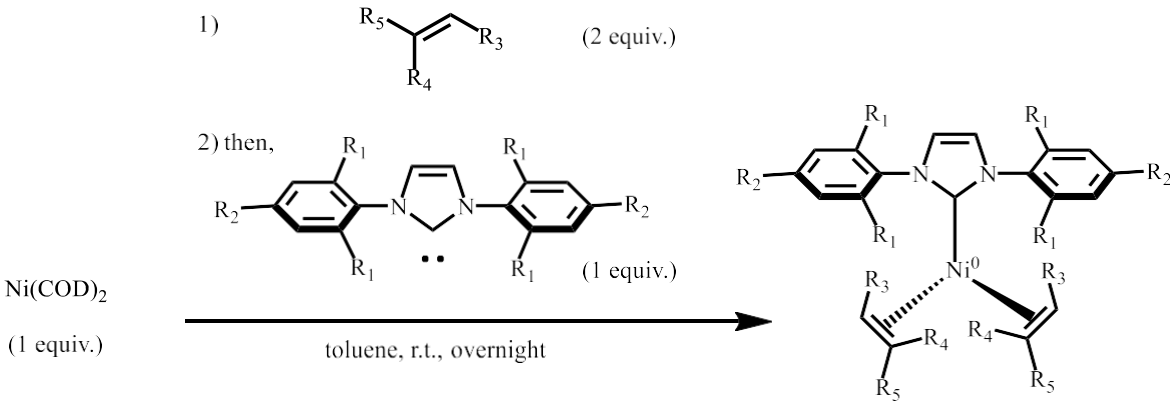

3-20, Ni(IMes)(dMeFu)$_2$: R_1, R_2 = -Me, R_3, R_5 = -CO2Me, R_4 = -H
3-21: Ni(IMes)(dEtFu)$_2$: R_1, R_2 = -Me, R_3, R_5 = -CO2Et, R_4 = -H
3-22: Ni(IMes)(d-*i*-*Pr*Fu)$_2$: R_1, R_2 = -Me, R_3, R_5 = -CO2*i*-Pr, R_4 = -H
3-23: Ni(IMes)(d-*i*-BuFu)$_2$: R_1, R_2 = -Me, R_3, R_5 = -CO2*i*-Bu, R_4 = -H
3-24: Ni(IMes)(d-*t*-BuFu)$_2$: R_1, R_2 = -Me, R_3, R_5 = -CO2*t*-Bu, R_4 = -H
3-25: Ni(IMes)(MA)$_2$: R_1, R_2 = -Me, R_3, R4 = -H, R_5 = -CO2Me,
3-26: Ni(IMes)(MMA)$_2$: R_1, R_2 = -Me, R_3 = -H, R_5 = -CO2Me, R_4 = -Me
3-27:Ni(IPr^{*OMe})(PhA)$_2$: R_1 = -CHPh$_2$. R_2 = -OMe, R_3, R_4 = -H, R_5 = -CO2Ph
3-28:Ni(IPr^{*OMe})(MA)$_2$: R_1 = -CHPh$_2$. R_2 = -OMe, R_3, R_4 = -H, R_5 = -CO2Me
3-2910: Ni(IPr)(MA)$_2$: R_1 = -*i*-Pr, R_2, R_3, R_4 = -H, R_5 = -CO2Me
3-30: Ni(IPr)(MMA)$_2$: R_1 = -*i*-Pr, R_2, R_3, = -H, R_4 = -Me, R_5 = -CO2Me
3-31: Ni(IPr)(PhA)$_2$: R_1 = -*i*-Pr, R_2, R_3, R_4 = -H, R_5 = -CO2Ph
3-32: Ni(IPr)(MA)$_2$: R_1 = -*i*-Pr, R_2, R_3, R_4 = -H, R_5 = -CO2Me
3-33: Ni(IPr)(PhA)$_2$: R_1 = -*i*-Pr, R_2, R_3, R_4 = -H, R_5 = -CO2P3

Figure 3-20. Discrete Ni(0)-NHC catalysts developed by Montgomery and co-workers.

Once a library of discrete Ni(0)-NHC catalysts was synthesized, their utility in the context of a reductive coupling of aldehydes and alkynes. Reaction progression analysis over an hour of reductive couplings was conducted for catalysts **3-20** to **3-26**. **3-20** and **3-21** showed little to no product formation, while **3-22** and **3-23** provided moderate yields, with **3-24 to 3-26** providing excellent yields. In a separate experiment, catalysts **3-21 to 3-26** were exposed to air for 24 hours and the reaction progression analysis repeated. Catalysts **3-22** and **3-25** were completely incompetent. While **3-21** and **3-23** performed comparably to the experiment when they were not exposed to air. **3-26** still provided some product, though in greatly reduced quantities. Catalyst **3-24** gave identical performance. While the air stability of **3-24** for greater lengths of time is

unknown, it is clear that the d-*t*-butyl fumarate ancillary ligand is unique in balancing reactivity with stability.[83]

Since the initial report, other groups have made important contributions to the literature. Though these are not discrete complexes, they do carry the advantage of being incredibly air-stable and undergo facile ligand substitution. Both the Engel and Cornella groups utilized the same strategy as the previously reported air-stable Ni(0) pre-catalysts to confer air-stability onto the catalyst by employing strong π-acids. Notably, both protocols utilize a Ni(II) source as the source of nickel for their synthesis (Figure 3-21).

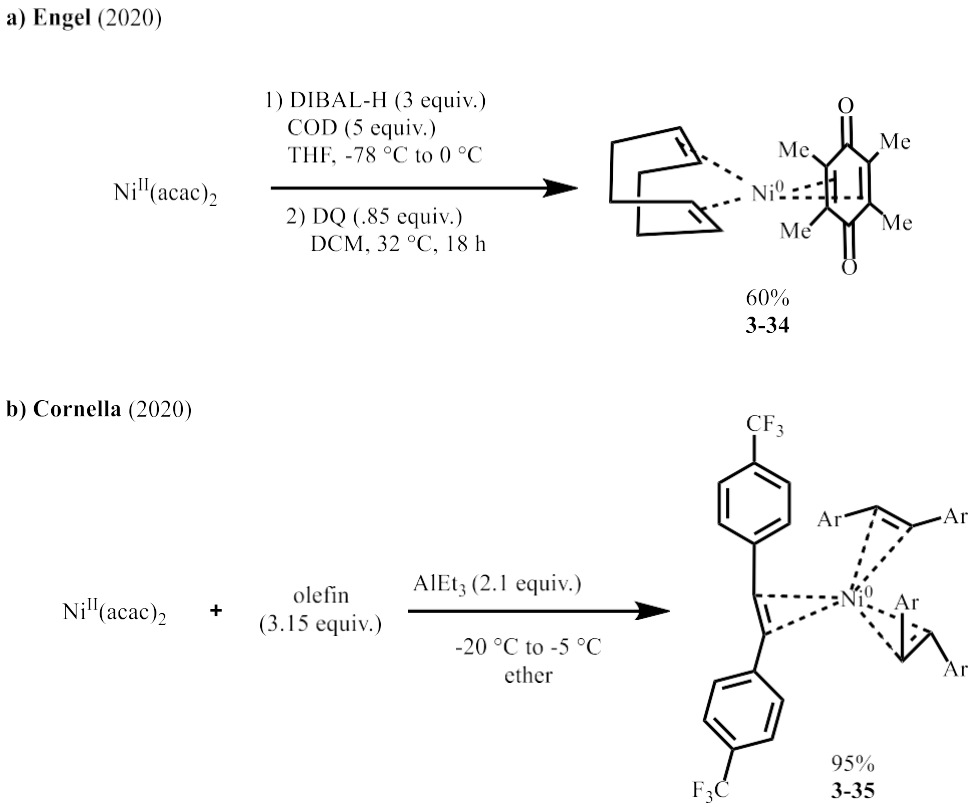

Figure 3-21. Examples of other air-stable Ni(0) pre-catalysts.

In work by Engel and co-workers, success was found in employing dihydroquinone (DQ) in combination with COD to create an 18-electron, air-stable Ni(0) complex. This contrasted work

by the Cornella group, which utilized electron deficient stilbenes as ligand to create air-stable 16-electron Ni(0) complexes. The competency of both catalysts was assessed in the context of several cross-coupling protocols and benchmarked against $Ni(COD)_2$ catalysts systems. The air-stable systems performed just as well if not better than $Ni(COD)_2$ in most cases.

3.5 Results and Discussion

3.5.1 Introduction

Though our group has been successful in designing air-stable, discrete Ni(0)-NHC catalysts, a limitation is that our synthesis currently relies upon $Ni(COD)_2$ and NHC free carbenes. These two measures limit the ability of others to readily synthesize these complexes and drive up the costs. With these considerations in mind, we were highly motivated to overcome these limitations.

3.5.2 Synthesis of Ni(IMes)(d-*t*-BuFu)$_2$ from the NHC Salt

An opportunity arose to enter another commercial partnership, wherein I provided 8g of catalyst **3-24** on a pilot scale. While synthesizing our patented catalyst from both Ni(II) and NHC salts would not have been on a viable time scale, at least making the improvement of utilizing the NHC salt seemed worthwhile to attempt (Figure 3-22).

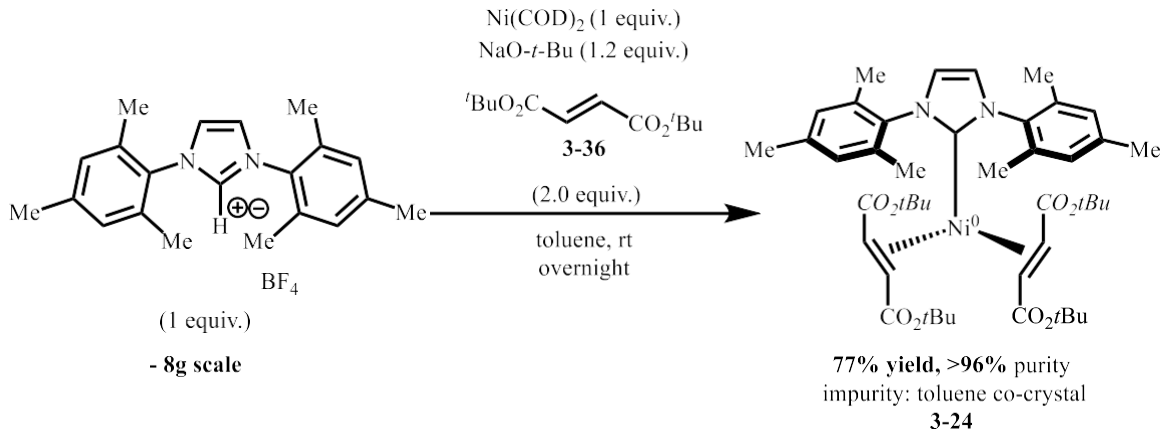

Figure 3-22. Large scale synthesis of Ni(IMes)(di-*t*-BuFu)$_2$ from the NHC salt.

To our excitement, this was easily achieved simply by pre-stirring the NHC salt with NaO-*t*-Bu for hours prior to adding the slurry to the wine, red solution Ni(COD)$_2$ and fumarate as per the usual protocol on a large scale.

3.5.3 Attempts to Form the Air-Stable Ni(IMes)(d-*t*-BuFu)$_2$ Complex from Ni(II) Salts Utilizing Ni(COD)$_2$ as a Transient Intermediate

The next challenge to address was synthesizing the discrete catalyst from Ni(II) salts. Initial attempts began with forming Ni(COD)$_2$ to serve as a transient intermediate from Ni(II) salts in a one-pot protocol (Figure 3-14). To realize this goal, an adaptation of the Baker protocol, which used $Ni^{II}(acac)_2$ as the source of nickel and *n*-dibutylmagnesium as the reductant was explored (Figure 3-23).

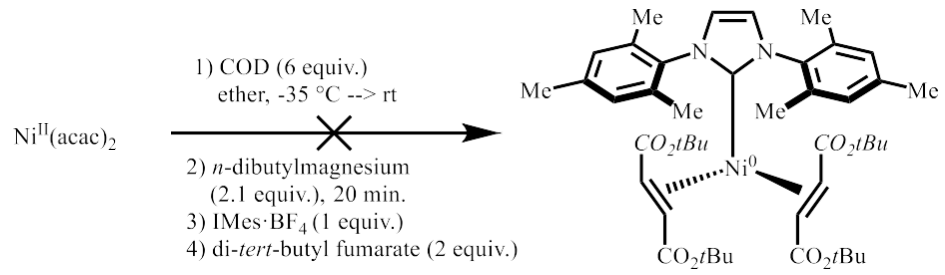

3-24

Figure 3-23. One-pot protocol for the synthesis of Ni(IMes)(di-*t*-BuFu)$_2$ via *n*-dibutylmagnesium.

After step 2, it was clear that Ni(COD)$_2$ had been formed as the solution turned the characteristic bright, orangish-yellow hue. In a departure from the typical protocol, the NHC salt was added first, because it was hypothesized that the remaining dibutyl magnesium would deprotonate the NHC, thus also quenching itself. This way, the fumarate could be added later with minimum threat of being destroyed. Unfortunately, this sequence of events led to the solution turning a dark brown color and only grey residues were isolated, indicating decomposition.

Alternatively, we were also intrigued by the Murakami protocol, which also utilized Ni^{II}(acac)$_2$ as the Ni(II) source. Where their strategy diverged, however, was that the reaction relied upon reduction of the Ni(II) salt by the formation of ketyl radicals that resulted from the deprotonation of a diol, which was generated by dimerization of xanthone under *hv* light. This reaction also worked well as described by Murakami and co-workers yielding by the characteristic orangish, yellow hue of Ni(COD)$_2$ after introducing methanol to quench the ketyl radicals, which caused the solution to be blue prior to the quench (Figure 3-24). This time, fumarate was added, followed by the NHC salt that had been pre-stirred with addition base. Once again, however, nothing desirable could be isolated from the complex reaction mixture.

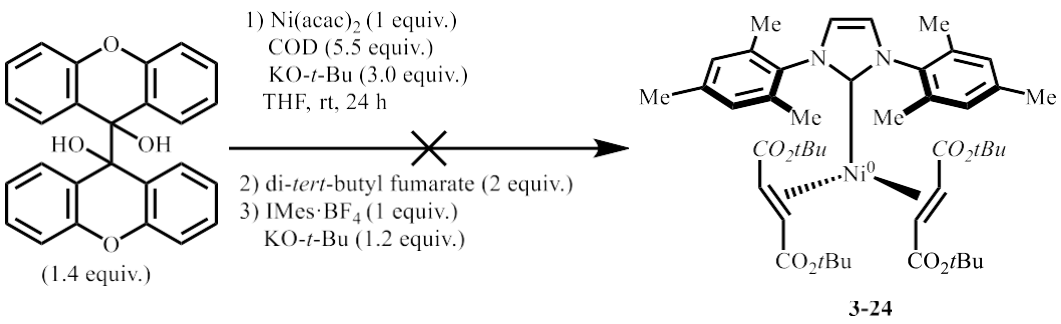

Figure 3-24. One-pot synthesis of Ni(IMes)(di-*t*-BuFu)$_2$ via the Murakami protocol.

The common denominator of both protocols is that the stoichiometry of both reactions is based upon the assumption that there is 100% formation of Ni(COD)$_2$. However, neither protocol provides full conversion of Ni(COD)$_2$, therefore the addition of 1 equivalent of NHC is likely to create both mono and bis-ligated Ni(0)-NHC complexes. Although the desired product is most likely formed after the addition of 2 equivalents of fumarate, the reaction mixture is complex and so the isolation of desired material was not possible. Therefore, the next approach would need to ensure that a 1:1 ratio of ligand to metal was established from the on-set.

3.5.4 Synthesizing the Air-Stable Ni(IMes)(d-*t*-BuFu)$_2$ Complex from Ni(II) Salts Utilizing Ni(IMes)(1,5-hexadiene) as a Transient Intermediate

To first asses the feasibility of attaining Ni(IMes)(d-*tert*-BuFu)$_2$ from Ni(IMes)(1,5-hexadiene), fumarate was added to a solution of Ni(IMes)(1,5-hexadiene) suspended in THF (Figure 3-25).

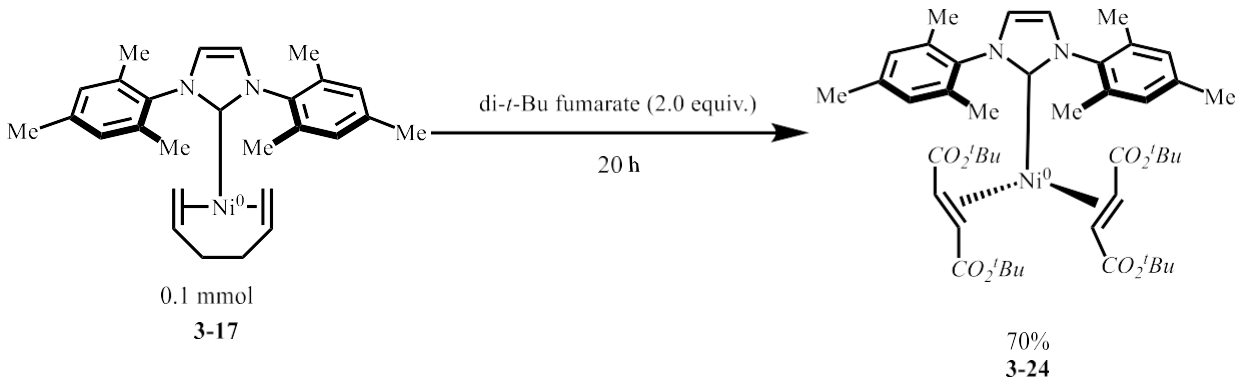

Figure 3-25. Synthesis of Ni(IMes)(di-*t*-BuFu)$_2$ from Ni(IMes)(1,5-hexadiene).

The reaction mixture immediately showed a favorable color transition upon the addition of fumarate signaling the formation of the desired Ni(0)-NHC complex and this was confirmed via isolation. We were next interested in synthesizing Ni(IMes)(d-*t*-BuFu)$_2$ in a one-pot protocol via this route. The issue regarding unknown stoichiometry of nickel to NHC in the aforementioned strategies was eliminated by pre-stirring $NiCl_2$ with the free carbene of IMes for 30 minutes to create the discrete Ni(II)-IMes complex before the addition of allyl Grignard reagent (Figure 3-26). By using 1.7 equivalents of allyl Grignard, it was ensured that no additional Grignard is left if the reaction mixture post addition, leaving no need for quenching steps later in the process. At the conclusion of this step, a 16 electron Ni(0)(1,5-hexadiene) complex is formed. Subsequent addition of fumarate provides the desired product.

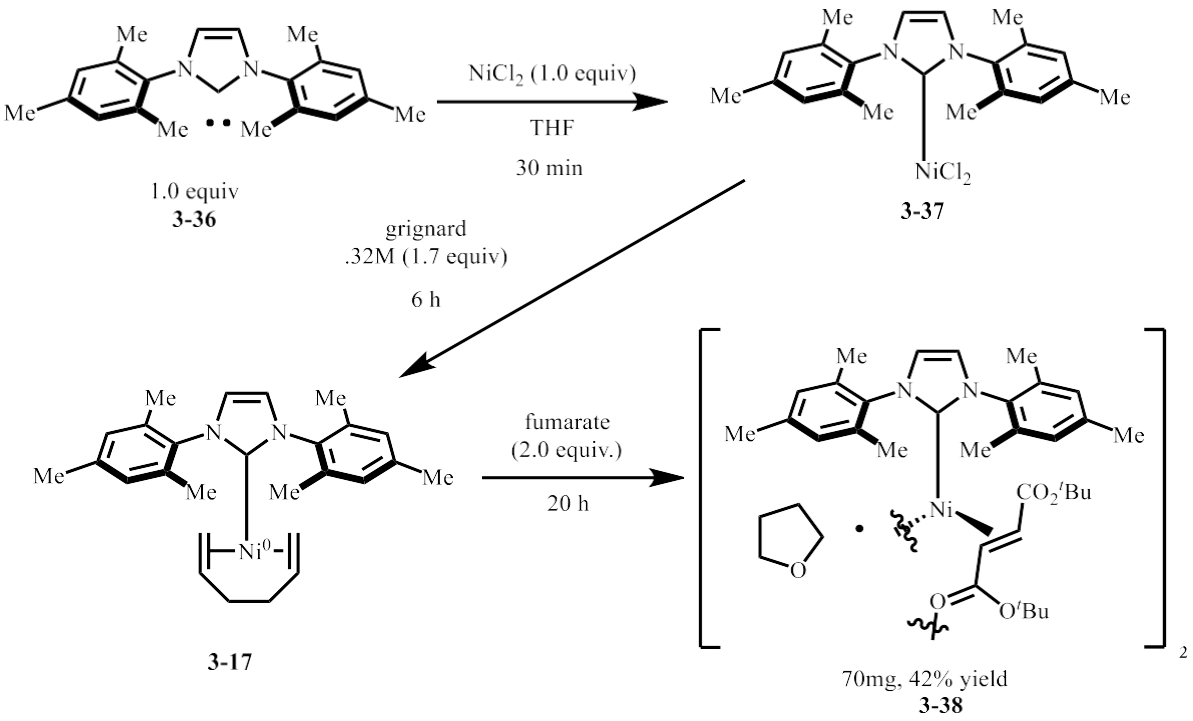

Figure 3-26. One-pot synthesis of Ni(IMes)(di-*t*-BuFu)$_2$ from Ni(II) salts.

Interestingly, the attempt to furnish **3-24** provided a complex that was purple in contrast with the darker orange of the known compound, **3-38**. ^{1}H NMR analysis suggests the formation of a dimeric complex as the ratio of NHC to tetrahydrofuran (THF) to fumarate is 1:1:1. This is precedented in the case of Ni(0)-NHC complexes with fumarates that possess a methyl group on the backbone. To further investigate this, several control reactions were executed, beginning with subjecting the idependantly synthesized Ni(IMes)(di-*tert*-BuFu)$_2$ complex to allylmagnesium chloride. The result was that the darkish orange solution formed a darkish, brown signifying some decomposition (Figure 3-27).

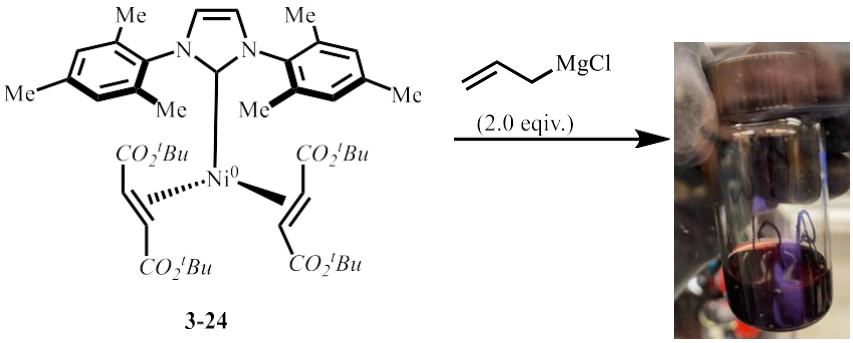

Figure 3-27. Addition of allyl Grignard to the independently synthesized Ni(IMes)(di-*t*-BuFu)$_2$ complex.

Conversiely, when 2 equivalents of magnesium chloride was added to the independantly synthesized complex, **3-24**, the darkish orange solution turned to the same, vibrant purple as was identified in the synthesis that utilized the allyl Grignard (Figure 3-28).

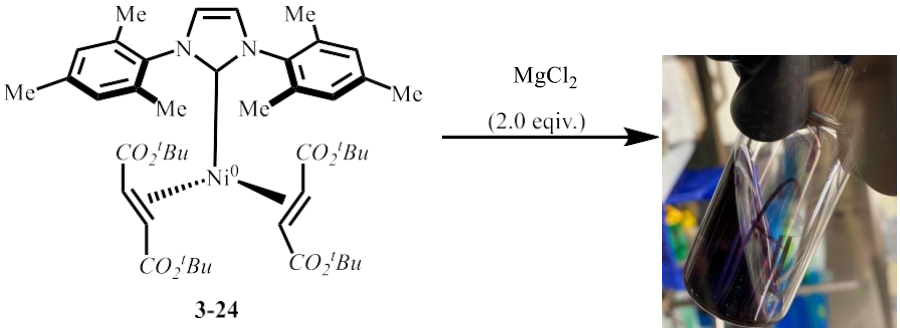

Figure 3-28. Addition of $MgCl_2$ to the independently synthesized Ni(IMes)(di-*t*-BuFu)$_2$ complex.

This result is of great import as it suggests that the formation of the dimeric complex is thermodynamically favorable and as such has implications regarding the performance of these compounds moving forward. One such benefit to performance could be that less stable discrete Ni(0) pre-catalysts that posses acrylates as opposed to fumarates as ancillary ligands may possess better air stability in their dimeric form, while still posessing higher reactivity while in solution.

3.6 Conclusions of Results and Discussion

The preliminary results of this project are highly encouraging, as 1) our discrete complexes, at least in the case of Ni(IMes)(d-*t*-BuFu)$_2$, can be synthesized from Ni(II) and NHC salts, and 2) unexpected dimer formation appears to occur in the presence of $MgCl_2$ as indicated by ^{1}H NMR. Although significant progress has been made, this work is in the early stages of development and more studies are required to unequivocally confirm the product and extend this chemistry to broader uses. Current efforts are aimed towards conducting extensive characterization of the alleged dimeric nickel complex. Future work would be best directed towards assessing the competency of this new complex in the context of catalytic reactions. Finally, more work needs to be done to understand if and how many other complexes can be formed into dimers by the addition of $MgCl_2$. Given that this occurs spontaneously, it is a thermodynamically favorable process and the implications of this need to be determined as they could have intriguing consequences on the stability of otherwise less stable catalyst systems like in the case of monomeric discrete nickel acrylate catalysts. However, once complete, this work shall encompass the three most desirable qualities of a discrete Ni(0) pre-catalysts being 1) air-stability, 2) possessing a well-defined catalyst structure, and 3) being sourced from cheap, and accessible starting materials.

Chapter 4

Supporting Information

4.1 General Experimental Details

Unless otherwise noted, all reactions were run in flame-dried or oven-dried (140 °C) sealed culture tubes equipped with magnetic stirrers, that were sealed in the glovebox. Solvents were purified under nitrogen using a solvent purification system (Innovative Technology, Inc. Model # SPS400-3 and PS-400-3) and sparged with nitrogen for one hour or distilled over calcium hydride and sparged with nitrogen for one hour. Diboron species (Combi-Blocks) were recrystallized from pentane, dried under high-vacuum for at least 4 hours before storing in a nitrogen filled glovebox. All silyloxyarenes and benyl silyl ethers were dried for at least four hours under high vacuum, before storage in an inert atmosphere glovebox. Anhydrous $Ni(acac)_2$ (Strem Chemicals), $Ni(COD)_2$ (Strem Chemicals), IPrMe·HCl (made from known procedure)[12,13], IMesMe·HCl (made from known procedure)[13], ICy·HCl (Sigma-Aldrich), IAd·HCl (Sigma-Aldrich), IPrCl·HCl (made from known procedure)[13], IPr·HCl (made from known procedure)[13], IMes·HCl (made from known procedure) [13], IPr*OMe·HCl (made from known procedure)[13], and *tert*-butoxide bases (Strem Chemicals) were stored and weighed in an inert atmosphere glovebox.

Analytical thin layer chromatography (TLC) was performed on Kieselgel 60 F254 (250 μm silica gel) glass plates and compounds were visualized with UV light and potassium permanganate stain. Flash column chromatography was performed using Kieselgel 60 (230-400 mesh) silica gel. As boronic esters have been known to partially decompose on silica gel, Kieselgel 60 (230-400 mesh) silica gel was often used instead, which was prepared from a reported procedure.[84] For many

substrates, improved yields ranging from 5-15% could be observed when the boric acid impregnated silica gel was employed. Eluent mixtures are reported as v:v percentages of the minor constituent in the major constituent. All compounds purified by column chromatography by hand, or on the biotage with hexanes/ethyl acetate and were sufficiently pure for use in further experiments unless otherwise indicated.

^{1}H NMR spectra were collected at 400 MHz on a Varian MR400, at 500 MHz on a Varian Inova 500 or Varian vnmrs 500, or at 700 MHz on a Varian vnmrs 700 instruments. The proton signal of the residual, non-deuterated solvent (δ 7.26 for $CHCl_3$ or 7.15 for C_6D_6) was used as the internal reference for ^{1}H NMR spectra. ^{13}C NMR spectra were completely heterodecoupled and measured at 126 MHz or 176 MHz. Chloroform-d (δ 77.00) was used as an internal reference. ^{11}B NMR spectra were collected at 128 MHz or 160 MHz. Note: The ^{13}C NMR signal for carbons attached to boron did not appear in the collected spectra due to the quadruple splitting of ^{11}B. High resolution mass spectra were recorded on a VG 70-250-s spectrometer manufactured by Micromass Corp. (Manchester UK) at the University of Michigan Mass Spectrometry Laboratory. GCMS analysis was carried out on a HP 6980 Series GC system with HP-5MS column (30 m x 0.250 mm x 0.25 μm). GC-FID analysis was carried out on a HP 6980N Series GC system with a HP-5 column (30 m x 0.32 mm x 0.25 μm).

4.2 Experimental Details for Chapter 2

4.2.1 General Procedures (A-B) for Chapter 2

4.2.1.1 General Procedure for the synthesis of silyloxyarenes (A):

In a round bottom flask, aryl alcohol (1 equiv.) was dissolved in DMF or CH_2Cl_2 (5.0 mL). The solution was then charged with imidazole (2 equiv.) and *tert*-butyldimethylchlorosilane (1.5 equiv.) and stirred until the starting alcohol was fully consumed. The reaction was diluted with 25 mL Et_2O or CH_2Cl_2, washed with deionized H_2O (3 × 25 mL), dried over Na_2SO_4, filtered, concentrated under reduced pressure, and purified by flash column chromatography (hexanes/ethyl acetate)on silica gel to afford the aryl silyl ether.

4.2.1.2 General Procedure for the $Ni(acac)_2$/IPr^{Me}•HCl promoted borylation of silyloxyarenes using B_2pin_2 (B):

In an inert atmosphere glovebox, a glass culture tube equipped with magnetic stir bar was charged with aryl silyl ether (1.0 equiv.), $Ni(acac)_2$ (10 mol%), IPr^{Me}•HCl (20 mol%), LiO-*t*-Bu (2.5 equiv.), B_2pin_2 (2.5 equiv.), and *c*-pentyl methyl ether (CPME) (0.3 M). The sealed culture tube was brought outside the glovebox and placed in a heated block set to 100 °C and stirred for 16 h, unless noted otherwise. The mixture was cooled to rt, diluted with EtOAc (3 mL). The mixture was then run through a silica plug, concentrated under reduced pressure, and purified by flash column chromatography (hexanes/ethyl acetate) on silica gel or boric acid impregnated silica gel to afford the desired product.

4.2.2 Discussion of C–H Over-borylation

4.2.2.1 Discussion regarding over-borylation and borylation of arene solvent (Figure 4-1):

We observed that toluene solvent undergoes C(sp^2) borylation under the reaction conditions to generate regioisomers of borylated toluene as byproducts in our initial reaction conditions for the borylation of silyloxyarenes. Chatani, and Itami[67,85] had previously reported the borylation of non-acidic, undirected C-H bonds (see S61for spectra). We found that the toluene solvent (ts1) could be borylated and that the silyloxyarenes could become over-borylated, thereby diminishing the yield of desired product. These appeared as a mixture of regioisomers, which are in accordance with the literature. This ultimately led to the utilization of CPME instead, which is inert to the reaction conditions and suppresses over-borylation.

The naphthyl systems and biphenyl systems lacking substitution at the 4–position was most prone to over-borylation, while isolated aromatic systems showed little of this byproduct. One such example of this is in the over-borylation of product **1**. See page 165 for spectra.

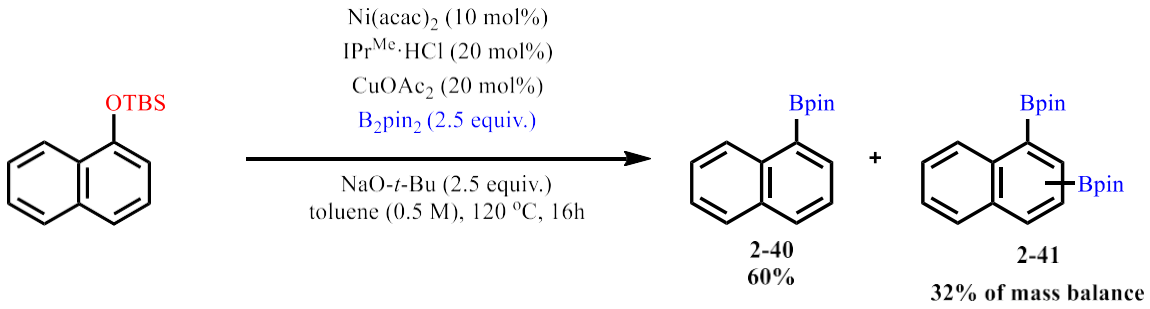

Figure 4-1. Over-borylation of desired product and solvent.

HRMS(EI-AutoSpec-Q) m/z: [M] calc'd for $C_{22}H_{30}B_2O_4$ 380.2330; found 380.2330.

4.2.3 Known Starting Material for Chapter 2

The following substrates were prepared according to literature procedures:

tert-butyldimethyl(naphthalen-2-yloxy)silane[13]

tert-butyldimethyl(naphthalen-1-yloxy)silane[13]

([1,1'-biphenyl]-3-yloxy)(*tert*-butyl)dimethylsilane[13]

([1,1'-biphenyl]-4-yloxy)(*tert*-butyl)dimethylsilane[13]

tert-butyldimethyl(phenoxy)silane[86]

tert-butyl(4-(*tert*-butyl)phenoxy)dimethylsilane[13]

tert-butyldimethyl(o-tolyloxy)silane[87]

tert-butyl(2-ethylphenoxy)dimethylsilane[88]

([1,1'-biphenyl]-2-yloxy)(*tert*-butyl)dimethylsilane[89]

tert-butyldimethyl((3-methyl-[1,1'-biphenyl]-4-yl)oxy)silane[12]

tert-butyldimethyl((5,6,7,8-tetrahydronaphthalen-2-yl)oxy)silane[2]

tert-butyl(4-methoxyphenoxy)dimethylsilane[90]

tert-butyl(3-methoxyphenoxy)dimethylsilane[91]

4-((*tert*-butyldimethylsilyl)oxy)-N,N-dimethylaniline[92]

4-(3-((*tert*-butyldimethylsilyl)oxy)phenyl)morpholine[13]

3-((*tert*-butyldimethylsilyl)oxy)aniline[93]

2-((*tert*-butyldimethylsilyl)oxy)-9H-carbazole[13]

2-(4-((*tert*-butyldimethylsilyl)oxy)phenyl)pyridine[13]

tert-butyl((4'-((*tert*-butyldimethylsilyl)oxy)-[1,1'-biphenyl]-4-yl)methoxy)dimethylsilane[13]

tert-butyldimethyl(naphthalen-2-ylmethoxy)silane[93]

(benzyloxy)(*tert*-butyl)dimethylsilane[94]

tert-butyl((3-methoxybenzyl)oxy)dimethylsilane[95]

([1,1'-biphenyl]-4-ylmethoxy)(tert-butyl)dimethylsilane[13]

4.2.4 New Starting Material for Chapter 2

1-(3-((*tert*-butyldimethylsilyl)oxy)phenyl)-1H-indole (2-72):

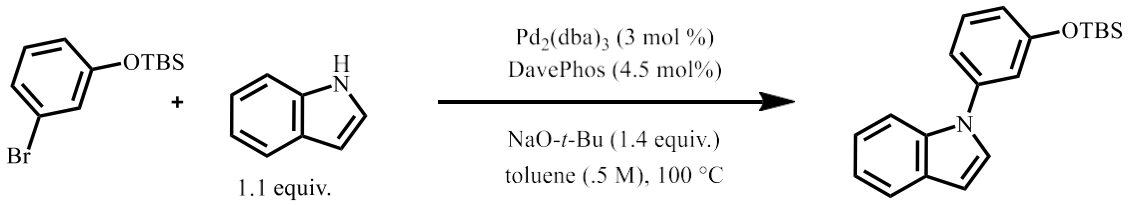

Figure 4-2. Synthesis of *n*-arylated indole substrate.

Using a modified procedure,[69] an oven-dried microwave vial was charged with $Pd_2(dba)_3$ (96 mg, 0.11 mmol), DavePhos (54 mg, 0.16 mmol, 4.5 mol %), indole (452 mg, 3.85 mmol), and NaO-*t*-Bu (67 mg, 0.7 mmol). The test tube was capped with a septum, purged with argon, (3-bromophenoxy)(*tert*-butyl)dimethylsilane (1.0 g, 3.5 mmol) followed by toluene (7 mL, 0.5 M) The sealed microwave vial was removed from the glovebox, and reaction mixture was heated at 100 °C in an oil bath with stirring for 16 h. The reaction mixture was cooled to room temperature, diluted with diethyl ether, filtered through a pad of celite, and concentrated in vacuo. The crude residue was purified by flash chromatography on silica gel (hexanes and ethyl acetate) providing a clear oil (0.9 g, 80% yield).

^{1}H NMR (500 MHz, $CDCl_3$) δ 7.68 (d, *J* = 7.8 Hz, 1H), 7.59 (d, *J* = 8.2 Hz, 1H), 7.35 (t, *J* = 8.0 Hz, 1H), 7.33 (d, *J* = 3.2 Hz, 1H), 7.26 – 7.20 (m, 1H), 7.20 – 7.14 (m, 1H), 7.14 – 7.05 (m, 1H), 6.99 (t, *J* = 2.2 Hz, 1H), 6.84 (ddd, *J* = 8.2, 2.4, 1.1 Hz, 1H), 6.67 (d, *J* = 3.2 Hz, 1H), 1.01 (s, 9H), 0.25 (d, *J* = 1.0 Hz, 6H).

^{13}C NMR (126 MHz, $CDCl_3$) δ 156.7, 140.9, 135.8, 130.2, 129.3, 127.9, 122.3, 121.1, 120.3, 118.2, 117.3, 116.2, 110.6, 103.5, 25.7, 18.2, -4.3.

HRMS(ESI-TOF) m/z: $[M+H]^+$ calc'd for $C_{20}H_{25}NOSi$ 324.1784; found, 324.1777.

4.2.5 Borylation of Silyloxyarenes

4,4,5,5-tetramethyl-2-(naphthalen-1-yl)-1,3,2-dioxaborolane; compound, 2-40

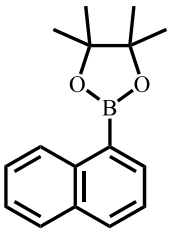

Following general procedure B, $Ni(acac)_2$ (7.7 mg, 0.03 mmol), IPr^{Me}•HCl (27.2 mg, 0.06 mmol), LiO-*t*-Bu (60.0 mg, 0.75 mmol), B_2pin_2 (192.0 mg, 75 mmol), and *tert*-butyldimethyl(naphthalen-1-yloxy)silane (77.4 mg, 0.3 mmol) at 100 °C for 16 h gave a crude residue which was purified by flash chromatography (hexanes/ethyl acetate) to afford the desired product as a white solid (46.5 mg, 0.183 mmol, 55% yield) as the average of three trials.

^{1}H NMR (500 MHz, $CDCl_3$): δ 8.84 – 8.64 (m, 1H), 8.08 (dd, *J* = 6.9, 1.4 Hz, 1H), 7.93 (d, *J* = 8.2 Hz, 1H), 7.83 (dd, *J* = 8.3, 1.4 Hz, 1H), 7.59 – 7.37 (m, 3H), 1.43 (s, 12H).

^{13}C NMR (126 MHz, $CDCl_3$): δ 136.1, 134.9, 132.4, 130.8, 127.6, 127.5, 125.5, 124.7, 124.2, 82.9, 24.2. The carbon directly attached to the boron atom was not detected due to quadrupolar broadening.

^{11}B NMR (128 MHz, $CDCl_3$): δ 31.5.

The spectral data matched the literature.[96]

4,4,5,5-tetramethyl-2-(naphthalen-2-yl)-1,3,2-dioxaborolane; compound, 2-43

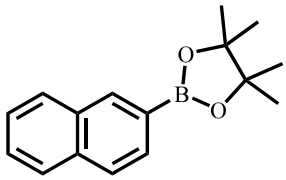

Following general procedure B, $Ni(acac)_2$ (7.7 mg, 0.03 mmol), IPr^{Me}•HCl (27.2 mg, 0.06 mmol), LiO-*t*-Bu (60.0 mg, 0.75 mmol), B_2pin_2 (192.0 mg, 75 mmol), and *tert*-butyldimethyl(naphthalen-2-yloxy)silane (77.4 mg, 0.3 mmol) at 100 °C for 16 h gave a crude residue which was purified by flash chromatography (hexanes/ethyl acetate) to afford the desired product as a white solid (45.7 mg, 0.18 mmol, 60% yield).

^{1}H NMR (700 MHz, $CDCl_3$): δ 8.37 (d, *J* = 3.6 Hz, 1H), 7.88 (d, *J* = 7.4 Hz, 1H), 7.83 (dd, *J* = 5.7, 3.3 Hz, 3H), 7.53 – 7.44 (m, 2H), 1.39 (dd, *J* = 3.7, 2.0 Hz, 12H).

^{13}C NMR (176 MHz, $CDCl_3$): δ 136.3, 135.1, 132.8, 130.4, 128.7, 127.7, 127.0, 127.0, 125.8, 83.9, 24.9. The carbon directly attached to the boron atom was not detected due to quadrupolar broadening.

^{11}B NMR (128 MHz, $CDCl_3$): δ 30.4.

The spectral data matched the literature. [96]

2-([1,1'-biphenyl]-3-yl)-4,4,5,5-tetramethyl-1,3,2-dioxaborolane; compound, 2-42

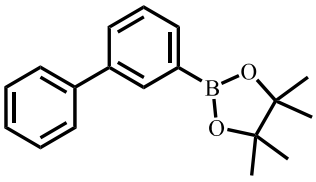

Following general procedure B, $Ni(acac)_2$ (7.7 mg, 0.03 mmol), IPr^{Me}•HCl (27.2 mg, 0.06 mmol), LiO-*t*-Bu (60.0 mg, 0.75 mmol), B_2pin_2 (192.0 mg, 75 mmol), and ([1,1'-biphenyl]-3-yloxy)(*tert*-butyl)dimethylsilane (85.3 mg, 0.3 mmol) at 100 °C for 16 h gave a crude residue

which was purified by flash chromatography (hexanes/ethyl acetate) to afford the desired product as a colorless oil (59.6 mg, 0.21 mmol, 68% yield) as an average over two trials.

^{1}H NMR (500 MHz, $CDCl_3$): δ 8.05 (d, *J* = 1.9 Hz, 1H), 7.79 (dt, *J* = 7.4, 1.3 Hz, 1H), 7.69 (dt, *J* = 7.9, 1.5 Hz, 1H), 7.65 – 7.58 (m, 2H), 7.44 (dt, *J* = 11.5, 7.7 Hz, 3H), 7.36 – 7.30 (m, 1H), 1.36 (s, 12H).

^{13}C NMR (176 MHz, $CDCl_3$): δ 141.2, 140.6, 133.7, 133.5, 130.0, 128.6, 128.2, 127.3, 127.2, 83.9, 24.9. The carbon directly attached to the boron atom was not detected due to quadrupolar broadening.

^{11}B NMR (128 MHz, $CDCl_3$): δ 31.0.

The spectral data matched the literature. [96]

2-([1,1'-biphenyl]-4-yl)-4,4,5,5-tetramethyl-1,3,2-dioxaborolane; compound, 2-44

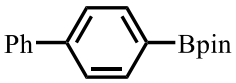

Following general procedure B, $Ni(acac)_2$ (7.7 mg, 0.03 mmol), IPr^{Me}•HCl (27.2 mg, 0.06 mmol), LiO-*t*-Bu (60.0 mg, 0.75 mmol), B_2pin_2 (192.0 mg, 75 mmol), and ([1,1'-biphenyl]-4-yloxy)(*tert*-butyl)dimethylsilane (85.3 mg, 0.3 mmol) at 100 °C for 16 h gave a crude residue which was purified by flash chromatography (hexanes/ethyl acetate) to afford the desired product as a white solid (78.7 mg, 0.28 mmol, 93% yield) as an average over two trials.

^{1}H NMR (500 MHz, $CDCl_3$): δ 7.89 (d, *J* = 7.9 Hz, 2H), 7.64 – 7.58 (m, 4H), 7.44 (t, *J* = 7.6 Hz, 2H), 7.36 (t, *J* = 7.4 Hz, 1H), 1.37 (s, 12H).

^{13}C NMR (126 MHz, $CDCl_3$): δ 143.4, 140.5, 135.2, 128.3, 127.0, 126.7, 126.0, 83.3, 24.4. The carbon directly attached to the boron atom was not detected due to quadrupolar broadening.

^{11}B NMR (128 MHz, $CDCl_3$): δ 30.8.

The spectral data matched the literature. [96]

4,4,5,5-tetramethyl-2-phenyl-1,3,2-dioxaborolane; compound, 2-45

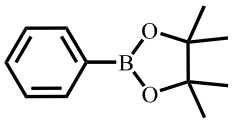

Following general procedure B, $Ni(acac)_2$ (7.7 mg, 0.03 mmol), IPr^{Me}•HCl (27.2 mg, 0.06 mmol), LiO-*t*-Bu (60.0 mg, 0.75 mmol), B_2pin_2 (192.0 mg, 75 mmol), *tert*-butyldimethyl(phenoxy)silane (62.5 mg, 0.3 mmol) at 100 °C for 16 h gave a crude residue which was purified by flash chromatography (hexanes/ethyl acetate) to afford the desired product as a colorless oil (49.0 mg, 0.21 mmol, 80% yield) as an average over three trials.

^{1}H NMR (500 MHz, $CDCl_3$): δ 7.81 (d, *J* = 7.1 Hz, 2H), 7.46 (t, *J* = 7.3 Hz, 1H), 7.37 (t, *J* = 7.2 Hz, 2H), 1.35 (s, 12H).

^{13}C NMR (126 MHz, $CDCl_3$): δ 134.3, 130.8, 127.3, 83.3, 24.4. The carbon directly attached to the boron atom was not detected due to quadrupolar broadening.

^{11}B NMR (128 MHz, $CDCl_3$): δ 30.9.

The spectral data matched the literature. [96]

2-(4-(*tert*-butyl)phenyl)-4,4,5,5-tetramethyl-1,3,2-dioxaborolane; compound, 2-46

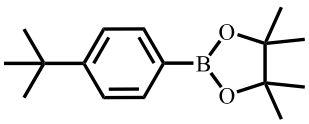

Following general procedure B, $Ni(acac)_2$ (7.7 mg, 0.03 mmol), IPr^{Me}•HCl (27.2 mg, 0.06 mmol), LiO-*t*-Bu (60.0 mg, 0.75 mmol), B_2pin_2 (192.0 mg, 75 mmol), and *tert*-butyl(4-(tert-

butyl)phenoxy)dimethylsilane (79.4 mg, 0.3 mmol) at 100 °C for 16 h gave a crude residue which was purified by flash chromatography (hexanes/ethyl acetate) to afford the desired product as a white solid (64.1 mg, 0.25 mmol, 83% yield) as an average over two trials.

^{1}H NMR (700 MHz, $CDCl_3$): δ 7.78 – 7.74 (m, 2H), 7.42 – 7.39 (m, 2H), 1.33 (d, *J* = 0.7 Hz, 12H), 1.32 (d, *J* = 0.7 Hz, 9H).

^{13}C NMR (176 MHz, $CDCl_3$): δ 154.5 134.7, 124.7, 83.6, 34.9, 31.2, 24.9. The carbon directly attached to the boron atom was not detected due to quadrupolar broadening.

^{11}B NMR (128 MHz, $CDCl_3$): δ 30.3.

The spectral data matched the literature. [96]

4,4,5,5-tetramethyl-2-(*o*-tolyl)-1,3,2-dioxaborolane; compound, 2-47

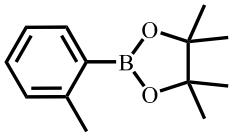

Following general procedure B, $Ni(acac)_2$ (7.7 mg, 0.03 mmol), IPr^{Me}•HCl (27.2 mg, 0.06 mmol), LiO-*t*-Bu (60.0 mg, 0.75 mmol), B_2pin_2 (192.0 mg, 75 mmol), *tert*-butyldimethyl(*o*-tolyloxy)silane (65.4 mg, 0.3 mmol) at 100 °C for 16 h gave a crude residue which was purified by flash chromatography (hexanes/ethyl acetate) to afford the desired product as a colorless oil (46.9 mg, 0.21 mmol, 75% yield) as an average over two trials.

^{1}H NMR (500 MHz, $CDCl_3$): δ 7.76 (d, *J* = 7.0 Hz, 1H), 7.31 (t, *J* = 7.0 Hz, 1H), 7.16 (d, *J* = 7.0 Hz, 2H), 2.54 (s, 3H), 1.34 (s, 12H).

^{13}C NMR (126 MHz, $CDCl_3$): δ 144.3, 135.4, 130.3, 129.3, 124.2, 82.9, 24.4, 21.7. The carbon directly attached to the boron atom was not detected due to quadrupolar broadening.

^{11}B NMR (128 MHz, $CDCl_3$): δ 31.0.

The spectral data matched the literature. [96]

2-(2-ethylphenyl)-4,4,5,5-tetramethyl-1,3,2-dioxaborolane; compound, 2-48

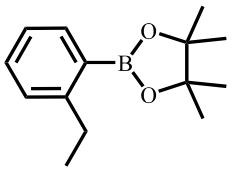

Following general procedure B, $Ni(acac)_2$ (7.7 mg, 0.03 mmol), IPr^{Me}•HCl (27.2 mg, 0.06 mmol), LiO-*t*-Bu (60.0 mg, 0.75 mmol), B_2pin_2 (192.0 mg, 75 mmol), *tert*-butyl(2-ethylphenoxy)dimethylsilane (70.9 mg, 0.3 mmol) at 100 °C for 16 h gave a crude residue which

was purified by flash chromatography (hexanes/ethyl acetate) to afford the desired product as a colorless oil (35.6 mg, 0.15 mmol, 51% yield) as an average over two trials.

^{1}H NMR (500 MHz, $CDCl_3$): δ 7.81 – 7.74 (m, 1H), 7.39 – 7.33 (m, 1H), 7.22 – 7.14 (m, 2H), 2.91 (tt, *J* = 7.9, 4.8 Hz, 2H), 1.34 (s, 12H), 1.19 (ddt, *J* = 8.3, 6.4, 2.6 Hz, 3H).

^{13}C NMR (126 MHz, $CDCl_3$): δ 151.0, 135.5, 130.5, 127.9, 124.4, 82.9, 28.4, 24.4, 16.7. The carbon directly attached to the boron atom was not detected due to quadrupolar broadening.

^{11}B NMR (128 MHz, $CDCl_3$): δ 31.1.

The spectral data matched the literature.[97]

2-([1,1'-biphenyl]-2-yl)-4,4,5,5-tetramethyl-1,3,2-dioxaborolane; compound, 2-49

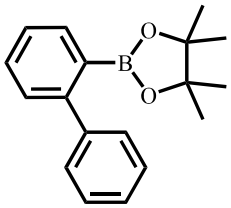

Following general procedure B, $Ni(acac)_2$ (7.7 mg, 0.03 mmol), IPr^{Me}•HCl (27.2 mg, 0.06 mmol), LiO-*t*-Bu (60.0 mg, 0.75 mmol), B_2pin_2 (192.0 mg, 75 mmol), and ([1,1'-biphenyl]-2-yloxy)(*tert*-butyl)dimethylsilane (85.3 mg, 0.3 mmol) at 100 °C for 16 h gave a crude residue which was purified by flash chromatography (hexanes/ethyl acetate) to afford the desired product as a colorless oil (57.0 mg, 0.21 mmol, 68% yield) as an average over two trials.

^{1}H NMR (700 MHz, $CDCl_3$): δ 7.71 (d, *J* = 7.6 Hz, 1H), 7.45 (t, *J* = 7.6 Hz, 1H), 7.41 – 7.31 (m, 7H), 1.20 (d, *J* = 2.4 Hz, 12H).

^{13}C NMR (176 MHz, $CDCl_3$): δ 147.0, 142.7, 133.9, 129.5, 128.6, 128.4, 127.2, 126.3, 125.8, 83.2, 24.4. The carbon directly attached to the boron atom was not detected due to quadrupolar broadening.

^{11}B NMR (128 MHz, $CDCl_3$): δ 31.4.

The spectral data matched the literature. [96]

4,4,5,5-tetramethyl-2-(3-methyl-[1,1'-biphenyl]-4-yl)-1,3,2-dioxaborolane; compound, 2-50

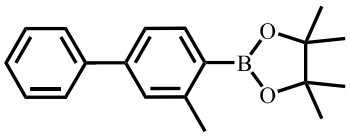

Following general procedure B, $Ni(acac)_2$ (7.7 mg, 0.03 mmol), IPr^{Me}•HCl (27.2 mg, 0.06 mmol), LiO-*t*-Bu (60.0 mg, 0.75 mmol), B_2pin_2 (192.0 mg, 75 mmol), and *tert*-butyldimethyl((3-methyl-[1,1'-biphenyl]-4-yl)oxy)silane (89.55 mg, 0.3 mmol) at 100 °C for 16 h gave a crude residue which was purified by flash chromatography (hexanes/ethyl acetate) to afford the desired product as a colorless oil (71.6 mg, 0.24 mmol, 81% yield).

^{1}H NMR (700 MHz, $CDCl_3$): 7.84 (d, *J* = 7.7 Hz, 1H), 7.61 (dd, *J* = 8.0, 1.4 Hz, 2H), 7.43 (t, *J* = 7.6 Hz, 2H), 7.40 (d, *J* = 7.0 Hz, 2H), 7.35 (d, *J* = 7.5 Hz, 1H), 2.61 (s, 3H), 1.36 (s, 12H).

^{13}C NMR (176 MHz, $CDCl_3$): δ 144.9, 142.9, 140.6, 136.0, 128.2, 128.1, 126.9, 126.7, 123.0, 82.9, 24.4, 21.9. The carbon directly attached to the boron atom was not detected due to quadrupolar broadening.

^{11}B NMR (128 MHz, $CDCl_3$): δ 31.0.

HRMS(EI-AutoSpec-Q) m/z: [M] calc'd for $C_{19}H_{23}BO_2$ 294.1791; found, 294.1791.

4,4,5,5-tetramethyl-2-(5,6,7,8-tetrahydronaphthalen-2-yl)-1,3,2-dioxaborolane;

compound, 2-51

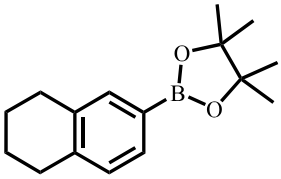

Following general procedure B, $Ni(acac)_2$ (7.7 mg, 0.03 mmol), IPr^{Me}•HCl (27.2 mg, 0.06 mmol), LiO-*t*-Bu (60.0 mg, 0.75 mmol), B_2pin_2 (192.0 mg, 75 mmol), and *tert*-butyldimethyl((5,6,7,8-tetrahydronaphthalen-2-yl)oxy)silane (78.7 mg, 0.3 mmol) at 100 °C for 16 h gave a crude residue which was purified by flash chromatography (hexanes/ethyl acetate) to afford the desired product as a colorless oil (61.9 mg, 0.24 mmol, 79% yield) as an average over three trials.

^{1}H NMR (700 MHz, $CDCl_3$): δ 7.55 – 7.50 (m, 2H), 7.08 (d, *J* = 7.5 Hz, 1H), 2.77 (d, *J* = 5.4 Hz, 4H), 1.79 (qd, *J* = 3.8, 1.8 Hz, 4H), 1.35 – 1.32 (m, 12H).

^{13}C NMR (176 MHz, $CDCl_3$): δ 140.3, 136.1, 135.3, 131.3, 128.2, 83.1, 29.2, 28.7, 24.4, 22.8, 22.7. The carbon directly attached to the boron atom was not detected due to quadrupolar broadening.

^{11}B NMR (128 MHz, $CDCl_3$): δ 30.8.

The spectral data matched the literature.[98]

2-(4-methoxyphenyl)-4,4,5,5-tetramethyl-1,3,2-dioxaborolane; compound, 2-52

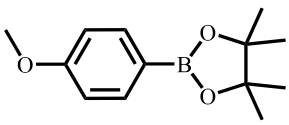

Following general procedure B, $Ni(acac)_2$ (7.7 mg, 0.03 mmol), IPr^{Me}•HCl (27.2 mg, 0.06 mmol), LiO-*t*-Bu (60.0 mg, 0.75 mmol), B_2pin_2 (192.0 mg, 75 mmol), and *tert*-butyl(4-methoxyphenoxy)dimethylsilane (71.4 mg, 0.3 mmol) at 100 °C for 16 h gave a crude residue which was purified by flash chromatography (hexanes/ethyl acetate) to afford the desired product and 12' as an inseparable mixture as a pale-yellow oil (17.6 mg, 0.08 mmol, 25% yield, 92% purity) as an average over two trials.

^{1}H NMR (700 MHz, $CDCl_3$): δ 7.77 – 7.73 (m, 2H), 6.91 – 6.87 (m, 2H), 3.82 (s, 3H), 1.33 (s, 12H). The peak at 7.80 ppm observable in the hard copy of the spectra belongs to the impurity, which was integrated to calculate percent purity.

^{13}C NMR (126 MHz, $CDCl_3$): δ 162.1, 136.5, 113.3, 83.5, 55.1, 24.9. The carbon directly attached to the boron atom was not detected due to quadrupolar broadening.

^{11}B NMR (160 MHz, $CDCl_3$) δ 30.4.

The spectral data matched the literature. [96]

1,4-bis(4,4,5,5-tetramethyl-1,3,2-dioxaborolan-2-yl)benzene; compound 2-52'

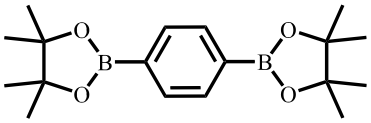

This product is formed in the reaction to make compound 2-52, which results from a subsequent borylation of the methoxy group. It tends to co-elute with compound 2-52, making isolation challenging, though it streaks enough such that it can be isolated separately accounting for 10% of the mass balance.

^{1}H NMR (500 MHz, $CDCl_3$) δ 7.80 (s, 4H), 1.35 (s, 24H).

^{13}C NMR (126 MHz, $CDCl_3$) δ 133.9, 83.8, 24.9.

^{11}B NMR (160 MHz, $CDCl_3$) δ 30.7. The carbon directly attached to the boron atom was not detected due to quadrupolar broadening.

The spectral data matched the literature. [96]

2-(3-methoxyphenyl)-4,4,5,5-tetramethyl-1,3,2-dioxaborolane; compound, 2-53

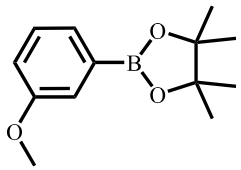

Following general procedure B, $Ni(acac)_2$ (7.7 mg, 0.03 mmol), IPr^{Me}•HCl (27.2 mg, 0.06 mmol), LiO-*t*-Bu (60.0 mg, 0.75 mmol), B_2pin_2 (192.0 mg, 75 mmol), and *tert*-butyl(3-methoxyphenoxy)dimethylsilane (71.4 mg, 0.3 mmol) at 100 °C for 16 h gave a crude residue which was purified by flash chromatography (hexanes/ethyl acetate) to afford the desired product as a pale-yellow oil (45.6 mg, 0.19 mmol, 65% yield) as an average over two trials.

^{1}H NMR (700 MHz, $CDCl_3$) δ 7.40 (dt, *J* = 7.3, 1.1 Hz, 1H), 7.33 (d, *J* = 2.8 Hz, 1H), 7.29 (dd, *J* = 8.2, 7.2 Hz, 1H), 7.01 (ddd, *J* = 8.2, 2.8, 1.1 Hz, 1H), 3.83 (s, 3H), 1.35 (s, 12H).

^{13}C NMR (176 MHz, $CDCl_3$) δ 159.0, 128.9, 127.2, 118.7, 117.9, 83.8, 55.2, 24.9. The carbon directly attached to the boron atom was not detected due to quadrupolar broadening.

^{11}B NMR (128 MHz, $CDCl_3$) δ 30.8.

The spectral data matched the literature. [96]

***N,N*-dimethyl-4-(4,4,5,5-tetramethyl-1,3,2-dioxaborolan-2-yl)aniline; compound, 2-54**

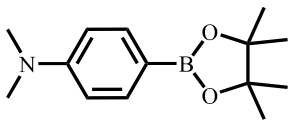

Following general procedure B, $Ni(acac)_2$ (7.7 mg, 0.03 mmol), IPr^{Me}•HCl (27.2 mg, 0.06 mmol), LiO-*t*-Bu (60.0 mg, 0.75 mmol), B_2pin_2 (192.0 mg, 75 mmol), and 4-((*tert*-butyldimethylsilyl)oxy)-*N*,*N*-dimethylaniline (75.4 mg, 0.3 mmol) at 100 °C for 16 h gave a crude residue which was purified by flash chromatography (hexanes/ethyl acetate) to afford the desired product as a white solid (30.3 mg, 0.12 mmol, 40% yield) as an average over two trials.

^{1}H NMR (400 MHz, $CDCl_3$): δ 7.72 – 7.67 (d, 2H), 6.69 (d, *J* = 8.1 Hz, 2H), 2.99 (s, 6H), 1.33 (d, *J* = 1.5 Hz, 12H).

^{13}C NMR (126 MHz, $CDCl_3$) δ 152.5, 136.1, 111.2, 83.2, 40.1, 24.8. The carbon directly attached to the boron atom was not detected due to quadrupolar broadening.

^{11}B NMR (160 MHz, $CDCl_3$) δ 30.9.

The spectral data matched the literature.[99]

4-(3-(4,4,5,5-tetramethyl-1,3,2-dioxaborolan-2-yl)phenyl)morpholine; compound, 2-55

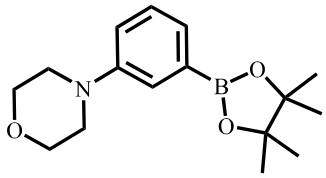

Following general procedure B, $Ni(acac)_2$ (7.7 mg, 0.03 mmol), IPr^{Me}•HCl (27.2 mg, 0.06 mmol), LiO-*t*-Bu (60.0 mg, 0.75 mmol), B_2pin_2 (192.0 mg, 75 mmol), and 4-(3-((*tert*-butyldimethylsilyl)oxy)phenyl)morpholine (86.7 mg, 0.3 mmol) at 100 °C for 16 h gave a crude residue which was purified by flash chromatography (hexanes/ethyl acetate) to afford the desired product as a clear oil (71.0 mg, 0.25 mmol, 83% yield) as an average over three trials.

^{1}H NMR (700 MHz, $CDCl_3$): δ 7.38 – 7.32 (m, 2H), 7.29 (t, *J* = 7.7 Hz, 1H), 7.02 (d, *J* = 8.2 Hz, 1H), 3.86 (t, *J* = 5.2 Hz, 4H), 3.19 (t, *J* = 4.4 Hz, 4H), 1.34 (d, *J* = 1.6 Hz, 12H).

^{13}C NMR (176 MHz, $CDCl_3$): δ 150.1, 128.0, 126.0, 121.2, 118.2, 83.1, 66.4, 48.9, 24.7. The carbon directly attached to the boron atom was not detected due to quadrupolar broadening.

^{11}B NMR (128 MHz, $CDCl_3$): δ 30.8.

The spectral data matched the literature.[100]

3-(4,4,5,5-tetramethyl-1,3,2-dioxaborolan-2-yl)aniline; compound, 2-56

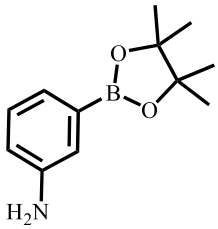

Following general procedure B, $Ni(acac)_2$ (7.7 mg, 0.03 mmol), IPr^{Me}•HCl (27.2 mg, 0.06 mmol), LiO-*t*-Bu (60.0 mg, 0.75 mmol), B_2pin_2 (192.0 mg, 75 mmol), 3-((*tert*-butyldimethylsilyl)oxy)aniline (67.0 mg, 0.3 mmol) at 100 °C for 16 h gave a crude residue which was purified by flash chromatography (hexanes/ethyl acetate) to afford the desired product as a colorless oil (18.4 mg, 0.08 mmol, 28% yield) as an average over two trials.

^{1}H NMR (700 MHz, $CDCl_3$): δ 7.21 (d, *J* = 7.4 Hz, 1H), 7.17 (td, *J* = 7.6, 2.5 Hz, 1H), 7.13 (d, *J* = 2.8 Hz, 1H), 6.79 (dd, *J* = 7.7, 3.2 Hz, 1H), 3.63 (s, 2H), 1.34 – 1.33 (m, 12H).

^{13}C NMR (176 MHz, $CDCl_3$): δ 145.5, 128.4, 124.7, 120.8, 117.8, 83.4, 24.6. The carbon directly attached to the boron atom was not detected due to quadrupolar broadening.

^{11}B NMR (128 MHz, $CDCl_3$): δ 31.0.

The spectral data matched the literature.[30]

9-methyl-2-(4,4,5,5-tetramethyl-1,3,2-dioxaborolan-2-yl)-9H-carbazole; compound, 2-57

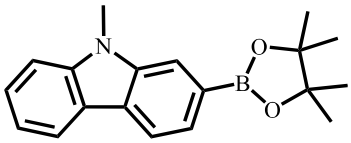

Following general procedure B, $Ni(acac)_2$ (7.7 mg, 0.03 mmol), IPr^{Me}•HCl (27.2 mg, 0.06 mmol), LiO-*t*-Bu (60.0 mg, 0.75 mmol), B_2pin_2 (192.0 mg, 75 mmol), 2-((*tert*-butyldimethylsilyl)oxy)-9-methyl-9H-carbazole (93.5 mg, 0.3 mmol) at 100 °C for 16 h gave a crude residue which was purified by flash chromatography (hexanes/ethyl acetate) to afford the desired product as a colorless oil (70.0 mg, 0.23 mmol, 76% yield) as an average over two trials.

^{1}H NMR (500 MHz, $CDCl_3$): δ 8.11 (t, *J* = 7.3 Hz, 2H), 7.90 (s, 1H), 7.70 (d, *J* = 7.7 Hz, 1H), 7.50 (t, *J* = 7.6 Hz, 1H), 7.41 (d, *J* = 8.3 Hz, 1H), 7.23 (t, *J* = 7.3 Hz, 1H), 3.90 (d, *J* = 2.6 Hz, 3H), 1.41 (d, *J* = 2.7 Hz, 12H).

^{13}C NMR (126 MHz, $CDCl_3$): δ 140.9, 140.0, 125.7, 124.7, 124.5, 122.0, 120.2, 119.0, 118.2, 114.4, 108.0, 83.2, 28.5, 24.4. The carbon directly attached to the boron atom was not detected due to quadrupolar broadening.

^{11}B NMR (128 MHz, $CDCl_3$): δ 31.4.

The spectral data matched the literature.[64]

2-(4-(4,4,5,5-tetramethyl-1,3,2-dioxaborolan-2-yl)phenyl)pyridine; compound, 2-58

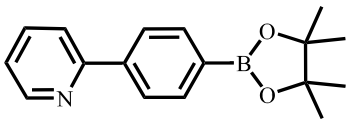

Following general procedure B, $Ni(acac)_2$ (7.7 mg, 0.03 mmol), IPr^{Me}•HCl (27.2 mg, 0.06 mmol), LiO-*t*-Bu (60.0 mg, 0.75 mmol), B_2pin_2 (192.0 mg, 75 mmol), 2-(4-((*tert*-butyldimethylsilyl)oxy)phenyl)pyridine (85.5 mg, 0.3 mmol) at 100 °C for 16 h gave a crude

residue which was purified by flash chromatography (hexanes/ethyl acetate) to afford the desired product as a colorless oil (41.3 mg, 0.15 mmol, 49% yield).

^{1}H NMR (500 MHz, $CDCl_3$) δ 8.74 (s, 1H), 8.02 (d, *J* = 7.8 Hz, 2H), 7.93 (d, *J* = 7.8 Hz, 2H), 7.81 (s, 2H), 7.29 (s, 1H), 1.37 (s, 12H)

^{13}C NMR (126 MHz, $CDCl_3$) δ 157.2, 149.7, 141.8, 136.8, 135.2, 126.1, 122.4, 120.9, 83.9, 24.9. The carbon directly attached to the boron atom was not detected due to quadrupolar broadening.

^{11}B NMR (160 MHz, $CDCl_3$) δ 30.6.

The spectral data matched the literature. [96]

1-(3-(4,4,5,5-tetramethyl-1,3,2-dioxaborolan-2-yl)phenyl)-1H-indole; compound, 2-59

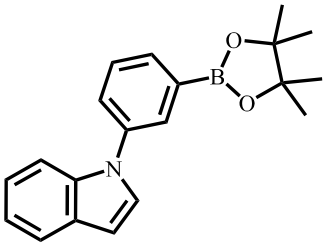

Following general procedure B, $Ni(acac)_2$ (7.7 mg, 0.03 mmol), IPr^{Me}•HCl (27.2 mg, 0.06 mmol), LiO-*t*-Bu (60.0 mg, 0.75 mmol), B_2pin_2 (192.0 mg, 75 mmol), 1-(3-((*tert*-butyldimethylsilyl)oxy)phenyl)-1H-indole (85.5 mg, 0.3 mmol) at 100 °C for 16 h gave a crude residue which was purified by flash chromatography (hexanes/ethyl acetate) to afford the desired product as a colorless oil (54.6 mg, 0.17 mmol, 57% yield).

^{1}H NMR (500 MHz, $CDCl_3$): δ 7.91 – 7.87 (m, 1H), 7.76 (dt, *J* = 7.3, 1.2 Hz, 1H), 7.65 (dt, *J* = 7.7, 1.0 Hz, 1H), 7.59 (ddd, *J* = 7.9, 2.3, 1.2 Hz, 1H), 7.53 – 7.47 (m, 2H), 7.34 (d, *J* = 3.2 Hz,

1H), 7.19 (ddd, *J* = 8.3, 7.0, 1.3 Hz, 1H), 7.13 (ddd, *J* = 7.9, 7.0, 1.1 Hz, 1H), 6.64 (dd, *J* = 3.3, 0.9 Hz, 1H), 1.33 (s, 12H).

^{13}C NMR (126 MHz, $CDCl_3$): δ 138.8, 135.4, 132.2, 130.1, 128.7, 128.4, 127.6, 126.7, 121.7, 120.5, 119.7, 110.0, 102.9, 83.6, 24.4. The carbon directly attached to the boron atom was not detected due to quadrupolar broadening.

^{11}B NMR (128 MHz, $CDCl_3$): δ 30.6.

HRMS(ESI-TOF) m/z: $[M+H]^+$ calc'd for $C_{20}H_{23}BNO_2$ 320.1822; found, 320.1818.

4,4,5,5-tetramethyl-2-(naphthalen-2-ylmethyl)-1,3,2-dioxaborolane; compound, 2-60

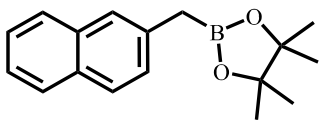

Following general procedure B, $Ni(acac)_2$ (7.7 mg, 0.03 mmol), IPr^{Me}•HCl (27.2 mg, 0.06 mmol), LiO-*t*-Bu (60.0 mg, 0.75 mmol), B_2pin_2 (192.0 mg, 75 mmol), *tert*-butyldimethyl(naphthalen-2-ylmethoxy)silane (85.5 mg, 0.3 mmol) at 100 °C for 16 h gave a crude residue which was purified by flash chromatography (hexanes/ethyl acetate) to afford the desired product as a white solid (54.7 mg, 0.20 mmol, 76% yield) as an average over three trials.

^{1}H NMR (700 MHz, $CDCl_3$): δ 7.77 (d, *J* = 8.1 Hz, 1H), 7.73 (t, *J* = 9.1 Hz, 2H), 7.61 (s, 1H), 7.42 (t, *J* = 7.4 Hz, 1H), 7.38 (t, *J* = 7.4 Hz, 1H), 7.33 (dd, *J* = 8.4, 1.7 Hz, 1H), 2.45 (s, 2H), 1.23 (s, 12H).

^{13}C NMR (176 MHz, $CDCl_3$): δ 135.9, 133.4, 131.1, 127.8, 127.2, 127.1, 126.8, 126.2, 125.2, 124.2, 83.1, 24.3. The carbon directly attached to the boron atom was not detected due to quadrupolar broadening.

^{11}B NMR (128 MHz, $CDCl_3$): δ 33.1.

The spectral data matched the literature.[101]

2-([1,1'-biphenyl]-4-ylmethyl)-4,4,5,5-tetramethyl-1,3,2-dioxaborolane; compound, 2-61

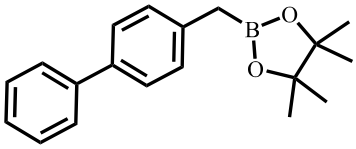

Following general procedure B, $Ni(acac)_2$ (7.7 mg, 0.03 mmol), IPr^{Me}•HCl (27.2 mg, 0.06 mmol), LiO-*t*-Bu (60.0 mg, 0.75 mmol), B_2pin_2 (192.0 mg, 75 mmol), ([1,1'-biphenyl]-4-ylmethoxy)(*tert*-butyl)dimethylsilane (89.6 mg, 0.3 mmol) at 100 °C for 16 h gave a crude residue which was purified by flash chromatography (hexanes/ethyl acetate) to afford the desired product as a colorless oil (53.9 mg, 0.18 mmol, 60% yield) as an average over three trials.

^{1}H NMR (500 MHz, $CDCl_3$): δ 7.60 – 7.56 (m, 2H), 7.49 – 7.47 (m, 2H), 7.41 (t, *J* = 7.7 Hz, 2H), 7.31 (td, *J* = 7.2, 1.2 Hz, 1H), 7.26 (d, *J* = 8.0 Hz, 2H), 2.34 (s, 2H), 1.25 (s, 12H).

^{13}C NMR (126 MHz, $CDCl_3$): δ 140.7, 137.3, 137.2, 128.8, 128.1, 126.5, 126.4, 126.3, 82.9, 24.2. The carbon directly attached to the boron atom was not detected due to quadrupolar broadening.

^{11}B NMR (128 MHz, $CDCl_3$) δ 33.6

The spectral data matched the literature.[34]

(benzyloxy)(*tert*-butyl)dimethylsilane; compound, 2-62

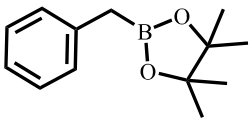

Following general procedure B, $Ni(acac)_2$ (7.7 mg, 0.03 mmol), IPr^{Me}•HCl (27.2 mg, 0.06 mmol), LiO-*t*-Bu (60.0 mg, 0.75 mmol), B_2pin_2 (192.0 mg, 75 mmol), (benzyloxy)(*tert*-butyl)dimethylsilane (67.0 mg, 0.3 mmol) at 100 °C for 16 h gave a crude residue which was purified by flash chromatography (hexanes/ethyl acetate) to afford the desired product as a colorless oil (36.0 mg, 0.17 mmol, 55% yield) as an average over two trials.

^{1}H NMR (500 MHz, $CDCl_3$): δ 7.25 – 7.22 (m, 2H), 7.20 – 7.17 (m, 2H), 7.12 (td, *J* = 7.1, 1.5 Hz, 1H), 2.29 (s, 2H), 1.23 (s, 12H).

^{13}C NMR (126 MHz, $CDCl_3$): δ 138.1, 128.4, 127.7, 124.6, 82.8, 24.2. The carbon directly attached to the boron atom was not detected due to quadrupolar broadening.

^{11}B NMR (128 MHz, $CDCl_3$): δ 33.0

The spectral data matched the literature.[102]

2-(3-methoxybenzyl)-4,4,5,5-tetramethyl-1,3,2-dioxaborolane; compound, 2-63

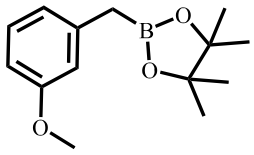

Following general procedure B, $Ni(acac)_2$ (7.7 mg, 0.03 mmol), IPr^{Me}•HCl (27.2 mg, 0.06 mmol), LiO-*t*-Bu (60.0 mg, 0.75 mmol), B_2pin_2 (192.0 mg, 75 mmol), *tert*-butyl((3-methoxybenzyl)oxy)dimethylsilane (75.7 mg, 0.3 mmol) at 100 °C for 16 h gave a crude residue which was purified by flash chromatography (hexanes/ethyl acetate) to afford the desired product as a colorless oil (35.0 mg, 0.14 mmol, 50% yield) as an average over two trials.

^{1}H NMR (700 MHz, $CDCl_3$): δ 7.15 (t, *J* = 7.9 Hz, 1H), 6.78 (d, *J* = 7.5 Hz, 1H), 6.75 (t, *J* = 2.1 Hz, 1H), 6.68 (dd, *J* = 8.2, 2.6 Hz, 1H), 3.78 (s, 3H), 2.28 (s, 2H), 1.24 (s, 12H).

^{13}C NMR (176 MHz, $CDCl_3$): δ 158.9, 139.6, 128.6, 120.9, 114.0, 109.8, 82.9, 54.5, 24.2. The carbon directly attached to the boron atom was not detected due to quadrupolar broadening.

^{11}B NMR (128 MHz, $CDCl_3$) δ 31.5.

The spectral data matched the literature.[103]

4-(4'-(((tert-butyldimethylsilyl)oxy)methyl)-[1,1'-biphenyl]-4-yl)morpholine; compound, 2-76

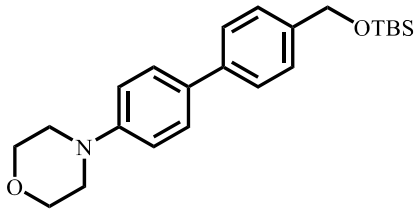

In the glovebox, an oven-dried microwave vial containing a magnetic stir bar was charged with *tert*-butyl((4'-((*tert*-butyldimethylsilyl)oxy)-[1,1'-biphenyl]-4-yl)methoxy)dimethylsilane (2.4 g, 5.6 mmol), $Ni(COD)_2$ (160 mg, 0.58 mmol), IPr^{Me}•HCl (526.5 mg, 1.2 mmol), NaO-*t*-Bu (1.4 g, 14.5 mmol.), toluene (11.2 mL, 0.5 M) and morpholine (0.76 mL, 8.7 mmol), which had been distilled over CaH_2. The sealed microwave vial was brought outside the glovebox and placed in an oil bath heated to 120 °C and stirred for 16 h. The mixture was allowed to cool to room temperature, diluted with EtOAc, run over a silica plug, concentrated under reduced pressure, and purified by flash column chromatography (hexanes/ethyl acetate) on silica gel to afford the desired product as a white solid (1.7g, 79% yield).

^{1}H NMR (500 MHz, $CDCl_3$) δ 7.56 – 7.50 (m, 4H), 7.37 (d, *J* = 7.7 Hz, 2H), 7.01 – 6.95 (m, 2H), 4.78 (s, 2H), 3.92 – 3.86 (m, 4H), 3.24 – 3.18 (m, 4H), 0.96 (s, 9H), 0.12 (s, 6H).

^{13}C NMR (126 MHz, $CDCl_3$) δ 150.5, 139.7, 139.4, 132.6, 127.7, 126.5, 126.4, 115.8, 66.9, 64.8, 49.2, 26.0, 18.5, -5.2.

HRMS(ESI-TOF) m/z: $[M+H]^+$ calc'd for $C_{23}H_{34}NO_2Si$ 384.2359; found, 384.2359.

4-(4'-((4,4,5,5-tetramethyl-1,3,2-dioxaborolan-2-yl)methyl)-[1,1'-biphenyl]-4-yl)morpholine; compound, 2-77

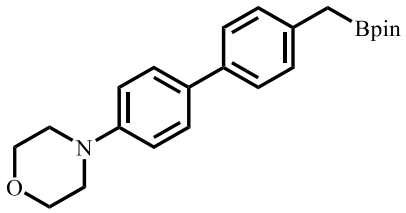

In an inert atmosphere glovebox, an oven-dried 25 mL RBF equipped with a magnetic stir bar was charged with 4-(4'-(((*tert*-butyldimethylsilyl)oxy)methyl)-[1,1'-biphenyl]-4-yl)morpholine (1 g, 2.6 mmol), $Ni(acac)_2$ (67 mg, 0.26 mmol), IPr^{Me}•HCl (236 mg, 0.52 mmol), LiO-*t*-Bu (520 mg, 6.5 mmol.), CPME (8.8 mL, 0.5 M) and B_2pin_2 (1.6 g, 6.5 mol). The sealed microwave vial was brought outside the glovebox and placed in an oil bath heated to 120 °C and stirred for 16 h. The mixture was allowed to cool to room temperature, diluted with EtOAc, run over a silica plug, concentrated under reduced pressure, and purified by flash column chromatography (hexanes/ethyl acetate) on silica gel to afford the desired product as a white solid (0.76 g, 77% yield).

^{1}H NMR (500 MHz, $CDCl_3$) δ 7.56 – 7.49 (m, 2H), 7.48 – 7.43 (m, 2H), 7.24 (d, *J* = 7.9 Hz, 2H), 7.00 – 6.94 (m, 2H), 3.91 – 3.86 (m, 4H), 3.23 – 3.17 (m, 4H), 2.34 (s, 2H), 1.26 (s, 12H).

^{13}C NMR (126 MHz, $CDCl_3$) δ 150.2, 137.3, 136.9, 132.8, 129.3, 127.5, 126.4, 115.7, 83.4, 66.9, 49.2, 24.7. The carbon directly attached to the boron atom was not detected due to quadrupolar broadening.

^{11}B NMR (160 MHz, $CDCl_3$) δ 33.0.

HRMS(ESI-TOF) m/z: $[M+H]^+$ calc'd for $C_{23}H_{31}BNO_3$ 380.2397; found, 380.2395.

***tert*-butyldimethyl((4'-(4,4,5,5-tetramethyl-1,3,2-dioxaborolan-2-yl)-[1,1'-biphenyl]-4-yl)methoxy)silane; compound, 2-75**

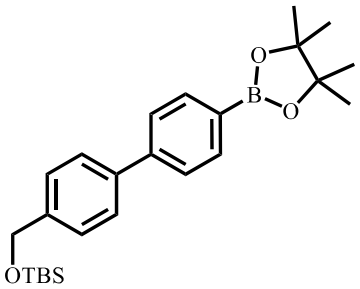

Following general procedure B, $Ni(acac)_2$ (7.7 mg, 0.03 mmol), IPr^{Me}•HCl (27.2 mg, 0.06 mmol), LiO-*t*-Bu (60.0 mg, 0.75 mmol), B_2pin_2 (192.0 mg, 75 mmol), *tert*-butyl((4'-((tert-butyldimethylsilyl)oxy)-[1,1'-biphenyl]-4-yl)methoxy)dimethylsilane (127 mg, 0.3 mmol) at 100 °C for 16 h gave a crude residue which was purified by flash chromatography (hexanes/ethyl acetate) to afford the desired product as an off white solid as an inseparable mixture (75.6 mg, 0.18 mmol, 61% yield, 2.7:1 of 2-75:di-borylation).

^{1}H NMR (500 MHz, $CDCl_3$): δ 7.87 (dd, *J* = 8.0, 3.4 Hz, 2H), 7.60 (dd, *J* = 9.2, 7.5 Hz, 4H), 7.40 (d, *J* = 7.9 Hz, 2H), 4.79 (s, 2H), 1.36 (s, 12H), 0.96 (s, 9H), 0.12 (s, 6H).

^{13}C NMR (126 MHz, $CDCl_3$): δ 143.7, 140.9, 139.6, 135.2, 129.5, 127.1, 126.5, 126.3, 83.8, 64.7, 26.0, 24.9, 18.4, -5.2.

^{11}B NMR (160 MHz, $CDCl_3$): 31.2.

HRMS(EI-AutoSpec-Q) m/z: [M] calc'd for $C_{25}H_{37}BO_3Si$ 424.2605; found, 424.2601.

4,4,5,5-tetramethyl-2-((4'-(4,4,5,5-tetramethyl-1,3,2-dioxaborolan-2-yl)-[1,1'-biphenyl]-4-yl)methyl)-1,3,2-dioxaborolane, 2-75'

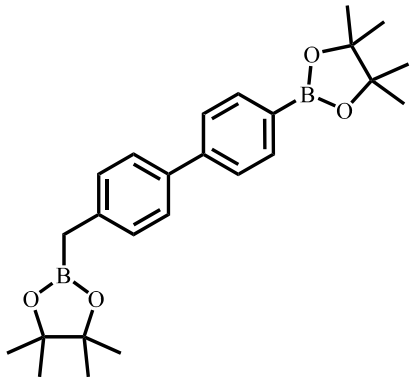

This compound results from di-borylating both silyl ethers. Its formation is made evident by its confirmation via HRMS. Additionally, the benzylic proton peak in the ^{1}H NMR at 2.4 ppm is consistent with the chemical shift of the benzylic protons in the anologous compound, 22.

HRMS(EI-AutoSpec-Q) m/z: [M] calc'd for $C_{25}H_{34}B_2O_4$ 420.2643; found, 420.2649.

4.3 Experimental Details for Chapter 3

4.3.1 Procedures for Catalyst Synthesis

4.3.2 Synthesis of di-*tert*-Butyl Fumarate, 3-36

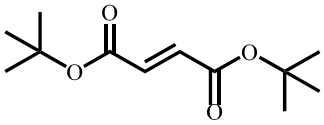

In the glovebox, lithium *tert*-butoxide (8.4g, 105.1 mmol) was added to a flame dried 50 mL RBF that was equipped with a magnetic stir bar and an oven-dried addition funnel. An appropriately sized rubber septum was used to seal the apparatus, and this was then brought outside of the glovebox. THF (14 mL, 3.75 M) was added via the addition funnel, and the solution was cooled to 0 °C via an ice bath while stirring. Fumaryl chloride (5.65 mL, 52.6 mmol) was added dropwise via the addition funnel. **Warning**: This is very concentrated and after each drop, some smoke appears. The reaction should be diluted further. The ice bath was then removed, and the

reaction mixture was allowed to stir overnight. The crude product was extracted from water with ether x3, washed with brine, dried over magnesium sulfate, filtered, and concentrated. The crude material was filtered through silica gel (5% EtOAc/hexanes) and concentrated, resulting in a light yellow crystalline solid. This was dissolved in the minimum quantity of pentane at rt and recrystallized at -78 °C. The resulting white crystals were collected by filtration and washed with cold pentanes. The filtrate was concentrated and re-subjected to the recrystallization conditions to yield a second batch of desired product, yielding in total 7.8g, 60% yield.

^{1}H NMR (401 MHz, $CDCl_3$): δ 6.67 (d, *J* = 1.1 Hz, 2H), 1.50 (s, 18H).

The spectral data matched the literature.[83]

4.3.3 Synthesis of Nickel Catalysts

4.3.3.1 Synthesis of Bis(di-tert-butyl fumarate)(1,3-bis(2,4,6-trimethylphenyl)imidazol-2-ylidene)nickel(0) from the NHC Salt, 3-24

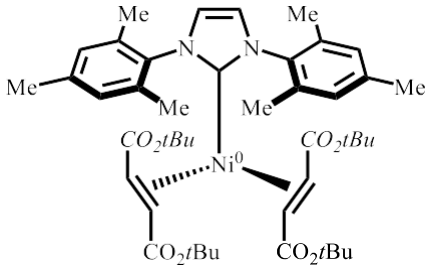

In the glovebox, an oven-dried 20 mL vial equipped with a magnetic stir bar was charged with NaO-*t*-Bu (115.4 mg, 1.2 mmol), IMes•BF_4 (392.2 mg, 1.00 mmol), and 3 mL toluene (freeze-pump-thawed) with stirring. This resulted in a slurry with an off yellow hue. After 3 hours and 40 minutes later, an oven-dried 20 mL vial equipped with a magnetic stir bar was charged with $Ni(COD)_2$ (275.1 mg, 1.00 mmol), di-*tert*-butyl fumarate (456.6 mg, 2.00 mmol), and 3 mL toluene. The metal/olefin solution became a red, clear solution after 15 minutes, at which point,

the base/ligand solution had stirred for 4 hours. At this time, the base/ligand solution was added to the metal/olefin solution, slowly. 1-2 mL of toluene was used to aid in the transfer of the base/ligand solution. The reaction became dark red and was allowed to stir overnight. The crude reaction mixture was filtered over celite. Then, all volatiles were removed *in vacuo* leaving behind a red amorphous solid. After this, 5 mL of pentane was added to the flask and walls of the flask were scraped. The pentane was subsequently removed *in vacuo,* which expedites the removal of COD. After all volatiles were removed a reddish, orange solid remained. The crude product was taken up in ~12 mL of pentane to produce a solution containing a significant amount of precipitate was filtered and washed with pentane. This resulted in a solid that appeared pure via ^{1}H NMR. The filtrate, still somewhat cloudy, was then transferred to a 20 mL vial and stored in the freezer at -20 °C overnight. The reddish orange product was isolated via immediate filtration. ^{1}H NMR analysis confirmed that this was also desired product, so the two batches were combined and dried via high vacuum; which, resulted in an orange powder 77% yield (627 mg).

^{1}H NMR (500 MHz, C_6C_6): δ 7.05 (s, 2H), 6.90 (s, 2H), 6.41 (s, 2H), 4.51 (d, *J* = 11.1 Hz, 2H), 3.79 (d, *J* = 11.1 Hz, 2H), 2.36 (s, 6H), 2.19 (s, 6H), 2.14 (s, 6H), 1.48 (s, 18H), 1.28 (s, 18H).

^{13}C NMR (126 MHz, C_6C_6): δ 189.0, 171.7, 168.3, 137.9, 136.40, 135.9, 133.8, 130.4, 129.1, 124.1, 78.6, 78.5, 65.3, 58.2, 28.2, 28.1, 20.8, 20.0, 19.9.

The spectral data matched the literature.[83]

Storage: Ni(IMes)(di-tert-butyl fumarate)$_2$ is air-sensitive over prolonged periods of time and should be stored in an inert atmosphere.

4.3.3.2 Attempted Synthesis of Bis(di-tert-butyl fumarate)(1,3-bis(2,4,6-trimethylphenyl)imidazol-2-ylidene)nickel(0) via *In-Situ Preparation of Ni(COD)$_2$ via n*-dibutylmagnesium.

In the glovebox, an oven-dried vial equipped with a magnetic stir bar was charged with anhydrous Ni(acac)$_2$ (25.6 mg, 0.10 mmol), COD (220 µL, 73.6 µmol) followed by THF (0.8 mL). The vial was placed inside of an aluminum block, then placed in the glovebox freezer until cooled to -35 °C. Upon reaching the desired temperature, the aluminum block was removed from the freezer and placed on a magnetic stir plate with stirring set to 600 rpm. Then, di-*tert*-butylmagnesium (220 µL)was added dropwise and permitted to stir for 10 minutes, upon which, a bright yellow precipitate had been observed, indicating the formation of Ni(COD)$_2$. Then, IMes●BF$_4$ (39.2 mg, 0.10 mmol) was added to the crude reaction mixture followed by di-*tert*-butyl fumarate (50.2 mg, 0.22 µmol) and permitted to stir overnight. The crude reaction was filtered over celite, washed with THF, and concentrated. The mixture was then taken up in the minimum amount of THF and pentanes were added until precipitation ceased. This turbid mixture was then filtered over a glass-fritted filter. The filter cake was a grey color, and no desired product was observed.

4.3.3.3 Attempted Synthesis of Bis(di-tert-butyl fumarate)(1,3-bis(2,4,6-trimethylphenyl)imidazol-2-ylidene)nickel(0) via *In-Situ* Preparation of Ni(COD)$_2$ via Ketyl Radical Route

In the glovebox, an oven-dried vial equipped with a magnetic stir bar was charged with the diol (55 mg, 0.14 mmol), anhydrous Ni(acac)$_2$ (26 mg, 0.10 mmol), and COD (67 µL, 550 µmol) were placed in a flask under a nitrogen atmosphere. THF (2 mL) was added to the flask to give an emerald, green solution. To the solution was added KO-*t*-Bu (34 mg, 0.30 mmol) at room

temperature to turn the color to deep blue, indicating the formation of a ketyl radical. After 30 h, MeOH (0.33 mL) was added to quench the remaining ketyl radical, and the color turned to yellow, indicating successful formatting of $Ni(COD)_2$. To the crude reaction was added di-*tert*-butyl fumarate (46 mg, 0.20 mmol), which was allowed to stir for about 5 minutes followed by the free carbene of IMes (30 mg, 0.10 mmol). The solution darkened and possessed an orangish tint, which is a good sign. This was permitted to stir overnight. The crude reaction was filtered over celite, washed with THF, and concentrated. The mixture was then taken up in the minimum amount of THF and pentanes were added until precipitation ceased. This turbid mixture was then filtered over a glass-fritted filter. Despite the promising throughout the process, the filter cake was a grey color, and no desired product was observed.

4.3.3.4 Synthesis of Bis(di-tert-butyl fumarate)(1,3-bis(2,4,6-trimethylphenyl)imidazol-2-ylidene)nickel(0)from Ni(IMes)(1,5-hexadiene), 3-24

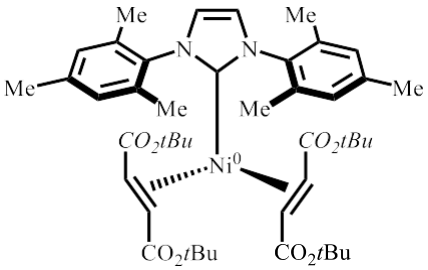

In the glovebox, an oven-dried 20 mL vial equipped with a magnetic stir bar was charged with, Ni(IMes)(1,5-hexadiene) (45 mg, 0.10 mmol), and 3 mL THF (freeze-pump-thawed) with stirring, resulting in a light orange hue. Then, di-*tert*-butyl fumarate (46 mg, 0.20 mmol) was added, forming a darker, orange color and the reaction was permitted to stir overnight at room temperature. Then, all volatiles were removed *in vacuo* leaving behind a red amorphous solid. After this, 5 mL of pentane was added to the flask and walls of the flask were scraped. The pentane was subsequently removed *in vacuo,* which expedites the removal of 1,5-hexadiene. After all

volatiles were removed a reddish, orange solid remained. The crude product was dissolved in the minimal amount of ether followed by the addition of pentane until cessation of precipitate formation, which was then filtered over a glass-fritted filter to provide 59 mg of **3-24** in 70% yield. Of the desired product.

^{1}H NMR (500 MHz, C_6D_6) δ 7.05 (s, 2H), 6.90 (s, 2H), 6.41 (s, 2H), 4.51 (d, *J* = 11.1 Hz, 2H), 3.79 (d, *J* = 11.1 Hz, 2H), 2.36 (s, 6H), 2.19 (s, 6H), 2.14 (s, 6H), 1.48 (s, 18H), 1.28 (s, 18H).

^{13}C NMR (126 MHz, C_6D_6) δ 188.95, 171.71, 168.29, 137.91, 136.40, 135.93, 133.83, 130.41, 129.05, 124.07, 78.64, 78.51, 65.29, 58.18, 28.15, 28.12, 20.78, 20.04, 19.90.

The spectral data matched the literature.[83]

4.3.3.5 Attempted Synthesis of Bis(di-tert-butyl fumarate)(1,3-bis(2,4,6-trimethylphenyl)imidazol-2-ylidene)nickel(0) via In-Situ Preparation of Ni(IMes)(1,5-hexadiene) Resulting in a Proposed Dimeric Complex, 3-38

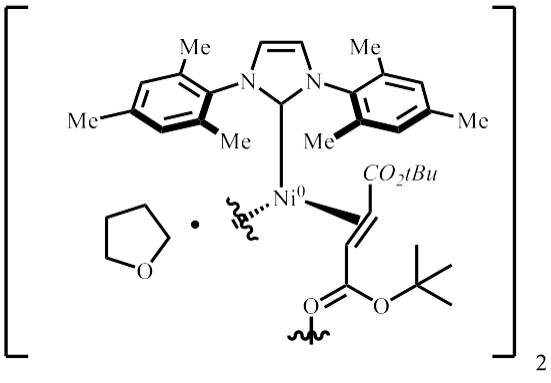

In the glovebox, an oven-dried vial equipped with a magnetic stir bar was charged with $NiCl_2$ (25.9 mg, 0.200 mmol) IMes free carbene(60.9 mg, 0.200 mmol), followed by 2 mL of THF and this was permitted to stir for 30 min. Allylmagnesium chloride (0.17 mL, 2 M) taken up in THF (1.0 mL, 0.32 M) and the solution immediately turned the desired orangish color. After 6 hours of stirring at RT, di-*tert*-butyl fumarate (91.3 mg, 0.400 mmol) was added, and the solution

turned a dark, bluish purple. After stirring overnight, the solution was concentrated, filtered over a celite plug and washed with THF resulting in a violet filtrate. This was concentrated and the minimal amount (about 1 mL) of ether was added followed by pentanes until precipitation ceased. This was then filtered over a fritted funnel via a Schenk tube resulting in a purple powder. Upon drying, the powder became a light blueish hue (70 mg, 42% yield). ^{1}H NMR shows a mystery product, which appears as though it might be a dimeric complex based off the color and that the stoichiometry of NHC:THF:Fumarate is 1:1:1. Additionally, dimers of these discrete Ni(0) pre-catalysts are also purple.

^{1}H NMR (500 MHz, C_6D_6): δ 7.09 (s, 2H), 6.74 (s, 2H), 6.08 (s, 2H), 3.59 (s, 4H), 2.64 (d, *J* = 10.4 Hz, 1H), 2.44 (s, 6H), 2.31 (d, *J* = 10.3 Hz, 1H), 2.18 (s, 6H), 1.96 (s, 6H), 1.69 (s, 9H), 1.41 (s, 4H), 1.30 (d, *J* = 1.7 Hz, 9H).

4.3.3.6 Control Experiment Subjecting Independently Synthesized Bis(di-tert-butyl fumarate)(1,3-bis(2,4,6-trimethylphenyl)imidazol-2-ylidene)nickel(0) to AllylMagnesium Chloride

In the glovebox, an oven-dried vial equipped with a magnetic stir bar was charged with Bis(di-tert-butyl fumarate)(1,3-bis(2,4,6-trimethylphenyl)imidazol-2-ylidene)nickel(0) (21 mg, .025 mmol), which had been independently synthesized followed by THF. Then, allylmagnesium chloride (25 µL, 50 µmol) was added and the color turned a brownish color, which was not indicative of the proposed dimeric complex, but rather, complex degradation.

4.3.3.7 Control Experiment Subjecting Independently Synthesized Bis(di-tert-butyl fumarate)(1,3-bis(2,4,6-trimethylphenyl)imidazol-2-ylidene)nickel(0) to $MgCl_2$.

In the glovebox, an oven-dried vial equipped with a magnetic stir bar was charged with Bis(di-tert-butyl fumarate)(1,3-bis(2,4,6-trimethylphenyl)imidazol-2-ylidene)nickel(0) (21 mg,

.025 mmol), which had been independently synthesized followed by THF. Then, $MgCl_2$ (4.8 mg, .050 mmol) was added, and the color turned to the same violet color, which was indicative of the proposed dimeric complex.

4.4 NMR Spectra

1-(3-((*tert*-butyldimethylsilyl)oxy)phenyl)-1H-indole (2-72)

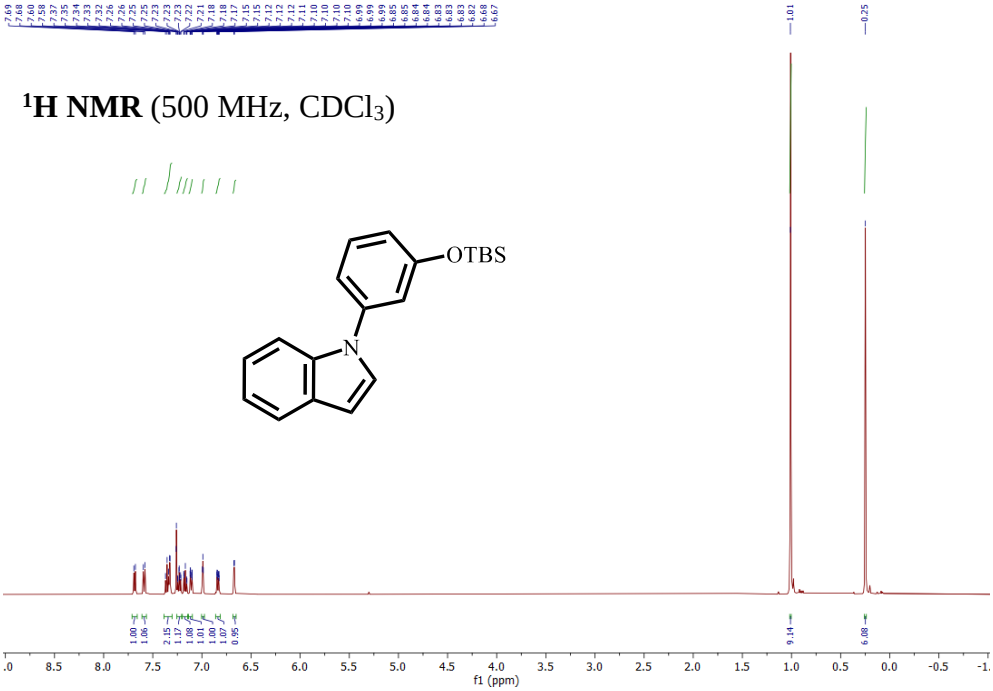

Figure 4-3. ^{1}H of 1-(3-((*tert*-butyldimethylsilyl)oxy)phenyl)-1H-indole (2-72).

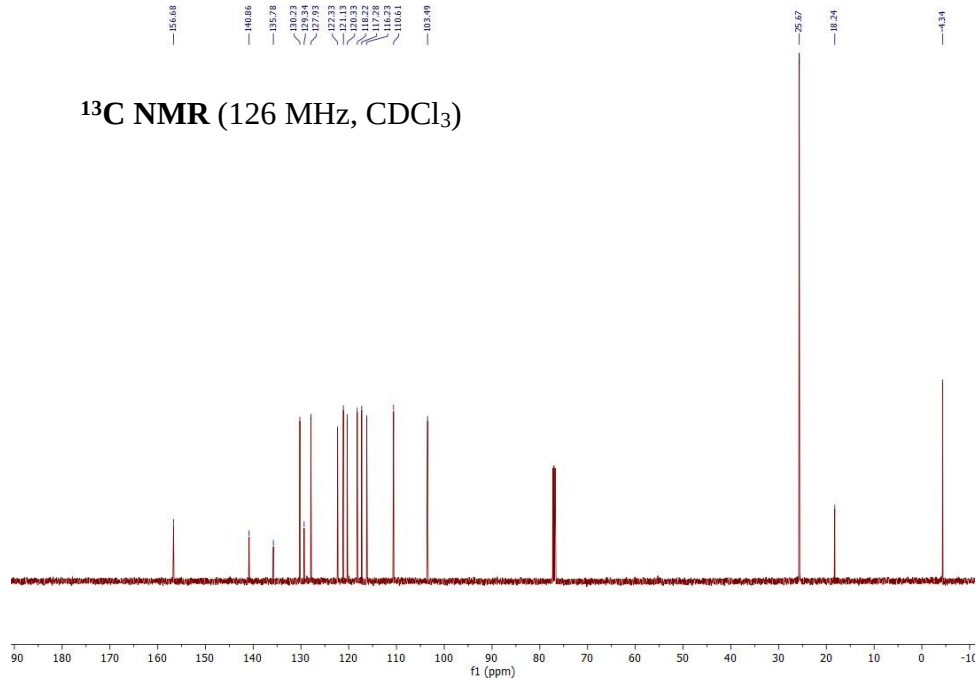

Figure 4-4. ^{13}C of 1-(3-((*tert*-butyldimethylsilyl)oxy)phenyl)-1H-indole (2-72).

4,4,5,5-tetramethyl-2-(naphthalen-1-yl)-1,3,2-dioxaborolane **(2-40)**

^{1}H NMR (500 MHz, $CDCl_3$)

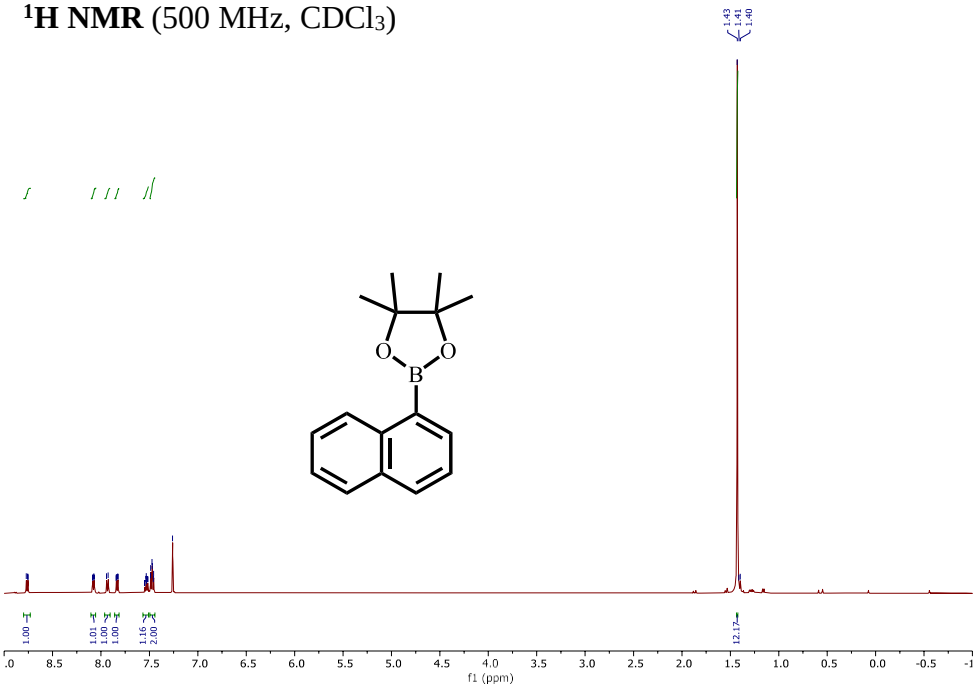

Figure 4-5. ^{1}H of 4,4,5,5-tetramethyl-2-(naphthalen-1-yl)-1,3,2-dioxaborolane (2-40).

^{13}C NMR (126 MHz, $CDCl_3$)

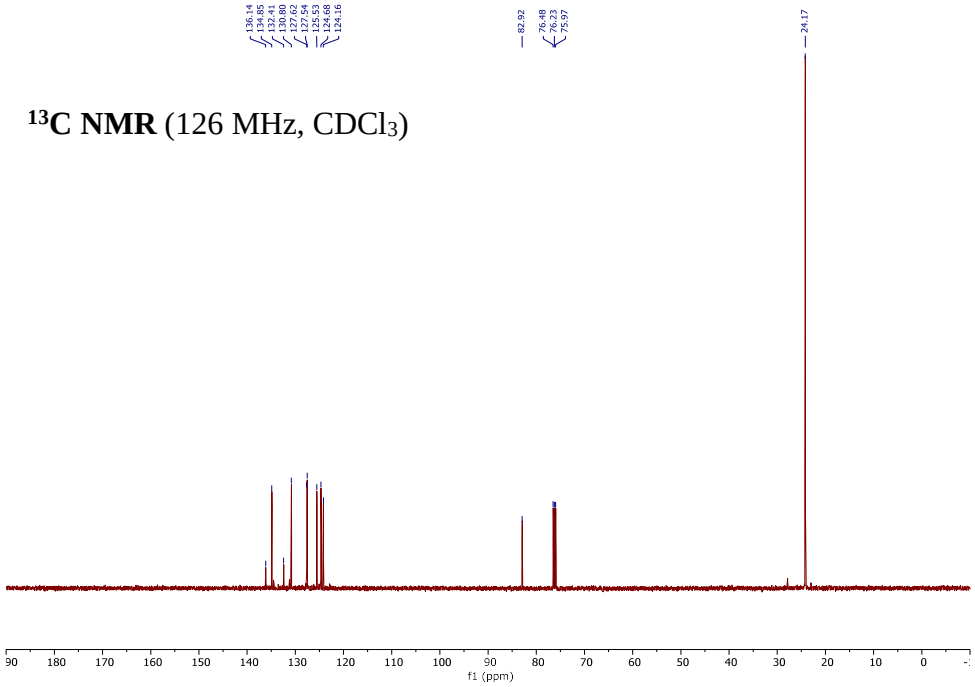

Figure 4-6. ^{13}C of 4,4,5,5-tetramethyl-2-(naphthalen-1-yl)-1,3,2-dioxaborolane (2-40).

4,4,5,5-tetramethyl-2-(naphthalen-2-yl)-1,3,2-dioxaborolane **(2-43)**

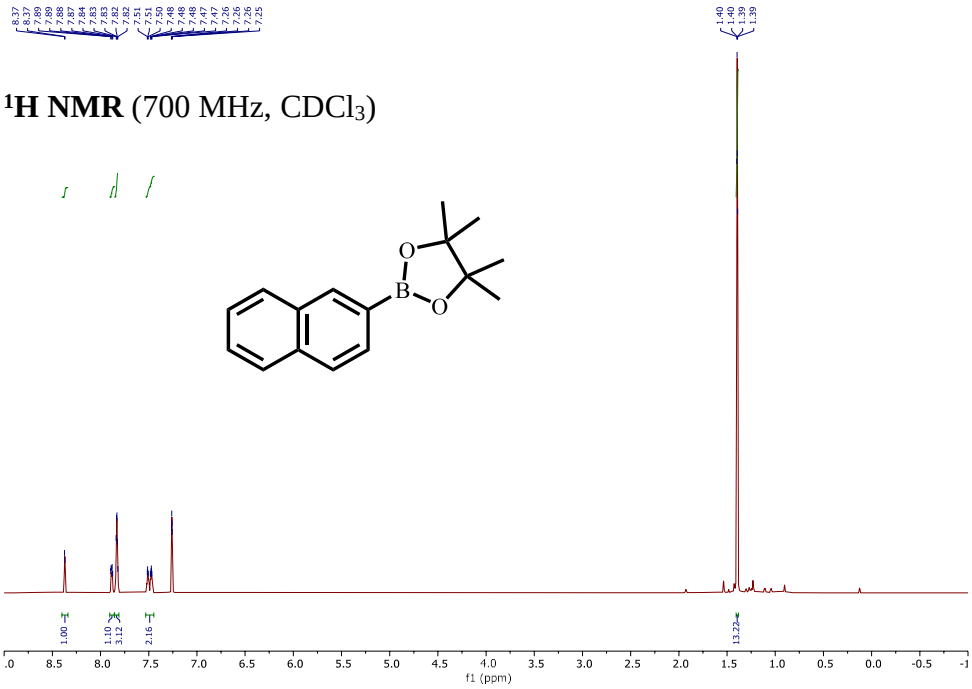

Figure 4-7. [1]H of 4,4,5,5-tetramethyl-2-(naphthalen-2-yl)-1,3,2-dioxaborolane (2-43).

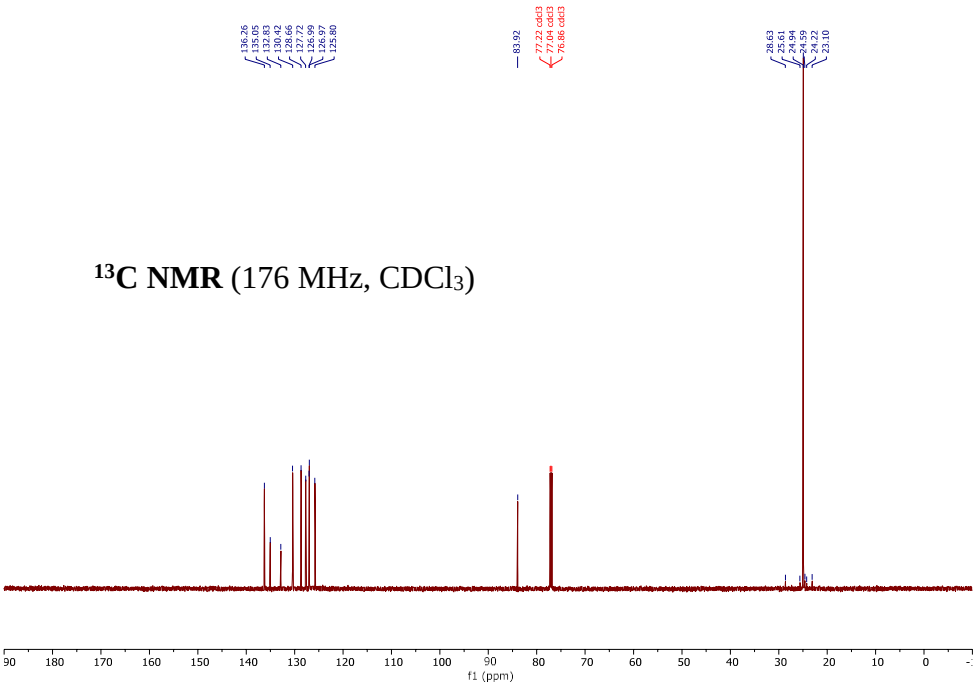

Figure 4-8. [13]C of 4,4,5,5-tetramethyl-2-(naphthalen-2-yl)-1,3,2-dioxaborolane (2-43)

2-([1,1'-biphenyl]-3-yl)-4,4,5,5-tetramethyl-1,3,2-dioxaborolane (2-42)

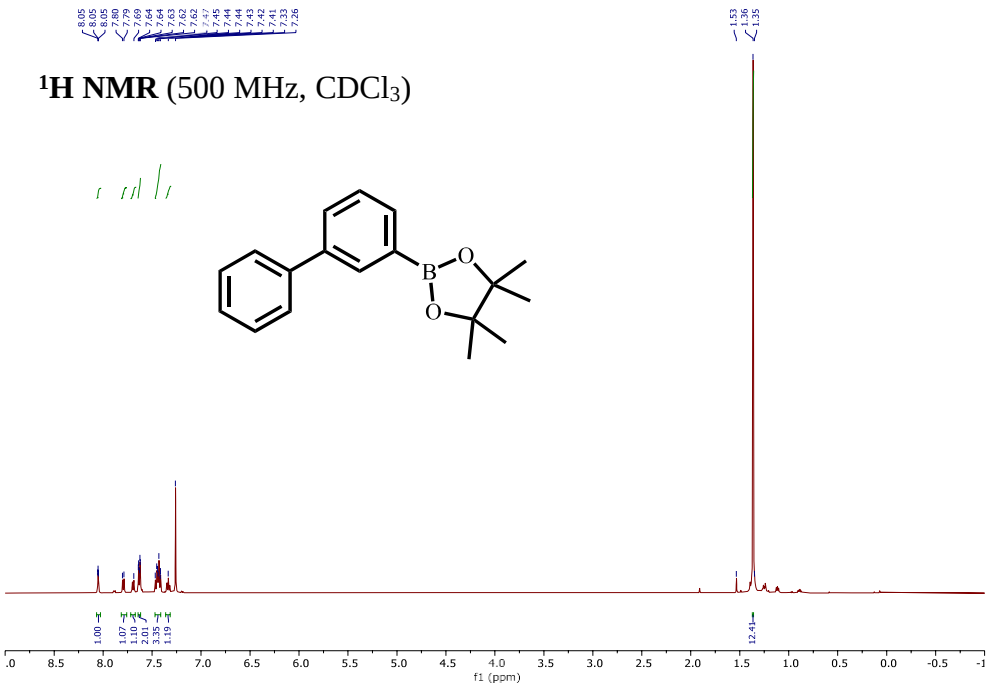

Figure 4-9. ^{1}H of 2-([1,1'-biphenyl]-3-yl)-4,4,5,5-tetramethyl-1,3,2-dioxaborolane (2-42).

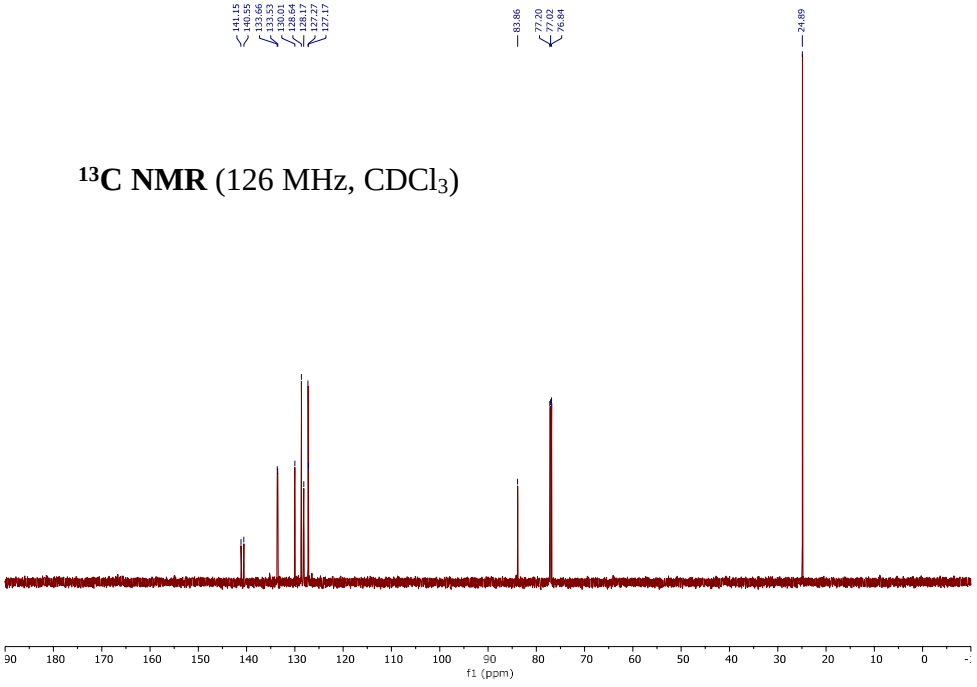

Figure 4-10. ^{13}C of 2-([1,1'-biphenyl]-3-yl)-4,4,5,5-tetramethyl-1,3,2-dioxaborolane (2-42).

2-([1,1'-biphenyl]-4-yl)-4,4,5,5-tetramethyl-1,3,2-dioxaborolane (2-44)

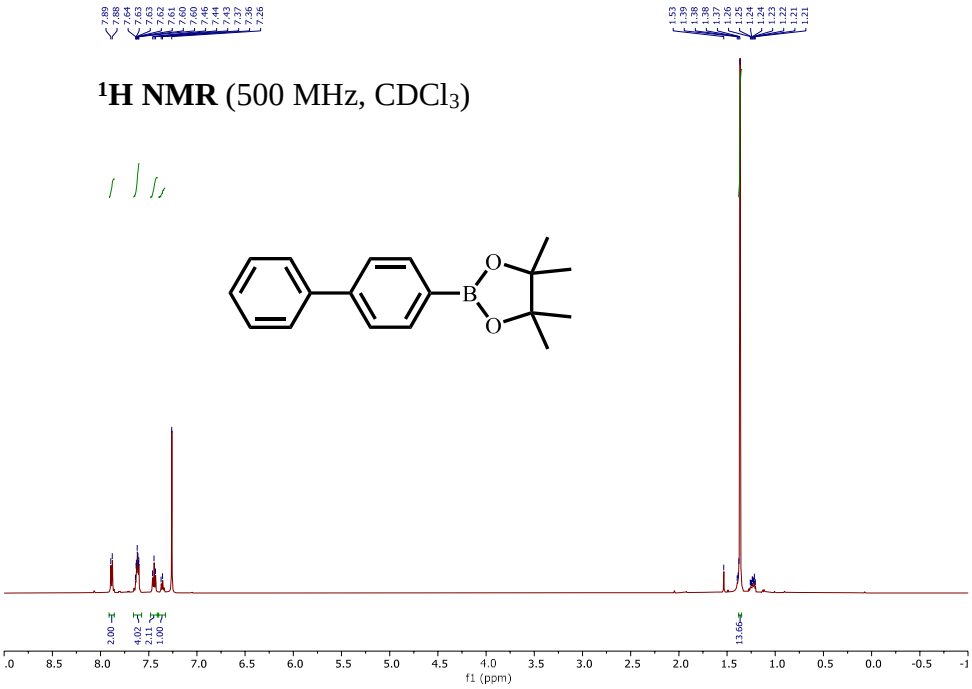

Figure 4-11. [1]H of 2-([1,1'-biphenyl]-4-yl)-4,4,5,5-tetramethyl-1,3,2-dioxaborolane (2-44).

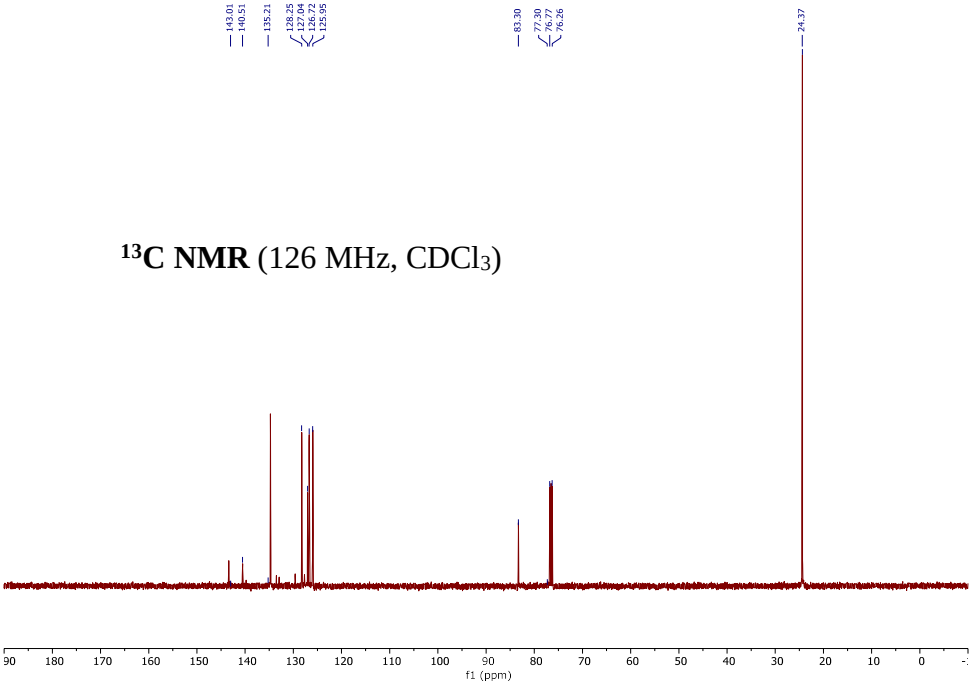

Figure 4-12. [13]C of 2-([1,1'-biphenyl]-4-yl)-4,4,5,5-tetramethyl-1,3,2-dioxaborolane (2-44).

4,4,5,5-tetramethyl-2-phenyl-1,3,2-dioxaborolane **(2-45)**

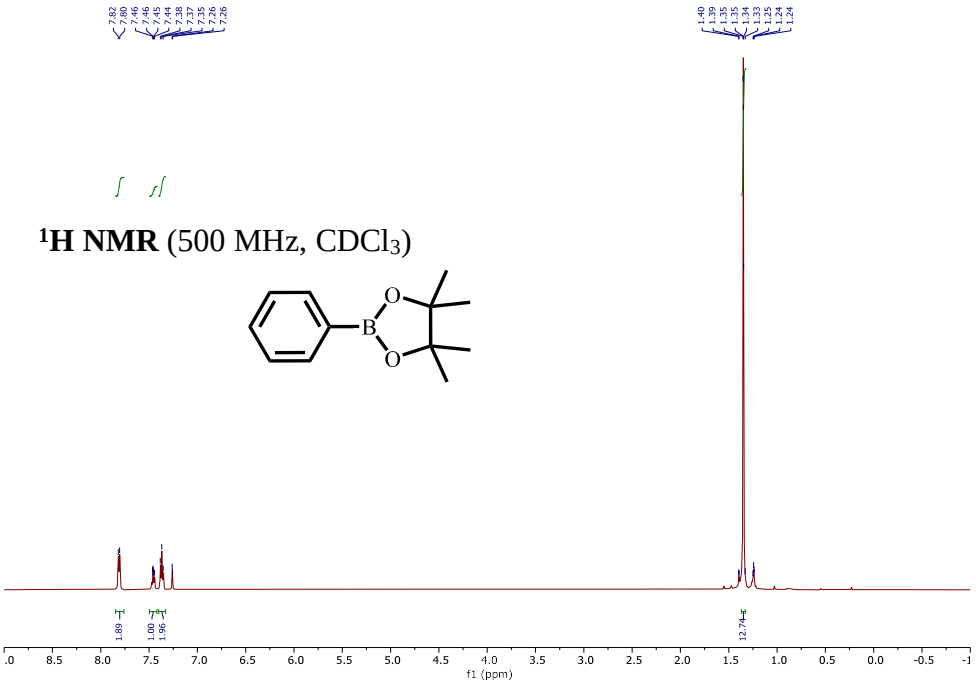

^{1}H NMR (500 MHz, $CDCl_3$)

Figure 4-13. ^{1}H of 4,4,5,5-tetramethyl-2-phenyl-1,3,2-dioxaborolane (2-45).

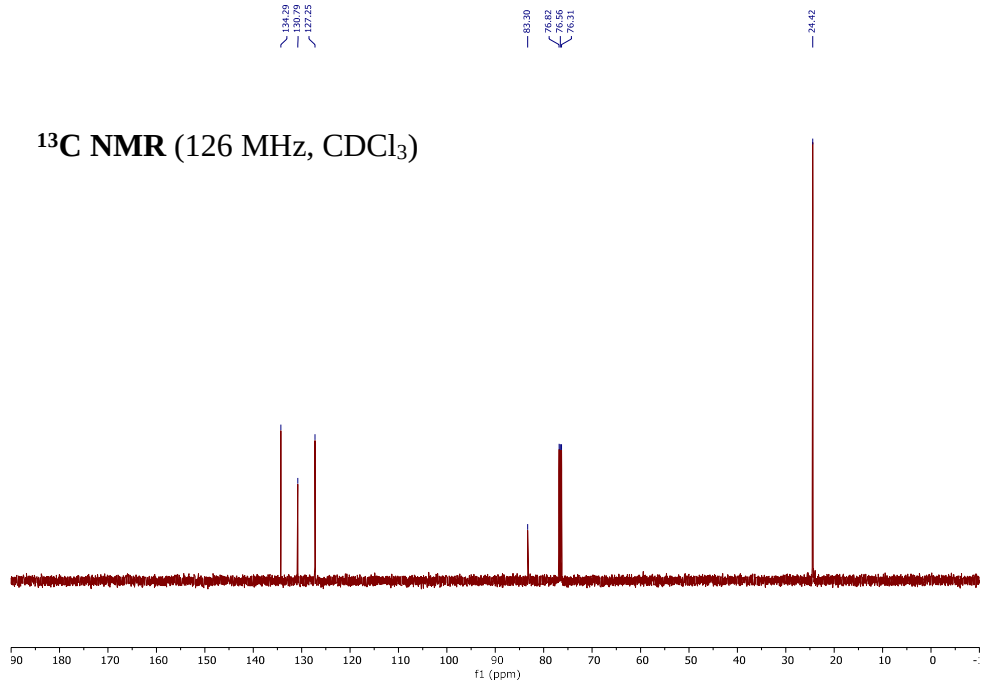

^{13}C NMR (126 MHz, $CDCl_3$)

Figure 4-14. ^{13}C of 4,4,5,5-tetramethyl-2-phenyl-1,3,2-dioxaborolane (2-45).

2-(4-(*tert*-butyl)phenyl)-4,4,5,5-tetramethyl-1,3,2-dioxaborolane (2-46)

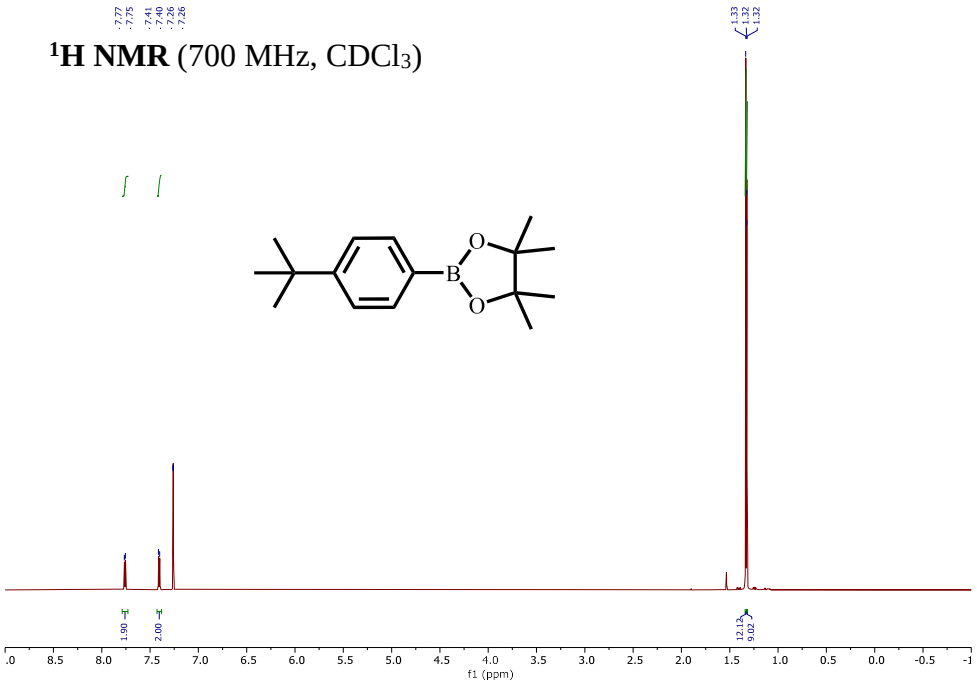

Figure 4-15. ^{1}H of 2-(4-(*tert*-butyl)phenyl)-4,4,5,5-tetramethyl-1,3,2-dioxaborolane (2-46).

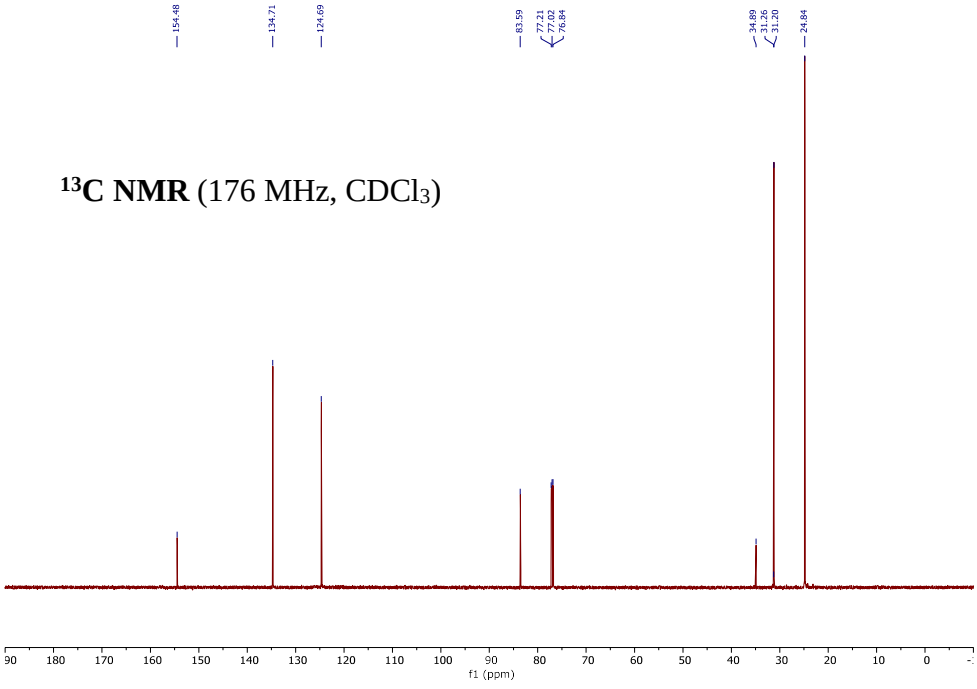

Figure 4-16. ^{13}C of 2-(4-(*tert*-butyl)phenyl)-4,4,5,5-tetramethyl-1,3,2-dioxaborolane (2-46).

4,4,5,5-tetramethyl-2-(*o*-tolyl)-1,3,2-dioxaborolane **(2-47)**

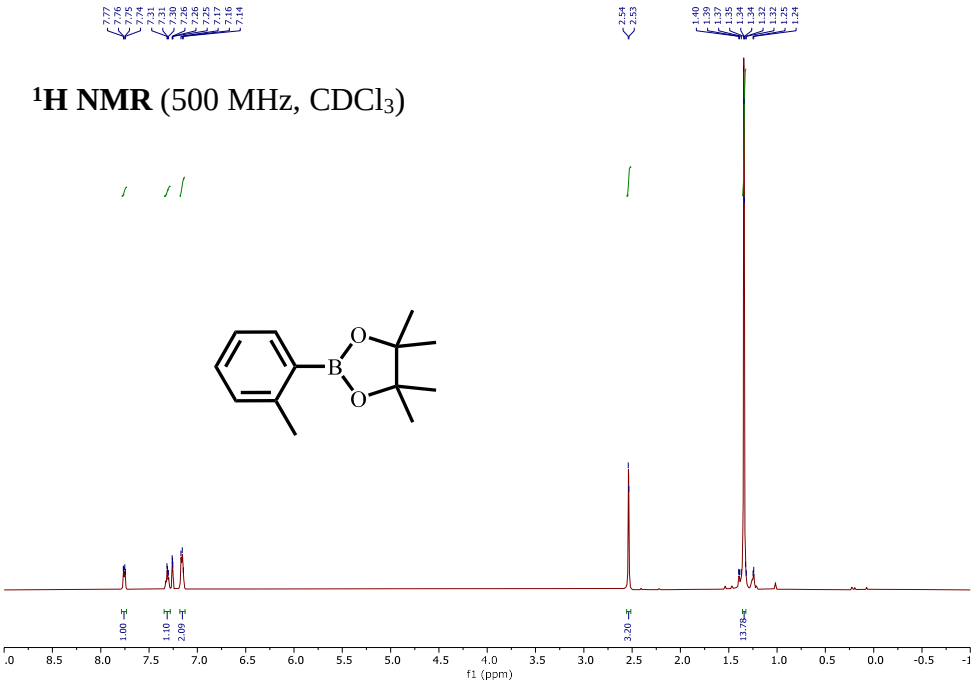

Figure 4-17. ^{1}H of 4,4,5,5-tetramethyl-2-(*o*-tolyl)-1,3,2-dioxaborolane (2-47).

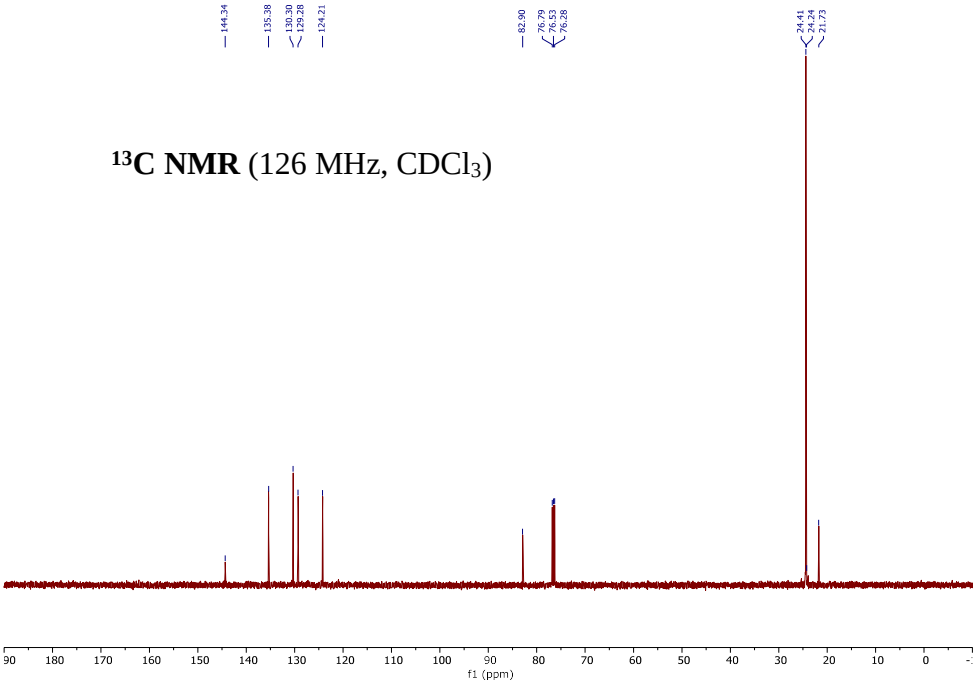

Figure 4-18. ^{13}C of 4,4,5,5-tetramethyl-2-(*o*-tolyl)-1,3,2-dioxaborolane (2-47).

2-(2-ethylphenyl)-4,4,5,5-tetramethyl-1,3,2-dioxaborolane **(2-48)**

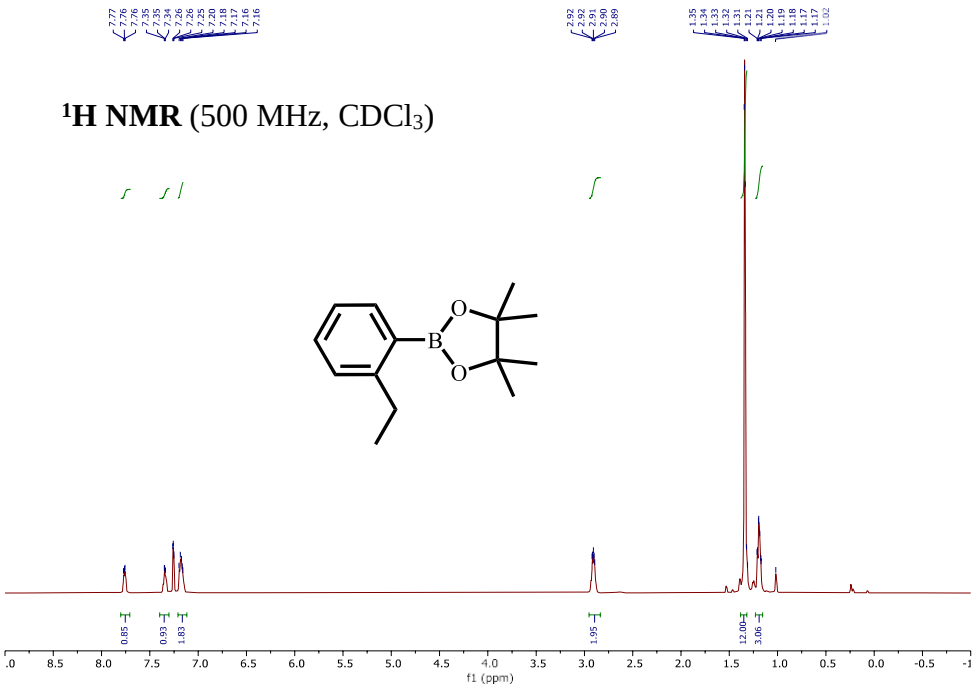

^{1}H NMR (500 MHz, $CDCl_3$)

Figure 4-19. ^{1}H of 2-(2-ethylphenyl)-4,4,5,5-tetramethyl-1,3,2-dioxaborolane (2-48).

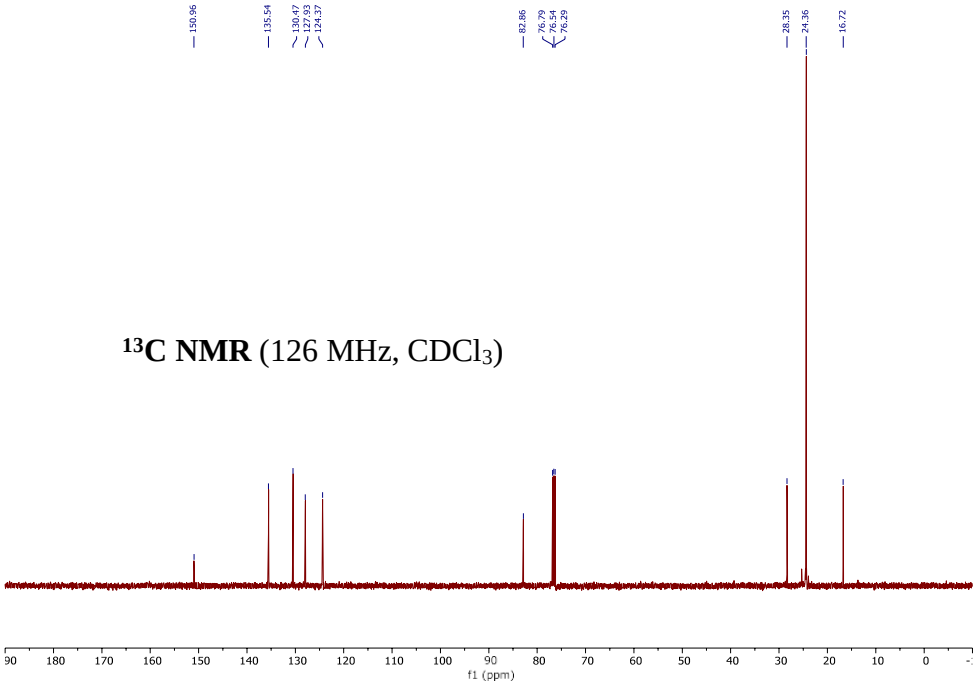

^{13}C NMR (126 MHz, $CDCl_3$)

Figure 4-20. ^{13}C of 2-(2-ethylphenyl)-4,4,5,5-tetramethyl-1,3,2-dioxaborolane (2-48).

2-([1,1'-biphenyl]-2-yl)-4,4,5,5-tetramethyl-1,3,2-dioxaborolane (2-49)

^{1}H NMR (700 MHz, $CDCl_3$)

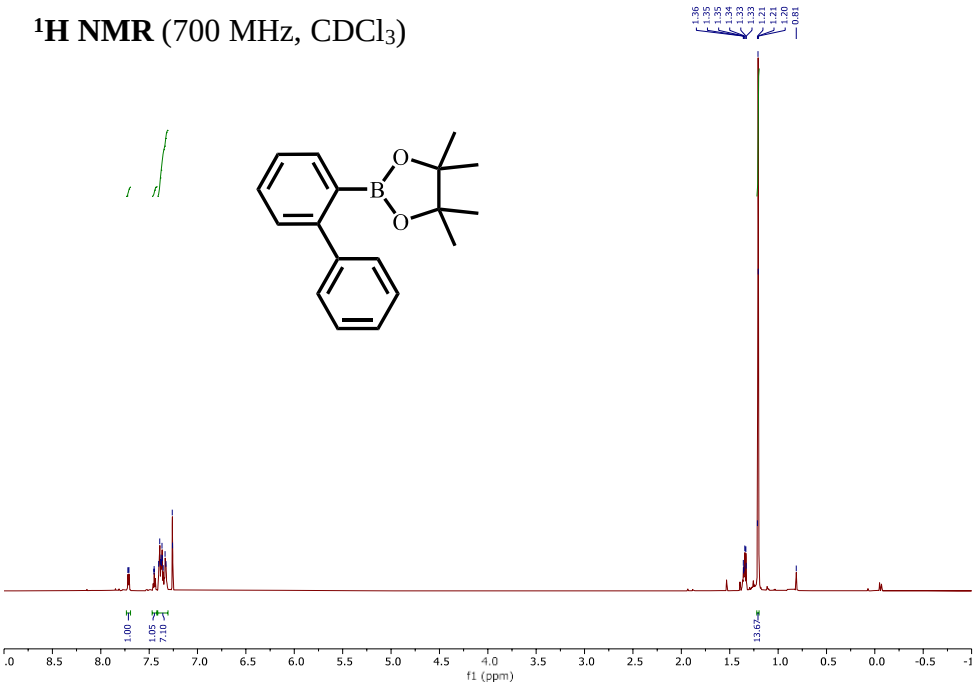

Figure 4-21. ^{1}H of 2-([1,1'-biphenyl]-2-yl)-4,4,5,5-tetramethyl-1,3,2-dioxaborolane (2-49).

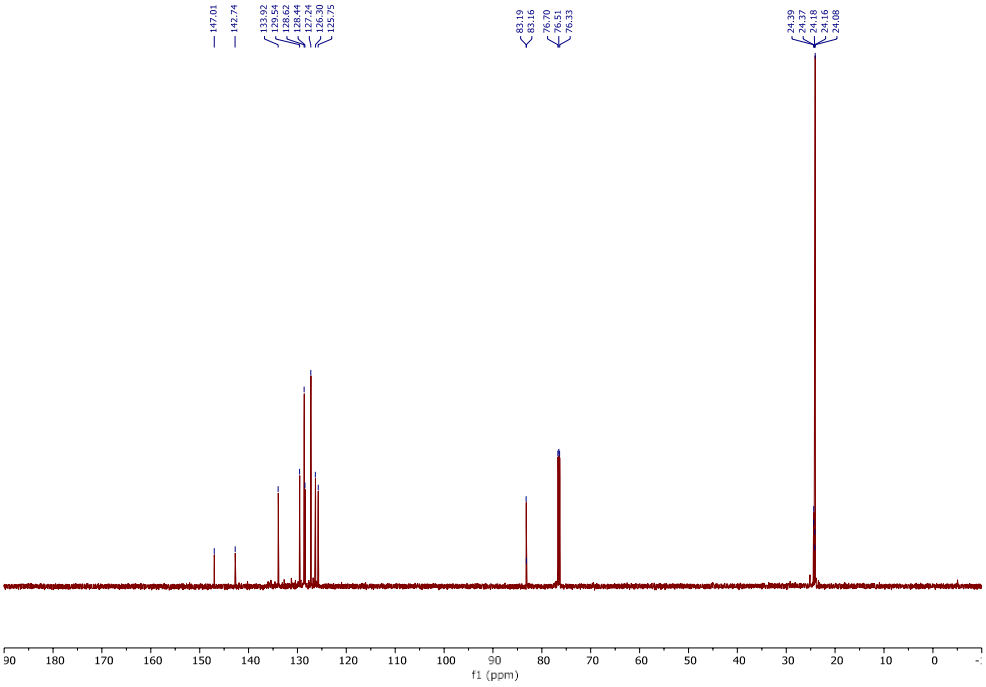

Figure 4-22. ^{13}C of 2-([1,1'-biphenyl]-2-yl)-4,4,5,5-tetramethyl-1,3,2-dioxaborolane (2-49).

4,4,5,5-tetramethyl-2-(3-methyl-[1,1'-biphenyl]-4-yl)-1,3,2-dioxaborolane (2-50)

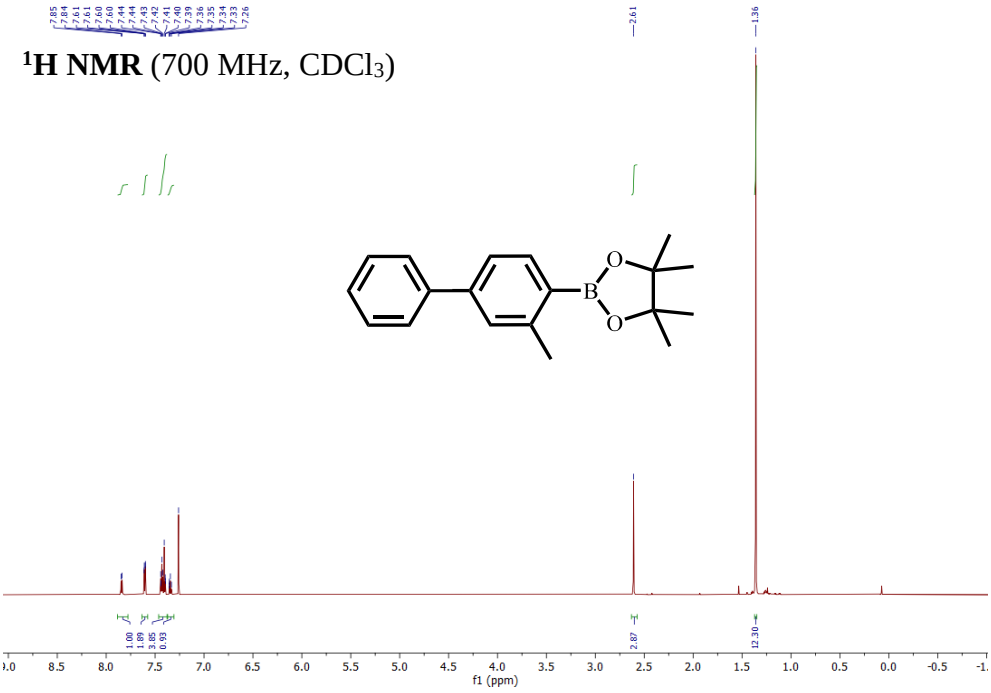

Figure 4-23. ^{1}H of 4,4,5,5-tetramethyl-2-(3-methyl-[1,1'-biphenyl]-4-yl)-1,3,2-dioxaborolane (2-50).

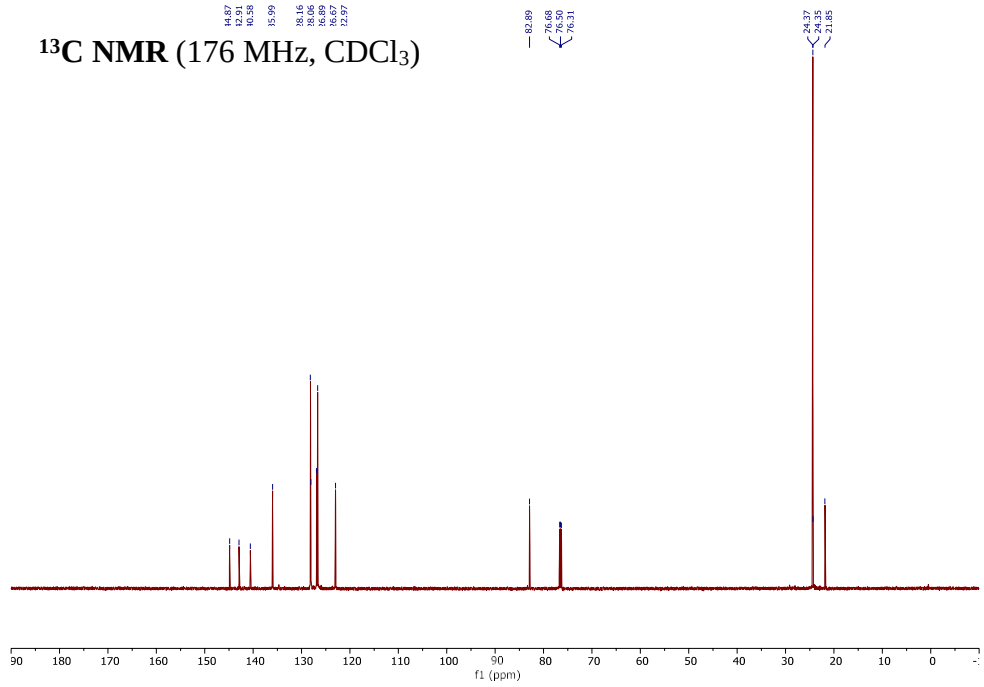

Figure 4-24. ^{13}C of 4,4,5,5-tetramethyl-2-(3-methyl-[1,1'-biphenyl]-4-yl)-1,3,2-dioxaborolane (2-50).

^{11}B NMR (128 MHz, $CDCl_3$)

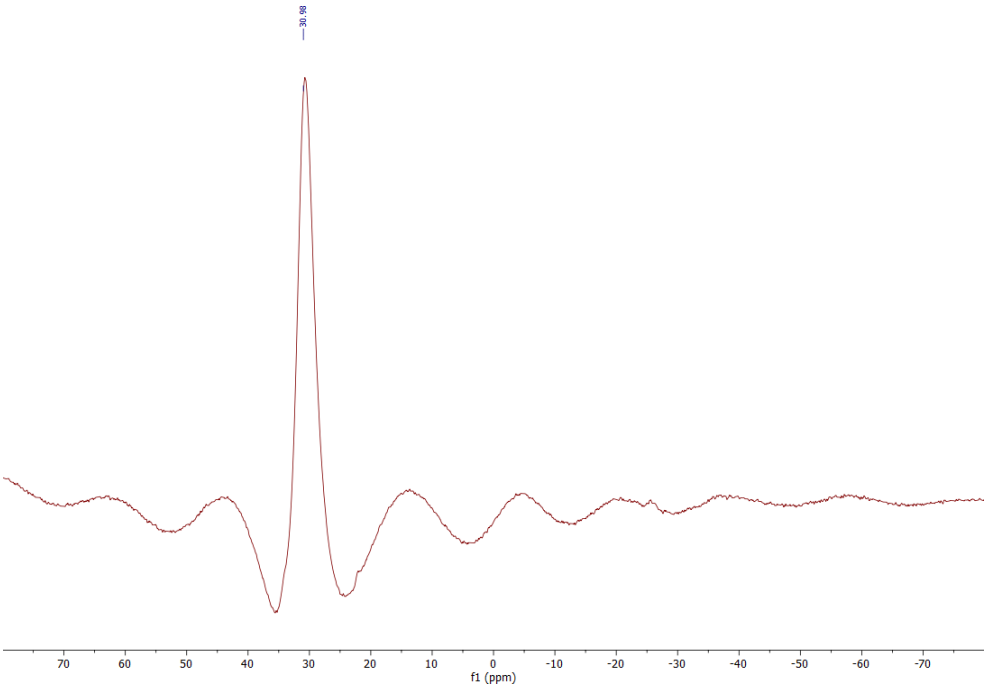

Figure 4-25. ^{11}B of 4,4,5,5-tetramethyl-2-(3-methyl-[1,1'-biphenyl]-4-yl)-1,3,2-dioxaborolane (2-50).

4,4,5,5-tetramethyl-2-(5,6,7,8-tetrahydronaphthalen-2-yl)-1,3,2-dioxaborolane (2-51)

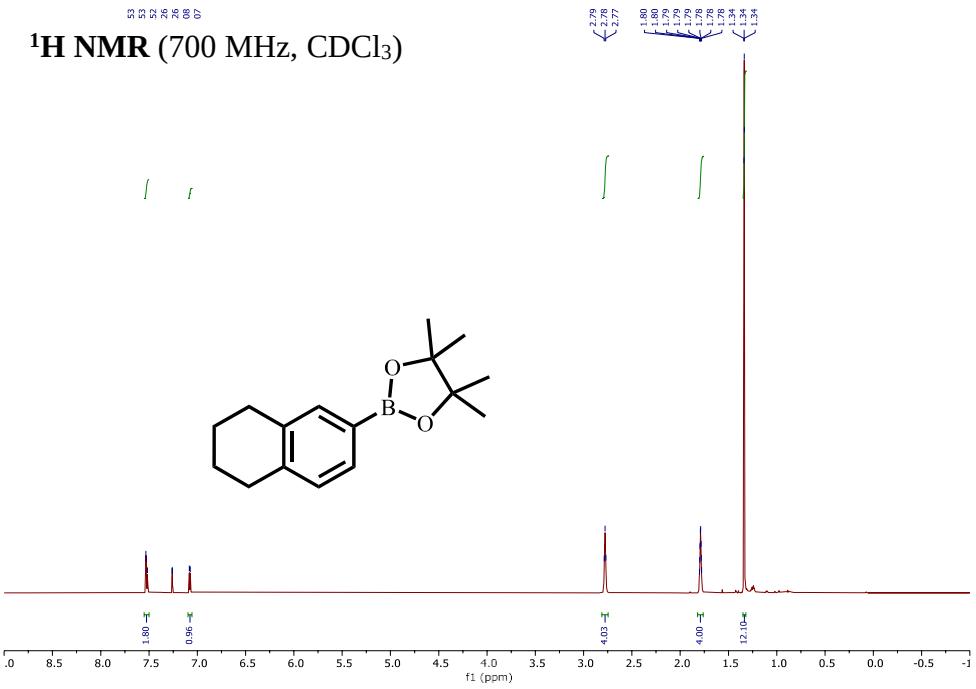

Figure 4-26. ^{1}H of 4,4,5,5-tetramethyl-2-(5,6,7,8-tetrahydronaphthalen-2-yl)-1,3,2-dioxaborolane (2-51).

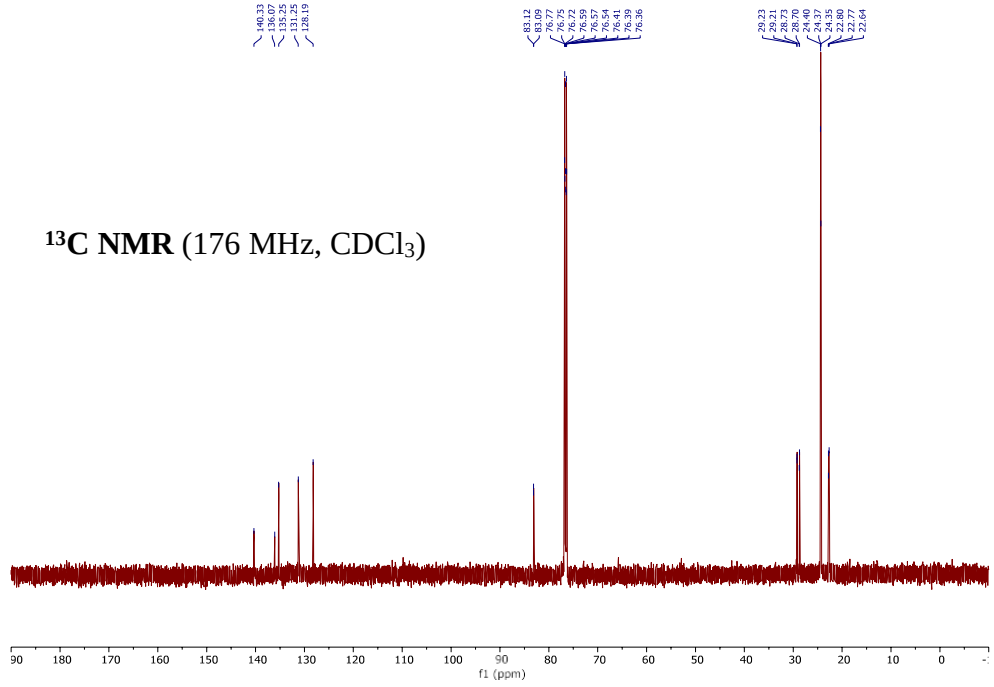

Figure 4-27. ^{13}C of 4,4,5,5-tetramethyl-2-(5,6,7,8-tetrahydronaphthalen-2-yl)-1,3,2-dioxaborolane (2-51).

2-(4-methoxyphenyl)-4,4,5,5-tetramethyl-1,3-dioxolane **(2-52)**

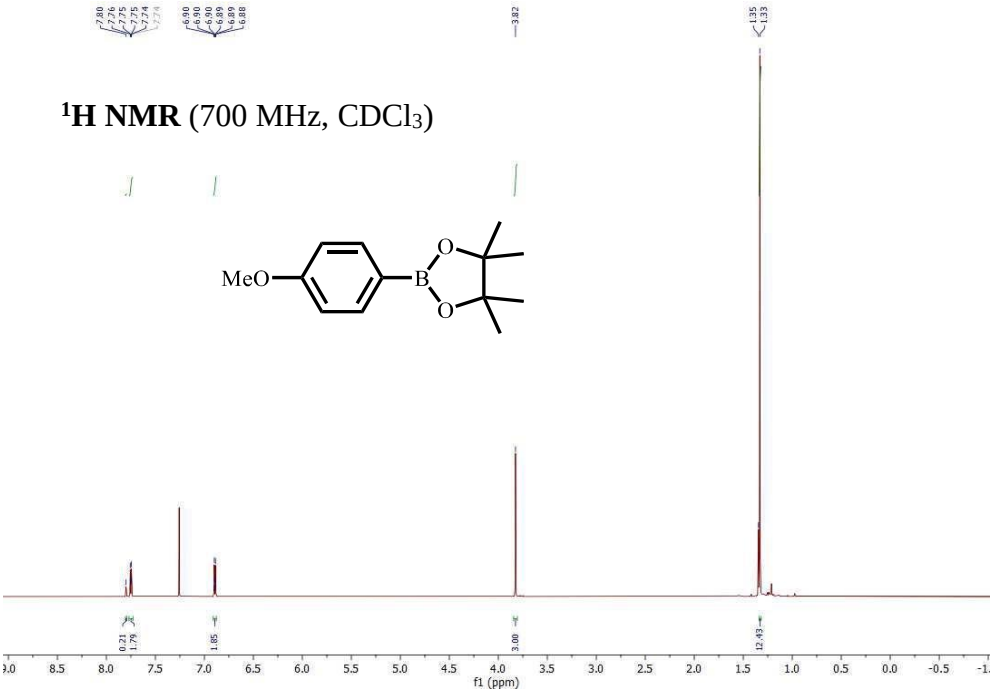

Figure 4-28. [1]H of 2-(4-methoxyphenyl)-4,4,5,5-tetramethyl-1,3-dioxolane (2-52).

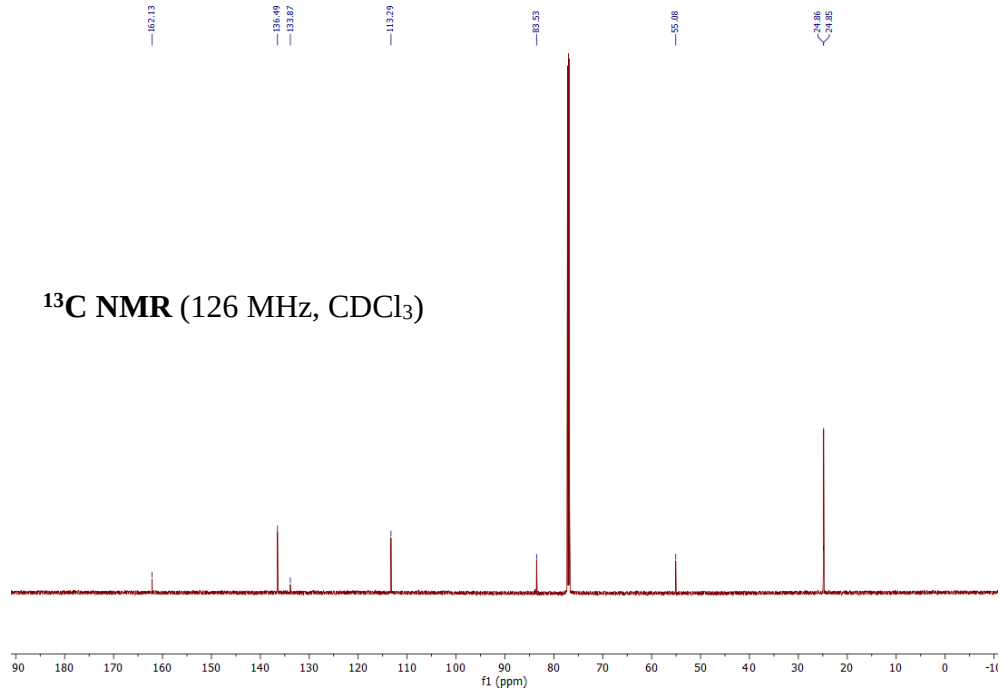

Figure 4-29. [13]C of 2-(4-methoxyphenyl)-4,4,5,5-tetramethyl-1,3-dioxolane (2-52).

1,4-bis(4,4,5,5-tetramethyl-1,3,2-dioxaborolan-2-yl)benzene (2-52')

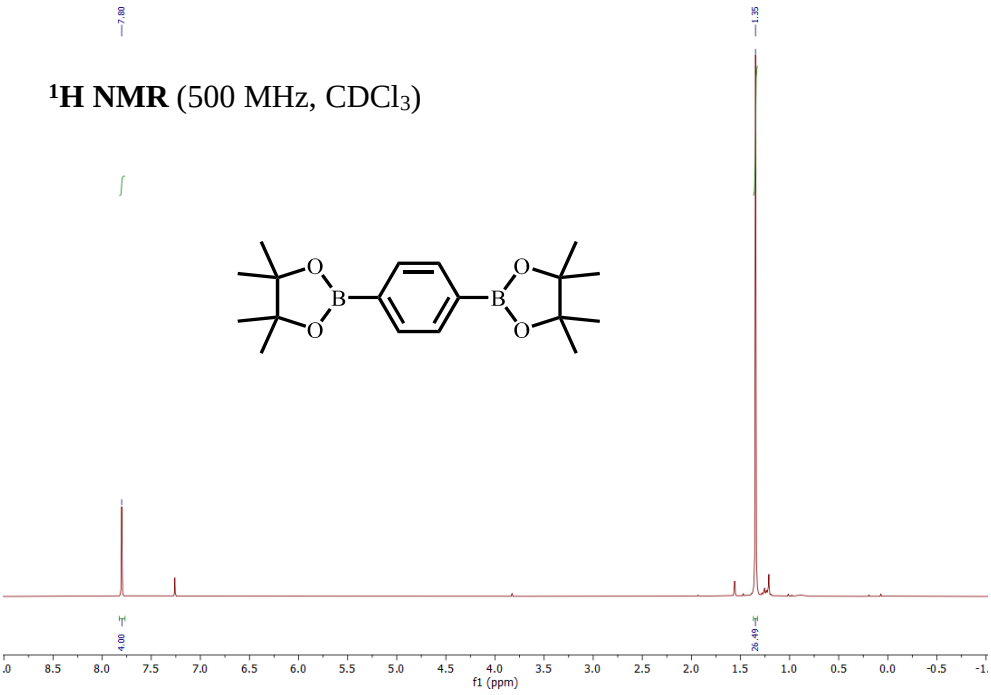

Figure 4-30. [1]H of 1,4-bis(4,4,5,5-tetramethyl-1,3,2-dioxaborolan-2-yl)benzene (2-52').

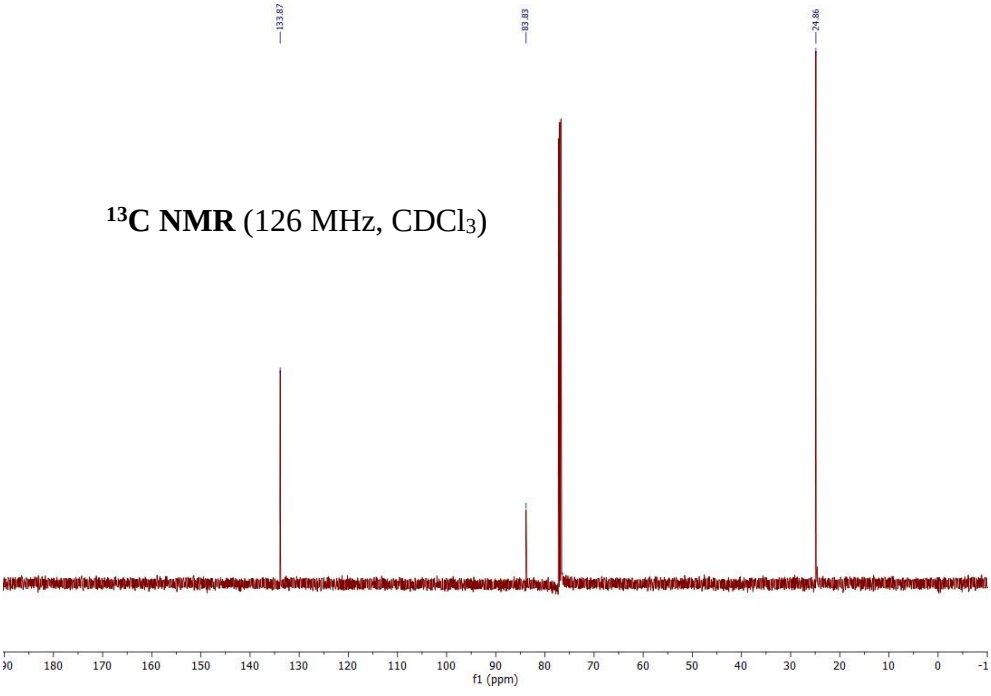

Figure 4-31. [13]C of 1,4-bis(4,4,5,5-tetramethyl-1,3,2-dioxaborolan-2-yl)benzene (2-52').

2-(3-methoxyphenyl)-4,4,5,5-tetramethyl-1,3-dioxolane **(2-53)**

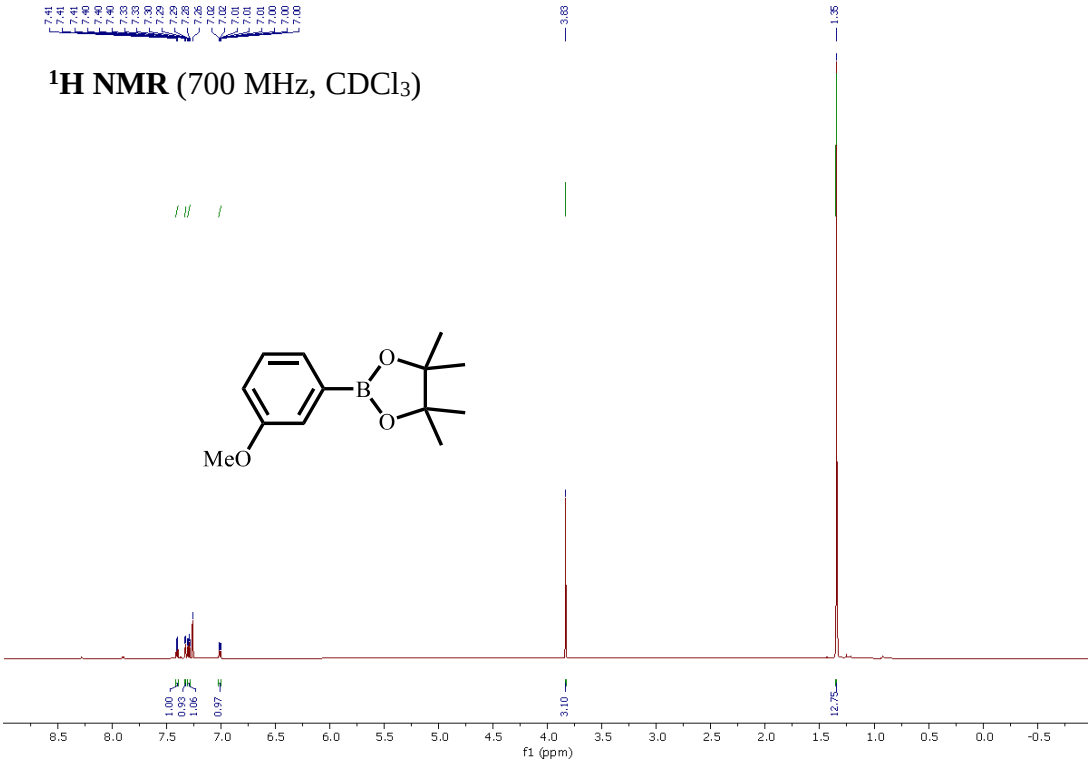

Figure 4-32. [1]H of 2-(3-methoxyphenyl)-4,4,5,5-tetramethyl-1,3-dioxolane (2-53).

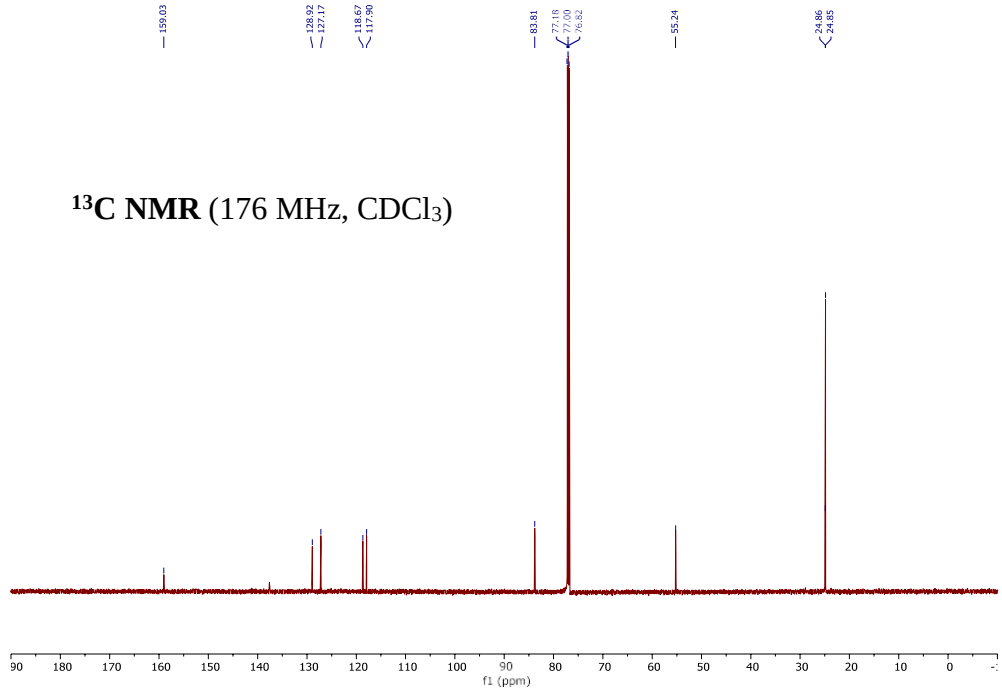

Figure 4-33. [13]C of 2-(3-methoxyphenyl)-4,4,5,5-tetramethyl-1,3-dioxolane (2-53).

***N*,*N*-dimethyl-4-(4,4,5,5-tetramethyl-1,3,2-dioxaborolan-2-yl)aniline** **(2-54)**

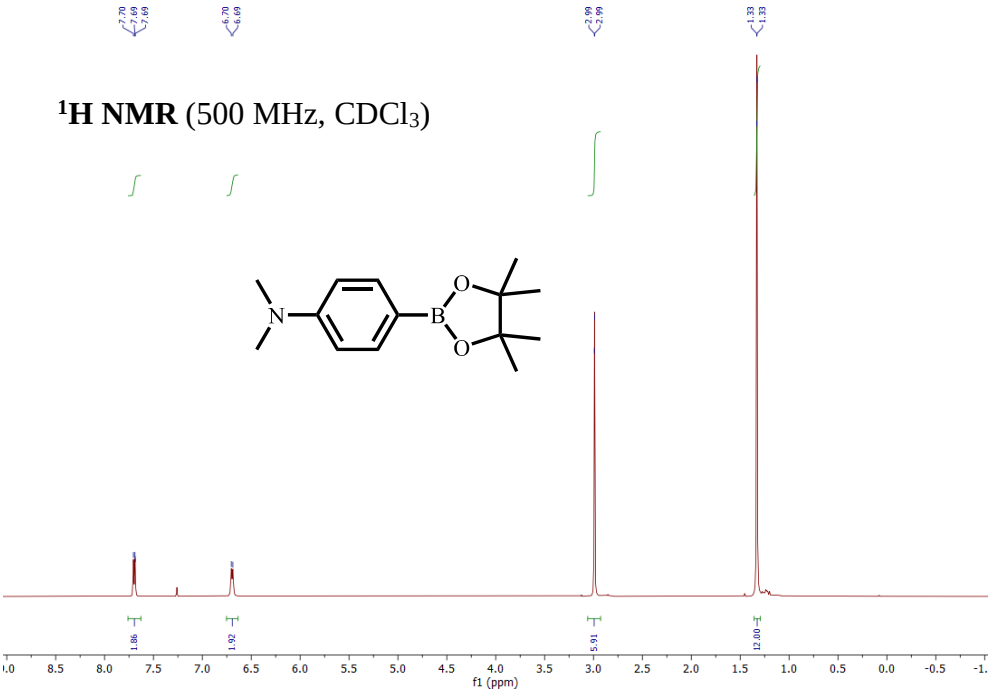

Figure 4-34. ^{1}H of *N*,*N*-dimethyl-4-(4,4,5,5-tetramethyl-1,3,2-dioxaborolan-2-yl)aniline (2-54).

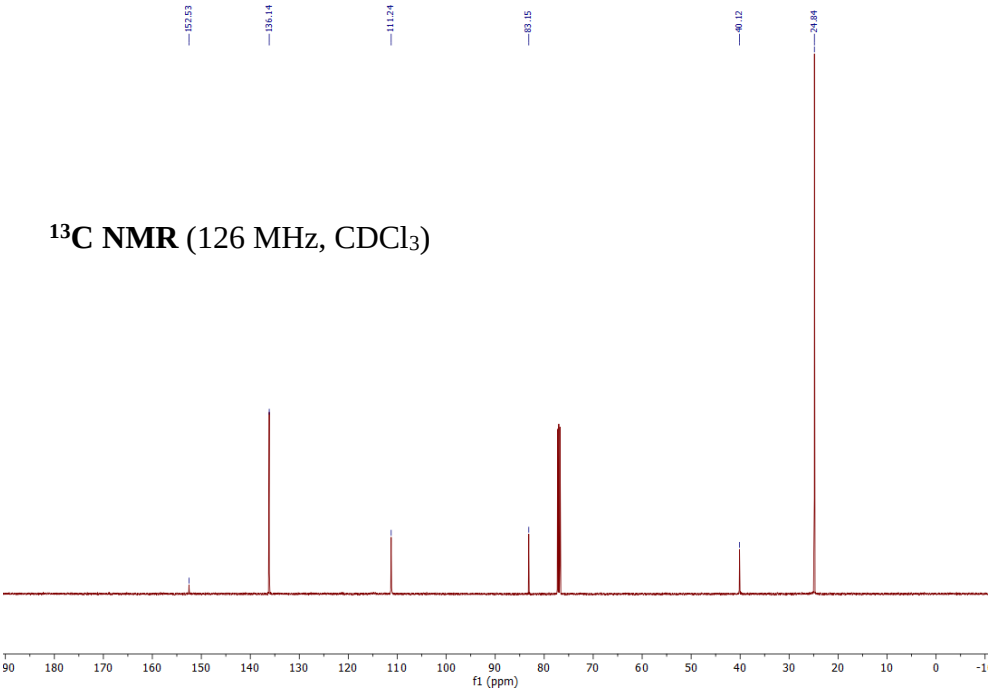

Figure 4-35. ^{13}C of *N*,*N*-dimethyl-4-(4,4,5,5-tetramethyl-1,3,2-dioxaborolan-2-yl)aniline (2-54).

4-(3-(4,4,5,5-tetramethyl-1,3,2-dioxaborolan-2-yl)phenyl)morpholine (2-55)

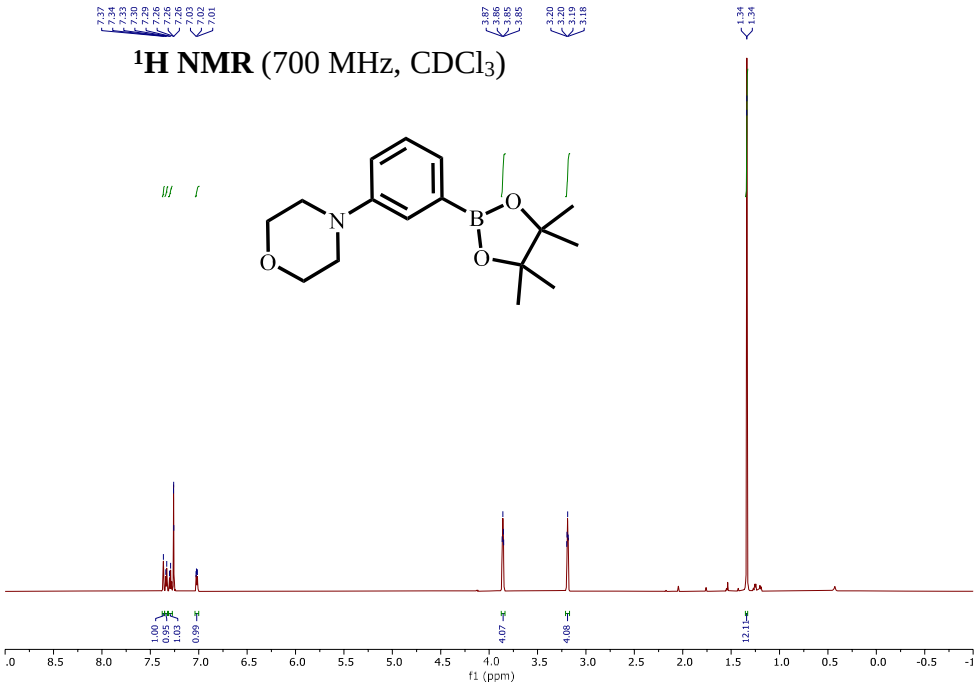

Figure 4-36. ^{1}H of 4-(3-(4,4,5,5-tetramethyl-1,3,2-dioxaborolan-2-yl)phenyl)morpholine (2-55).

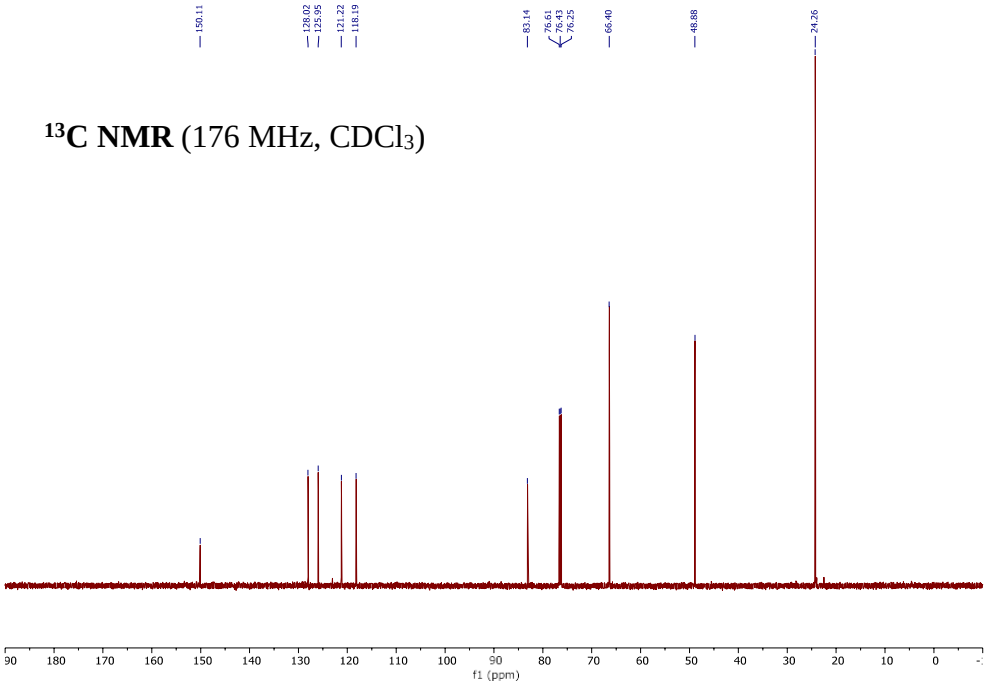

Figure 4-37. ^{13}C of 4-(3-(4,4,5,5-tetramethyl-1,3,2-dioxaborolan-2-yl)phenyl)morpholine (2-55).

3-(4,4,5,5-tetramethyl-1,3,2-dioxaborolan-2-yl)aniline **(2-56)**

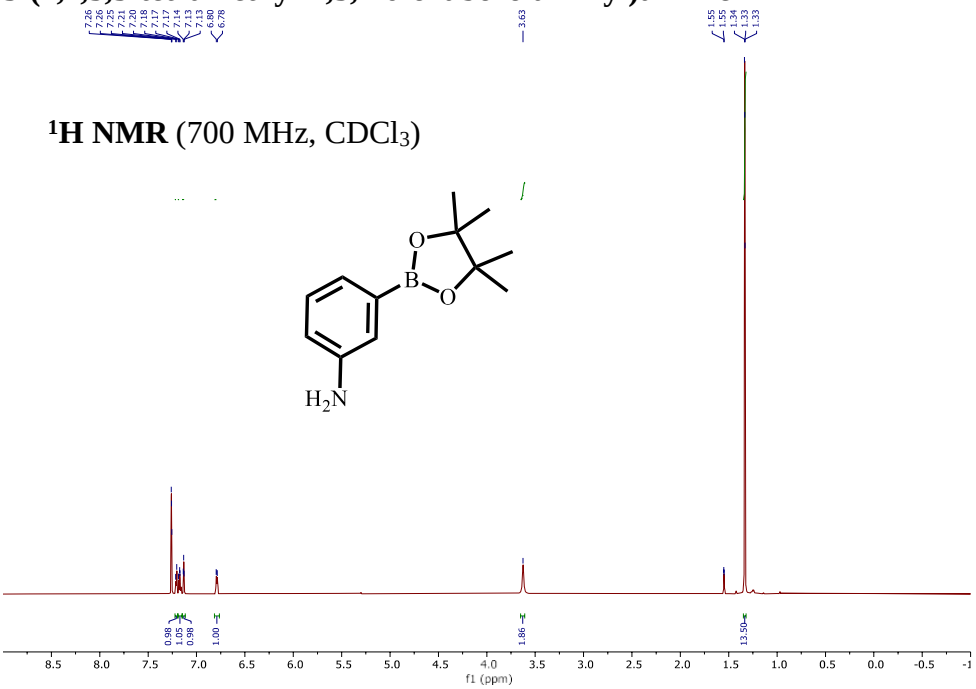

Figure 4-38. ^{1}H of 3-(4,4,5,5-tetramethyl-1,3,2-dioxaborolan-2-yl)aniline (2-56).

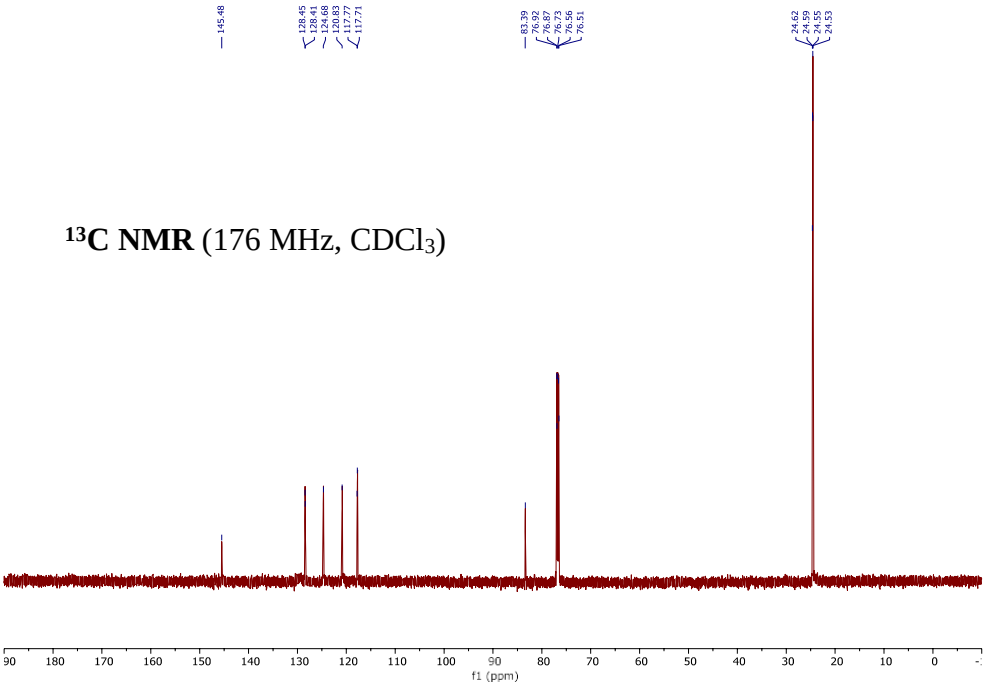

Figure 4-39. ^{13}C of 3-(4,4,5,5-tetramethyl-1,3,2-dioxaborolan-2-yl)aniline (2-56).

9-methyl-2-(4,4,5,5-tetramethyl-1,3,2-dioxaborolan-2-yl)-9H-carbazole (2-57)

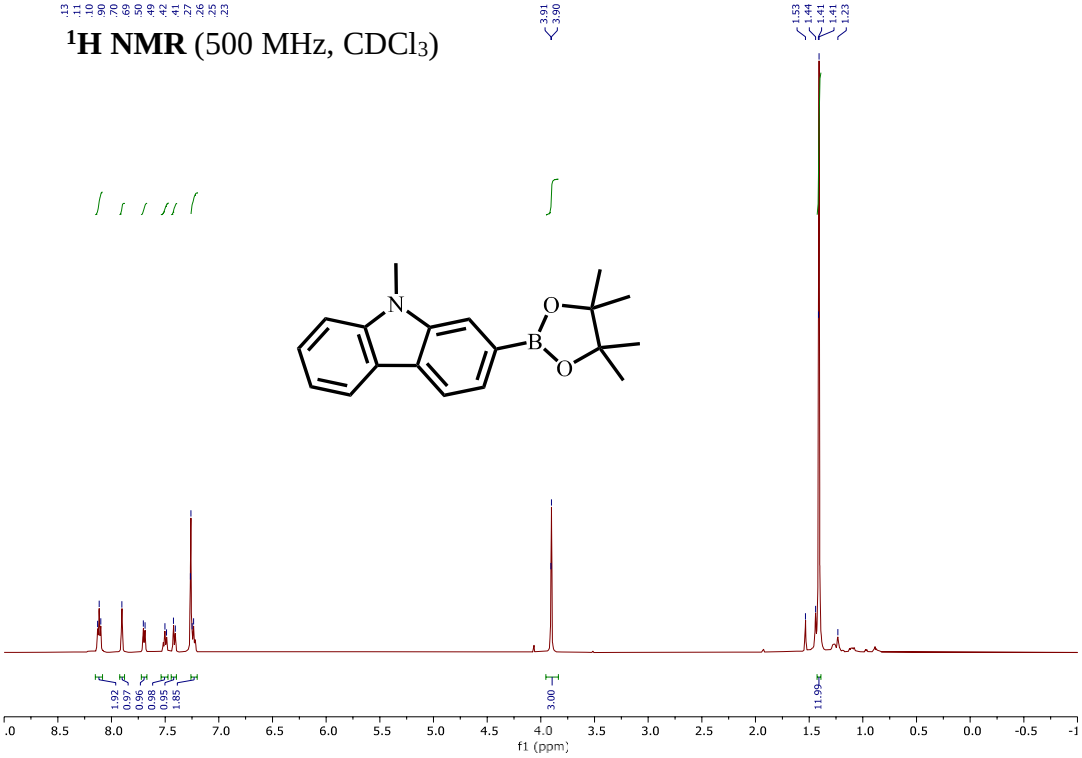

Figure 4-40. ^{1}H of 9-methyl-2-(4,4,5,5-tetramethyl-1,3,2-dioxaborolan-2-yl)-9H-carbazole (2-57).

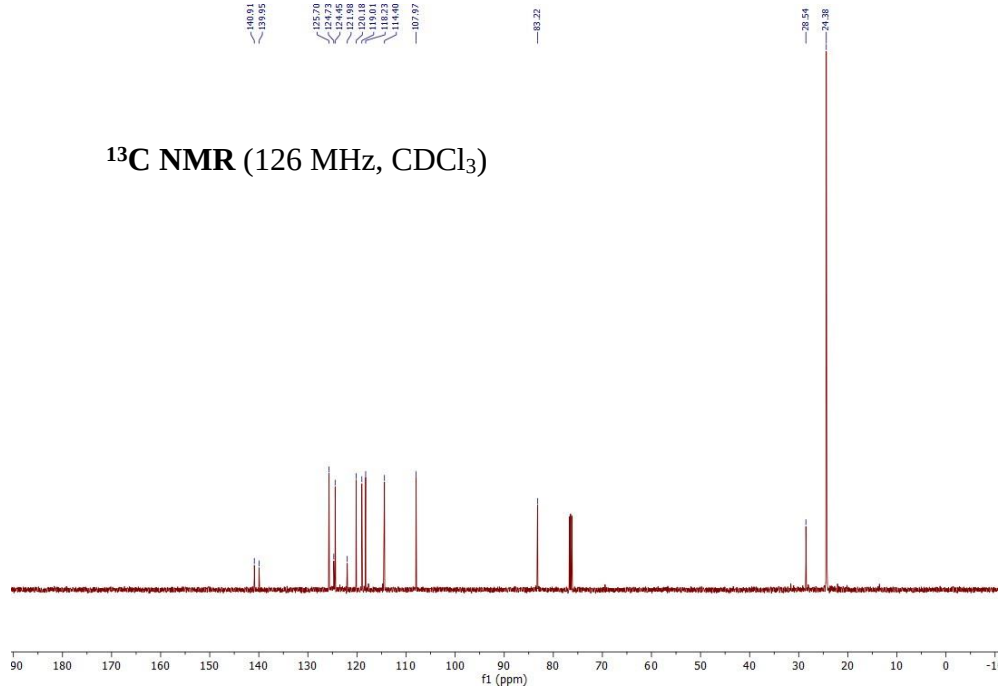

Figure 4-41. ^{13}C of 9-methyl-2-(4,4,5,5-tetramethyl-1,3,2-dioxaborolan-2-yl)-9H-carbazole (2-57).

2-(4-(4,4,5,5-tetramethyl-1,3,2-dioxaborolan-2-yl)phenyl)pyridine (2-58)

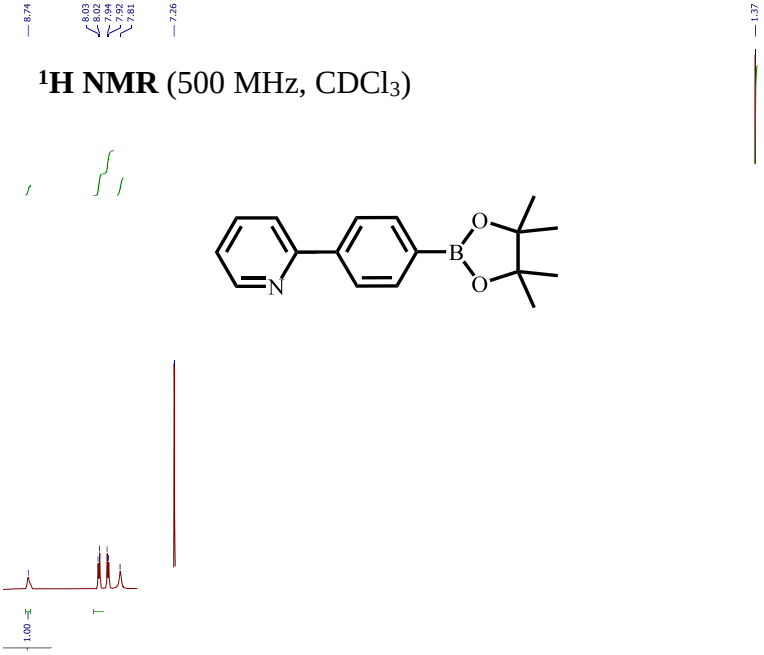

Figure 4-42. ^{1}H of 2-(4-(4,4,5,5-tetramethyl-1,3,2-dioxaborolan-2-yl)phenyl)pyridine (2-58).

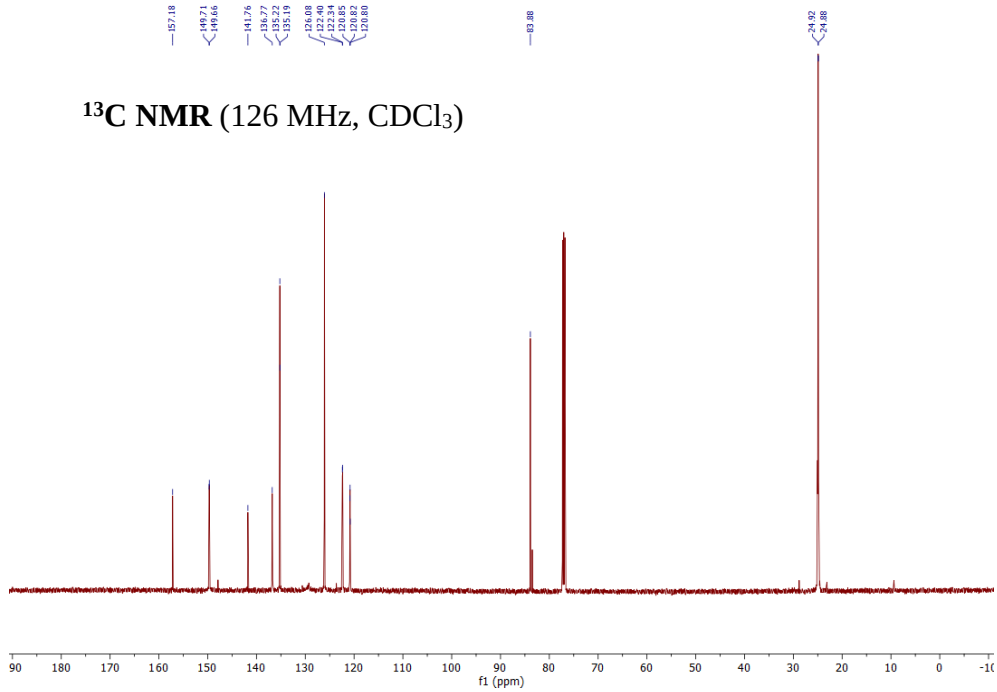

Figure 4-43. ^{13}C of 2-(4-(4,4,5,5-tetramethyl-1,3,2-dioxaborolan-2-yl)phenyl)pyridine (2-58).

1-(3-(4,4,5,5-tetramethyl-1,3,2-dioxaborolan-2-yl)phenyl)-1H-indole (2-59)

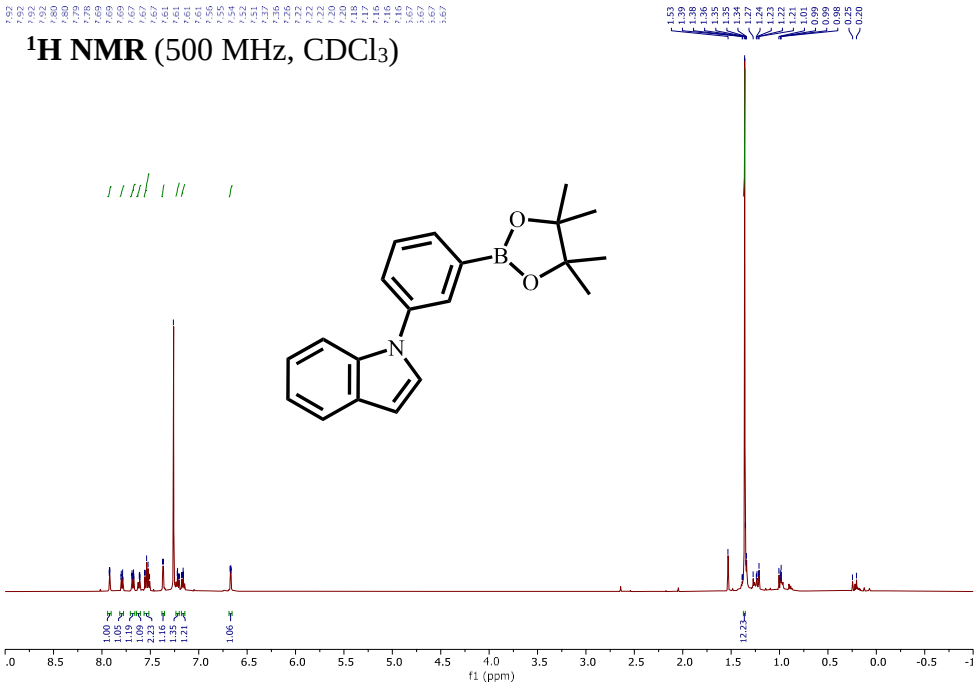

Figure 4-44. ^{1}H of 1-(3-(4,4,5,5-tetramethyl-1,3,2-dioxaborolan-2-yl)phenyl)-1H-indole (2-59).

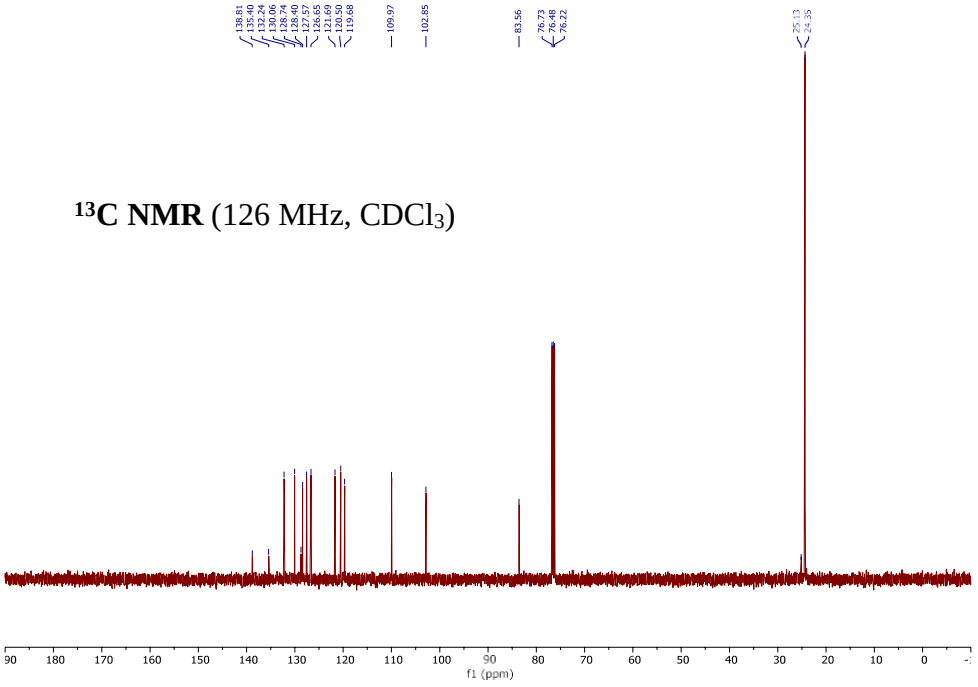

Figure 4-45. ^{13}C of 1-(3-(4,4,5,5-tetramethyl-1,3,2-dioxaborolan-2-yl)phenyl)-1H-indole (2-59).

^{11}B NMR (128 MHz, $CDCl_3$)

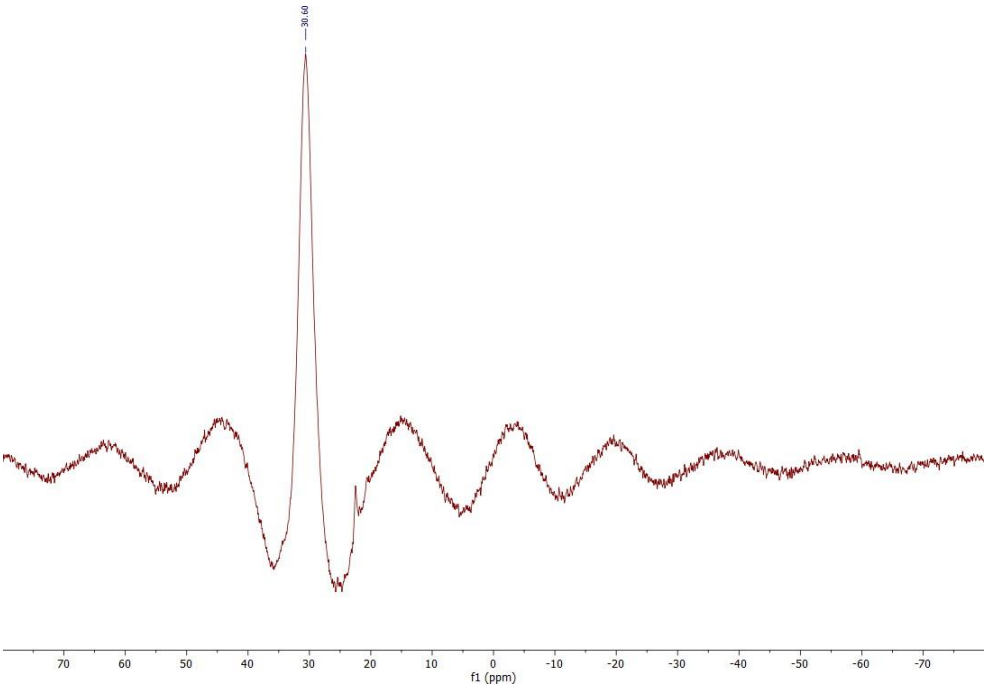

Figure 4-46. ^{11}B of 1-(3-(4,4,5,5-tetramethyl-1,3,2-dioxaborolan-2-yl)phenyl)-1H-indole (2-59).

4,4,5,5-tetramethyl-2-(naphthalen-2-ylmethyl)-1,3,2-dioxaborolane (2-60)

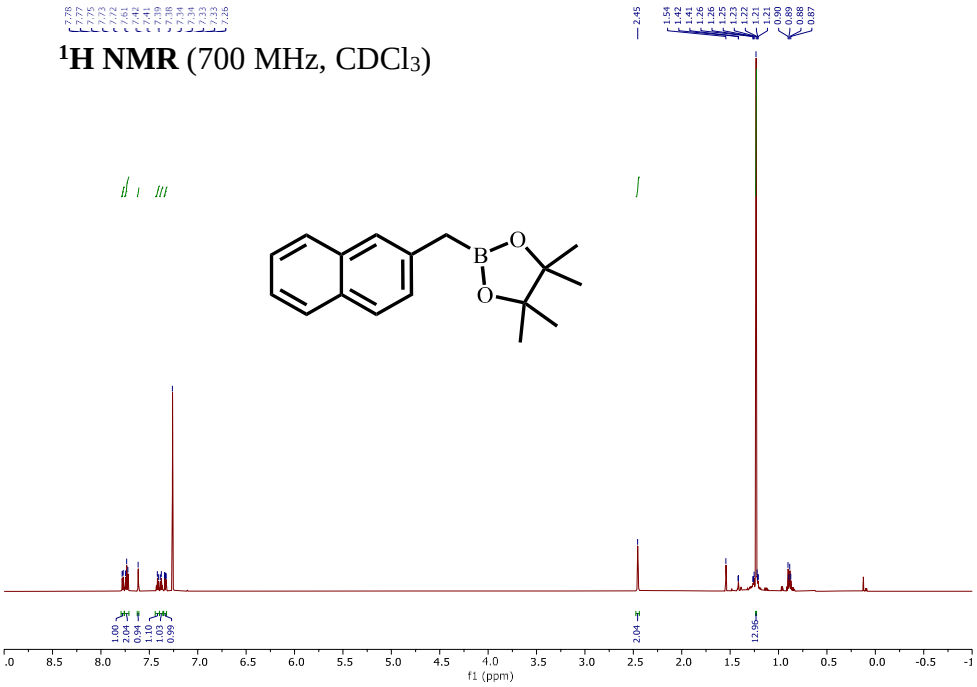

Figure 4-47. ^{1}H of 4,4,5,5-tetramethyl-2-(naphthalen-2-ylmethyl)-1,3,2-dioxaborolane (2-60).

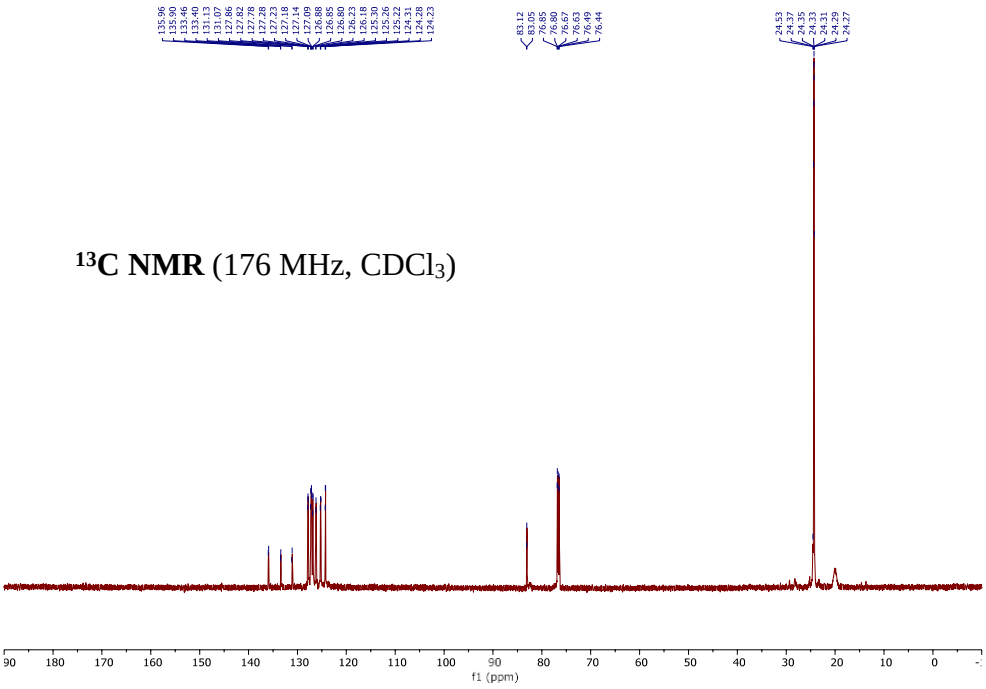

Figure 4-48. ^{13}C of 4,4,5,5-tetramethyl-2-(naphthalen-2-ylmethyl)-1,3,2-dioxaborolane (2-60).

2-([1,1'-biphenyl]-4-ylmethyl)-4,4,5,5-tetramethyl-1,3,2-dioxaborolane (2-61)

^{1}H NMR (500 MHz, $CDCl_3$)

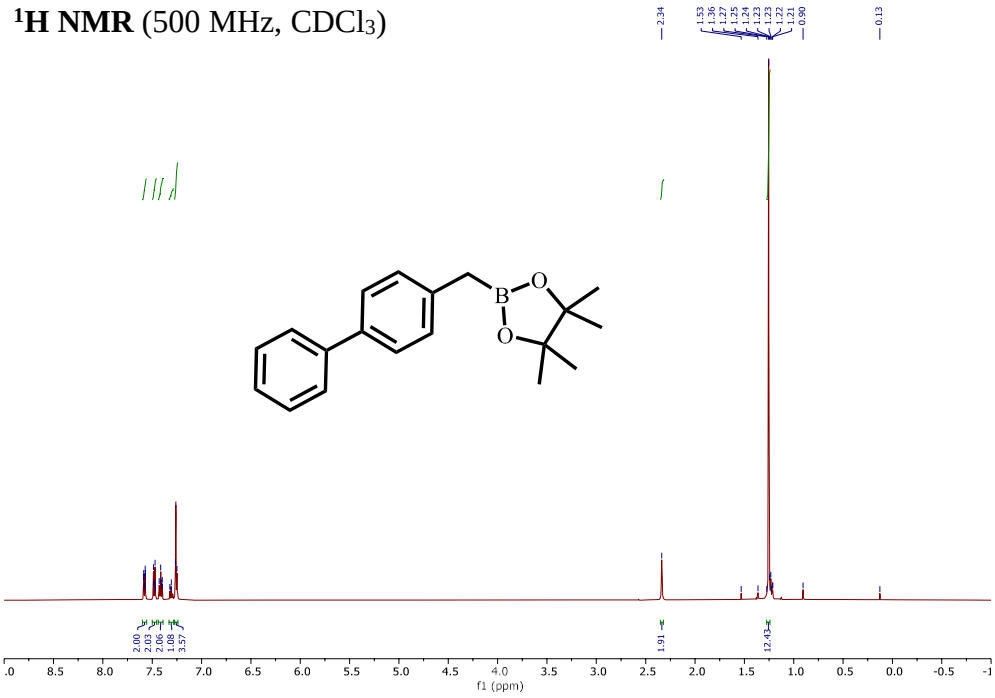

Figure 4-49. ^{1}H of 2-([1,1'-biphenyl]-4-ylmethyl)-4,4,5,5-tetramethyl-1,3,2-dioxaborolane (2-61).

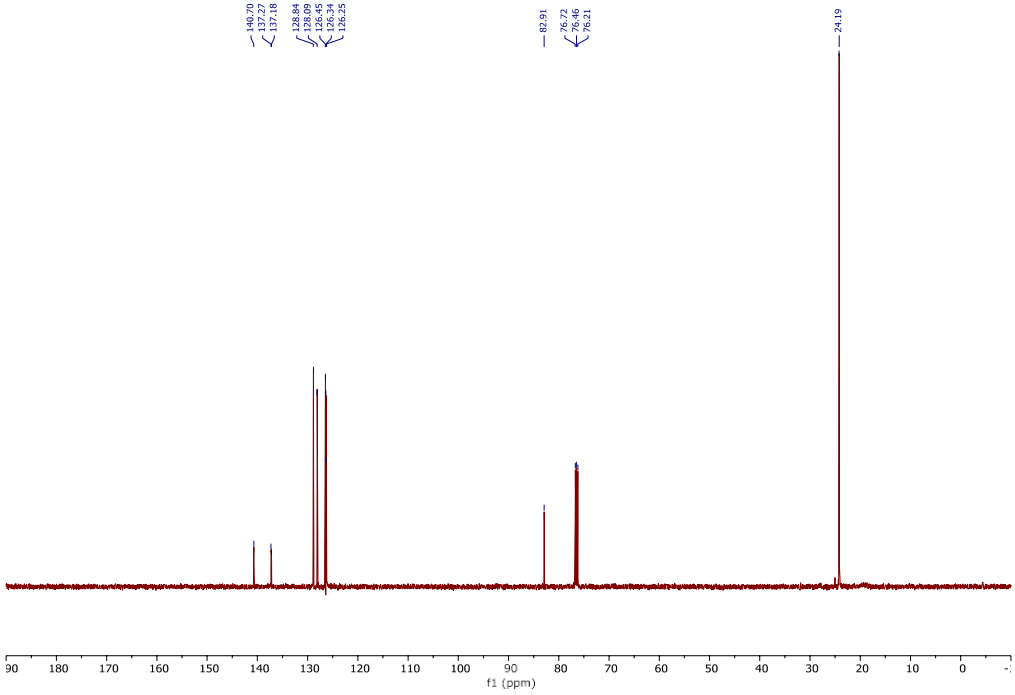

Figure 4-50. ^{13}C of 2-([1,1'-biphenyl]-4-ylmethyl)-4,4,5,5-tetramethyl-1,3,2-dioxaborolane (2-61).

2-benzyl-4,4,5,5-tetramethyl-1,3,2-dioxaborolane **(2-62)**

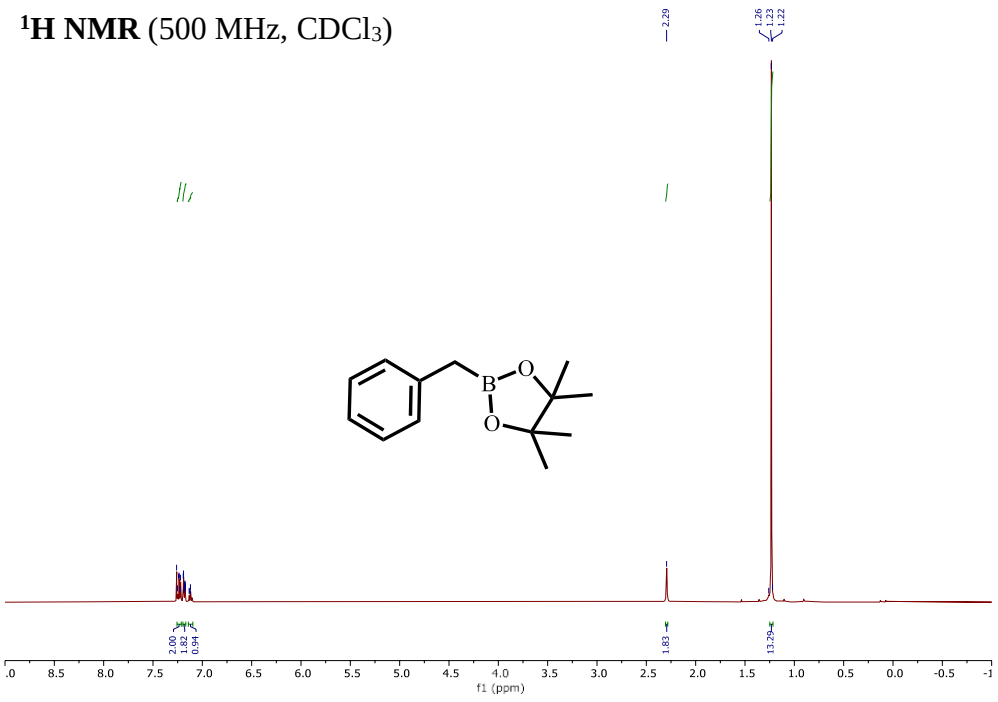

Figure 4-51. [1]H of 2-benzyl-4,4,5,5-tetramethyl-1,3,2-dioxaborolane (2-62).

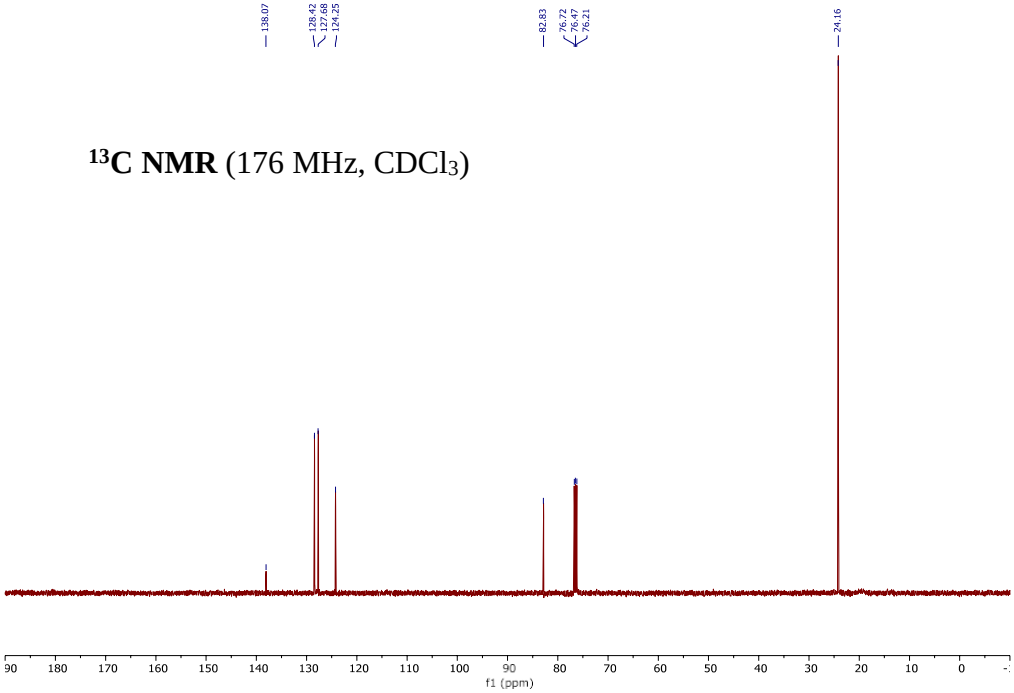

Figure 4-52. [13]C of 2-benzyl-4,4,5,5-tetramethyl-1,3,2-dioxaborolane (2-62).

2-(3-methoxybenzyl)-4,4,5,5-tetramethyl-1,3,2-dioxaborolane **(2-63)**

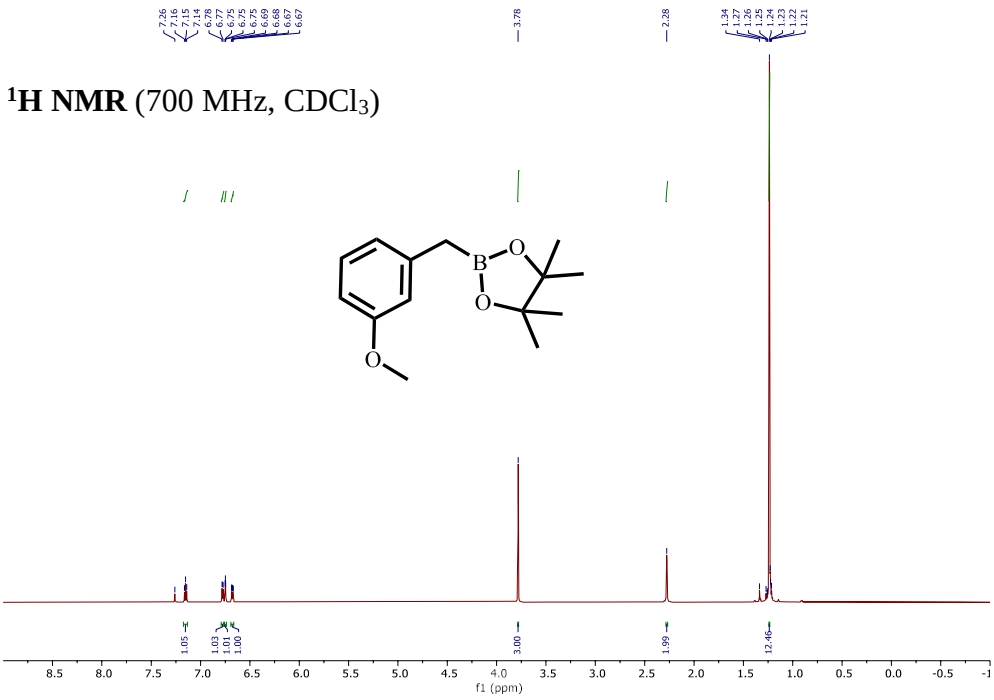

Figure 4-53. [1]H of 2-(3-methoxybenzyl)-4,4,5,5-tetramethyl-1,3,2-dioxaborolane (2-63).

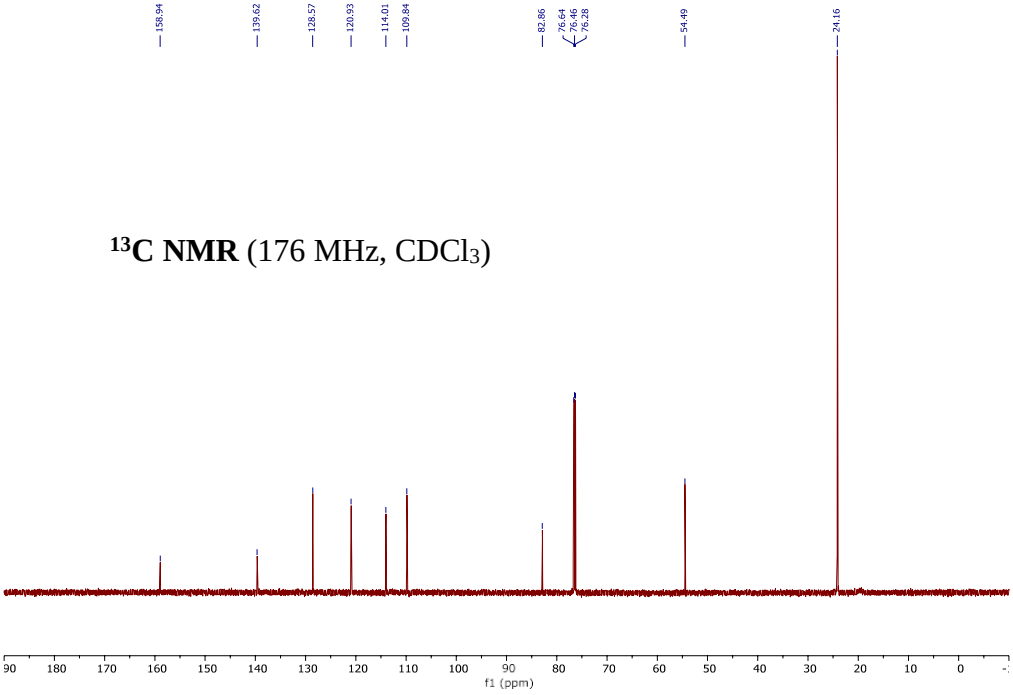

Figure 4-54. [13]C of 2-(3-methoxybenzyl)-4,4,5,5-tetramethyl-1,3,2-dioxaborolane (2-63).

4-(4'-(((*tert*-butyldimethylsilyl)oxy)methyl)-[1,1'-biphenyl]-4-yl)morpholine (2-76)

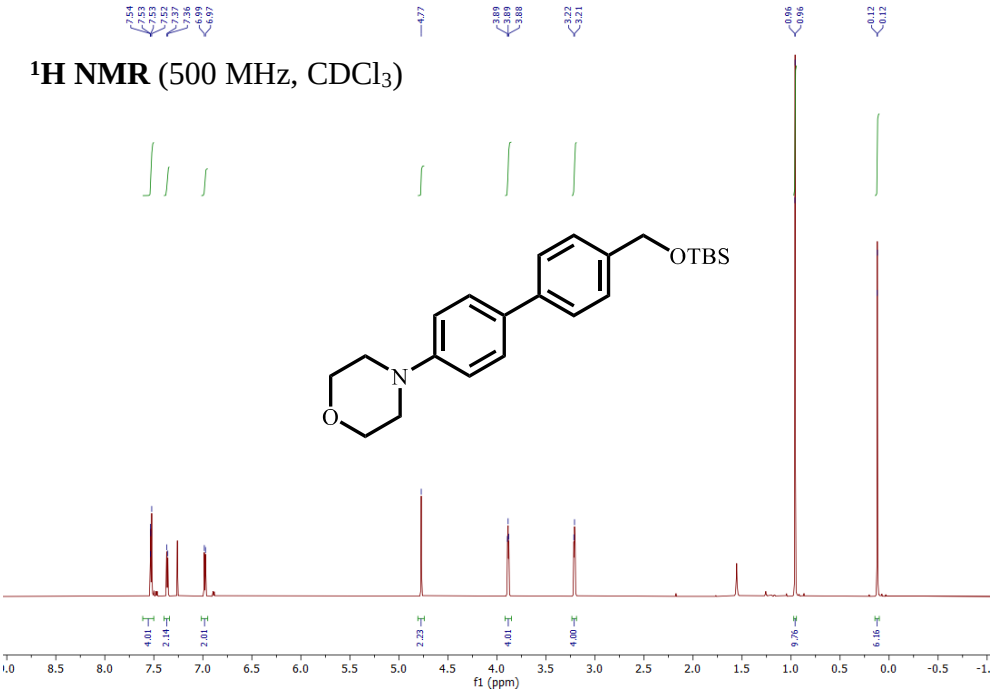

Figure 4-55. ^{1}H of 4-(4'-(((*tert*-butyldimethylsilyl)oxy)methyl)-[1,1'-biphenyl]-4-yl)morpholine (2-76).

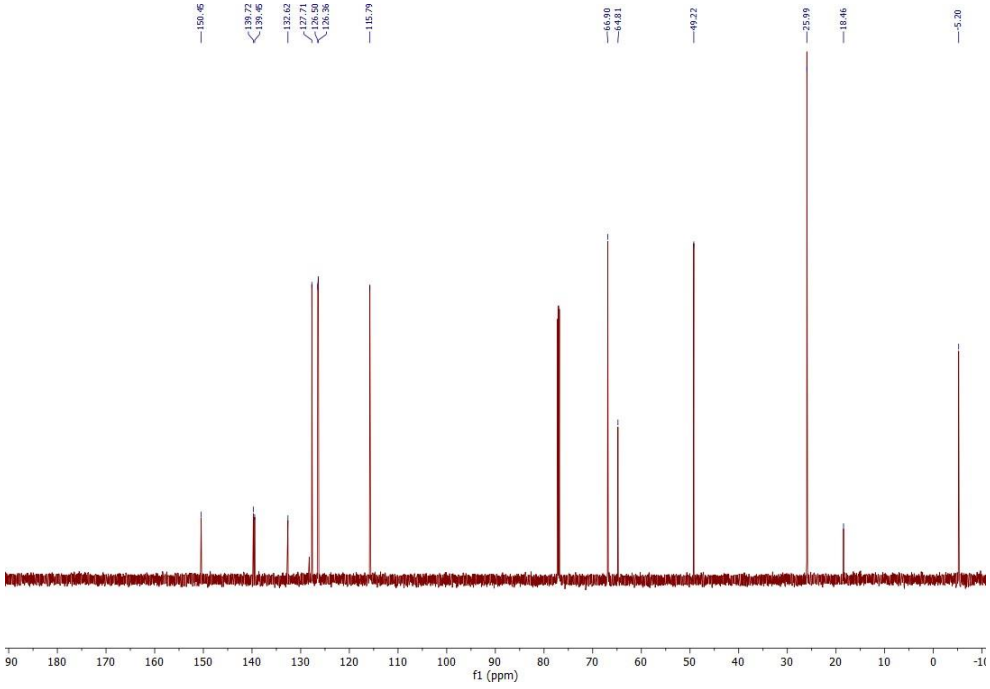

Figure 4-56. ^{13}C of 4-(4'-(((*tert*-butyldimethylsilyl)oxy)methyl)-[1,1'-biphenyl]-4-yl)morpholine (2-76).

4-(4'-((4,4,5,5-tetramethyl-1,3,2-dioxaborolan-2-yl)methyl)-[1,1'-biphenyl]-4-yl)morpholine (2-77)

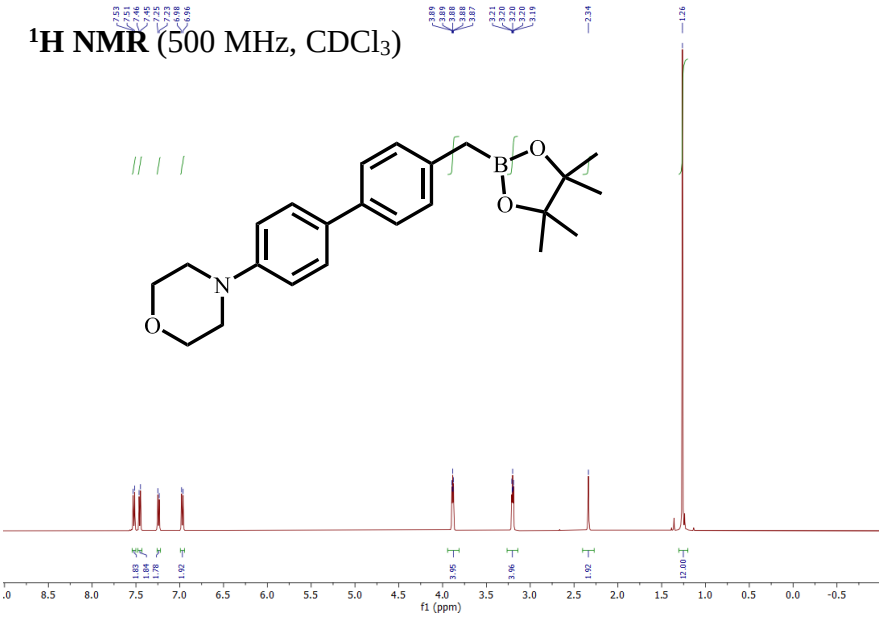

Figure 4-57. ^{1}H of 4-(4'-((4,4,5,5-tetramethyl-1,3,2-dioxaborolan-2-yl)methyl)-[1,1'-biphenyl]-4-yl)morpholine(2-77).

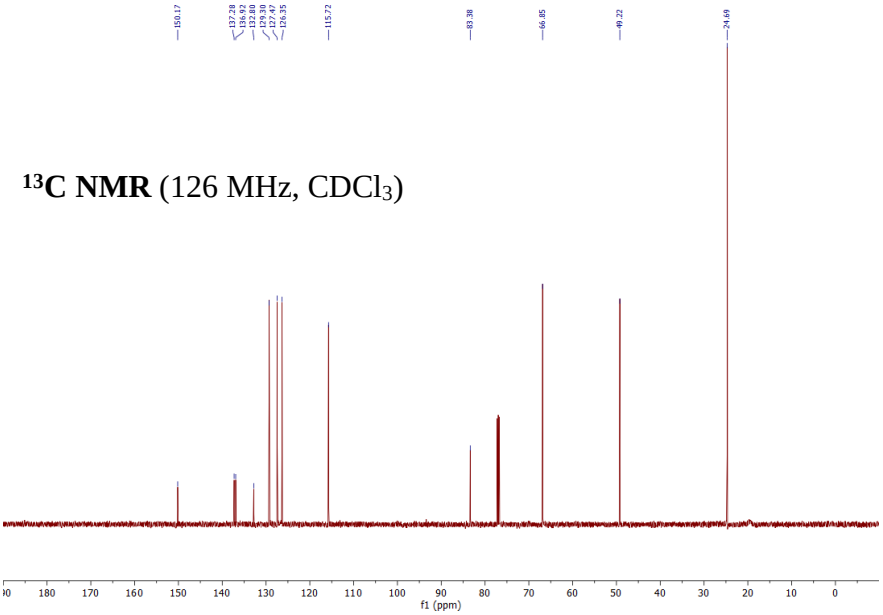

Figure 4-58. ^{13}C of 4-(4'-((4,4,5,5-tetramethyl-1,3,2-dioxaborolan-2-yl)methyl)-[1,1'-biphenyl]-4-yl)morpholine(2-77).

^{11}B NMR (160 MHz, $CDCl_3$)

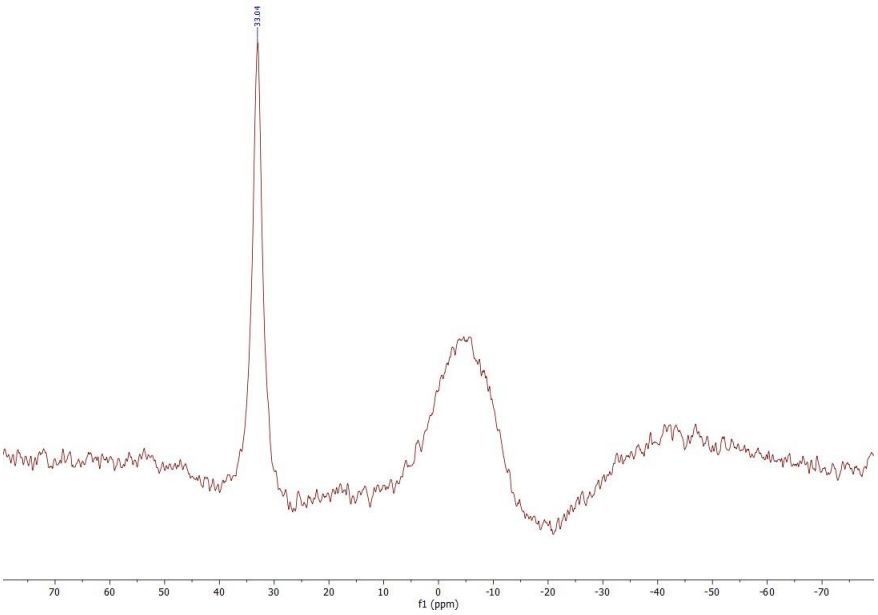

Figure 4-59. ^{11}B of 4-(4'-((4,4,5,5-tetramethyl-1,3,2-dioxaborolan-2-yl)methyl)-[1,1'-biphenyl]-4-yl)morpholine(2-77).

tert-butyldimethyl((4'-(4,4,5,5-tetramethyl-1,3,2-dioxaborolan-2-yl)-[1,1'-biphenyl]-4-yl)methoxy)silane (2-75)

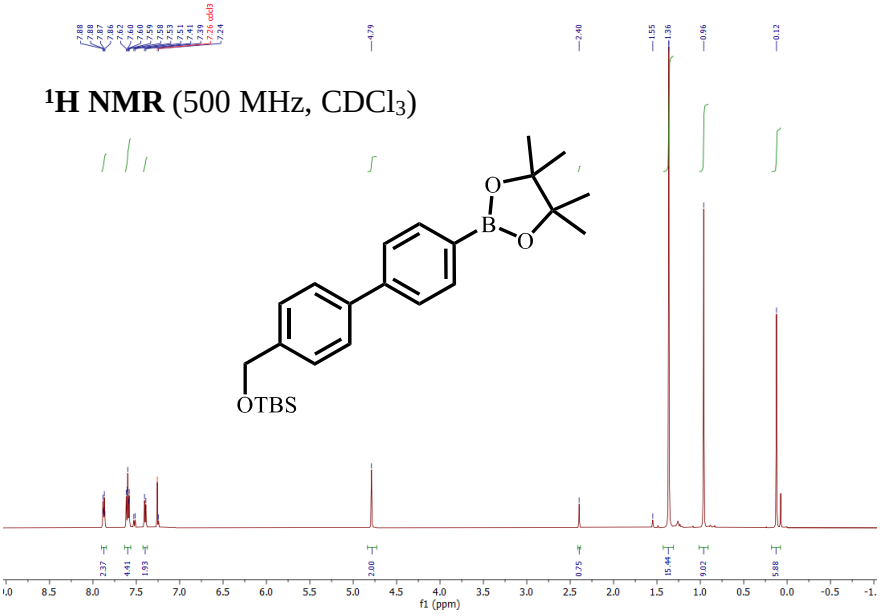

Figure 4-60. ^{1}H of *tert*-butyldimethyl((4'-(4,4,5,5-tetramethyl-1,3,2-dioxaborolan-2-yl)-[1,1'-biphenyl]-4-yl)methoxy)silane (2-75).

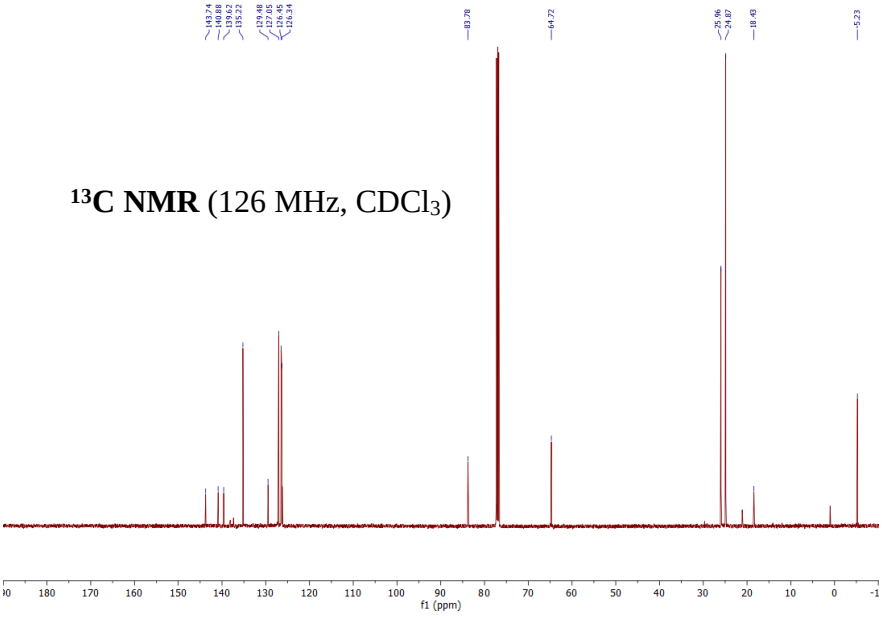

Figure 4-61. ^{13}C of *tert*-butyldimethyl((4'-(4,4,5,5-tetramethyl-1,3,2-dioxaborolan-2-yl)-[1,1'-biphenyl]-4-yl)methoxy)silane (2-75)

^{11}B NMR (160 MHz, $CDCl_3$)

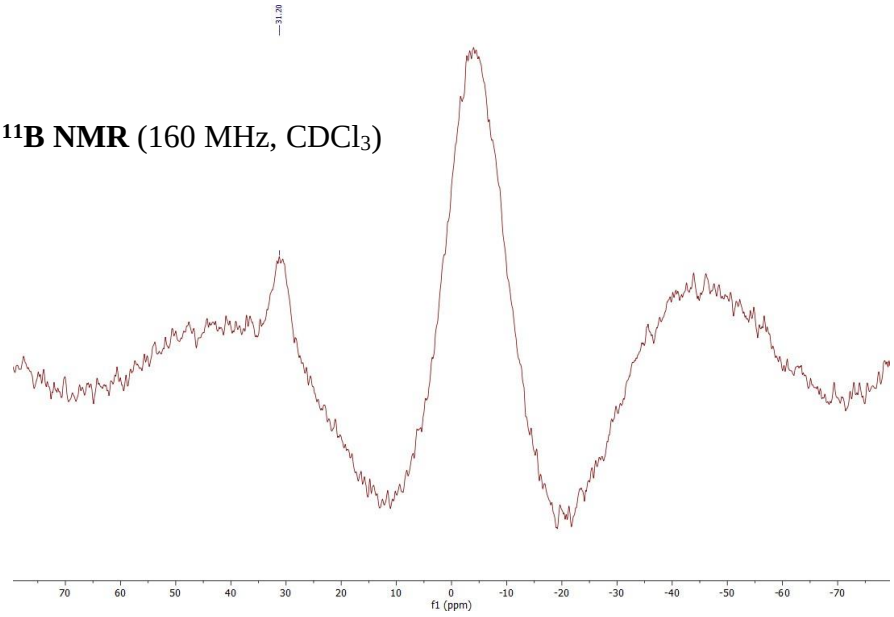

Figure 4-62. ^{11}B of *tert*-butyldimethyl((4'-(4,4,5,5-tetramethyl-1,3,2-dioxaborolan-2-yl)-[1,1'-biphenyl]-4-yl)methoxy)silane (2-75).

4,4,5,5-tetramethyl-2-(naphthalen-2-yl)-1,3,2-dioxaborolane and regioisomers (2-41)

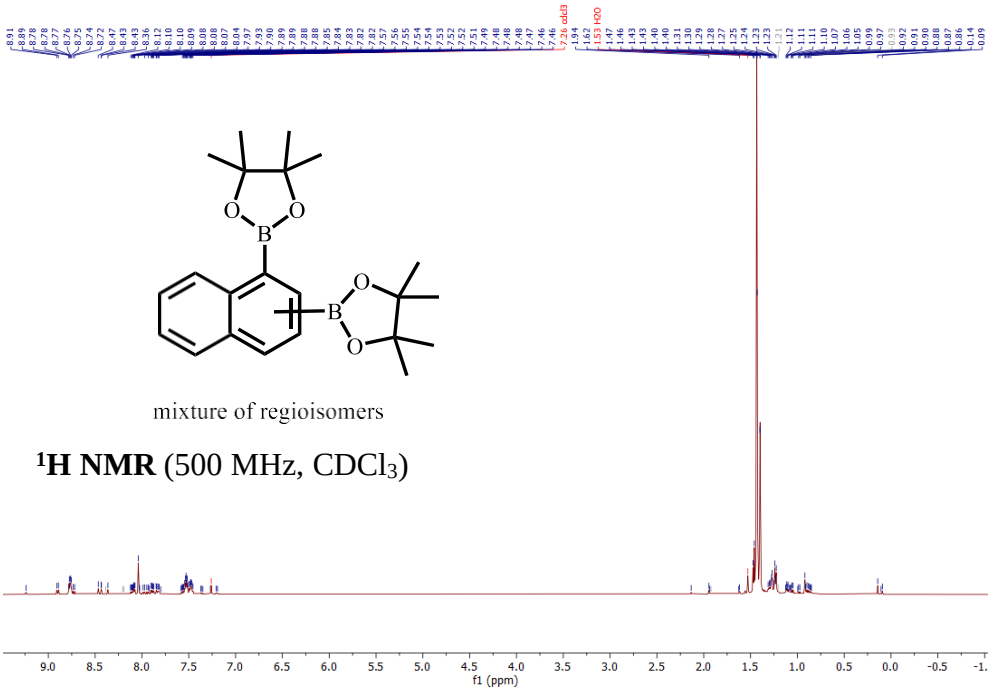

Figure 4-63. ^{1}H of 4,4,5,5-tetramethyl-2-(naphthalen-2-yl)-1,3,2-dioxaborolane and regioisomers (2-41).

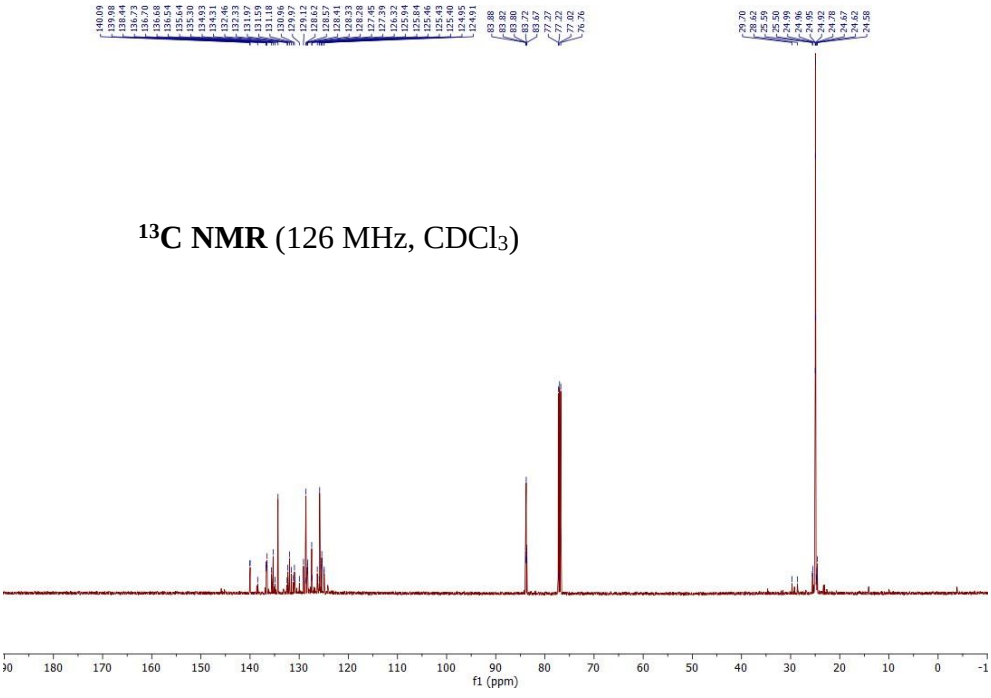

Figure 4-64. ^{13}C of 4,4,5,5-tetramethyl-2-(naphthalen-2-yl)-1,3,2-dioxaborolane and regioisomers (2-41).

Bis(di-tert-butyl fumarate)(1,3-bis(2,4,6-trimethylphenyl)imidazol-2-ylidene)nickel(0) (**3-24**)

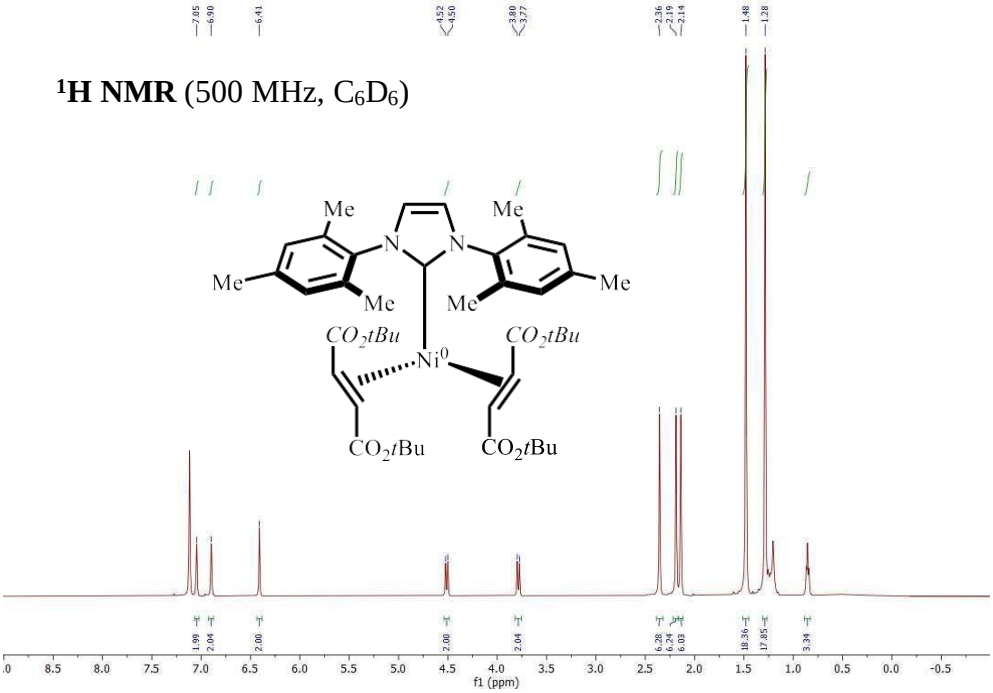

Figure 4-65. [1]H of Bis(di-tert-butyl fumarate)(1,3-bis(2,4,6-trimethylphenyl)imidazol-2-ylidene)nickel(0) (3-24).

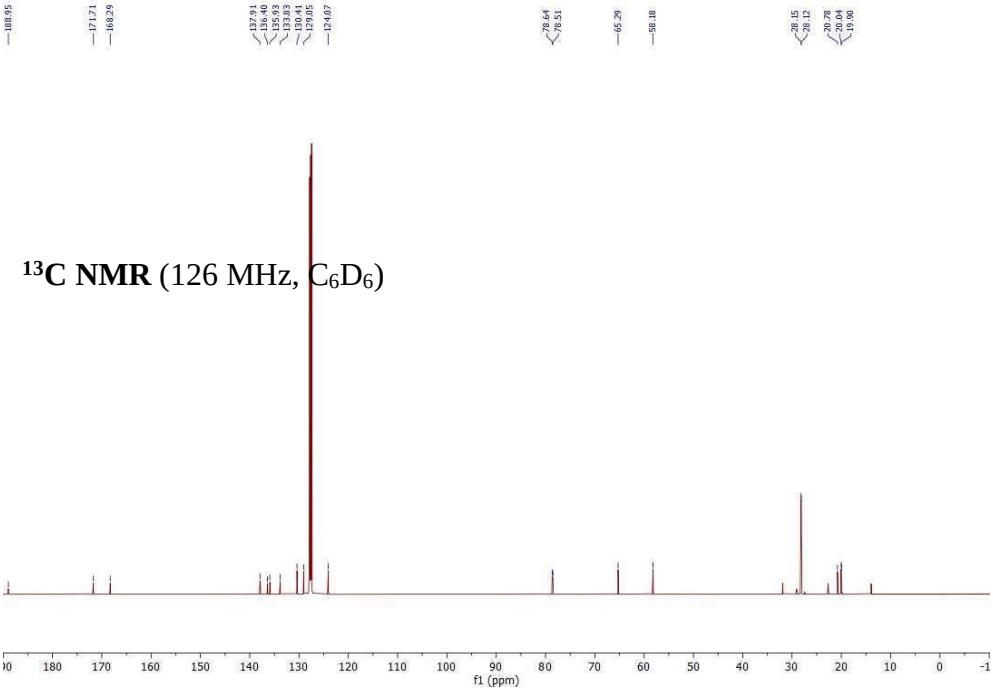

Figure 4-66. [13]C of Bis(di-tert-butyl fumarate)(1,3-bis(2,4,6-trimethylphenyl)imidazol-2-ylidene)nickel(0) (3-24).

di-*tert*-Butyl Fumarate (3-36)

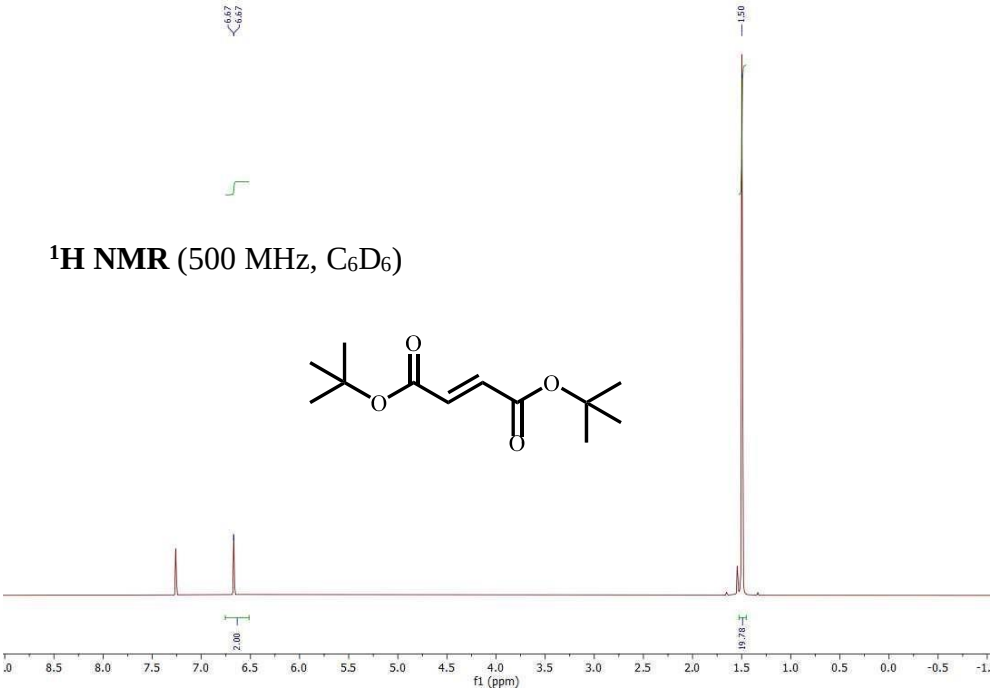

Figure 4-67. ^{1}H of di-tert-Butyl Fumarate (3-36).

Bis(di-tert-butyl fumarate)(1,3-bis(2,4,6-trimethylphenyl)imidazol-2-ylidene)nickel(0) (3-38)

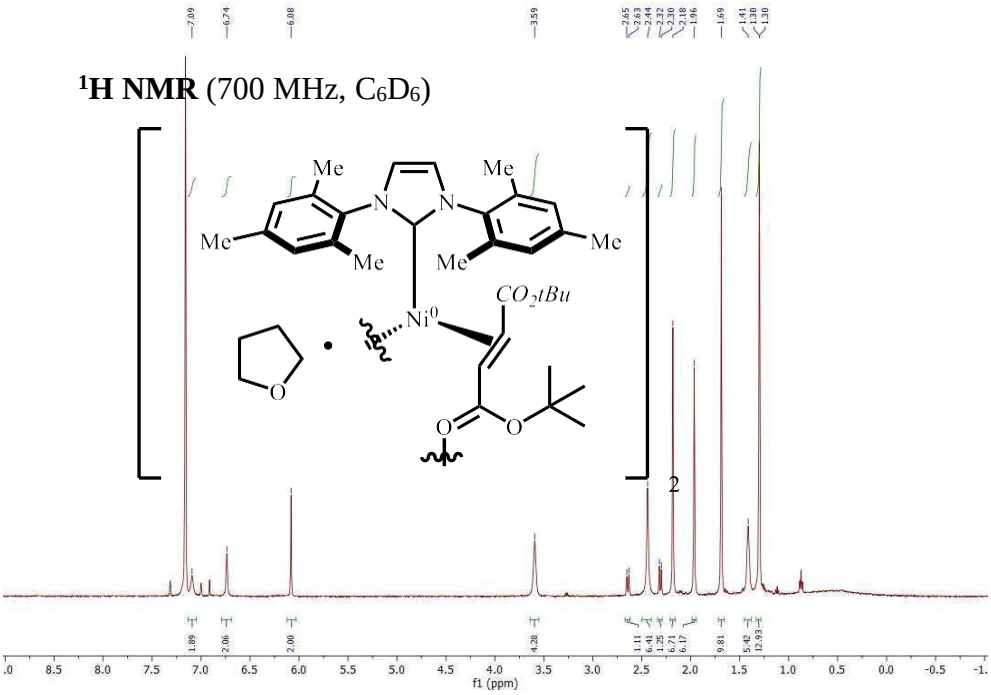

Figure 4-68. [1]H of Bis(di-tert-butyl fumarate)(1,3-bis(2,4,6-trimethylphenyl)imidazol-2-ylidene)nickel(0) (3-38).

References

(1) Ludwig, J. R.; Schindler, C. S. Catalyst: Sustainable Catalysis. *Chem* **2017**, *2*, 313–316. https://doi.org/10.1016/j.chempr.2017.02.014.

(2) Tasker, S. Z.; Standley, E. A.; Jamison, T. F. Recent Advances in Homogeneous Nickel Catalysis. *Nature* **2014**, *509*, 299–309. https://doi.org/10.1038/nature13274.

(3) Chemistry, T. *The Chemistry of Painting*; 1925; 116. https://doi.org/10.1038/116799a0.

(4) Kärkäs, M. D.; Matsuura, B. S.; Monos, T. M.; Magallanes, G.; Stephenson, C. R. J. Transition-Metal Catalyzed Valorization of Lignin: The Key to a Sustainable Carbon-Neutral Future. *Org. Biomol. Chem.* **2016**, *14*, 1853–1914. https://doi.org/10.1039/c5ob02212f.

(5) Biffis, A.; Centomo, P.; Del Zotto, A.; Zecca, M. Pd Metal Catalysts for Cross-Couplings and Related Reactions in the 21st Century: A Critical Review. *Chem. Rev.* **2018**, *118*, 2249–2295. https://doi.org/10.1021/acs.chemrev.7b00443.

(6) Tobisu, M.; Chatani, N. Cross-Couplings Using Aryl Ethers via C-O Bond Activation Enabled by Nickel Catalysts. *Acc. Chem. Res.* **2015**, *48*, 1717–1726. https://doi.org/10.1021/acs.accounts.5b00051.

(7) Qiu, Z.; Li, C. J. Transformations of Less-Activated Phenols and Phenol Derivatives via C-

O Cleavage. *Chem. Rev.* **2020**, *120*, 10454–10515. https://doi.org/10.1021/acs.chemrev.0c00088.

(8) Zeng, H.; Qiu, Z.; Domínguez-Huerta, A.; Hearne, Z.; Chen, Z.; Li, C. J. An Adventure in Sustainable Cross-Coupling of Phenols and Derivatives via Carbon-Oxygen Bond Cleavage. *ACS Catal.* **2017**, *7*, 510–519. https://doi.org/10.1021/acscatal.6b02964.

(9) Bajo, S.; Laidlaw, G.; Kennedy, A. R.; Sproules, S.; Nelson, D. J. Oxidative Addition of Aryl Electrophiles to a Prototypical Nickel(0) Complex: Mechanism and Structure/Reactivity Relationships. *Organometallics* **2017**, *36*, 1662–1672. https://doi.org/10.1021/acs.organomet.7b00208.

(10) Pein, W. L.; Wiensch, E. M.; Montgomery, J. Nickel-Catalyzed Ipso-Borylation of Silyloxyarenes via C – O Bond Activation. *Chem Rxiv* **2021**, 1–5. https://doi.org/10.1021/acs.orglett.1c01280.

(11) Pein, W. L.; Wiensch, E. M.; Montgomery, J. Nickel-Catalyzed Ipso-Borylation of Silyloxyarenes via C–O Bond Activation. *Org. Lett.* **2021**, 4588–4592. https://doi.org/10.1021/acs.orglett.1c01280.

(12) Wiensch, E. M.; Montgomery, J. Nickel-Catalyzed Amination of Silyloxyarenes through C–O Bond Activation. *Angew. Chemie - Int. Ed.* **2018**, *57*, 11045–11049. https://doi.org/10.1002/anie.201806790.

(13) Wiensch, E. M.; Todd, D. P.; Montgomery, J. Silyloxyarenes as Versatile Coupling

Substrates Enabled by Nickel-Catalyzed C-O Bond Cleavage. *ACS Catal.* **2017**, *7*, 5568–5571. https://doi.org/10.1021/acscatal.7b02025.

(14) Entz, E. D.; Russell, J. E. A.; Hooker, L. V.; Neufeldt, S. R. Small Phosphine Ligands Enable Selective Oxidative Addition of Ar-O over Ar-Cl Bonds at Nickel(0). *J. Am. Chem. Soc.* **2020**, *142*, 15454–15463. https://doi.org/10.1021/jacs.0c06995.

(15) Reeves, E. K.; Entz, E. D.; Neufeldt, S. R. Chemodivergence between Electrophiles in Cross-Coupling Reactions. *Chem. - A Eur. J.* **2021**, *27*, 6161–6177. https://doi.org/10.1002/chem.202004437.

(16) Montgomery, J. Organonickel Chemistry. *Organometallics Synth.* **2013**, 319–428. https://doi.org/10.1002/9781118651421.ch3.

(17) Fricke, C.; Schoenebeck, F. Organogermanes as Orthogonal Coupling Partners in Synthesis and Catalysis. *Acc. Chem. Res.* **2020**. https://doi.org/10.1021/acs.accounts.0c00527.

(18) Guan, B. T.; Xiang, S. K.; Wu, T.; Sun, Z. P.; Wang, B. Q.; Zhao, K. Q.; Shi, Z. J. Methylation of Arenes via Ni-Catalyzed Aryl C-O/F Activation. *Chem. Commun.* **2008**, *2*, 1437–1439. https://doi.org/10.1039/b718998b.

(19) Dankwardt, J. W. Nickel-Catalyzed Cross-Coupling of Aryl Grignard Reagents with Aromatic Alkyl Ethers: An Efficient Synthesis of Unsymmetrical Biaryls. *Angew. Chemie - Int. Ed.* **2004**, *43*, 2428–2432. https://doi.org/10.1002/anie.200453765.

(20) Xie, L. G.; Wang, Z. X. Cross-Coupling of Aryl/Alkenyl Ethers with Aryl Grignard

Reagents through Nickel-Catalyzed C-O Activation. *Chem. - A Eur. J.* **2011**, *17*, 4972–4975. https://doi.org/10.1002/chem.201003731.

(21) Yang, Z. K.; Wang, D. Y.; Minami, H.; Ogawa, H.; Ozaki, T.; Saito, T.; Miyamoto, K.; Wang, C.; Uchiyama, M. Cross-Coupling of Organolithium with Ethers or Aryl Ammonium Salts by C−O or C−N Bond Cleavage. *Chem. - A Eur. J.* **2016**, *22*, 15693–15699. https://doi.org/10.1002/chem.201603436.

(22) Hooshmand, S. E.; Heidari, B.; Sedghi, R.; Varma, R. S. Recent Advances in the Suzuki-Miyaura Cross-Coupling Reaction Using Efficient Catalysts in Eco-Friendly Media. *Green Chem.* **2019**, *21*, 381–405. https://doi.org/10.1039/c8gc02860e.

(23) Wu, P.; Givskov, M.; Nielsen, T. E. Reactivity and Synthetic Applications of Multicomponent Petasis Reactions. *Chem. Rev.* **2019**, *119*, 11245–11290. https://doi.org/10.1021/acs.chemrev.9b00214.

(24) West, M. J.; Fyfe, J. W. B.; Vantourout, J. C.; Watson, A. J. B. Mechanistic Development and Recent Applications of the Chan-Lam Amination. *Chem. Rev.* **2019**, *119*, 12491–12523. https://doi.org/10.1021/acs.chemrev.9b00491.

(25) Trippier, P. C.; McGuigan, C. Boronic Acids in Medicinal Chemistry: Anticancer, Antibacterial and Antiviral Applications. *Medchemcomm* **2010**, *1*, 183–198. https://doi.org/10.1039/c0md00119h.

(26) Leermann, T.; Leroux, F. R.; Colobert, F. Highly Efficient One-Pot Access to

Functionalized Arylboronic Acids via Noncryogenic Bromine/Magnesium Exchanges. *Org. Lett.* **2011**, *13*, 4479–4481. https://doi.org/10.1021/ol2016252.

(27) Hafner, A.; Meisenbach, M.; Sedelmeier, J. Flow Chemistry on Multigram Scale: Continuous Synthesis of Boronic Acids within 1 S. *Org. Lett.* **2016**, *18*, 3630–3633. https://doi.org/10.1021/acs.orglett.6b01681.

(28) Wan, C. W.; Burghart, A.; Chen, J.; Bergström, F.; Johansson, L. B. .; Wolford, M. F.; Kim, T. G.; Topp, M. R.; Hochstrasser, R. M.; Burgess, K. Anthracene - BODIPY Cassettes: Syntheses and Energy Transfer. *Chem. - A Eur. J.* **2003**, *9*, 4430–4441. https://doi.org/10.1002/chem.200304754.

(29) Jin, S.; Dang, H. T.; Haug, G. C.; He, R.; Nguyen, V. D.; Nguyen, V. T.; Arman, H. D.; Schanze, K. S.; Larionov, O. V. Visible Light-Induced Borylation of C-O, C-N, and C-X Bonds. *J. Am. Chem. Soc.* **2020**, *142*, 1603–1613. https://doi.org/10.1021/jacs.9b12519.

(30) Ji, H.; Cai, J.; Gan, N.; Wang, Z.; Wu, L.; Li, G.; Yi, T. Palladium-Catalyzed Borylation of Aryl (Pseudo)Halides and Its Applications in Biaryl Synthesis. *Chem. Cent. J.* **2018**, *12*, 6–13. https://doi.org/10.1186/s13065-018-0510-6.

(31) Zhou, Q.; Srinivas, H. D.; Zhang, S.; Watson, M. P. Accessing Both Retention and Inversion Pathways in Stereospeci Fi c, Nickel-Catalyzed Miyaura Borylations of Allylic Pivalates. **2016**. https://doi.org/10.1021/jacs.6b07396.

(32) Huang, K.; Yu, D. G.; Zheng, S. F.; Wu, Z. H.; Shi, Z. J. Borylation of Aryl and Alkenyl

Carbamates through Ni-Catalyzed C-O Activation. *Chem. - A Eur. J.* **2011**, *17*, 786–791. https://doi.org/10.1002/chem.201001943.

(33) Quasdorf, K. W.; Antoft-Finch, A.; Liu, P.; Silberstein, A. L.; Komaromi, A.; Blackburn, T.; Ramgren, S. D.; Houk, K. N.; Snieckus, V.; Garg, N. K. Suzuki-Miyaura Cross-Coupling of Aryl Carbamates and Sulfamates: Experimental and Computational Studies. *J. Am. Chem. Soc.* **2011**, *133*, 6352–6363. https://doi.org/10.1021/ja200398c.

(34) Zarate, C.; Martin, R. Ipso- Borylation of Aryl Ethers via Ni-Catalyzed C − OMe Cleavage. **2015**, No. entry 5. https://doi.org/10.1021/jacs.5b03955.

(35) Crouch, R. D. Synthetic Communications Reviews: Recent Advances in Silyl Protection of Alcohols. *Synth. Commun.* **2013**, *43*, 2265–2279. https://doi.org/10.1080/00397911.2012.717241.

(36) Crouch, R. D. Selective Monodeprotection of Bis-Silyl Ethers. *Tetrahedron* **2004**, *60*, 5833–5871. https://doi.org/10.1016/j.tet.2004.04.042.

(37) Lalonde, M.; Chan, T.H. Use of Organosilicon Reagents as PRotective Groups in Organic Synthesis. *Synthesis*, **1985**, *9*, 817–845. https://doi.org/101055/s-1985-31361.

(38) Hiller, N. de J.; do Amaral e Silva, N. A.; Tavares, T. A.; Faria, R. X.; Eberlin, M. N.; de Luna Martins, D. Arylboronic Acids and Their Myriad of Applications Beyond Organic Synthesis. *European J. Org. Chem.* **2020**, *2020*, 4841–4877. https://doi.org/10.1002/ejoc.202000396.

(39) Chen, J. Q.; Li, J. H.; Dong, Z. B. A Review on the Latest Progress of Chan-Lam Coupling Reaction. *Adv. Synth. Catal.* **2020**, *362*, 3311–3331. https://doi.org/10.1002/adsc.202000495.

(40) Fernandes, R. A.; Bhowmik, A.; Yadav, S. S. Advances in Cu and Ni-Catalyzed Chan-Lam-Type Coupling: Synthesis of Diarylchalcogenides, Ar2-X (X = S, Se, Te). *Org. Biomol. Chem.* **2020**, *18*, 9583–9600. https://doi.org/10.1039/d0ob02035d.

(41) Vantourout, J. C.; Miras, H. N.; Isidro-Llobet, A.; Sproules, S.; Watson, A. J. B. Spectroscopic Studies of the Chan-Lam Amination: A Mechanism-Inspired Solution to Boronic Ester Reactivity. *J. Am. Chem. Soc.* **2017**, *139*, 4769–4779. https://doi.org/10.1021/jacs.6b12800.

(42) Kalinski, C.; Lemoine, H.; Schmidt, J.; Burdack, C.; Kolb, J.; Umkehrer, M.; Ross, G. Multicomponent Reactions as a Powerful Tool for Generic Drug Synthesis. *Synthesis (Stuttg).* **2008**, *24*, 4007–4011. https://doi.org/10.1055/s-0028-1083239.

(43) Beisel, T.; Manolikakes, G. A Palladium-Catalyzed Three-Component Synthesis of Arylmethylsulfonamides. *Synth.* **2016**, *48*, 379–386. https://doi.org/10.1055/s-0035-1560910.

(44) Buskes, M. J. Discovery and Development. *Genet. Eng. Biotechnol. News* **2014**, *34*, 12. https://doi.org/10.1089/gen.34.08.07.

(45) Yan, G.; Yang, M.; Wu, X. Synthetic Applications of Arylboronic Acid via an Aryl Radical

Transfer Pathway. *Org. Biomol. Chem.* **2013**, *11*, 7999–8008. https://doi.org/10.1039/c3ob41851k.

(46) Demir, A. S.; Reis, Ö.; Emrullahoglu, M. Generation of Aryl Radicals from Arylboronic Acids by Manganese (III) Acetate : Synthesis of Biaryls and Heterobiaryls Described . In Aromatic Solvents , in Situ Generated Aryl Radicals Afford the Corresponding Biaryls In. *J. Org. Chem.* **2003**, *68*, 578–580.

(47) Kvasovs, N.; Gevorgyan, V. Contemporary Methods for Generation of Aryl Radicals. *Chem. Soc. Rev.* **2021**, *50*, 2244–2259. https://doi.org/10.1039/d0cs00589d.

(48) Of, D.; Acid, P. Feb., 1931. **1931**, *2784*, 711–723.

(49) Brown, H. C.; Cole, T. E.; Srebnik, M. Organoboranes. 40. A Simple Preparation of Borinic Esters from Organolithium Reagents and Selected Boronic Esters. *Organometallics* **1985**, *4*, 1788–1792. https://doi.org/10.1021/om00129a019.

(50) Ishiyama, T.; Murata, M.; Miyaura, N. Palladium(0)-Catalyzed Cross-Coupling Reaction of Alkoxydiboron with Haloarenes: A Direct Procedure for Arylboronic Esters. *J. Org. Chem.* **1995**, *60*, 7508–7510. https://doi.org/10.1021/jo00128a024.

(51) Euzenat, L.; Horhant, D.; Ribourdouille, Y.; Alcaraz, G.; Vaultier, M. Monomeric (Dialkylamino)Boranes: A New and Efficient Boron Source in Palladium Catalyzed C-B Bond Formation with Aryl Halides. *Chem. Commun.* **2003**, *3*, 2280–2281. https://doi.org/10.1039/b306874a.

(52) Chow, W. K.; Yuen, O. Y.; Choy, P. Y.; So, C. M.; Lau, C. P.; Wong, W. T.; Kwong, F. Y. A Decade Advancement of Transition Metal-Catalyzed Borylation of Aryl Halides and Sulfonates. *RSC Adv.* **2013**, *3*, 12518–12539. https://doi.org/10.1039/c3ra22905j.

(53) Mkhalid, I. A. I.; Barnard, J. H.; Marder, T. B.; Murphy, J. M.; Hartwig, J. F. C-H Activation for the Construction of C-B Bonds. *Chem. Rev.* **2010**, *110*, 890–931. https://doi.org/10.1021/cr900206p.

(54) Murphy, J. M.; Tzschucke, C. C.; Hartwig, J. F. One-Pot Synthesis of Arylboronic Acids and Aryl Trifluoroborates by Ir-Catalyzed Borylation of Arenes. *Org. Lett.* **2007**, *9*, 757–760. https://doi.org/10.1021/ol062903o.

(55) Xu, L.; Wang, G.; Zhang, S.; Wang, H.; Wang, L.; Liu, L.; Jiao, J.; Li, P. Recent Advances in Catalytic C−H Borylation Reactions. *Tetrahedron* **2017**, *73*, 7123–7157. https://doi.org/10.1016/j.tet.2017.11.005.

(56) Waltz, K. M.; Muhoro, C. N.; Hartwig, J. F. C-H Activation and Functionalization of Unsaturated Hydrocarbons by Transition-Metal Boryl Complexes. *Organometallics* **1999**, *18*, 3383–3393. https://doi.org/10.1021/om990113v.

(57) Larsen, M. A.; Hartwig, J. F. Iridium-Catalyzed C-H Borylation of Heteroarenes: Scope, Regioselectivity, Application to Late-Stage Functionalization, and Mechanism. *J. Am. Chem. Soc.* **2014**, *136*, 4287–4299. https://doi.org/10.1021/ja412563e.

(58) Baquero, A. Recent Advances on Mechanistic Studies on C─H Activation Catalyzed by

Base Metals. **2018**, 1001–1058.

(59) Lohrengel, M. *Encyclopedia of Applied Electrochemistry*; **2014**. https://doi.org/10.1007/978-1-4419-6996-5.

(60) Hong, J.; Liu, Q.; Li, F.; Bai, G.; Liu, G.; Li, M.; Nayal, O. S.; Fu, X.; Mo, F. Electrochemical Radical Borylation of Aryl Iodides. *Chinese J. Chem.* **2019**, *37*, 347–351. https://doi.org/10.1002/cjoc.201900001.

(61) Cao, Z.; Luo, F.; Shi, W.; Shi, Z. Organic Chemistry Fronteirs Direct Borylation of Benzyl Alcohol and Its Analogues in the Absence of Bases. **2015**, 1505–1510. https://doi.org/10.1039/c5qo00243e.

(62) Mao, L.; Szabó, K. J.; Marder, T. B. Synthesis of Benzyl-, Allyl-, and Allenyl-Boronates via Copper-Catalyzed Borylation of Alcohols. *Org. Lett.* **2017**, *19*, 1204–1207. https://doi.org/10.1021/acs.orglett.7b00256.

(63) Miura, H.; Hachiya, Y.; Nishio, H.; Fukuta, Y.; Toyomasu, T.; Kobayashi, K.; Masaki, Y.; Shishido, T. Practical Synthesis of Allyl, Allenyl, and Benzyl Boronates through SN1′-Type Borylation under Heterogeneous Gold Catalysis. *ACS Catal.* **2021**, *11*, 758–766. https://doi.org/10.1021/acscatal.0c03771.

(64) Kinuta, H.; Tobisu, M.; Chatani, N. Rhodium-Catalyzed Borylation of Aryl 2-Pyridyl Ethers through Cleavage of the Carbon-Oxygen Bond: Borylative Removal of the Directing Group. *J. Am. Chem. Soc.* **2015**, *137*, 1593–1600. https://doi.org/10.1021/ja511622e.

(65) Wititsuwannakul, T.; Tantirungrotechai, Y.; Surawatanawong, P. Density Functional Study of Nickel N-Heterocyclic Carbene Catalyzed C-O Bond Hydrogenolysis of Methyl Phenyl Ether: The Concerted β-H Transfer Mechanism. *ACS Catal.* **2016**, *6*, 1477–1486. https://doi.org/10.1021/acscatal.5b02058.

(66) H, C. ChemComm Nickel-Catalyzed Borylation of Arenes and Indoles. *Chem. Commun.* **2015**, *51*, 6508–6511. https://doi.org/10.1039/C5CC01378J.

(67) Zhang, H. hrrt. Aromatic C─H Borylation by Nickel Catalysis. **2015**, 779–781. https://doi.org/10.1246/cl.150154.

(68) Xu, L.; Chung, L. W.; Wu, Y. Mechanism of Ni-NHC Catalyzed Hydrogenolysis of Aryl Ethers : Roles of the Excess Base. **2016**. https://doi.org/10.1021/acscatal.5b02089.

(69) Old, D. W.; Harris, M. C.; Buchwald, S. L. Efficient Palladium-Catalyzed N -Arylation of Indoles. **2000**, No. 14.

(70) Downes, M.; Verdecia, M. A.; Roecker, A. J.; Hughes, R.; Hogenesch, J. B.; Kast-Woelbern, H. R.; Bowman, M. E.; Ferrer, J. L.; Anisfeld, A. M.; Edwards, P. A.; Rosenfeld, J. M.; Alvarez, J. G. A.; Noel, J. P.; Nicolaou, K. C.; Evans, R. M. A Chemical, Genetic, and Structural Analysis of the Nuclear Bile Acid Receptor FXR. *Mol. Cell* **2003**, *11*, 1079–1092. https://doi.org/10.1016/S1097-2765(03)00104-7.

(71) Cornella, J.; Martin, R. Combined Experimental and Theoretical Study on the Reductive Cleavage of Inert C − O Bonds with Silanes: Ruling out a Classical Ni(0)/Ni(II) Catalytic

Couple and Evidence for Ni(I) Intermediates. **2013**, No. 0. https://doi.org/10.1021/ja311940s.

(72) Cordova, M.; Wodrich, M. D.; Meyer, B.; Sawatlon, B.; Corminboeuf, C. Data-Driven Advancement of Homogeneous Nickel Catalyst Activity for Aryl Ether Cleavage. *ACS Catal.* **2020**, *10*, 7021–7031. https://doi.org/10.1021/acscatal.0c00774.

(73) Niwa, T.; Ochiai, H.; Watanabe, Y.; Hosoya, T. Ni/Cu-Catalyzed Defluoroborylation of Fluoroarenes for Diverse C-F Bond Functionalizations. *J. Am. Chem. Soc.* **2015**, *137*, 14313–14318. https://doi.org/10.1021/jacs.5b10119.

(74) Standley, E. A.; Smith, S. J.; Müller, P.; Jamison, T. F. A Broadly Applicable Strategy for Entry into Homogeneous Nickel(0) Catalysts from Air-Stable Nickel(II) Complexes. *Organometallics* **2014**, *33*, 2012–2018. https://doi.org/10.1021/om500156q.

(75) Lei, A.; Shi, W.; Liu, C.; Liu, W. *Related Titles Handbook of Reagents for Organic Synthesis -Catalyst Components for Coupling Catalysis in Asymmetric Synthesis 2e Modern Tools for the Synthesis of Complex Bioactive Cross-Coupling Reactions*.

(76) Hachiya, H.; Hirano, K.; Satoh, T.; Miura, M. Oxidative Nickel-Air Catalysis in C-H Arylation: Direct Cross-Coupling of Azoles with Arylboronic Acids Using Air as Sole Oxidant. *ChemCatChem* **2010**, *2*, 1403–1406. https://doi.org/10.1002/cctc.201000223.

(77) Lo, P. K. T.; Chen, Y.; Willis, M. C. Nickel(II)-Catalyzed Synthesis of Sulfinates from Aryl and Heteroaryl Boronic Acids and the Sulfur Dioxide Surrogate DABSO. *ACS Catal.* **2019**,

9, 10668–10673. https://doi.org/10.1021/acscatal.9b04363.

(78) Clarke, C.; Incerti-Pradillos, C. A.; Lam, H. W. Enantioselective Nickel-Catalyzed Anti-Carbometallative Cyclizations of Alkynyl Electrophiles Enabled by Reversible Alkenylnickel E/Z Isomerization. *J. Am. Chem. Soc.* **2016**, *138*, 8068–8071. https://doi.org/10.1021/jacs.6b04206.

(79) Luo, F. X.; Cao, Z. C.; Zhao, H. W.; Wang, D.; Zhang, Y. F.; Xu, X.; Shi, Z. J. Nickel-Catalyzed Oxidative Coupling of Unactivated C(Sp3)-H Bonds in Aliphatic Amides with Terminal Alkynes. *Organometallics* **2017**, *36*, 18–21. https://doi.org/10.1021/acs.organomet.6b00529.

(80) Broggi, J.; Terme, T.; Vanelle, P. Organic Electron Donors as Powerful Single-Electron Reducing Agents in Organic Synthesis. *Angew. Chemie - Int. Ed.* **2014**, *53*, 384–413. https://doi.org/10.1002/anie.201209060.

(81) Nett, A. J.; Montgomery, J.; Zimmerman, P. M. Entrances, Traps, and Rate-Controlling Factors for Nickel-Catalyzed C-H Functionalization. *ACS Catal.* **2017**, *7*, 7352–7362. https://doi.org/10.1021/acscatal.7b02919.

(82) Todd, D. P.; Thompson, B. B.; Nett, A. J.; Montgomery, J. Deoxygenative C-C Bond-Forming Processes via a Net Four-Electron Reductive Coupling. *J. Am. Chem. Soc.* **2015**, *137*, 12788–12791. https://doi.org/10.1021/jacs.5b08448.

(83) Nett, A. J.; Canellas, S.; Higuchi, Y.; Robo, M. T.; Kochkodan, J. M.; Haynes, M. T.;

Kampf, J. W.; Montgomery, J. Stable, Well-Defined Nickel(0) Catalysts for Catalytic C-C and C-N Bond Formation. *ACS Catal.* **2018**, *8*, 6606–6611. https://doi.org/10.1021/acscatal.8b02187.

(84) Hitosugi, S.; Tanimoto, D.; Nakanishi, W.; Isobe, H. A Facile Chromatographic Method for Purification of Pinacol Boronic Esters. *Chem. Lett.* **2012**, *41*, 972–973. https://doi.org/10.1246/cl.2012.972.

(85) Furukawa, T.; Tobisu, M.; Chatani, N. Nickel-Catalyzed Borylation of Arenes and Indoles via C-H Bond Cleavage. *Chem. Commun.* **2015**, *51*, 6508–6511. https://doi.org/10.1039/c5cc01378j.

(86) Baker, M. S.; Phillips, S. T. A Two-Component Small Molecule System for Activity-Based Detection and Signal Amplification: Application to the Visual Detection of Threshold Levels of Pd(II). *J. Am. Chem. Soc.* **2011**, *133*, 5170–5173. https://doi.org/10.1021/ja108347d.

(87) Qing, Z.; Takacs, J. M. Click-Connected Ligand Scaffolds: Macrocyclic Chelates for Asymmetric Hydrogenation. *Org. Lett.* **2008**, *10*, 545–548. https://doi.org/10.1021/ol702890s.

(88) Izquierdo, J.; Orue, A.; Scheidt, K. A. A Dual Lewis Base Activation Strategy for Enantioselective Carbene-Catalyzed Annulations. *J. Am. Chem. Soc.* **2013**, *135*, 10634–10637. https://doi.org/10.1021/ja405833m.

(89) Manley, D. W.; McBurney, R. T.; Miller, P.; Walton, J. C.; Mills, A.; O'Rourke, C. Titania-Promoted Carboxylic Acid Alkylations of Alkenes and Cascade Addition-Cyclizations. *J. Org. Chem.* **2014**, *79*, 1386–1398. https://doi.org/10.1021/jo4027929.

(90) Shirley, H. J.; Bray, C. D. Spiroketal Formation by Cascade Oxidative Dearomatization: An Approach to the Phorbaketal Skeleton. *European J. Org. Chem.* **2016**, *2016*, 1504–1507. https://doi.org/10.1002/ejoc.201501370.

(91) Bourke, D. G.; Collins, D. J. Conversion of 7-Methoxy-3,4-Dihydro-2H-1-Benzopyran-2-One into the Corresponding Dimethyl Ortho Ester. *Tetrahedron* **1997**, *53*, 3863–3878. https://doi.org/10.1016/S0040-4020(97)00007-0.

(92) Blechta, V.; Šabata, S.; Sýkora, J.; Hetflejš, J.; Soukupová, L.; Schraml, J. The Effect of Solvent Accessible Surface on Hammett-Type Dependencies of Infinite Dilution ^{29}Si and ^{13}C NMR Shifts in Ring Substituted Silylated Phenols Dissolved in Chloroform and Acetone. *Magn. Reson. Chem.* **2012**, *50*, 128–134. https://doi.org/10.1002/mrc.2860.

(93) Petronijevic, F. R.; Wipf, P. Total Synthesis of (( )-Cycloclavine and (( )-5- Epi -Cycloclavine. **2011**, No. 5, 7704–7707.

(94) Jadhav, A. H.; Kim, H. A Mild, Efficient, and Selective Deprotection of Tert-Butyldimethylsilyl (TBDMS) Ethers Using Dicationic Ionic Liquid as a Catalyst. *Tetrahedron Lett.* **2012**, *53*, 5338–5342. https://doi.org/10.1016/j.tetlet.2012.07.108.

(95) Carbonylative, P.; Produce, H. T.; Lactones, B. E. @ X « w Tocr. **1991**, 6506–6507.

(96) Dai, P. F.; Ning, X. S.; Wang, H.; Cui, X. C.; Liu, J.; Qu, J. P.; Kang, Y. B. Cleavage of C(Aryl)−CH 3 Bonds in the Absence of Directing Groups under Transition Metal Free Conditions. *Angew. Chemie - Int. Ed.* **2019**, *58*, 5392–5395. https://doi.org/10.1002/anie.201901783.

(97) Ahammed, S.; Nandi, S.; Kundu, D.; Ranu, B. C. One-Pot Suzuki Coupling of Aromatic Amines via Visible Light Photocatalyzed Metal Free Borylation Using t-BuONO at Room Temperature. *Tetrahedron Lett.* **2016**, *57*, 1551–1554. https://doi.org/10.1016/j.tetlet.2016.02.097.

(98) Oda, S.; Ueura, K.; Kawakami, B.; Hatakeyama, T. Multiple Electrophilic C-H Borylation of Arenes Using Boron Triiodide. *Org. Lett.* **2020**, *22*, 700–704. https://doi.org/10.1021/acs.orglett.9b04483.

(99) Verma, P. K.; Mandal, S.; Geetharani, K. Efficient Synthesis of Aryl Boronates via Cobalt-Catalyzed Borylation of Aryl Chlorides and Bromides. *ACS Catal.* **2018**, *8*, 4049–4054. https://doi.org/10.1021/acscatal.8b00536.

(100) Devine, W.; Woodring, J. L.; Swaminathan, U.; Amata, E.; Patel, G.; Erath, J.; Roncal, N. E.; Lee, P. J.; Leed, S. E.; Rodriguez, A.; Mensa-Wilmot, K.; Sciotti, R. J.; Pollastri, M. P. Protozoan Parasite Growth Inhibitors Discovered by Cross-Screening Yield Potent Scaffolds for Lead Discovery. *J. Med. Chem.* **2015**, *58*, 5522–5537. https://doi.org/10.1021/acs.jmedchem.5b00515.

(101) Zarate, C.; Manzano, R.; Martin, R. Ipso- Borylation of Aryl Ethers via Ni-Catalyzed C-

OMe Cleavage. *J. Am. Chem. Soc.* **2015**, *137*, 6754–6757. https://doi.org/10.1021/jacs.5b03955.

(102) Qiu, Z.; Zhu, M.; Zheng, L.; Li, J.; Zou, D.; Wu, Y.; Wu, Y. Regioselective α-Benzylation of 3-Iodoazetidine via Suzuki Cross-Coupling. *Tetrahedron Lett.* **2019**, *60*, 1321–1324. https://doi.org/10.1016/j.tetlet.2019.04.008.

(103) Endo, K.; Ohkubo, T.; Shibata, T. Chemoselective Suzuki Coupling of Diborylmethane for Facile Synthesis of Benzylboronates. *Org. Lett.* **2011**, *13*, 3368–3371. https://doi.org/10.1021/ol201115k.